2015

DUAL FUNCTIONS FOR INSULINOMA-ASSOCIATED 1 IN RETINAL DEVELOPMENT

Marie A. Forbes-Osborne
University of Kentucky, maforb2@gmail.com

STUDENT AGREEMENT:

I represent that my thesis or dissertation and abstract are my original work. Proper attribution has been given to all outside sources. I understand that I am solely responsible for obtaining any needed copyright permissions. I have obtained needed written permission statement(s) from the owner(s) of each third-party copyrighted matter to be included in my work, allowing electronic distribution (if such use is not permitted by the fair use doctrine) which will be submitted to UKnowledge as Additional File.

I hereby grant to The University of Kentucky and its agents the irrevocable, non-exclusive, and royalty-free license to archive and make accessible my work in whole or in part in all forms of media, now or hereafter known. I agree that the document mentioned above may be made available immediately for worldwide access unless an embargo applies.

I retain all other ownership rights to the copyright of my work. I also retain the right to use in future works (such as articles or books) all or part of my work. I understand that I am free to register the copyright to my work.

REVIEW, APPROVAL AND ACCEPTANCE

The document mentioned above has been reviewed and accepted by the student's advisor, on behalf of the advisory committee, and by the Director of Graduate Studies (DGS), on behalf of the program; we verify that this is the final, approved version of the student's thesis including all changes required by the advisory committee. The undersigned agree to abide by the statements above.

Marie A. Forbes-Osborne, Student

Dr. Ann C. Morris, Major Professor

Dr. David F. Westneat, Director of Graduate Studies

DUAL FUNCTIONS FOR INSULINOMA-ASSOCIATED 1 IN RETINAL DEVELOPMENT

_____

DISSERTATION

_____

A dissertation submitted in partial fulfillment of the requirements for the degree of Doctor of Philosophy in the College of Arts and Sciences at the University of Kentucky

By
Marie A. Forbes-Osborne
Lexington, Kentucky
Director: Ann C. Morris, Associate Professor of Biology
Lexington, Kentucky
2015

ABSTRACT OF DISSERTATION

DUAL FUNCTIONS FOR INSULINOMA-ASSOCIATED 1 IN RETINAL DEVELOPMENT

Proper visual system function requires tightly controlled proliferation of a pool of relatively homogeneous retinal progenitor cells, followed by the stepwise specification and differentiation of multiple distinct cell types. These retinal cells, both neuronal and glial, must be generated in the correct numbers, and the correct laminar location to permit the formation of synaptic connections between individual cell types. After synapses are made, constant signaling is required as part of normal retinal function, and to maintain cellular identity and connectivity. These processes rely on both extrinsic and intrinsic signaling, with regulation of gene expression by cascades of transcription factors having a key role. While considerable work has been done to identify key regulators of retinal development, maturation, and homeostasis, many factors remain unidentified or poorly characterized, either at large or within the retina.

One such factor is Insulinoma-associated 1 (*Insm1*). Known to function in endocrine cell, sympathetic and monoaminergic neuron, and olfactory epithelial cell differentiation and maturation, Insm1 is also a regulator of cell cycle progression in the adrenal system and cerebral cortex. Although *Insm1* was previously considered a transcriptional regulator, recently, non-nuclear functions have also been identified. However, the retinal function of *Insm1* remained a mystery. To determine the role of *Insm1* in retinal development, I characterized the retinal expression pattern of *Insm1*, as well as the effect of perturbation of *Insm1* expression levels at both the cellular and molecular level. Chapter 1 of this dissertation provides an overview of the retina and its development, vision and retinal degenerative diseases, and a review of *Insm1* expression and function in tissues outside the retina. Chapter 2 presents data generated from the knockdown of the retinal-expressed zebrafish co-ortholog of *Insm1, insm1a,* which demonstrated a requirement for *insm1a* in proper differentiation of photoreceptor cells. Additionally, these experiments showed a cell cycle regulatory function for *insm1a* in retinal development. Characterization of a zebrafish *insm1a* mutant and functional examination of *insm1a* truncation variants is discussed in Chapter 3. Chapter 4 presents data from an RNA-Seq analysis of wild-type and *Insm1* knockout mouse retinas at two developmental time points, and details transcriptional changes during retinal development in the absence of *Insm1*. Finally, Chapter 5 discusses the conclusions from the data generated for this dissertation, additional studies identified as the result of this work, and the implications of these results on our understanding of retinal development.

KEYWORDS: Retina, Photoreceptor, Insm1, Development, Zebrafish, Mouse

Marie A. Forbes-Osborne
Student's Signature

December 10, 2015
Date

DUAL FUNCTIONS FOR INSULINOMA-ASSOCIATED 1 IN RETINAL DEVELOPMENT

By

Marie A. Forbes-Osborne

Ann C. Morris
Director of Dissertation

David F. Westneat
Director of Graduate Studies

December 10, 2015
Date

F*or MB*
Really, Really.

ACKOWLEDGEMENTS

"Hard work spotlights the character of people: some turn up their sleeves, some turn up their noses, and some don't turn up at all." –Sam Ewing

Throughout life (and especially during graduate school) this quote has inspired me, and I have committed to always being the type person who turns up their sleeves. However, hard work seldom occurs in a vacuum, and good company can make difficult tasks far easier. Though this dissertation bears only my name, it is built on the hard work and knowledge of innumerable others.

First, I owe more than I can ever express to my mother, Antoinette Forbes. She taught me the value of hard work and dedication from childhood. She made me a voracious learner, and more importantly, a limitless questioner. She never stifled my curiosity and showed me the value and importance of questions without answers. For this and so much more, I am forever grateful.

Second, I would like to thank my doctoral advisor, Dr. Ann Morris. Far beyond simply giving knowledge, Ann gave me a toolbox to solve nearly any problem that presented itself. She also gave me the freedom to explore, experiment and make (not mention learn from) mistakes, all while being ready to swoop in and save the day if I couldn't figure it out on my own. This made me a better scientist, and gave me the opportunity to learn to be independent, without fear of failing. She also showed me that excellent science must be accompanied by excellent writing and engaging presentation skills. Her continued support has been essential to my growth and success in the lab and in life.

I would also like to express my gratitude to the members of my committee. Dr. Pete Mirabito, who offered me unbelievable support and guidance from the lab to the classroom. His emphasis on understanding *why* and *how* have forever changed the way that I look at and solve problems. Dr. Randal Voss, whose questions and observations often forced me outside my comfort zone. Without a doubt, this made me a more thorough researcher and a better student of science and the world. Dr. Liz Debski, who always held me to exceptionally high standards, and showed me the importance in being certain of the underlying facts and the best ways to present them. Lastly, Dr. Jayakrishna Ambati, who helped me understand the importance of making research work for the betterment of society, and the value of using basic science and simple techniques to answer real world difficult questions. Their assistance has been invaluable to me throughout.

My initial research experiences came from Dr. Rebecca Kellum. Without her support and assistance I would never have found the passion for research. I will be forever grateful to her for all that she has done for me.

Day to day, I have been fortunate to have amazing lab mates and department colleagues, who made the daily grind more enjoyable. Dr. Lakshmi Pillai-Kastoori, my batch-

mate and confidant. I am forever thankful for her support and friendship. Wen Wen, who attacks every obstacle with unending enthusiasm. Every task is possible when untaken so positively. Stephen Wilson, who showed me the value of taking every opportunity to enjoy the high points, while never letting the low points destroy you. Cagney (CC) Coomer, who has brought a new vibrancy to the lab in the last year, and has reminded me how important it is to pass on what we have learned. Sara Perkins, our fabulous technician, who kept things together for all of us. Whether supporting us at the bench or keeping us in line, none of this work would be possible without her. She has also become one of my best friends during this time, and has made my life better in more ways than I can ever express. Michelle Geidt, who has been a great friend, always ready to shore up flagging energy any way possible. Melissa Keinath and Stephanie Bryant for a listening ear and copious help when the science got ahead of my abilities. Thank you all.

I have also been fortunate to mentor some of the best students imaginable. Meredith Stone was my first undergraduate and showed me the value of teaching and mentorship. Sana Aslam, an amazing high school student, who at 15 joined the lab and for almost 3 years has been working tirelessly alongside me. She is inspiring in her passion for science and for the world at large. Thank you both for reminding me every day why we do this.

My experience in graduate school would have far different without the assistance of the administrative staff. Beverly Taulbee, solver of problems, Cheryl Edward, Monica Decker, Seth Taylor, Jacqueline Burke and Jacqueline Lee. Thank you for all the help, guidance, and support.

Finally, I would like to thank my family. My partner in life and best friend, Sam Osborne, who has anchored me and kept me sane. Without him, I would not have been able to make it through. To my parents, my mother and bonus-father Cecil Johnson, who have been amazingly supportive during these years. My grandmother, Beatrice Purdy, for a lifetime of support and encouragement. My parents and sister in-law, Corb, Becky and Lydia Osborne who have forgiven the long nights and holidays required for this dissertation, and who have encouraged and supported both Sam and me throughout. You have all been safe ports in this rough journey of life, and I love you all.

Finally, I would like to thank the Department of Biology and Gertrude F. Ribble, whose gift to the department provided monetary support for summer and year-long fellowships, as well as research grants to fund interesting projects. I am also grateful to have received a travel fellowship for the ARVO annual meeting from the National Eye Institute. Financial support to Ann Morris from the National Eye Institute (NIH/R01), The Pew Biomedical Scholars Program, and Fight for Sight funded the research discussed in this dissertation.

TABLE OF CONTENTS

LIST OF TABLES

LIST OF FIGURES

CHAPTER 1: VISION, INSM1 AND DEVELOPMENT

Marie Forbes-Osborne

Department of Biology, University of Kentucky, Lexington, Kentucky 40506-0225

KEYWORDS: Vision, retinal development, Insm1

1.1 Introduction

The word vision is derived from the Latin verb videre, "to see" and is defined as the act or power of sensing with the eyes. Vision is a fundamental biological process which influences nearly every aspect of our lives. As small children, we fear darkness, imbuing it with almost mystical powers. As adults, we fear loss of vision more than any other sensory deficit. A 2014 poll conducted for Research! America and the Alliance for Eye and Vision Research, found that Americans fear vision loss more than cancer, HIV/AIDS, and Alzheimer's Disease.

Proper visual function requires the development of multiple complex tissues derived from different embryonic origins, the formation of correct connections between cells in different regions of the head, and successful integration of sensory input between these cells. Improper development of or damage to any of the cells involved this process can result in vision loss or blindness. The National Eye Institute estimates that the cost of vision loss and eye disease in the United States exceeds $68 billion annually, and that more than 1 in 10 Americans suffer from vision loss or eye disease. Worldwide nearly 250 million people suffer from visual impairment, and a further 40 million people are functionally blind.

The neural tissue of the eye, the retina, is an outgrowth of the vertebrate brain, and therefore a part of the central nervous system (CNS). Like much of the mammalian central nervous system, the retina is unable to regenerate neurons lost to injury or disease. Despite recent advances, effective cell-based transplantation therapies to treat retinal degenerative

diseases and acute retinal injuries remain a long way from implementation. To replace lost retinal neurons with cells grown in culture, we must be able to efficiently grow individual cell types, as well as uncover the mechanisms that will permit proper integration and survival of the implanted cells. One promising avenue of research is to determine how some animals are able to naturally repair retinal damage, and thus determine what the human eye may require to accomplish regeneration.

This chapter will provide an overview of retinal morphology and development, including relevant retinal connections and molecular signals associated with proper visual function. Additionally, we will review the available information about *Insm1* in development. Throughout, we will follow the established nomenclature. Gene names will be italicized, with all letters capitalized for humans and non-human primates, first letters capitalized for rodents, and all letters lowercase for other vertebrates. Protein names will follow the same, but will not be italicized.

1.1.1 Vision and the eye

Vision begins in the eye. Light enters through the lens at the anterior of the eye. After traveling through the vitreous, the light reaches the intrinsically photoreceptive retina. The retina is a highly organized, multilayered tissue, which lines the back of the eye. The retina receives a light stimulus, converts it to electrical and chemical signals, and transmits the signal to the visual centers of the brain. Once received, the brain decodes the signal to reproduce an image of the world around us with a high degree of fidelity and in remarkable detail[1].

During embryonic development, the complex tissue of the retina, composed of 7 distinct cell types arranged in 3 highly interconnected layers, is created from a single sheet of relatively homogeneous pseudo-stratified neuroepithelia. Underlying proper retinal development is a highly regulated, tightly controlled network of cell-intrinsic factors and cell-extrinsic signals,

which interact to control proliferation, migration, and step-wise specification of retinal progenitor cells [2-4]. Tightly controlled expression of cascades of transcriptional regulators provide the basis for much of the cell-intrinsic regulation, and their misexpression can result in significant eye abnormalities.

1.1.2 Cells of the vertebrate retina and their connections

The vertebrate neural retina is composed of 6 neuronal cell types and 1 resident glial cell, the Müller glia. The nuclei of these cells are found in one of 3 cell layers: the outer nuclear layer (ONL), the inner nuclear layer (INL) or the ganglion cell layer (GCL). The processes of the cells extend into one of 2 plexiform layers: the outer plexiform layer (OPL), where ONL and INL cells synapse, and the inner plexiform layer (IPL), where INL and GCL cells synapse [1].

The ONL contains the cell bodies of the rod and cone photoreceptor cells (PRCs). The PRCs are light receiving cells responsible for phototransduction, whereby the received light stimulus is converted into neural impulses. The rod PRCs are extremely sensitive, some can be activated by a single photon of light, and are responsible for mediating low-light, monochromatic vision (night vision) (Luo, 2008). The cone PRCs require significantly more light stimulus, but are capable of producing finely detailed, full color vision. Multiple cone subtypes that respond to different wavelengths of light have been identified. This wavelength sensitivity is created by the expression of variants of the opsin visual pigment, and is the basis for color vision. The human retina contains 3 cone subtypes: blue cones, expressing S-opsin; green cones, expressing M-opsin; and red cones, expressing L-opsin [5]. The rod and cone PRCs have outer segments, which contain membranous disks (in the rods) or folds (in the cones) studded with the transmembrane opsin proteins. These outer segments are closely associated with the retinal pigmented epithelium (RPE) at the back of the eye. The RPE aids in the normal clearance of shed PRC outer segments and in recycling of the opsin bound chromophores, which undergo a

conformational change upon reception of a light stimulus [6]. The PRCs send processes into the OPL, where they form synapses with the processing interneurons of the INL.

The INL contains cell bodies of 3 neuronal cell types: the bipolar cells, amacrine cells, and horizontal cells; as well as the cell bodies of the single resident glial cell, the Müller glia. Although the Müller glia have cell bodies in the INL, their processes span the thickness of the retina. Müller glia act as support cells for the retinal neurons; for example they regulate environmental conditions (ions and neurotransmitters), remove debris, and provide physical support)by increasing the tensile strength of the retinal tissue) [7-9]. Multiple subtypes have been identified for each of the INL's interneurons, with at least 12 bipolar cell subtypes, 3 horizontal cell subtypes, and more than 25 amacrine cell subtypes identified in the primate retina [10-13]. The interneurons receive, integrate, and modulate signals received from the PRCs, after which the signal is transmitted to the retinal ganglion cells (RGCs) through the amacrine and bipolar cell processes in the IPL.

The RGCs have cell bodies in the GCL. They receive inputs from bipolar and amacrine cells in the INL, and then transmit the signal to the brain. To accomplish this, the RGCs have very long axons, which bundle together to form the optic nerve. The optic nerve directly connects the retina to the visual centers of the brain [14].

1.1.3 Development of the vertebrate retina

Development of the vertebrate retina has been the subject of significant study, including the molecular signals required to achieve proper levels of proliferation, step-wise specification of individual cell populations, timing of cell cycle exit, and eventual differentiation of each neuronal type, in the proper location, to permit the formation of correct connections with surrounding neurons.

1.1.3.1 Birth order of retinal neurons is highly conserved

In many species, including mouse and zebrafish, the first cells to differentiate in the retina are the RGCs, and the last to begin differentiating are the Müller glia [4, 15, 16]. In the mouse, differentiation of the amacrine and horizontal cells and cone photoreceptors overlap highly with the differentiation of the RGCs, though the RGCs do begin differentiating first. Similarly, the timing of differentiation of bipolar cells, rod photoreceptors, and Müller glia is very similar, though the Müller glia are the last to begin differentiating (Figure 1.2A) [15-17]. This differentiation occurs from the center of the developing retina and progresses towards the retinal periphery in the mouse [17].

Unlike in the mouse, zebrafish RGC differentiation is largely complete before the onset of amacrine, horizontal, and bipolar cell differentiation (Figure 1.2B). Differentiation of these INL cells, likewise, does not overlap significantly with differentiation of the photoreceptor cells. Cone photoreceptors are generated first, as the initiation of rod photoreceptor differentiation in the zebrafish is delayed and extended. The Müller glia remain the final cell to begin differentiation, though their genesis overlaps significantly with that of the rod photoreceptor cells. Another difference in zebrafish is that neurogenesis occurs in a fan-shaped wave, which originates at the ventral-most portion of the eye and proceeds through ventro-nasal to the dorsal and the ventro-temporal regions[18] .

1.1.3.2 Proliferation and specification of retinal stem cells are tightly controlled processes

The pseudo-stratified neuroepithelium of the early retina is a relatively homogeneous population of retinal progenitor cells (RPCs). Proliferation of these progenitors is maintained initially by several downstream effectors of the extrinsic Notch signaling pathway, including *Hes1* and *Hes5* [19], in conjunction with the expression of intrinsic pro-cell cycle progression factors, such as *CyclinD1* and members of the Retinoblastoma protein family (*Rb1*, *p107* and

p130) [20]. The initiation of cell cycle exit requires the downregulation of these factors, as well as the upregulation of cell cycle exit factors, such as $p27^{Kip1}$ and $p57^{Kip2}$[21]. Overlapping this proliferative phase and continuing thereafter are a series of gene expression events by which the eventual cell fate potential of subsets of the multipotent pool of RPCs become successively more restricted. As with the regulation of proliferation, this early competence restriction relies on both extrinsic (including *Hh* and FGFs) and intrinsic (transcription factor) signals [19, 22].

Expression of the basic-helix-loop-helix transcription factor *Math5/Atoh7,* in conjunction with the POU-domain containing transcription factor *Brn3b/c,* is required to specify RGCs. Mice lacking *Math5* fail to generate mature RGCs, but rather produce additional cone PRCs[23]. Similarly, in mice lacking *Brn3b* or *Brn3c*, few RGCs develop and optic nerve outgrowth is severely impaired. The double ablation of both *Brn3b* and *Brn3c* indicates that while these genes overlap in some functions, specifically in their ability to promote RGC differentiation, they also possess separate functions as well, with *Brn3c* being essential to optic nerve outgrowth [19, 24] .

Specification of INL cells is highly intertwined, with multiple specification factors shared amongst the 3 cell types. Expression of *Foxn4* promotes both horizontal and amacrine cell fate [25]. *Foxn4* acts through the required genes *Math3*, *NeuroD1*, and *Ptf1α* to specify amacrine cell fate [26, 27]. Alone, neither *Math3* nor *NeuroD1* were sufficient to generate amacrine cells in overexpression studies. The addition of *Pax6* to *NeuroD1* allowed the production of0 amacrine cells, while the addition of *Pax6* to *Math3* overexpression shifted cells to the horizontal cell fate. Together, these data indicate a finely tuned cell fate specification cascade, producing both amacrine and horizontal cells from a pool of progenitors that have maintained at least a portion of their plasticity.

Amacrine cell subtype specification is also controlled by expression of additional transcription factors. For example, GABAergic amacrine cells require *Bhlhb5*, while glycinergic

amacrine cells require *Barhl2* [25, 28]. In addition to *Foxn4* and *Ptf1α*, the expression of *Prox1*, which is both essential and sufficient, is required for horizontal cell specification [29, 30]. Bipolar cell fate specification, like other INL cells, requires *Math3* expression. However, in the absence of *Math3*, no apparent defects in retinogenesis were detected, and misexpression of *Math3* only promoted rod PRC genesis [27]. However, when *Math3* and *Ascl1* expression were abolished, bipolar cells were completely lost, and the cells normally specified as bipolar cells were transformed into Müller glia cells [31]. Additionally, *Chx10/Vsx2* gene expression is required for bipolar cell differentiation, as bipolar cells are missing in the absence of *Chx10/Vsx2*. *Chx10/Vsx2* is not sufficient for bipolar cell maturation however, as misexpression generates INL cells that fail to fully differentiate [27, 30].

Specification and differentiation of the PRCs is perhaps the best studied of all the retinal cell types. Rod and cone PRCs arise from a common progenitor pool, which expresses the required transcription factors *Otx2* and *Crx*, as well as *NeuroD1* and *Ascl1*. *Otx2* directly transactivates *Crx*, and in the absence of *Otx2* amacrine cells are generated in place of the PRCs. Similarly, deletion of *Crx* results in the loss of most, though not all PRCs [32]. Together this suggests that while *Otx2* and *Crx* are necessary for proper PRC development, additional factors are also involved. Misexpression of *NeuroD1* resulted in the enhanced generation of rod photoreceptor cells, indicating that *NeuroD1* is one such factor [26]. *Crx*, either alone or through other factors like *Rorß* [33], induces expression of pro-rod PRC genes, *Nrl* and *Nr2e3* [34-36]. Expression of rod PRC promoting genes, especially *Nr2e3*, suppresses cone cell specific genes, and permits the expression of additional rod photoreceptor genes, including the rod visual pigment, rhodopsin (Rho) [32]. In *Crx* expressing cells which do not receive the necessary signals to become rod PRCs, expression of cone-specific factors occurs instead. Expression of *Trß2* inhibits *S-opsin* (*Opn1sw*) expression while promoting *M-opsin* (*Opn1mw*) expression. Other

factors, including *Rxrγ* and *Rorα*, interact with *Trß2* to specify *S*-, *L*- and *M-opsin* expressing cone PRC specification and differentiation, but the exact mechanisms and gene interactions are currently unknown [33, 37, 38].

Cell specification and differentiation must be followed by maturation and maintenance of the eventual cell fate. This is accomplished through continued control of gene expression, proper processing and transport of functional proteins or protein subunits, and creation of proper neuron connections between cells [32]. Failure to complete any of these functions could lead to degeneration and eventual cell death within the retina, causing one of a multitude of retinal degenerative diseases.

1.1.4 Diseases of the retina

Dozens of genetic disorders that cause visual system defects have been characterized in human patients, representing at least 10% of all described genetic disorders [39]. Between 1 in 2000 and 1 in 3500 people worldwide have a genetic defect that negatively affects vision. The causative genetic lesions underlying these conditions have been traced to more than 120 loci, and more than 75 genes. Many inherited retinal diseases directly affect the PRCs or their connecting cells within the eye. The causative genes include phototransduction genes, retinal cell synapse formation and maintenance genes, and opsin regeneration genes, but also include many genes with either pan-neuronal or whole body expression. These conditions include non-syndromic diseases, such as Retinitis Pigmentosa (RP), Cone-Rod Dystrophy (CRD), Congenital Stationary Night Blindness (CSNB), and Leber's Congenital Amaurosis (LCA), as well as syndromic diseases including Joubert's, Bardet-Biedl and Usher's Syndromes, and Refsum's disease [39-41]. Multiple independent mutations have been identified for many of these diseases and multiple diseases have been linked to single genes, creating a complex picture of the many mechanisms by which visual function may be impaired.

Genetic diseases of the eye include both stable and degenerative conditions. Many of the stable conditions arise from a developmental defect, which results in the loss of partial or whole visual function. This includes conditions as varied as color blindness and CSNB. The retinal degenerative disorders may result from developmental deficits or may occur later in life as the result of improper maintenance of retinal cells or their connections, which leads to premature retinal cell death. Non-syndromic retinal degenerative diseases include RP, CRD, LCA, and many others. Often classified clinically by their age of onset and disease progression, considerable overlap in both symptoms and genetic causes are observed for many of these conditions. Additionally, considerable heterogeneity in causative genetic mutations, disease progression and eventual outcome also exist both within and between diseases [40-42]. For some individual mutations, disease severity and onset differ significantly even with a single family.

RP and CRD are similar progressive diseases, and share both causative genes and retinal disease pathologies. In RP, primary degeneration of the rod PRCs results in nyctalopia, or night blindness. This is followed by loss of peripheral cone PRCs leading to blind spots and eventual tunnel vision. Secondary cone PRC loss and retinal remodeling results in decreases in visual acuity, and for many patients eventual blindness [43]. CRD, unlike RP, is either a disease of primarily cone PRC degeneration or a disease where rod and cone PRCs are lost simultaneously. CRD patients experience decreased visual acuity and defects in color vision. These defects occur first in the central visual field with peripheral and night vision affected later. End stage RP and CRD are identical [44]. Both RP and CRD are highly genetically heterogeneous; inherited with autosomal dominant, autosomal recessive, and X-linked patterns, over 60 genes have been causatively linked to RP and over 30 to CRD. These include genes involved in eye development, photoreceptor maturation and maintenance, phototransduction, visual cycle genes and many others. While many of these genes are linked to only RP or CRD, others are implicated in both

[45], suggesting the potential for additional modifying loci or other factors in RP versus CRD pathology. Additional information concerning RP and RP-associated mutations, including our work to produce a panel of RP models in the zebrafish, may be found in Appendix I.

Unlike RP and CRD, CSNB is a stable (non-progressive) disease, which causes nyctalopia, nystagmus, strabismus, reduced visual acuity, and severe myopia. Unlike RP and CRD, individuals with CSNB have defects in retinal function at birth, which do not worsen over time. CSNB can be inherited through autosomal dominant, autosomal recessive and X-linked genes, with more than 10 identified loci. Many of the loci linked to CSNB are primarily expressed in bipolar cells and affect rod PRC to bipolar cell synapses [46-50]. Two genes linked to CSNB have also been linked to RP, though the specific mutations differ between the two conditions. For example, *PDE6B*, a rod specific phosphodiesterase, is mutated in both CSNB and RP, but the CSNB linked mutation is *H258N* (*His258-to-Asn*) [51], while *H557Y* (*His557-to-Tyr*), *R531X* (*Arg531-to-Term*) and other mutations are associated with RP [52].

LCA is an eye disorder affecting multiple eye components. Individuals with LCA often experience photophobia, nystagmus, severe hyperopia, keratoconus, and a lack of pupillary response. The visual impairment in LCA is generally stable, though some progression has been observed in a small number of patients. LCA associated mutations have been identified in genes affecting retinal development, PRC maturation and maintenance, and cilia formation, with defect in the thin connecting cilium separating the PRC inner and outer segments specifically [53, 54]. Of the 14 genes causatively linked to LCA, 3 have also been linked to CRD, 4 to RP, and 1 (*CRX*) to both CRD and RP, though again the residues changed differ between each [55-57].

The high degree of genetic heterogeneity observed within and between retinal degenerative diseases, coupled with the relatively small number of patients with each mutation makes the creation of good animal models of paramount importance. Models will permit us to

determine the mechanisms by which degeneration occurs, how cell death is initiated and identify potential avenues for therapeutic intervention. Unfortunately, few high quality *in vivo* models have been generated, and for many disease-associated mutations no models exist.

In addition to these genetic causes of vision loss, damage from physical trauma or comorbidities from other conditions, such as diabetes and aging, can also negatively impact vision [58, 59]. Because the eye is a part of the central nervous system, damage to retinal neurons is generally permanent. Currently, there are no effective treatments to replace damaged or lost retinal neurons. In order to develop vision-saving treatments, it is imperative to understand the transcriptional regulatory networks involved in the development and maintenance of retinal neurons, as well as to understand the mechanisms by which cells are lost and the responses of the retina to that cell loss. In addition to developing good animal models, models possessing the natural ability to regenerate retinal neurons are highly beneficial for examining the mechanism of retinal damage and for identifying and testing novel potential treatments. One organism which possesses this ability is the zebrafish (*Danio rerio*)[60].

1.2 The zebrafish as a model system

The zebrafish (*Danio rerio*) is a small fresh water teleost (ray finned) fish, native to the Ganges River system in western India and Bangladesh. Zebrafish have a strong history of use in general laboratory studies, and in particular in eye studies[61]. One of the most valuable features is its high fecundity, which allows studies to be highly powered. A single breeding pair can produce hundreds of eggs in a morning, and can be bred up to twice weekly. Fertilization is external, which allows ease of embryo collection as well as permitting direct observation of the developing embryos beginning at or very close to fertilization. Development of the embryos occurs very rapidly, with the first cell division occurring within 1 hour of fertilization. By 24 hours post fertilization (hpf), the developing embryo has a recognizable head, tail, eyes with distinct

lenses, and a beating heart [62]. This is equivalent to an E9.5 mouse [63] or a 3-4 week human embryo [64]. By 72 hpf, the bulk of embryonic development is completed, and the embryos respond to both light and touch stimuli. At 5 days post fertilization (dpf), the larvae are actively swimming and seeking food [62]. The larvae begin metamorphosis between 10 and 14 dpf, at which point they develop more adult-like fin features, grow scales, and start to show secondary sexual characteristics [65]. This process may last several weeks to months. With proper housing density and quality nutrition, zebrafish may become sexually mature in as little as 5-6 weeks, though peak fecundity is normally observed at 6-18 months of age.

1.2.1 Molecular techniques and the zebrafish

The zebrafish have a fully sequenced and annotated genome, and a wide variety of available genetic and molecular tools. Zebrafish can be used in both forward and reverse genetics studies, are capable of showing mosaic expression of both injected, *in vitro* transcribed mRNAs and promoter driven DNA [66], are capable of true transgenesis [67-69], and site specific recombination [70]. Developmental studies using morpholino-mediated gene knock downs are common [71, 72], and newly developed genome editing technologies also permit the creation of targeted mutations and site-specific knock-in lines [73-76] .

1.2.2 The zebrafish eye

The organization zebrafish retina is well conserved with other vertebrates. It contains four cone photoreceptor subtypes, blue, green and red cone photoreceptors, as are seen in humans, as well as an ultraviolet cone photoreceptor. Zebrafish also have rod photoreceptors. These cells are highly organized, forming a regular mosaic, wherein there are alternating rows of red/green double cones and blue/UV single cones. The rod PRCs are inserted into the mosaic at regular intervals [77]. Zebrafish are also capable of persistent and sustained

neurogenesis and proper reintegration of new neural cells into the existing retina [67-69], both as a function of their normal indeterminate growth and in response to injury or disease.

1.3 Insulinoma-Associated 1

Insulinoma-associated 1 (Insm1, formerly IA-1) is an evolutionarily conserved transcription factor, which was first isolated from a human insulinoma tumor subtraction library [78]. Insm1 was found to be absent in most adult tissues, but highly expressed in pheochromocytoma, medullary thyroid carcinoma, medulloblastoma, small cell lung carcinomas, glucagonoma insulinoma, and pituitary tumors, all of which arise from neuroendocrine cells [78, 79].

1.3.1 Insm1: gene and protein structure

Insm1 is a single exon gene (in human, chimp, mouse, rat, and multiple teleost species). The human *INSM1* gene encodes a 510 amino acid peptide containing an N-terminal SNAIL/GFI (SNAG) domain, a potential nuclear localization signal sequence (NLS), and 5 Cys_2-His_2 (C2H2) zinc finger motifs (Figure 1.1). The structure of the Insm1 protein is similar to the SNAIL, SLUG, GFI superfamily, which are known to act as transcriptional repressors [80].

Structural analysis of Insm1 identified 2 major domains. The N-terminal domain (human 1-250) is rich in proline, glycine, and alanine residues [81]. Many transcriptional regulators are known to contain proline-rich sequences, which function as domains for protein-protein interactions and mediate the activator/repressor activity [81-83], and in fact, murine Insm1 has been shown to interact with CAP/SORBS1 (an SH3 domain containing protein) in the regions at or near these proline rich domains [80]. Additionally, the N-terminal motif of Insm1 contains four highly conserved dibasic amino acids (human 8-9, 11-12, 221-222, 227-228), which are known to act as recognition sites for cleavage of peptide hormone precursors, including insulin, pancreatic polypeptide (PP), somatostatin, and glucagon. This domain also contains a potential

amidation signal sequence (human 198-201); the addition of α-amide groups is a common modification amongst multiple active neuroendocrine peptides [81, 84]. However, no evidence has been found to indicate that Insm1 is either cleaved or α-amidated in any neuroendocrine tissue [81].

The C-terminal domain (human 251-510) contains 5 symmetrically oriented C2H2 zinc finger motifs. Two tandem repeats are spaced 45-46 amino acids on either side of a central singular motif. The Cys-His residues within each zinc finger are extremely well conserved, including the replacement of the second Histidine residue in zinc finger motif 1 with an Arginine in multiple species. The spacing of the zinc finger motifs suggests that Insm1 should bind DNA in a sequence specific manner, and a consensus DNA-binding sequence for Insm1, $T(^{G}/_{T})(^{C}/_{T})(^{C}/_{T})(^{T}/_{A})GGGG(^{G}/_{T})C(^{G}/_{A})$, has been identified [79]. The central GGGG motif is required for Insm1 protein to bind to target promoters, and regulation of the downstream target gene appears to require orientation-specific, directional binding of Insm1 to the promoter [79]. Bioinformatic analysis of a eukaryotic promoter database identified multiple potential targets of Insm1 regulation, including *Insulin (Ins)*, *NeuroD*/ß2, and *Insm1* itself [79, 85].

1.3.2 Homologs of INSM1

Homologs of *Insm1* have been identified in multiple species, with the highest degrees of conservation observed in the SNAG domain, dibasic amino acid motifs, NLS sequence upstream of the first zinc finger motif, and zinc finger motifs 1, 2 and 5.

The *C. elegans* homolog of *Insm1* (*egl-46*), is a 283 amino acid peptide, while the *Drosophila nerfin-1* gene is a 469 amino acid peptide. Both contain 3 zinc finger domains and have 18.2 and 22.6% identity to the human peptide, respectively.

Insm1 homologs have been identified in two teleost fish species. *Ol-insm1a* and *Ol-insm1b* are Medaka co-orthologs of the mammalian *Insm1* [86], while *insm1a* and *insm1b* are

the zebrafish co-orthologs[87]. *Ol-insm1a* encodes a 440 amino acid protein with 52.7% identity to the human INSM1, and *Ol*-insm1b encodes a 498 amino acid protein, with 49.4% identity to the human INSM1. The zebrafish co-orthologs of mammalian *Insm1*, *insm1a* and *insm1b,* encode a 383 amino acid protein with 62.9% identity to human INSM1 and a 453 amino acid protein with 57.4% identity to human INSM1, respectively.

In rodent models, homologs of *INSM1* have been identified in both the rat (*Rattus norvegicus*) and the mouse (*Mus musculus*). In the rat, the *Insm1* gene is predicted to encode a 436 amino acid protein with 76.7% identity to the human protein. While other features are conserved, the third zinc finger motif is absent from the rat homolog [81]. In the mouse, the *Insm1* gene encodes a 521 amino acid peptide that shows 92.2% identity with the human INSM1.

1.3.3 Expression and function of INSM1 homologs in invertebrates and teleost fishes

Insm1 expression is generally restricted to development. Expression has been observed in the developing neuroendocrine system (in the pancreas; thymus, thyroid, and adrenal glands; and in the enteric cells of the gastrointestinal tract) and nervous systems (including the forebrain, midbrain, hindbrain, cerebellum, olfactory epithelium, and eye [88], neurogenic regions of the adult brain [89], and tumors of neuroendocrine origin [81] in a number of mammalian species.

C. elegans egl-46 and *Drosophila nerfin-1* are both developmentally expressed during early CNS development, and are known to be involved in neuronal differentiation. *Egl-46* and *nerfin-1* are both expressed transiently, with both genes absent in mature glia and neurons [81, 90-92]. The 3'UTR of *nerfin-1* was shown to possess binding sites for 18 distinct miRNAs, which were shown to play a role in post-transcriptional regulation of *nerfin-1* expression [93]. Similar regulation in vertebrate *Insm1* homologs has not been examined.

In Medaka, *Ol-insm1a* was shown to have a similar, albeit weaker, function compared to *Ol-insm1b*. Onset of *Ol-insm1b* expression corresponds to the timing of optic bud formation, and is first detected in the developing head. Expression increases during brain development and *Ol-insm1b* mRNA was detected in the developing telencephalon, several midbrain structures (including the optic tectum, torus semicircularis, and pretectal regions), several structures in the hypothalamus (including the suprachiasmatic nucleus (SCN), thalamic and preoptic regions), as well as in the habenular nuclei, scattered cells in the hindbrain, and the developing retina. Strong expression was also seen in the developing pancreas [86]. In the developing optic tectum and retina, *Ol-insm1b* was found to be present in differentiating zones, but absent in both proliferative zones and mature neuronal zones. In contrast to other species, *Ol-insm1b* expression remained strongly expressed in some regions of the adult brain, including in the olfactory bulbs, SCN, and some regions of the hypothalamus[86] .

Unlike the Medaka co-orthologs, zebrafish *insm1a* appears to be maternally deposited. Both *insm1a* and *insm1b* increase in expression during embryonic development, peak at 48 hpf, and are not detectable in most adult tissues. This corresponds with the neurogenic period of zebrafish development [87]. *Insm1a* and *insm1b* have similar but distinct expression patterns. Both co-orthologs are expressed in the developing olfactory placode, tegmentum, ventral diencephalon, hindbrain, and pancreas as well as in other regions of the brain. While both *insm1a* and *insm1b* are expressed in a subset of neurons in the spinal cord, the pattern of the 2 genes is different, with *insm1b* expressed in motorneurons, interneurons, and Rohan-beard neurons while, *insm1a* is absent from the Rohon-Beard neurons and restricted to the ventral motorneurons. Only *insm1a* expression is observed in the retina [87, 88, 94], and the pattern is similar to that which was observed in Medaka [86]. Additionally, *insm1a* has been shown to be

upregulated in response to damage or degeneration in neuronal tissues including the eye [94, 95].

1.3.4 Expression and function of mouse and human Insm1

In both mouse and human, *Insm1* is expressed in the developing brain (including the forebrain, midbrain, hindbrain, cerebellum, hypothalamus, olfactory epithelium), as well as in the developing retina, pancreas and gastrointestinal tract [80, 89, 96-101]. The function of *Insm1* has been closely examined in a subset of these tissues. These studies indicate both an absolute requirement for *Insm1* in embryonic development, as two independently generated mouse models where *Insm1* is globally deleted are embryonic lethal, and a complex and tissue specific role for *Insm1* during development. They also provide evidence for a wide array of molecules which either act upon or are influenced by *Insm1* expression.

1.3.4.1 Pancreatic Insm1 acts in cell differentiation and maturation

The pancreas contains 5 types of endocrine cells: α-, ß-, δ-, ε- and PP cells, which produce glucagon, insulin, somatostatin, ghrelin and pancreatic polypeptide, respectively. These cell types arise from a pancreatic and intestinal primordia, which also forms exocrine and ductal tissues in the pancreas, as well as the enteric endocrine cells scattered throughout the intestines and stomach [102-105]. Similar to the endocrine cells of the pancreas, these enteric endocrine cells produce an array of hormones including cholecystokinin, neurotensin, serotonin, substance P, and others [106]. A similar developmental programming has been determined to control the development of both the pancreatic and intestinal endocrine cells (Figure 1.3A) [98, 102-105].

Careful examination of a mouse knock-out line by Gierl et al., in which the *Insm1* coding region (but not the 5' and 3' UTRs) was replaced with *ß-galactosidase*, showed that all endocrine cells of the pancreas express *Insm1*, both developmentally (beginning as early as E9.5) and persistently. No cells of the ductal or exocrine lineage in the pancreas were seen to

express *Insm1*. Nearly all the *ß-galactosidase* expressing cells also expressed one of the pancreatic hormones at both E18.5 and in the adult pancreas (97.6 and 99.5% respectively).

When *Insm1* expression was entirely abolished in this model, α-cell differentiation was delayed. Even after the numbers of α-cells recovered, glucagon production remained low. ß-cells were more greatly affected by ablation of *Insm1*, with few mature (insulin expressing) ß-cells observed. No transdifferentiation of putative ß-cells into δ-, ε-, or PP-cells was observed. Interestingly, while expression of *Glucagon*, *Insulin*, *Somatostatin*, and the enteric endocrine derived *Neuropeptide Y* were decreased in the absence of *Insm1*, *Pancreatic Polypeptide* and G*hrelin* showed no change in expression levels. Additionally, all the genes involved in hormone processing and secretion examined were significantly reduced in the absence of *Insm1*, suggesting a role for *Insm1* in the maturation of all the endocrine cell types of the pancreas and gut. *Insm1* was determined to have no effect on the early proliferation of pancreatic progenitor cells, but rather to affect the eventual survival of at least the ß- and δ-cells in the pancreas.

Similarly, *Insm1* expression was shown to have no effect on enteric endocrine cell proliferation. Instead, *Insm1* is required to initiate and maintain expression of the secretory machinery in these cells [98]. Taken together, these experiments suggest that *Insm1* functions primarily in cell differentiation and maturation in the both murine endocrine pancreas and enteric endocrine cells.

1.3.4.2 Insm1 in the developing cerebral cortex

In the developing mammalian cerebral cortex, progenitor cells are classified by where they undergo mitosis. The first group, collectively called APs (apical progenitors), includes the neuroepithelia cells, the primary progenitor cells of the CNS (and their daughter cells), radial glia, and the short neural precursors. These cells are defined by their apical-basal polarity, where the apical surface of the plasma membrane associates with the ventricular surface [97,

107-111]. The second group, called the BPs (basal progenitors), non-surface dividing progenitor cells, or intermediate progenitors, are defined by their ability to divide away from the ventricular wall, in the basal region of the ventricular zone (VZ) or the subventricular zone (SVZ). BPs arise from APs, and are critical to the expansion of the mammalian cerebral cortex. This expansion is thought to be a result of the abventricular BP cell divisions, which permit BPs to expand their population, and therefore the eventual neuronal population they produce, to a greater extent than would be possible with only ventricular surface mitoses. Many of the genes defining and regulating BP genesis and expansion are still unknown, as are the signals driving the shift from AP to BP [97, 111-115].

In the hindbrain and midbrain regions of the mouse, *Insm1* expression is observed as early as E9.5, and spreads caudally through the spinal cord (by E11) and rostrally to the telencephalon. Telencephalon expression expands from the ventral to the dorsal, with expression in the dorsal telencephalon first observed at E10. Early *Insm1* expression levels are very low, but increase rapidly through E11.5, with abundant expression in both the VZ and SVZ [97]. Although *Insm1* is expressed in both APs and BPs in the VZ, *Insm1* expression is highest in basal cell bodies. *Insm1* mRNA was not seen to be coexpressed with ßIII-tubulin, a marker of early neurons, suggesting that the basal cells are not newborn neurons. Insm1 was observed to co-localize with the mitotic marker phosphohistone H3 (PH3) in both APs and BPs; and nearly all mitotic BPs throughout neurogenesis express *Insm1*. The pattern of *Insm1* expression is nearly identical to that of *Tis21*, a known panneurogenic factor [97, 111]. Panneurogenic factors identify a population of progenitor cells undergoing neurogenic, rather that proliferative, cell division. In these experiments, coexpression of *Insm1* and *Tis21* was seen in almost all E10.5 APs and BPs, with 80% *Tis21*/*Insm1* positive, 13% *Insm1* positive only, 2% *Tis21* positive only, and 5% *Tis21*/*Insm1* negative. Additionally, expression in other brain regions, including the

external granule cell layer of the cerebellum, the dentate gyrus of the hippocampus, and the wall of the lateral ventricle also mirrored known patterns of neurogenesis in those regions. Taken together, this may suggest a panneurogenic role for *Insm1* in the developing hindbrain (Figure 1.3D) [97].

Both the global *Insm1* knock-out described previously and forced premature expression (FPE) studies were used to determine the specific function of *Insm1* in the developing cerebral cortex. In the absence of *Insm1*, a decrease in the radial thickness of the neocortex was observed beginning at E13.5 and increasing in severity through E16.5 (when the lethality of the knock-out is complete). This change in thickness was especially severe in the SVZ and cortical plate. Decreased ßIII-tubulin and Tbr1 (markers of postmitotic neurons) staining, coupled with no changes in cell death in these regions, suggests that *Insm1* may function in the generation of cortical neurons from BPs. Mitotic BPs, identified by PH3 expression, were decreased, while mitotic APs were slightly though not significantly increased throughout. A concurrent increase in the thickness of the VZ was observed to be coupled with increased mitotic cells in the VZ. The increased mitotic VZ cells led to both a radial and a lateral expansion of the VZ, and suggests that in the absence of Insm1, genesis of BPs from APs is impaired. This impairment in BP genesis results in both more total cells and more cycling cells in the VZ, and an impairment of SVZ formation, expansion, and subsequent neurogenesis.

FPE of *Insm1* was induced by electroporating VZ neuroepithelial cells of E10.5 ex-utero embryos with a plasmid driving constitutive *Insm1* expression. Whole-embryos were cultured for 24 hours, resulting in about 1/3 of neuroepithelial cells expressing Insm1. In cells with FPE of *Insm1*, basal mitoses increased more than 2-fold, and apical mitoses decreased by more than half. Double labeling experiments in conjunction with Insm1 FPE showed an increase in cell cycle length in the VZ. S-phase incorporation of the thymidine analog BrdU was decreased by 20% in

Insm1 FPE cells, with no accumulation of the early neurogenic marker, ßIII-tubulin, to suggest that these cells had exited the cell cycle. Additional experiments determined that 90% of the *Insm1* FPE cells in the VZ remained positive for the cell proliferation marker Pcna, indicating that these cells remained in the cell cycle. The increase in basal mitoses after *Insm1* FPE produced cells which expressed *Tbr1*, similarly to cells produced by normal basal mitoses in later development. However, expression of the panneurogenic marker *Tis21* was not observed in the majority of these induced basal mitoses, indicating that while FPE of *Insm1* is sufficient to induce *Tbr1* expression, it is not sufficient to induce *Tis21* expression. Taken together, this suggests that *Insm1* can induce basal mitoses, but in the absence of other still unknown factors, this results in the generation of additional BPs, which then self-amplify at the expense of generating neurogenic progenitor cells [97].

1.3.4.3 Two functions for Insm1 in the sympatho-adrenal system

Sympatho-adrenal precursors are derived from neural crest cells. These precursors, which all express Insm1 at E10.5, eventually give rise to the secondary sympathetic ganglia, the chromaffin cells of the adrenal medulla and extra-adrenal chromaffin tissues [116-118]. A common set of genes has been identified for both the differentiation of sympatho-adrenal precursors, sympathetic neurons, and chromaffin cells, and for catecholamine biosynthesis by these cell types [118, 119]. Initial migration and differentiation of neural crest cells leads to the formation of the primary sympathetic ganglion chain [117, 120, 121]. Initiation of differentiation, as well as early maturation, of these cell types requires expression of an array of transcriptional factors, including *Phox2b*, *Mash1*/*Ascl1*, *Hand 2*, and *Gata2/3*, as well as a number of pan-neuronal factors (Figure 1.3C and reviewed in [122]). At E12.5, a subset of sympatho-adrenal cells migrate to the anlage of the adrenal gland, and at E14.5 begin to differentiate into chromaffin cells.

The function of Insm1 in the developing sympatho-adrenal system was examined in a third study using the same knock-out line described above. In the absence of *Insm1*, differentiation of sympatho-adrenal precursors that go on to form the secondary sympathetic ganglia was determined to initiate correctly, and proliferation at E10.5 was comparable to *Insm1* wild-type and heterozygous knock-out siblings. However, at both E11.5 and E12.5 proliferation rates were greatly decreased. Proliferation returned to normal by E14.5, but the size of the secondary sympathetic ganglia remained significantly smaller. Throughout, no changes in apoptosis were observed. Taken together, these studies suggest that in the secondary sympathetic ganglia, *Insm1* is primarily acting on proliferation of early progenitor cells. This starkly contrasts with functional data obtained for the chromaffin cells produced from the same sympatho-adrenal precursor population.

When *Insm1* expression was abolished, the number of chromaffin cells was similar at E14.5, but greatly decreased by E18.5. Analysis of proliferation, using BrdU, showed no changes in proliferation between E14.5 and E18.5. Instead, the 2.5-fold decrease in chromaffin cells was accounted for by a concomitant increase in apoptosis. Additionally, terminal differentiation of the chromaffin cells was perturbed, with decreases in expression of catecholamine synthesis and chromogranin genes much greater than would be expected from a 2.5-fold reduction in chromaffin cells. These experiments implicate *Insm1* in differentiation, maturation and survival of the adrenal cells arising from the sympatho-adrenal lineage, with no apparent effect on the proliferation of precursors. In total, with Insm1 primarily affecting proliferation of sympathoadrenal precursors that produce the sympathetic ganglia (but not chromaffin cells), as well as enhancing the survival, differentiation and maturation of chromaffin cells (but not sympathetic ganglia), these experiments suggests distinct functions for *Insm1* in two populations arising from a single progenitor pool [101],

1.3.4.4 Insm1 in the specification of monoaminergic neurons of the hindbrain

Monoaminergic neurons are defined by their ability to produce one of several monoamine signaling molecules, including serotonin, dopamine, noradrenaline and adrenaline. As multiple subtypes of monoaminergic neurons arise from either a single progenitor pool, or a progenitor pool that also gives rise to other neuronal subtypes, the eventual neurotransmitter phenotype of these cells is intrinsically tied to both precursor cell fate determination and progenitor cell differentiation [122]. For example, although they arise from separate progenitor pools, all monoaminergic progenitor cells in the developing hindbrain are known to express *Ascl1* during their differentiation (Figure 1.3B). Similarly, despite arising from separate progenitor pools, both the central and peripheral nervous system's noradrenergic neurons express *Ascl1* during their development[99]. While this suggests that *Ascl1* is at the core of a regulatory program for all these cell types, the mechanism by which *Ascl1* confers identity is currently unknown.

Noradrenergic (NA) neurons are primarily observed in a single large nucleus, the locus coeruleus (LC). The LC arises from progenitors in the dorsal portion of the metencephalon. While additional NA neurons have been identified in scattered nuclei throughout the hindbrain, little is known about their development and specification. NA neurons are some of the earliest born brain neurons, and are generated between E9 and E10.5 in the mouse. While many of the genes identified in the specification of hindbrain NA neurons are similar to those identified in peripheral sympathetic neuron specification, the order of expression is distinct in the two cell populations.

In both peripheral and hindbrain NA neurons, BMP signaling directly regulates the expression of *Ascl1*. In the periphery, BMPs also induce expression of *Phox2b*. *Ascl1* and *Phox2b* in turn activate *Phox2a*, *Hand2* and *Gata3*, in a complex regulatory network with multiple cross-

regulatory actions, resulting in the eventual activation of catecholamine biosynthesis enzymes *dopamine-ß-hydroxylase* (*Dbh*) and *tyrosine hydroxylase* (*Th*). In the hindbrain, however, the BMP mediated induction of *Ascl1* is followed by *Ascl1* induction of *Phox2a*, *Phox2a* induction of *Phox2b*, and *Phox2b* induction of *Dbh* and *Th*. Additional, not yet identified factors are required for specification in both systems, and the exact interactions between factors remain unknown.

Insm1 gene expression in the neural hindbrain overlaps with both LC precursors and a subset of the ventral neuroepithelial progenitors, which will become the Visceral Motor (VM) and Serotonergic (5-HT) neurons. LC precursors at E10.5, are highly expressing *Insm1*. This expression was determined to overlap completely with that of *Phox2a*. However, by E11.5, *Insm1* expression had been greatly down regulated in these LC cells, while *Phox2a* expression remained high. By E12.5, these cells were determined to be highly differentiated, expressing both *Th* and *Dbh*, indicating that *Insm1* expression is transient, and lapses prior to NA neuron maturation.

When *Insm1* expression was abolished, using the knock-out described previously, the numbers of differentiated, *Th*-expressing cells were greatly reduced at both E10.5 and E12.5. However, this deficit was transient, as *Th*-positive cell number recovered by E16.5. No changes in *Ascl1*, *Phox2a/b*, *Dbh* or other LC differentiation markers were observed, and there did not appear to be a global delay in differentiation. Taken together, this indicates that *Ascl1* and *Insm1* act sequentially and not combinatorially on NA development in the hindbrain, and that together they act as core regulators of parallel biosynthesis pathways in NA neuronal development [99].

Serotonergic (5-HT), dopaminergic (DA), and (non-monoaminergic) visceral motor (VM) neurons arise from the ventral neuroepithelial progenitors near the floor plate. Initially, signaling by *Shh* specifies this progenitor cell subpopulation. The VM neurons are the first to

differentiate, followed by DA neurons (at E9.5 and E10 respectively). The first 5-HT neurons are detectable at E11.5, but are fully specified by E10.75[122]. The specification of 5-HT neurons is known to require expression of several different transcription factors depending on location. The ventral most progenitors require expression of *Nkx2.2*, while the dorsal nuclei require *Gata3*. Both populations of 5-HT neurons express *Pet1* after becoming post-mitotic. By E12.5, 5-HT neurogenesis is nearly complete[99]. The temporal mechanism and sequential gene expression profiles (though not the specific genes) underlying generation of these cell types is strikingly similar to that observed in the step-wise specification of the neural retina.

Initially expression of *Insm1* in the 5-HT progenitor cells of the hindbrain is seen at E9.5, overlapping completely with *Phox2b*, and partially with *Ascl1* and *Nkx2.2*. *Insm1* continues to be weakly expressed at E12.5 in 5-HT neurons. Pulse labeling experiments determined that *Insm1* expression occurs at or near the final S-phase of the progenitor cells. Inversely, *Ascl1* expression is observed only in cycling progenitors, and few cells are seen expressing both *Ascl1* and *Insm1*. ChIP studies determined that *Ascl1* directly binds the *Insm1* promoter. *Ascl1* has been shown to regulate multiple post-mitotic determinants of 5-HT cell fate, including *tryptophan hydroxylase* expression, despite being expressed only in cycling cells. This regulation was determined to require the interaction of *Ascl1* and *Insm1*[99].

In the absence of *Insm1*, the VM neurons differentiate normally, and ßIII-tubulin staining showed no changes in neurogenesis. However, *serotonin* levels were severely reduced in 5-HT neurons at E12.5, as were levels of multiple cell fate specification genes, including *Pet1* and *Lmx1b*. This suggests that *Insm1* acts in regulating both cell fate determination and serotonin biosynthesis. By E16.5 the aggregate nuclei were greatly reduced in size, but neither changes in specification gene expression nor changes in cell death were observed, in the absence of Insm1.

Taken together, these experiments indicate that *Insm1* and *Ascl1* are the core regulators of both 5-HT cell fate determination and serotonin biosynthesis.

1.3.4.5 Insm1 expression in the development of the olfactory epithelium

A second mouse strain, in which the entire *Insm1* locus is deleted (including both coding and noncoding sequences), was used to study to role of *Insm1* in the development of the olfactory epithelia. During normal development, the olfactory epithelium is divided into 2 regions, apical and basal, each containing a distinct population of cells. In the apical region are progenitors, which divide early to produce additional progenitors and later to form the sustentacular glia. A subset of the progenitors produced apically will migrate into the basal region, undergo a terminal, symmetric cell division, and produce neurons [123-125]. The molecular signatures defining these cell populations and the signals that drive the transition from proliferative to neurogenic and apical to basal are poorly understood.

Global deletion of *Insm1* resulted in no change in the total number of olfactory epithelia cells during embryonic development (from E12.5-E18.5). Additionally, no changes in apoptosis were observed, and both cell cycle length and number of cycling progenitor cells were consistent throughout development (Figure 1.3E). However an increase in the number of apical cells and a decrease in the number of basal cells was observed starting at E14.5. Coupled with an increase in apical mitoses and a decrease in basal (neurogenic) mitoses, this suggests that in the absence of *Insm1*, progenitors fail to migrate basally and therefore fail to undergo terminal neurogenic division to produce olfactory neurons.

Sequential labeling experiments showed that in the olfactory epithelium, similar to the Medaka optic tectum and retina, *Insm1* expression is limited to the basal progenitors during mitosis and intermediate cells (whether dividing or not), and expression is not observed in apical progenitors or mature neurons. This suggests that *Insm1* expression is activated in apical cells as

they are migrating to the basal region, preparing for their final mitotic division and beginning to differentiate [100].

1.3.4.6 INSM1 in human development

Human *INSM1* expression is seen in the developing spinal cord, dorsal root ganglia, hindbrain and midbrain as early as 37 days post ovulation (dpo). At 50-51 dpo, *INSM1* in the hindbrain is observed in the rhombic lip, in regions that will produce Purkinje cells in the cerebellum and granule cell precursors, as well as in the basal cells of the olfactory epithelium. At 56 dpo *INSM1* expression is limited to the basal edge of the cerebral cortex, including the ganglionic eminence, as well as to the thalamus and regions of the hindbrain. The pattern of expression within all these areas is similar to that observed in mouse development, with *INSM1* absent from the apical, rapidly proliferative cells near the ventricle, and from the basal, mature neurons, but present in a subset of either the intermediate progenitors or nascent neurons at the interface of these apical and basal cells [89].

1.3.5 Interactions of Insm1 with other cellular factors

Much of the study concerning *Insm1* activity has been focused on descriptive studies outlining the function of *Insm1* within specific tissues or determining genes regulated by Insm1 binding to their promoters. The latter of these have identified *Insm1* binding sites in the promoters of *Insulin*, *NeuroD*/ß2, and *Insm1* itself, and have described Insm1 primarily as a repressor of target genes [79, 85, 126, 127]. INSM1 has been shown to interact with CyclinD1 (CCND1), and through CCND1 with HDAC1 and HDAC3. This interaction leads to repression of targeted promoter regions [127]. Additionally, INSM1 also interacts with several spliceoforms of the SORBS1 gene (CAP2, CAP3, and CAP4) [80, 128]. CAP, an adaptor protein, is a known regulator of insulin-induced glucose transport, acting through the insulin receptor [129]. Interestingly, additional studies have shown that *INSM1* expression activates rather than

represses expression of other factors, including *Pax6* and *Nkx6.1* [130, 131]. While this could be the result of indirect activity on these promoters (through INSM1 repression of a repressor of *Pax6* or *Nkx6.1*), chromatin modification assays indicate that INSM1 alone enhances acetylation of histone H4 (compared with H3 acetylation by other known activators), leading to enhanced expression of target genes [130].

1.3.5.1 Insm1 and cell cycle regulation

Insm1 has been implicated in cell cycle regulation, through the ability of INSM1 to directly bind CCND1. The interaction of INSM1 and CCND1 was determined to occur through the N-terminal proline-rich region (amino acids 43-58). CCND1 is normally complexed with CDK4, which results in the activation of CDK4. Activated CDK4 phosphorylates the retinoblastoma protein (RB), causing the release of E2F and the activation of pro-cell cycle progression genes. When *INSM1* expression was induced in cultured cells (both Cos-7 and Panc-1), the levels of phosphorylated RB were dramatically reduced, compared to uninduced controls. Total RB levels were unchanged, suggesting that the induction of *INSM1* did not affect *RB* transcription, only RB phosphorylation. To determine the functional effect of this change in RB phosphorylation, cells were synchronized by serum starvation, with 80-90% in G_1/S phase. This was followed by activation with a serum pulse. In cells without *INSM1* induction, a significant portion of cells (up to 70%) had progressed to G_2/M phase within 24 hours. Induction of *INSM1* expression resulted in the majority of cells (80%) remaining in G_1/S phase. The cell cycle arrest was determined to be mediated through *INSM1* interference with CCND1/CDK4 interaction, as inducing additional expression of CCND1/CDK4 with Insm1 resulted in 60% of cells progressing to G_2/M. In a mouse model where Panc-1 cancer cells were implanted and allowed to produce tumors, induced *INSM1* expression was able to inhibit tumor growth by 70% compared to control tumors [132]. This is especially interesting, as *INSM1* expression has been shown to be activated in a number

of tumors. This might suggest that the induction of *INSM1* may be an attempt by these cancer cells to decrease or abolish improper proliferation, which ultimately fails, potentially as a result of mutation in RB or other factors within this regulatory cascade.

1.3.5.2 Insm1 and transdifferentiation

In cell culture, INSM1 expression was shown to result in the functional transdifferentiation of both an exocrine pancreatic acinar cell line (AR42J, originating from a rat pancreatic acinar adenocarcinoma) and a ductal cell population (Panc-1, originating from a human pancreatic carcinoma) into Insulin producing endocrine cells. While this transdifferentiation can be accomplished at low frequency (8% and 9.66% in AR42J and Panc-1 respectively) by expressing *INSM1* alone, transdifferentiation can be enhanced by co-expression of two additional Islet Transcription Factors (ITFs), *Pdx-1* and *NeuroD1* (25% and 19.75%) [130, 131]. While these transdifferentiated cells produce Insulin, they produce far less than normally derived mouse islet cells, with Insulin production from mouse islet cells over 400 fold greater than that produced by the transdifferentiated ductal cells [130]. The addition of induced expression of growth factors EGF and TGFß to the ITFs, greatly increased *Insulin* expression in the transdifferentiated acinar cells, though Insulin protein levels remained 100-fold lower than in mouse islet cells [131]. These studies provide additional consolidating evidence that *INSM1* acts to define pancreatic cell fate, but also suggest that the previously determined activity of *INSM1* as a transcriptional repressor is insufficient to explain the effect of *INSM1* in transdifferentiation. The ability of INSM1 to interact with growth factor signaling, especially in light of its known affinity for extra-nuclear regulators like CCND1, suggests a potential extra-nuclear role for INSM1.

1.3.5.3 Extra-nuclear function of Insm1

RACK1 is a cellular adaptor protein and Protein Kinase C receptor, which is known to interact with the IGF-1 receptor and the Insulin receptor and modulate their signaling activity. This modulation occurs through RACK1 inhibition of the PI3K pathway and subsequent decreases in AKT phosphorylation. Inversely, expression of *INSM1* in AR42J cells was shown to promote PI3K signaling and AKT phosphorylation. RACK1 and INSM1 were shown to interact, by yeast 2 hybrid assay and immunoprecipitation experiments. This interaction was determined by immunofluorescence experiments to be occurring in the extra-nuclear or cytoplasmic region of the cell, additional co-immunoprecipitations of cytoplasmic and nuclear fractions determined that INSM1 is physically associated with RACK1 in the cytoplasm only, and that RACK1 and INSM1 do not complex in the nucleus. The binding of RACK1 and INSM1 was determined to require the same proline-rich region as CCND1/INSM1 binding. To determine if the expression of INSM1 and subsequent increase in AKT phosphorylation was occurring as the result of INSM1 binding to RACK1 and removing the inhibition of PI3K signaling, cells were treated with a PI3K inhibitor and AKT phosphorylation was tested. Phosphorylation of AKT was reduced in these cells even when *INSM1* was expressed, indicating that PI3K is the pathway affected by the INSM1/RACK1 association [133].

Exogenous expression of *INSM1* also caused an increase in *NKX6.1* (Figure 1.3F). In vitro assays determined that this was not the result of direct activation of the *NKX6.1* promoter by INSM1. However, the levels of *NKX6.1* were directly correlated with the binding of RACK1 by INSM1, and to Insulin signal transduction. Interference with AKT phosphorylation by the inhibition of PI3K was unable to induce *NKX6.1*, suggesting no involvement of the PI3K pathway in this activity [133]. Together these experiments provide convincing evidence that INSM1 displays extra-nuclear activity, and that this activity can result in both changes in cell signaling,

and effect change on downstream gene expression separately without direct interaction with the affected promotor regions.

1.4 Rationale, Hypotheses and Specific Aims

The previously outlined experiments indicate several distinct functions for *Insm1* (Figure 1.3). With expression in a wide variety of tissues, from the pancreas to the brain to a large array of tumors, *Insm1* has been shown to directly repress transcription of multiple distinct promoter regions, as well as to engage in both nuclear and non-nuclear associations with regulators of cell cycle progression and cell signaling. *Insm1* has been determined to be a pan-neuronal marker, required for the specification of a subset of sympathetic neurons, as well as to act in the expansion of pools of progenitor cells in the adrenal system. It can direct the transdifferentiation of ductal and exocrine cells into Insulin producing cells and affect histone acetylation. The exact mechanisms of some of these activities have been determined, but there remain many open questions. Perhaps the most interesting here is: what is the function of *Insm1* in the retina? Touched upon lightly only in descriptive experiments, the function of *Insm1* in the retina remains a black box, waiting to be explored.

The aim of this dissertation was to determine the function of Insm1 in retinal cell proliferation and neurogenesis. The initial hypothesis was that Insm1 was required for rod PRC differentiation, specifically that Insm1 functions initially to bias a population of retinal progenitor cells toward a photoreceptor cell fate, and in later development acts to affect cell cycle exit and cell differentiation. Presented here is evidence supporting the requirement for Insm1 during both rod and cone PRC differentiation. Separately, we have shown a requirement for Insm1 in regulating cell cycle kinetics of retinal progenitor cells.

This work will be laid out in the following aims:

Specific Aims

I. Characterize the expression pattern of Insm1 in the developing retina.
    a. Using in situ hybridization, describe the expression of *Insm1a*, the retinal expressed zebrafish co-ortholog of mammalian *Insm1*

II. Characterize the effects of *Insm1* misexpression in the developing retina at the cellular and molecular level.
    a. Using morpholino mediated knockdown and mRNA overexpression, determine the function of *insm1a* in zebrafish retinal development.
        i. Comparison of *insm1a* morphant and control retinas using immunohistochemistry for cell identity and morphology.
        ii. Examination of cell cycle kinetics when *insm1a* is perturbed.

III. Identify molecular targets of Insm1 in the retina and place Insm1 within the photoreceptor cell transcriptional regulatory network.
    a. Using a candidate gene approach, identify genes with variable expression in the retina when *insm1a* is knocked down. Determine changes in expression using in situ hybridization and quantitative PCR.
    b. Using an unbiased approach, RNA-seq, identify genes with variable expression in the developing retina of the Insm1 knockout mouse. Validate a subset of the genes identified.

IV. Creation and characterization of *insm1a* mutants
    a. Determine the photoreceptor specific phenotype of the *insm1a_K141X* mutant using immunohistochemistry.
    b. Evaluate 3 *insm1a* variants for ability to rescue the *insm1a* morphant phenotype.

Aims I, II, and IIIa and are included in Chapter 2.

Aim IV is included in Chapter 3.

Aim IIIb is included in Chapter 4.

Chapter 1 Figures:

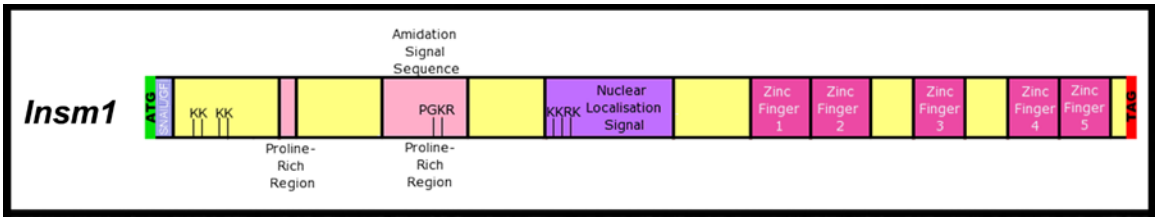

Figure 1.1: Schematic of Insm1

The single exon Insm1 gene encodes a peptide containing an N-terminal SNAIL/GFI (SNAG) domain (blue), a putative nuclear localization signal sequence (purple) and 5 C-terminal Zinc Finger DNA binding motifs (magenta). Two Proline-rich regions (pink) have been identified as protein-protein interaction sites.

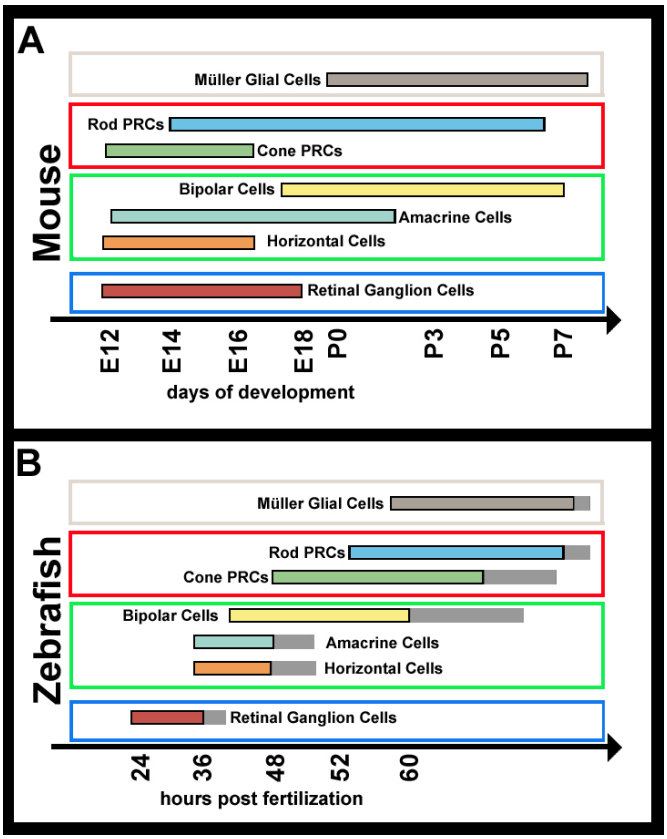

Figure 1.2 Timing of retinal neurogenesis in the mouse and zebrafish

In many species, including the mouse and the zebrafish, birth order for retinal neurons is highly conserved. The first cells to begin differentiating are the RGCs, while the last are the Müller glia. **A.** In the mouse, RGCs begin to differentiate at E12. Differentiation of the horizontal and amacrine cells in the INL and cone PRCs in the ONL begins shortly thereafter. Rod PRC differentiation begins near E14, and is a protracted event, lasting well into the postnatal period. Bipolar cells differentiate during late embryonic development and through the first week after birth, while onset of Müller glia differentiation occurs near birth. **B.** Differentiation of the zebrafish RGCs begins near 24 hpf, and is largely completed prior to the onset of amacrine and horizontal cell differentiation at 36 hpf. Bipolar cells begin to differentiation at 40 hpf, followed by cone PRC differentiation at 48hpf. Rod PRCs are observed beginning at 55 hpf and Müller glia near 60 hpf. (RGC, retinal ganglion cell; E12, embryonic day 12; INL, inner nuclear layer; PRC, photoreceptor cells; E14, embryonic day 14 ONL, outer nuclear layer; hpf, hours post fertilization)

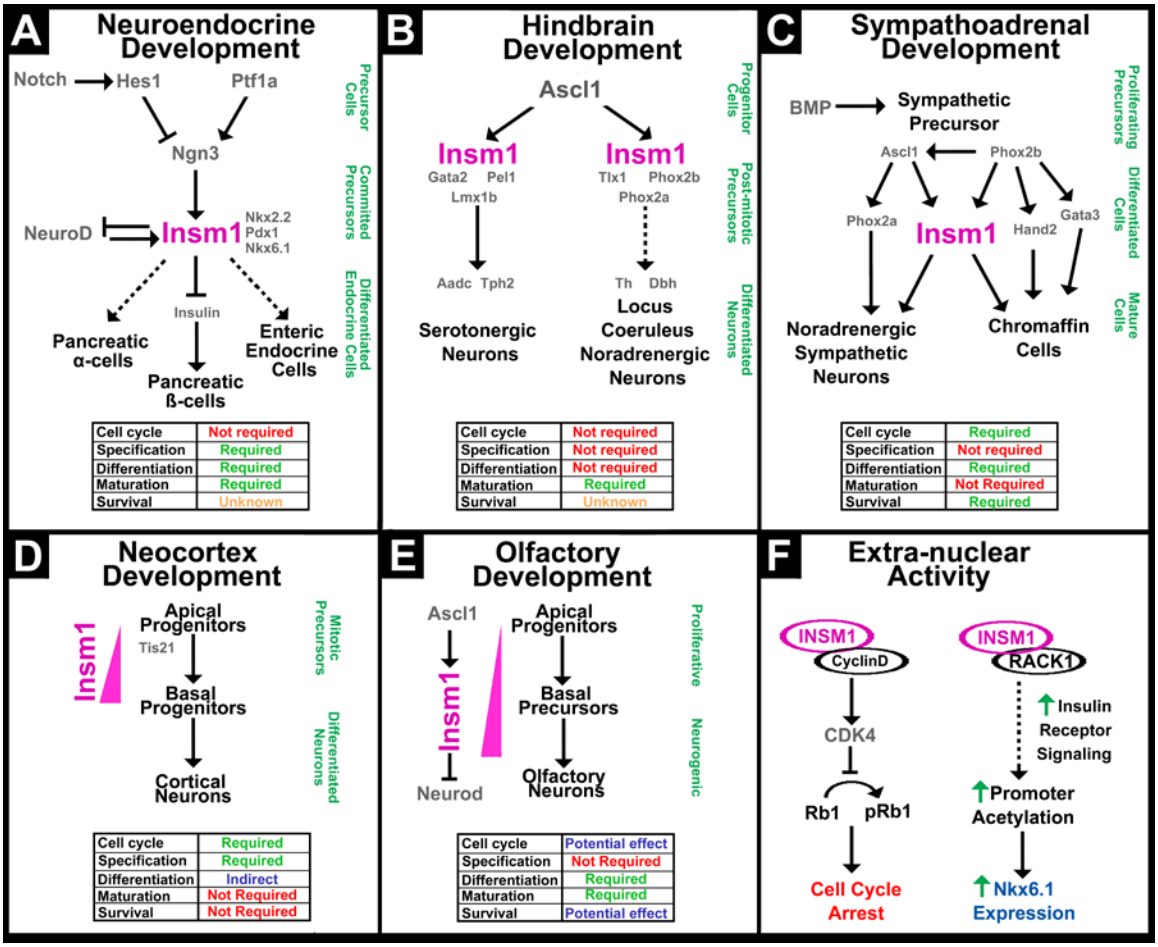

Figure 1.3: Insm1 activity is highly variable

A. In neuroendocrine development, Insm1 is downstream of Notch signaling, and is required for specification, differentiation and maturation of pancreatic ß-cells and enteric endocrine cells. Timing and maturation of pancreatic α-cells is also Insm1 dependent. **B.** In the developing hindbrain, Insm1 expression is downstream of Ascl1, and acts through multiple intermediaries (including Gata2, Phox2a, and Tlx1) to drive maturation of serotonergic, and noradrenergic neurons and neurons of the locus coeruleus. Insm1 is not required for proliferation, specification or differentiation in the hindbrain. **C.** In the developing sympathoadrenal system, Insm1 expression is downstream of BMP signaling, and a complex web of Insm1 interactions have been shown to regulate progenitor proliferation, terminal differentiation and survival of mature cells, but not to affect progenitor specification or maturation. **D.** During neocortical development, increasing Insm1 expression drives apical progenitors towards a basal cell fate, and Insm1 has been implicated in affecting proliferation through cell cycle length, and precursor specification and differentiation through both direct and indirect transcription factor activity. **E.**

Figure 1.3: Insm1 activity is highly variable (continued)

Olfactory development, like neocortical development depends heavily on the apical to basal transition of progenitor cells. Unlike in the neocortex, olfactory progenitors remain mitotic after undergoing the basal transition. Insm1 expression increases as cells prepare to shift basally, and remains high until the olfactory neurons are mature. Although Insm1 is not required for specification of these cells, it is essential in differentiation and maturation of the olfactory neurons, and may also affect cell cycle exit and cell survival. **F.** In addition to binding promoter regions and regulating downstream gene expression, Insm1 has also been shown to affect cell cycle and gene expression through extra-nuclear protein-protein interactions. Insm1 competitively binds CyclinD, interrupting the CyclinD/CDK4 association. This induces hypophosphorylation of the Rb1 protein, and leads to cell cycle arrest. Separately, Insm1 binding to Rack1 results in an increase in Insulin Receptor-mediated signaling, which results in increased acetylation of the Nkx6.1 promoter, and increases in Nxk6.1 expression. Both of these interactions have been shown to occur in the absence of nuclear localization and/or Insm1 association with DNA, clearly showing Insm1 activity in the absence of direct Insm1 transcriptional regulation.

CHAPTER 2: INSULINOMA-ASSOCIATED 1A (INSM1A) IS REQUIRED FOR PHOTORECEPTOR DIFFERENTIATION IN THE ZEBRAFISH RETINA

Marie A. Forbes-Osborne[1], Stephen G. Wilson[1], and Ann C. Morris[1]*

[1]Department of Biology, University of Kentucky, Lexington, KY 40506-0225

Key words: Insm1, photoreceptor, retinal development, cell cycle, zebrafish
Reprinted from: *Developmental Biology* 380(2): 157-171. (doi: 10.1016/j.ydbio.2013.05.021), Forbes-Osborne MA, Wilson SG, Morris AC. Insulinoma-associated 1a (Insm1a) is required for photoreceptor differentiation in the zebrafish retina, Pages 157-171, 2013. With permission from Elsevier.
N.B. For this dissertation, figure numbers, headings, and text were modified to match dissertation style; Supplemental Figures 2.S2 and 2.S3 were added.

2.1 Abstract

The zinc-finger transcription factor Insulinoma-associated 1 (Insm1, previously IA-1) is expressed in the developing nervous and neuroendocrine systems, and is required for cell type specific differentiation. Expression of Insm1 is largely absent in the adult, although it is present in neurogenic regions of the adult brain and zebrafish retina. While expression of Insm1 has also been observed in the embryonic retina of numerous vertebrate species, its function during retinal development has remained unexplored. Here, we demonstrate that in the developing zebrafish retina, *insm1a* is required for photoreceptor differentiation. *Insm1a*-deficient embryos were microphthalmic and displayed defects in rod and cone photoreceptor differentiation. Rod photoreceptor cells were more sensitive to loss of *insm1a* expression than were cone photoreceptor cells. Additionally, we provide evidence that *insm1a* regulates cell cycle progression of retinoblasts, and functions upstream of the bHLH transcription factors *ath5* and *neurod,* and the photoreceptor specification genes *crx* and *nr2e3*. Finally, we show that *insm1a*

is negatively regulated by Notch-Delta signaling. Taken together, our data demonstrate that Insm1 influences neuronal subtype differentiation during retinal development.

HIGHLIGHTS

- *Insm1a* is expressed during zebrafish retinal development and in adult rod photoreceptor progenitors
- Insm1a is required for photoreceptor differentiation
- Insm1a regulates cell cycle progression of retinoblasts
- Insm1a functions upstream of subtype specification genes and downstream of Notch signaling

2.2 Introduction

The vertebrate retina is an excellent model for studies of cellular differentiation during nervous system development, because all seven retinal cell types (6 neuronal and 1 glial), develop from a single pool of multipotent retinal progenitor cells (RPCs), demonstrate a precise laminar arrangement, and are generated in a conserved order of histogenesis [134, 135]. In order for the diverse array of retinal cell types to be generated in the proper numbers and at the appropriate times, RPC proliferation, migration and differentiation are tightly controlled by cell-intrinsic factors and cell-extrinsic signals [2, 30, 136]. Much of the intrinsic regulation is accomplished by spatio-temporally controlled expression of cascades of transcription factors (TFs). These TFs in turn regulate expression of other TFs, cell cycle genes, cell-fate specification genes and other genes of unknown function [3]. Although several TFs essential for these processes have been identified, our knowledge of the molecular determinants of cell type differentiation in the vertebrate retina remains incomplete.

Insulinoma-associated 1 (Insm1, formerly IA-1) is an evolutionarily conserved zinc finger transcription factor, which was first identified from a tumor subtraction library [78]. Insm1 expression is restricted to the developing nervous and neuroendocrine systems [81], neurogenic regions in the adult brain [89], and tumors of neuroendocrine origin [81]. Although very few direct target genes have been identified, Insm1 has been shown to regulate transcription of insulin and *NeuroD* in the developing pancreas, where Insm1 is essential for beta cell development [96, 127, 137].

Insm1 has been implicated both in the regulation of cell cycle progression [86, 97, 101, 132] as well as in cell fate specification [98, 99, 127]. Additionally, recent studies have identified a role for Insm1 in acinar cell trans-differentiation in vivo [131] and in Müller glia de-differentiation in the adult zebrafish retina following injury [95]. In a previous study, we

demonstrated that a zebrafish ortholog of Insm1, *insm1a*, is expressed in the developing retina in a spatiotemporal pattern that mirrors the progression of neurogenesis, and that it is also expressed in rod photoreceptor progenitor cells in the adult zebrafish retina [94]. Together, these data suggest that Insm1 regulates subtype differentiation, especially of photoreceptors in the developing retina. However, the precise function of Insm1 in retinal development has not yet been directly examined, and the embryonic lethality of Insm1 null mice [98] has precluded more detailed studies of the role of on Insm1 during murine retinogenesis.

In this study, we have used morpholino-mediated gene knockdown in zebrafish to examine the role of *insm1a* during retinal development. We show that *insm1a* is required for the proper differentiation of rod and cone photoreceptors, and that *insm1a* regulates RPC cell cycle kinetics. Additionally, we establish that *insm1a* lies upstream of the bHLH transcription factors *ath5* and *neurod*, as well as the photoreceptor specification genes *crx* and *nr2e3*, whereas it lies downstream of and is negatively regulated by Notch-Delta signaling. Taken together, our results identify *insm1a* as a novel intrinsic regulator of neuronal subtype differentiation in the developing vertebrate retina.

2.3 Methods

2.3.1 Zebrafish lines and maintenance

Zebrafish were bred, raised and maintained in accordance with established protocols for zebrafish husbandry [138]. Embryos and larvae were housed at 28°C, on a 14 h light:10 h dark cycle. Fish were anaesthetized with Ethyl 3-aminobenzoate methanesulfonate salt (MS-222, Tricaine, Sigma-Aldrich, St. Louis, MO). Embryos were staged as previously described [62]. Wild-type strains included the Ekwill strain (Ekwill Fish Farm, Gibsonton, FL), the AB strain obtained from the Zebrafish International Research Center (ZIRC, Eugene, OR) and hybrids produced by

crossing the Ekwill and AB strains. The Tg (XRho: gap43-mCFP) q13 transgenic line, hereafter called XOPS-mCFP, has been previously described [69, 94]. This line harbors a fluorescent mCFP reporter transgene under the control of a 5.5 kb Xenopus rhodopsin promoter. Expression of this transgene results in selective degeneration of the rod photoreceptor cells [94, 139]. The Tg (3.2TαC-EGFP) transgenic line, hereafter called TαC-EGFP, has been previously described [140], and was generously provided by Susan Brockerhoff (University of Washington, Seattle WA). The Tg (nyx:GAL4-VP16)q16a/ (UAS:gap43-YFP)q16b transgenic line, hereafter referred to as nyx::YFP, and the Tg (XlRho:EGFP)fl1 transgenic line (hereafter called XOPS-GFP) have both been previously described [77, 141], and were obtained from James Fadool (Florida State University, Tallahassee, FL). The Tg (gfap:GFP)mi2001 transgenic line (hereafter called *gfap*:GFP) has been previously described [142], and was obtained from ZIRC. All animal procedures were carried out in accordance with guidelines established by the University of Kentucky Institutional Animal Care and Use Committee.

2.3.2 Microinjections of morpholinos and mRNA

A translation-blocking antisense morpholino (MO) designed against *insm1a* was injected into fertilized embryos prior to the second cell division. Two non-overlapping morpholino sequences were used: MO1 (5'-GGTTGAAATCAGAGGCACACCT-3') and MO2 (5'-CGCCAGCTGAAAGGCACTTCA-3'). Both produced similar phenotypes; unless otherwise indicated, MO1 was used for all analyses described in this study. The *insm1a* MO1 was injected at 6.0-7.2 ng/embryo and the *insm1a* MO2 was injected at 7.2ng/embryo. Since injection of MO1 caused some toxicity to the embryos, an antisense *tp53* morpholino (p53MO) was co-injected to suppress cell death [143]. The p53MO (5'-GCGCCATTGCTTTGCAAGAATTG-3') was injected at 1.5-fold the amount of the *insm1a* MO. A standard control MO, targeting a mutant

variant of the human β-globin gene (5'-CCTCTTACCTCAGTTACAATTTATA-3'), was injected similarly to the *insm1a* MO. All morpholinos were synthesized by GeneTools, LLC (Philomath, OR).

Capped mRNA was synthesized from a cloned *insm1a* coding sequence lacking the morpholino binding site using the mMessage (T7 or Sp6) Kit (Ambion, Austin, TX) according to the manufacturer's instructions. mRNA was cleaned by column purification (RNeasy kit, Qiagen, Valencia, CA), followed by phenol-chloroform extraction and ethanol precipitation.

All injected embryos were transferred to fish water containing 0.003% 1-phenyl-2-thiourea (PTU) at 24 hours post fertilization (hpf) to inhibit pigmentation. Injected embryos were immobilized in depression slides at 48 and 72 hpf for live imaging.

2.3.3 Testing morpholino effectiveness

A pair of complementary oligonucleotides corresponding to the *insm1a* morpholino target sequence (Table 2.1) were synthesized and purified by HPLC (Biosynthesis, Lewisville, TX). The oligos were designed to produce overhangs complimentary to the ends produced by enzyme digestion of the pEF1α:GFP plasmid (Addgene plasmid 11154). The oligos were resuspended in oligo annealing buffer (10mM Tris pH 7.52, 50mM NaCl, 1mM EDTA) at 100ng/µl, and 1µg of each oligo was combined into a 50µl annealing reaction. The annealing reaction was heated at 95°C for 2 minutes and cooled to 25°C over 45 minutes. The annealed oligos were diluted 10-fold, and 1µl was ligated with 100 ng of double-digested pEF1α:GFP plasmid.

Wild-type embryos at the one-cell stage were co-injected with 100pg/embryo of pEF1α-GFP containing the *insm1a* MO1 binding site (pEF1 [illegible]MOBS:GFP) and either the control or the *insm1a* morpholino. Embryos were then screened each day from 1 through 5 dpf for expression of GFP.

2.3.4 RNA isolation

RNA was isolated from adult retinas or whole embryos at selected developmental time points. Adults were euthanized by rapid cooling as previously described [144].The eyes were dissected; the sclera, choroid and lens were removed. Retinas were transferred to tubes containing an RNA Stabilizer (RNALater, Ambion/Applied Biosystems). RNA was collected from pooled retinas using TRIzol Reagent (Life Technologies, Invitrogen), following the manufacturer's protocol, then treated with RNAse-Free DNAse I (Roche, Indianapolis, IN) to remove genomic DNA. RNA was collected from pooled embryos following a similar purification protocol.

2.3.5 Reverse transcription and quantitative PCR

Approximately 500ng of RNA was reverse transcribed into cDNA (GoScript Reverse Transcriptase System, Promega, Madison, WI) according to the manufacturer's instructions. Quantitative PCR (qPCR) was performed on an iCycler iQ Real Time PCR Detection System (Bio-Rad, Hercules, CA) using detection of SYBR Green incorporation, according to the manufacturer's instructions. Primer sequences used in qPCR are given in Table 2.1. Statistical analysis of the qPCR data was completed using SAS 9.3 software.

2.3.6 Preparation of digoxigenin labeled riboprobes

Digoxigenin (DIG)-labeled antisense and sense riboprobes were prepared from a linearized plasmid containing a portion of the coding region of the gene of interest by in vitro transcription with T7 or SP6 polymerase using the an RNA labeling kit (Roche Applied Science, Indianapolis, IN) according to the manufacturer's instructions. The *insm1a* and *neurod* plasmids were prepared by cloning PCR products into the pGEM T-easy vector (Promega) and pCR-TOPO (Invitrogen), and have been previously described [94, 145]. The *nr2e3* and *crx* plasmids were generously provided by Yuk Fai Leung (Purdue University, West Lafayette. IN), and have been

previously described [146-148]. The *atoh7/ath5* plasmid was a generous gift from Brian Link (Medical College of Wisconsin, Milwaukee, WI). The *ath5* probe sequence was subcloned into pGEM-T easy vector for probe synthesis, and the expression pattern matched previously published data [149].

2.3.7 Whole mount in situ hybridizations

Embryos and larvae were collected as described above. Tissues were fixed overnight at 4°C in freshly prepared 4% paraformaldehyde (PFA) prepared in PBS pH 7.0. Samples were dehydrated and stored in 100% methanol at -20°C for a minimum of 24 hours. Tissues were rehydrated through a graded PBST series (PBS, 0.1% Tween-20) and permeabilized in proteinase K (20µg/ml in PBST). After washing in triethanolamine (0.1 M TEA), tissues were acetylated using acetic anhydride, washed in TEA and PBST and refixed in 4% PFA in PBS. After additional PBST washes, samples were prehybridized in hybridization buffer (50% formamide, 5X Saline Sodium Citrate Buffer (SSC), 5mg/ml torula (yeast) RNA, 50µg/ml heparin sulfate, 0.1% Tween-20) for a minimum of 2 hours at 60°C. Riboprobes were hybridized to the tissue overnight at 60°C at a final concentration of 2ng/ul in hybridization buffer. Samples were washed through a graded SSC series at 60°C and 70°C, and a graded PBST series at room temperature, before blocking for a minimum of 2 hours at 4°C in PBST containing 2% BSA and 2% sheep serum. Samples were incubated overnight at 4°C with an anti-DIG-AP antibody (Roche) diluted 1:2500 in blocking buffer. The following day, samples were washed for 2 hours with multiple changes of blocking buffer, and equilibrated in NTMT buffer (0.1M Tris pH 9.5, 0.05M $MgCl_2$, 0.1M NaCl, 0.1% Tween-20) before coloration with 4-Nitro blue tetrazolium (NBT; Roche) and 5-bromo-4-chloro-3-indolyl-phosphate, 4-toluidine salt (BCIP; Roche) in NTMT. Coloration was halted by washing

with a stop solution (PBS pH5.5, 1mM EDTA). Whole embryos or dissected eyes were imaged on an inverted microscope (Eclipse Ti-U; Nikon Instruments, Melville, NY), using a 40X objective.

2.3.8 Histology and immunohistochemistry

Adult retinas or whole embryos were collected as described above. Tissues were fixed overnight at 4°C in freshly prepared 4% PFA. For immunolabeling, fixed embryos were cryoprotected in 10% sucrose in PBS for at least 3 hours and in 30% sucrose overnight at 4°C. Samples were mounted in OCT Medium (Ted Pella, Redding, CA) and frozen on dry ice. Ten to 12µm sections were cut on a cryostat (Leica CM 1850, Leica Biosystems, Buffalo Grove, IL), mounted on gelatin-coated slides, and dried overnight at room temperature. Before immunolabeling, sections were rehydrated and postfixed in 1% PFA for 10 minutes at room temperature. After 2 washes in PBS, and 2 washes in PBST, sections were blocked in PBST containing 1% BSA for at least 30 minutes at room temperature. Slides were incubated with primary antibody in PBST/BSA with 5% Normal Goat serum, overnight at 4°C in a humidified chamber. The following day, slides were washed 3 times in PBST, and incubated with secondary antibody in PBST/BSA for 1 hour at room temperature in the dark. Slides were washed 2 times with PBST, counterstained with DAPI (4', 6-diamidino-2-phenylindole, 1:10,000 dilution; Sigma-Aldrich) in PBS, and mounted in 40% glycerol in PBS. Images were obtained on an inverted fluorescent microscope (Eclipse Ti-U; Nikon Instruments), using a 40X objective.

The following antibodies were used: Zpr-1 (1:20 dilution), a monoclonal antibody that recognizes red and green cones (ZIRC); 4C12 (1:100 dilution), a monoclonal antibody that recognizes an unknown epitope on rods (Fadool J, Linser, P unpublished; a generous gift of James Fadool, FSU, Tallahassee, FL); Zn-8 (1:10 dilution), a monoclonal antibody that recognizes retinal ganglion cells (ZIRC); 5E11 (1:10 dilution), a monoclonal antibody that labels amacrine

cells (generously provided by James Fadool, FSU, Tallahassee FL) , HuC/D (1:20 dilution), a monoclonal antibody that recognizes retinal ganglion cells and amacrine cells (Invitrogen, Grand Island, NY); anti-PKCα (H300), a polyclonal antibody that recognizes bipolar cells (Santa Cruz Biotechnology, Santa Cruz, CA); anti-Prox1 (1:2000 dilution) a polyclonal antibody that recognizes horizontal cells (Millipore, Billerica, MA); anti-BrdU (clone B-33; 1:500 dilution), a mouse monoclonal antibody that marks cells in S phase of the cell cycle (Sigma-Aldrich); and anti-phospho-Histone H3 (Ser10;1:500 dilution), a polyclonal antibody that recognizes cells in late G2/M-phase (Millipore). Alexa Fluor 488 goat anti-mouse, 488 goat anti-rabbit, 546 goat anti-rabbit, 546 goat anti-mouse (Molecular Probes, Invitrogen), 647 goat anti-rabbit and Cy5 conjugated goat anti-mouse (Jackson ImmunoResearch, West Grove, PA) secondary antibodies were all used at 1:200 dilution.

2.3.9 Morphometric analysis

Control and *insm1a* morphant embryos were positioned in depression slides and imaged on an inverted microscope (Eclipse Ti-U; Nikon Instruments), using 4X and 20X objectives. Measurements were taken using the Nikon Elements software. The 4X images were used to measure total body length from the otic vesicle to the tip of the tail following the line of the spinal column The 20X images were used to measure the area of the eye by outlining the entire eye and the lens. The exclusion or inclusion of lenses was statistically irrelevant ($p<0.0001$ both with and without inclusion of the lens area), and all statistics reported here include lens measurements. All measurements were taken in triplicate. Additional measurements were taken if the variation was greater than 5% across the three measurements. SAS 9.3 was used for all statistical analyses.

2.3.10 Cell counts

Immunolabeled control and *insm1a* morphant cryosections containing three distinct cell layers and a lens were used for cell counts. Cells were counted a minimum of 3 times, and counts were averaged for statistical analysis. SAS 9.3 was used for all statistical analyses.

2.3.11 BrdU injection and immunohistochemistry

For cell cycle analysis, 30 hpf control and *insm1a* morphant embryos were dechorionated, anesthetized with MS-222, and transferred to an agarose microinjection plate. A 10mM solution of BrdU (Sigma-Aldrich) was injected into the yolk. The embryos were returned to 28°C, and collected at 0.5 hours post injection (hpi), 2 hpi, 4 hpi and 6 hpi. These correspond to 30.5, 32, 34 and 36 hpf, respectively. The embryos were fixed and cryoprotected as described above, and 10µm transverse cryosections were taken through the head.

Sections were immunolabeled as described above, with the addition of incubation in 2N HCl for 30-40 minutes in at 37°C prior to blocking. Following incubation with the secondary antibody, slides were washed 2 times with PBST then equilibrated twice in 2X SSC buffer. The slides were treated with 100µg/ml RNAse A (Qiagen) in 2X SSC, counterstained with propidium iodide (1µg/ml; Invitrogen), washed 2 times in 1X PBS and mounted in 40% glycerol in PBS. Images were obtained on an inverted fluorescent microscope (Eclipse Ti-U; Nikon Instruments), using a 40X objective.

2.3.12 Dual luciferase assays

HEK293 cells were transfected with varying amounts of the pcDNA3 mammalian expression vector (Invitrogen) containing the zebrafish *her4* cDNA, the pGL3 Firefly Luciferase reporter vector (Promega) containing an *insm1a* promoter cloned upstream of the luciferase

gene, and the pRL-TK vector (Promega), containing the *Renilla luciferase* gene driven by a ubiquitous tyrosine kinase promoter (to control for transfection efficiency) using Fugene 6 (Promega), following the manufacturer's instructions. The total amount of transfected DNA was kept constant across transfections, and transfection experiments were repeated a minimum of 3 times. Between 24 and 36 hours after transfection, when cells were at least 80% confluent, Firefly and Renilla luciferase activity were measured using the Dual Glo Luciferase Assay System (Promega). Data was analyzed as follows: Firefly luciferase (FFLuc) was baselined using an untransfected control (UTC) sample (=FFLuc – UTC) and normalized using the Renilla luciferase (RLuc). The Relative Luciferase Activity (RLA) was calculated as (FFLuc-UTC)/RLuc). The RLA was compared between experimental and control transfections, and statistical significance was determined by ANOVA using SAS 9.3 software.

2.3.13 DAPT treatment

Pharmacological inhibition of Notch-Delta signaling in embryonic zebrafish was accomplished using N- [N- (3, 5-Difluorophenacetyl)-L-alanyl]-S-phenylglycine t-butyl ester (DAPT), a γ-secretase inhibitor that prevents proteolytic cleavage of the Notch intracellular domain from the cell membrane. Embryos were partially dechorionated and transferred to pre-warmed embryo medium containing 100 µM DAPT in 1% DMSO (carrier). Time-matched sibling embryos in embryo medium with 1% DMSO served as carrier controls. Embryos were treated from 10.5 hpf until 28 hpf, when embryos were collected and processed for whole mount in situ hybridization as described above.

2.4 Results

2.4.1 Insm1a is expressed in adult rod progenitor cells and in the developing retina

We previously demonstrated that in the wild-type adult zebrafish, *insm1a* expression is very low or absent in the central retina, although it is present in the persistently neurogenic ciliary marginal zone (CMZ) [94]. In contrast, expression of *insm1a* is strongly upregulated in presumptive rod progenitor cells in a zebrafish model of chronic rod photoreceptor degeneration and regeneration (XOPS-mCFP). Rod progenitor cells can be identified by their location at the base of the outer nuclear layer (ONL) in the central retina, and by their expression of markers of cell proliferation and rod photoreceptor cell fate commitment [69, 94, 139]. To confirm that *insm1a* is expressed in proliferating rod progenitor cells, in situ hybridization with an *insm1a* probe was performed on retinal sections from adult XOPS-mCFP zebrafish that had been exposed to BrdU for four hours, followed by immunohistochemistry to detect BrdU incorporation. In XOPS-mCFP retinas, *insm1a*-positive cells were observed at the base of the ONL, and most (but not all) of the *insm1a*-positive cells were also BrdU-positive (Figure 2.1A-C). These data confirm our previously published results showing that in XOPS-mCFP retinas *insm1a* expression co-localizes with the S-phase marker *pcna* [94], and demonstrate that *insm1a* is expressed in rod progenitor cells in the adult zebrafish retina.

Using whole mount in situ hybridization (WISH), the onset of *insm1a* expression was first detected in the ventro-nasal region of the developing retina between 24 and 28 hpf (Figure 2.1D), which coincides with the initiation of the retinal neurogenic wave in zebrafish [150, 151]. The expression of *insm1a* continued to track the progression of neurogenesis, expanding in a counterclockwise fashion to the dorso-nasal retina at 36 hpf (Figure 2.1E), and then to the dorso-temporal quadrant of the retina by 48 hpf. This counterclockwise progression of *insm1a* expression in the sagittal plane was accompanied by a shift in expression from the central to

peripheral retina in the transverse plane, which we have described previously [94]. By 72 hpf, when retinal neurogenesis is largely complete, expression of *insm1a* was absent from the central differentiated retina and was only observed adjacent to the proliferative marginal zone at the retinal periphery (Figure 2.1G and [94]). Zebrafish possess two co-orthologs of the mammalian Insm1 gene, *insm1a* and *insm1b*. We did not observe expression of *insm1b* in the developing retina at any stage (data not shown), which agrees with a previous developmental study [87]. Taken together, the developmental expression pattern of *insm1a* in the retina suggests that it functions during the window when retinal progenitor cells (RPCs) are exiting the cell cycle to begin differentiation.

2.4.2 Insm1a morphants display a specific reduction in eye size

To examine the function of *insm1a* in retinal development, two different translation-blocking morpholinos (MOs) were designed to specifically knock down *insm1a* expression. Splice-blocking morpholinos could not be used against *insm1a* because it is a single-exon gene. Both MOs produced similar phenotypes when injected into 1-cell-stage embryos (data not shown). MO1 was used for all subsequent analysis unless otherwise stated. A standard control morpholino was used to control for non-specific phenotypes resulting from the microinjection procedure. The effectiveness of the *insm1a* MO at blocking translation was evaluated by co-injecting the morpholino along with an EF1α-GFP plasmid containing the *insm1a* morpholino binding site (pEF1α-MOBS:GFP). We compared the numbers of GFP-positive embryos injected with pEF1α-MOBS:GFP and the standard control morpholino to those injected with pEF1α-MOBS:GFP and the *insm1a* morpholino (Supplementary Figure 2.S1). This experiment showed that the *insm1a* morpholino was highly efficient and its translation-blocking activity lasted through 4 dpf. Because some non-specific cell death was observed in embryos injected with

either of the *insm1a* MOs, in all subsequent analyses we co-injected the *insm1a* MO with a morpholino for *tp53*, which has been shown to block apoptosis [71]. Survival of morpholino-injected and uninjected embryos between 8 and 24 hpf was not significantly different (one way ANOVA Pr > F = 0.44) across *insm1a* morphants (76.7±10.7%), control morphants (84.6±17.5%) and uninjected embryos (81.9±21.3%).

Control and *insm1a* morpholino-injected embryos were categorized based upon their morphology and developmental stage at 24 hpf using standard staging criteria [62]. At 24 hpf, morphological markers (including the presence or absence of a beating heart) were scored to determine developmental stage, and any individuals with developmental delay were categorized as "severe". Nearly all embryos injected with the standard control morpholino (Figure 2.2A, B) were at the correct developmental stage at 24 hpf (98%) and showed no overt morphological changes (93%). Any injected embryos that displayed pulmonary edema or other defects (5%) were not used for further analysis. Among the *insm1a* morphants without developmental delay (90%), the body shape, head shape, and presence/absence of pulmonary edema were scored at 48 hpf, and the embryos were categorized as mild, moderate or severe. *Insm1a* morphants in the "mild" category displayed no developmental delay or overt morphological changes when compared to control morphants. This category represented a very small number of *insm1a* morphants (2%). *Insm1a* morphants in the "moderate" category (Figure 2.2C, D) were also at the correct developmental stage, but displayed mild body torqueing, with a spinal curvature. Moderate category *insm1a* morphants displayed no other malformations of the body, and had no pulmonary edema. This category represented the majority of the *insm1a* morphants (74%). *Insm1a* morphants categorized as "severe" displayed significant body torque, with malformations of the tail. *Insm1a* morphants with significant pulmonary edema or any

global delay in development were also categorized as severe (24%). For all subsequent analyses, only *insm1a* morphants in the moderate phenotypic category were examined.

Measurements of eye size at 48 hpf revealed a significant reduction in eye area in the *insm1a* morphants compared to controls (Figure 2.2E). To determine whether this reduction in eye area was the result of an overall reduction in the body size of *insm1a* morphant embryos, the ratio of eye area to body length was compared in control and *insm1a* morphants. This analysis demonstrated that eye area was significantly reduced in *insm1a* morphants even when expressed as a ratio of eye area to body length (Figure 2.2G). To rule out off-target effects as a cause of the decrease in eye area in *insm1a* morphants, we co-injected the *insm1a* morpholino with an *in vitro* transcribed *insm1a* mRNA lacking the morpholino binding site. Co-injection of *insm1a* mRNA significantly increased the eye area at 48 hpf compared to *insm1a* morpholino injection alone (88% of the control eye area versus 66-70%, data not shown) demonstrating that the eye size reduction observed in *insm1a* morphants was due to a specific knockdown of *insm1a*.

We did not observe an increase in TUNEL-positive cells in *insm1a* morphant retinas (data not shown), suggesting that the reduced eye size is unlikely to be the result of increased cell death. We also attempted to investigate whether over-expression of *insm1a* alone resulted in larger eyes than controls. We did not detect an increase in eye size at 48 hpf using a dosage of *insm1a* mRNA similar to that used for the morpholino rescue. However, we were unable to test higher amounts of *insm1a* mRNA, because these were toxic to the embryos.

2.4.3 Knockdown of insm1a significantly impairs photoreceptor differentiation

Because *insm1a* was previously shown to be expressed in rod progenitor cells in the adult retina we next investigated whether knockdown of *insm1a* altered rod photoreceptor

development in the embryonic retina. Retinal cryosections were prepared from control and *insm1a* morphants at 3 dpf, and the number of rod photoreceptors per section was counted using either immunohistochemistry for a rod photoreceptor-specific antibody (4C12; Figure 2.3), or by counting GFP-positive cells in a rod photoreceptor-specific transgenic reporter line [77]; not shown). Using either method, *insm1a* morphants displayed greatly reduced numbers of rod photoreceptor cells at 3 dpf (Figure 2.3B), with an average of 2.55 rods per section, compared with control morphants, which contained an average of 41.13 rods per section. This represents a 93.7% decrease in rod photoreceptors in *insm1a* morphants compared with controls. Additionally, several retinal sections from 3 dpf *insm1a* morphants contained no detectable rods. Similar to our observation of eye size described above, co-injection of *insm1a* mRNA along with the *insm1a* MO significantly increased the rod photoreceptor number to an average of 32.98 rods per section, demonstrating that the lack of rod photoreceptors in *insm1a* morphants is due to a specific knockdown of *insm1a*.

Because rod photoreceptors display a protracted period of differentiation relative to cone photoreceptors and other retinal neurons [16, 18], we sought to determine whether rod photoreceptor number in *insm1a* morphants remained significantly reduced one day later in development. Retinal cryosections from 4 dpf control larvae contained an average of 55.74 rods per section; in contrast, rod photoreceptor number remained significantly lower in 4 dpf *insm1a* morphant retinal sections (Figure 2.3D), with an average of 14.54 rods per section. Because the number of rod photoreceptors increased from 3 to 4 dpf in *insm1a* morphant retinas, it is possible that knockdown of *insm1a* does not cause a complete arrest in rod photoreceptor differentiation. Alternatively, the small increase in rods may be due to incomplete knockdown of *insm1a*, although our data indicate that the *insm1a* morpholino is highly efficient through 4 dpf (Supplementary Figure 2.S1). In any case, our observation that the number of rod

photoreceptors in *insm1a* morphants was significantly lower than controls at both 3 and 4 dpf, suggests that differentiation of proper numbers of rod photoreceptors requires *insm1a* expression. We did not count rod photoreceptor number at later developmental stages in *insm1a* morphants, because of the concern that at 5 dpf and beyond the morpholino may no longer be effective at blocking translation (Supplementary Figure 2.S1).

Next, we investigated whether cone photoreceptor cell number was affected by the knockdown of *insm1a.* Cone number was scored on retinal cryosections from control and *insm1a* morphants either by counting GFP-positive cones in a cone photoreceptor-specific transgenic reporter line (TαC-EGFP; [140]; Figure 2.3), or by immunolabeling with the red/green cone antibody Zpr-1 (not shown). Using either method, we observed that differentiated cone photoreceptors were significantly reduced in *insm1a* morphants (average of 12.0 cones/section) compared to controls (average 73.17 cones/section) at 3 dpf (Figure 2.3C). This phenotype was specifically caused by knockdown of *insm1a*, because co-injection of the *insm1a* morpholino with *insm1a* mRNA lacking the morpholino binding site was able to significantly rescue cone photoreceptor number (average 67.39 cones/section).

Interestingly, when this experiment was repeated at 4 dpf, we observed that unlike the rods, cone photoreceptor differentiation had substantially recovered in *insm1a* morphant retinas (Figure 2.3D). However, we noticed that while the cone photoreceptors appeared continuous and well packed in control retinas, the cone photoreceptor layer in 4 dpf *insm1a* morphant retinas contained visible gaps in some regions. The gaps in cone photoreceptors were categorized as small if they were only 1-2 cells wide (Figure 2.3D' arrowhead) and large if they were >5 cells wide (Figure 2.3D' arrow); these gaps were observed in nearly all *insm1a* morphant retinal sections examined at 4 dpf (23/25), whereas they were never observed in control retinal sections (0/28). The number of cone photoreceptor gaps observed in individual

insm1a morphant retinal sections ranged from zero to fifteen, with an average of 3.86 gaps per section. The absence of cones in these gaps was accompanied by the presence of cells from the inner nuclear layer (INL) that had "breached" the outer plexiform layer (OPL). Overall, these data suggest that *insm1a* knockdown delays cone photoreceptor differentiation in addition to causing impaired rod photoreceptor differentiation. The cones appear to be less sensitive to the lack of *insm1a* than the rods, because they are able to recover to near control levels by 4 dpf. Moreover, *insm1a* knockdown (and the resulting reduction in differentiated photoreceptors at 3 dpf) may affect the integrity of the OPL, allowing cells from the INL to migrate into the ONL as a consequence.

2.4.4 Effect of insm1a knockdown on other retinal cell types

Photoreceptor cells are relatively late-born neurons in the zebrafish [18]. Therefore, it is possible that the delay in rod and cone photoreceptor differentiation observed in *insm1a* morphants reflects a more general delay in the differentiation of later born retinal cell types. To determine whether this is the case, we evaluated differentiation of the Müller glia, another late-differentiating cell type [152, 153] in the zebrafish retina. We counted the number of GFP-positive Müller cells in control and *insm1a* morphant retinal sections at 3 dpf, using the *gfap*:GFP transgenic zebrafish line, which specifically labels Müller glia in the retina [142, 154, 155]. Although the Müller cell bodies in *insm1a* morphant retinas were slightly less well aligned in the INL compared to controls (data not shown), the number of Müller cells was not significantly different in the *insm1a* morphants compared to controls at 3 dpf (Figure 2.4). This result suggests that the reduced photoreceptor cell number in *insm1a* morphants is not the consequence of an overall delay in the differentiation of late-appearing retinal cell types.

While Müller glia cell number was not reduced in *insm1a* morphants relative to controls, it is possible that knockdown of *insm1a* causes a neuronal-specific delay in differentiation. To determine if this was the case we evaluated differentiation of the other classes of retinal neurons, starting with the bipolar cells. Bipolar cells in control and *insm1a* morphant retinal sections at 3 dpf were identified using the nyx::YFP transgenic zebrafish line, which labels ON-bipolar cells, in combination with immunolabeling for the bipolar cell marker PKCα. Bipolar cell counts revealed a modest reduction (by approximately 22%) in *insm1a* morphants compared to controls (Figure 2.4). Furthermore, we observed that the bipolar cell terminal boutons in the inner plexiform layer (IPL) were less mature in *insm1a* morphants when compared to controls, appearing thinner and less intensely stained (data not shown). We repeated this experiment at 4 dpf to determine if the bipolar cell numbers would recover in the *insm1a* morphants, as we had observed with the cone photoreceptors. Although we observed an increase in the number of bipolar cells in *insm1a* morphants from 3 to 4 dpf, we found that the number of bipolar cells remained modestly reduced relative to controls. For the most part, at 4 dpf the morphology of the bipolar cells in *insm1a* morphants appeared very similar to the controls, with well-stratified terminal boutons in the IPL and nicely staining dendritic terminals in the OPL (Figure 2.5). However, there were some regions of the OPL where the bipolar processes were disrupted. These regions corresponded to the areas in which cells from the INL had breached the OPL. Bipolar cell bodies were sometimes observed in the breaches, at the level of the OPL (Figure 2.5B, arrowhead). Staining with fluor-conjugated phalloidin revealed that these OPL breaches lacked all neuronal processes (Figure 2.5B). Overall, these data suggest that a loss of *insm1a* causes a modest reduction in bipolar cell number, a delay in bipolar cell maturation, and compromises the integrity of the OPL.

Because the OPL was disrupted in some regions of the *insm1a* morphant retinas, we wondered whether this would affect the differentiation of horizontal cells, which are located directly adjacent to the OPL. To evaluate horizontal cell differentiation we immunolabeled retinal sections with the Prox1 antibody, which recognizes horizontal cells and precursors of horizontal, amacrine and bipolar cells. Mature horizontal cells could be distinguished from other Prox1-positive cells by their location (directly abutting the OPL) and the elongated, flattened morphology of their cell bodies. We observed that in 4 dpf *insm1a* morphant retinal sections, Prox1-positive cells were either absent at the OPL or lacked a mature horizontal cell morphology. In *insm1a* morphants, the Prox1-positive cells that were found near the OPL were rounder and more widely spaced than in the control embryos (Figure 2.5C, D). Interestingly, in regions of retinal sections where cone photoreceptors were present, we observed some Prox1-positive cells with a more mature horizontal cell morphology located directly adjacent to the cones (Figure 2.5D, arrows). However, even these cells were more widely spaced, rounder, and less well aligned with the border of the OPL than horizontal cells in sections from control retinas. Moreover, similar to our observation of bipolar cells, we found that at 4 dpf, some of the regions of the ONL where the OPL was disrupted contained Prox1-positive cells, indicating that cells from the INL had extended into the ONL (Figure 2.5D, arrowheads). Taken together, these data suggest that the knockdown of *insm1a* causes a delay in the maturation of the horizontal cells, perhaps as an indirect consequence of the delay in photoreceptor differentiation.

Although the OPL of *insm1a* morphants was disrupted in some areas, the rest of the *insm1a* morphant retina appeared nicely laminated and well organized. By DAPI staining, both the INL and the ganglion cell layer (GCL) in *insm1a* morphants appeared qualitatively similar to control retinas at 3 and 4 dpf. To determine if ganglion and amacrine cell differentiation was quantitatively altered after *insm1a* knockdown, we immunolabeled control and *insm1a*

morphant retinal sections with the HuC/D antibody, which labels the cell bodies of amacrine and ganglion cells. At both 3 and 4 dpf HuC/D-positive amacrine cells in the inner half of the INL appeared qualitatively similar in control and *insm1a* morphant retinal sections (data not shown). When we counted the number of HuC/D-positive cells in the INL, no significant difference was observed between control and *insm1a* morphants at 3 dpf (Figure 2.4). However, when HuC/D-positive cells in the GCL (which may include displaced amacrine cells as well as ganglion cells), were counted, we observed a 32.8% reduction in *insm1a* morphants compared to controls at 3 dpf (Figure 2.4). Interestingly, the number of HuC/D-positive cells in *insm1a* morphants did not significantly increase between 3 and 4 dpf (data not shown), which suggests that the reduced number of HuC/D-positive cells in *insm1a* morphants is not caused by a delay in differentiation.

2.4.5 Insm1a knockdown increases cell cycle length

Previous studies have shown that Insm1 physically interacts with cell cycle regulatory proteins [127, 132]. Therefore, one explanation for the reduced eye area and decrease in differentiated cell numbers in *insm1a* morphants is that loss of Insm1a results in a change in retinoblast cell cycle kinetics. To determine if cell cycle length was altered in *insm1a* morphants, the thymidine analog BrdU was injected into the yolk of 30 hpf control and morphant embryos. Embryos were collected at 0.5, 2, 4 and 6 hours post BrdU injection (hpi). Retinal cryosections were immunolabeled with anti-BrdU to label cells that were in S phase during the BrdU exposure window, and with anti-phosphohistone H3 (PH3), to mark cells that were in late G2/M phase at the time of collection.

At all time points, there were fewer BrdU-positive cells in *insm1a* morphant retinas compared to controls (Figure 2.6B). At 0.5 hpi (30.5 hpf), control sections contained numerous areas of BrdU-positive cells spanning the retina from the basal to apical surface; in contrast, the

insm1a morphants had fewer BrdU-positive cells at the apical side of the retina (Figure 2.6A). Additionally, at 2 hpi (32 hpf), *insm1a* morphants contained fewer BrdU-negative cells at the basal surface when compared with controls (Figure 2.6A), indicating a delay in cell cycle exit of retinal progenitors at this time. At 2, 4, and 6 hpi the number of PH3-positive cells was also reduced in *insm1a* morphants compared to controls (Figure 2.6C). Expressing the BrdU and PH3 cell counts from *insm1a* morphant retinal sections at 6 hpi as a percentage of the equivalent cell counts from control retinal sections revealed an approximate 50% and 65% reduction in the number of BrdU-positive and PH3-positive cells, respectively (Figure 2.6E). We noted that PH3-positive cells were observed only at the apical surface in both *insm1a* morphants and controls, indicating that knockdown of *insm1a* did not affect the location of mitoses in morphant retinas.

Although the altered pattern of BrdU incorporation in *insm1a* morphant retinas suggested a change in cell cycle kinetics, an alternative explanation is that knockdown of *insm1a* resulted in a reduction in the size of the optic primordia, which could explain the smaller eye and the reduced numbers of S- and G2/M-phase cells observed in *insm1a* morphant retinas compared to controls. To determine whether cell cycle length was altered in *insm1a* morphants, we tracked the proportion of cells that had traversed S phase and progressed into G2/M during the period of BrdU exposure. This metric, referred to as "percent labeled mitoses" [156] was calculated as follows:

$$\%\ labeled\ mitoses\ (\%LM) = \frac{PH3^{+}BrdU^{+}}{PH3^{+}}$$

The %LM should rise over time, as more cells complete S phase and progress to G2/M. Indeed, we observed that in both control and *insm1a* morphant retinas, the %LM increased over the time course of the BrdU pulse, demonstrating that knockdown of *insm1a* did not cause a complete arrest in progression from S to G2/M phase. However, the %LM was significantly reduced in *insm1a* morphants when compared to controls at 0.5, 2, and 6 hpi (Figure 2.6D). This

suggests that *insm1a* morphant retinal progenitors made the transition from S to G2/M more slowly than in controls. Taken together, these data indicate that the knockdown of *insm1a* causes a delay in cell cycle exit, due at least in part to an increase in the transition time from S-phase to G2/M-phase.

2.4.6 Insm1a acts upstream of the bHLH TFs Ath5 and Neurod

In the retina, as in other regions of the central nervous system, the precise coordination of cell cycle exit with cell fate specification is essential for generating the correct proportions of different cell types in the appropriate order. Because we observed changes in both cell cycle progression and neuronal differentiation in *insm1a* morphants, we next examined whether knockdown of *insm1a* altered expression of transcription factors known to regulate cell fate specification in the retina. Ath5/atoh7 is a basic helix-loop-helix (bHLH) transcription factor expressed during or after the terminal division of a subset of retinal progenitor cells [157-159]. In both zebrafish and mice mutant for *ath5*, retinal ganglion cells (RGCs) fail to differentiate [23, 158]. Interestingly, overexpression studies in the chick and lineage tracing studies in mouse suggest that *ath5* also contributes to the photoreceptor cell lineage [160, 161]. We examined the expression of *ath5* in control and *insm1a* morphants by WISH. At 33 hpf, control retinas displayed the expected circular fan-like pattern of strong *ath5* expression; in contrast, in *insm1a* morphant retinas expression of *ath5* was observed in a small patch of cells in the ventro-nasal retina, the location of initiation of *ath5* expression (Figure 2.7A). At 48 hpf, the peak of *ath5* expression had passed in control retinas and was confined to a subset of cells within the GCL. However, in *insm1a* morphant retinas *ath5* expression had spread throughout the inner retina, in a pattern that closely resembled the control retinas at 33 hpf (Figure 2.7A). Although the *ath5* probe signal appeared more intense in 48 hpf *insm1a* morphants than in controls, no significant

difference in transcript abundance was detected by quantitative RT-PCR (data not shown). This could be due to inter-embryo variability in *ath5* expression following *insm1a* knockdown. Overall, these data indicate that *insm1a* is required for proper developmental timing, but not the maintenance or patterning of *ath5* expression.

Neurod is another bHLH-transcription factor with known roles in cell cycle regulation, cell fate determination, and cellular differentiation [162]. In the developing zebrafish retina, Neurod promotes photoreceptor progenitor cell exit from the cell cycle, and may regulate early cone maturation [163]. In the differentiated zebrafish retina, *neurod* is expressed in amacrine cells, nascent cone photoreceptors near the retinal margin, and in progenitors of the rod lineage [147]. Additionally, Insm1 has been shown to regulate and be regulated by Neurod during mammalian pancreatic development [127]. To determine if Insm1a acts upstream of Neurod in the retina, we examined *neurod* expression using WISH. In control retinas at 48 hpf we observed a strong band of *neurod* expression in the developing photoreceptors in the ONL, and less intense *neurod* expression throughout the INL. In contrast, in *insm1a* morphant retinas expression was observed in a small patch of cells in the ventro-nasal retina, and diffusely in groups of cells scattered throughout the rest of the retina (Figure 2.7B). Interestingly, while *neurod* expression was decreased in the retinas of *insm1a* morphants, expression was strongly induced in the olfactory epithelium of *insm1a* morphants (Figure 2.7B, arrowheads). At 72 hpf, *neurod* expression in *insm1a* morphants appeared to have recovered such that it was qualitatively similar to controls, with expression observed in the ONL (Figure 2.7B, black bracket) and in the inner portion of the INL (Figure 2.7B, blue bracket). Taken together, these results suggest that *insm1a* is required for the proper timing, but not maintenance, of *neurod* expression in the developing retina. Moreover, since our results indicate that *insm1a* inhibits

neurod expression in the developing olfactory system but not in the retina, the genetic interaction between *insm1a* and *neurod* is likely to be context dependent.

2.4.7 Insm1a is required for proper temporal expression of photoreceptor-specific TFs

Because *insm1a* knockdown produced the most significant effects on the differentiation of rod and cone photoreceptors, we next sought to determine whether *insm1a* is required for the proper expression of TFs that specify photoreceptor cell fate. We first focused on the homeobox transcription factor *Crx*. *Crx* is expressed in late stage retinal progenitors just prior to differentiation, as well as in post-mitotic differentiated photoreceptor cells (both rods and cones) and in a subset of cells in the INL [164, 165]. *Crx* has been shown to directly bind and transactivate photoreceptor-specific genes in vitro [166, 167], as well as to regulate photoreceptor differentiation in vivo [168]. Knockdown of *crx* results in a dramatic decrease in photoreceptor-specific gene expression [168-170], and delayed cell cycle exit [165].

In control retinas at 48 hpf, *crx* was very strongly expressed in the developing ONL, and weakly in some cells of the INL. In 48 hpf *insm1a* morphant retinas however, *crx* was only strongly expressed in the ventro-nasal retina, with expression decreasing in a counterclockwise fashion across the rest of the retina (Figure 2.8A). Quantitative RT-PCR at 48 hpf confirmed that *crx* expression was reduced in *insm1a* morphants (by 2.7-fold) relative to controls (Figure 2.8C). By 72 hpf, *crx* expression in *insm1a* morphants and controls appeared qualitatively similar by WISH, with expression primarily in the ONL (Figure 2.8A). Thus, we conclude that the very low expression of *crx* at 48 hpf at least partially contributes to the reduced numbers of differentiated rod and cone photoreceptors in 3 dpf *insm1a* morphant retinas. Likewise, the recovery of cone photoreceptor differentiation we observed at 4 dpf in the *insm1a* morphants may be a consequence of the rebound in *crx* expression at 72 hpf.

To determine whether knockdown of *insm1a* alters rod photoreceptor specification, we examined the expression pattern of the rod-specific factor Nr2e3 in control and *insm1a* morphant retinas by WISH and quantitative RT-PCR. Nr2e3 is an orphan nuclear receptor expressed transiently in all developing photoreceptors in zebrafish, later becoming restricted to rod precursors and rod photoreceptors [145, 146, 171]. Nr2e3 binding sites have been shown to mediate both activation of rod-specific genes [172] and repression of cone-specific genes [146] in rod photoreceptor cells. Mutation of nr2e3 results in accumulation of cone-specific transcripts in S-cones, and progressive photoreceptor degeneration in the *rd7* mouse [172, 173]. In control retinas at 48 hpf, *nr2e3* was expressed in nascent photoreceptors in the developing ONL, as well as in scattered cells in the distal half of the INL, consistent with its previously described expression pattern (Figure 2.8B; [146, 171, 174]). In contrast, *nr2e3* expression was reduced to varying degrees in *insm1a* morphants at 48 hpf relative to controls. Approximately half of the *insm1a* morphant retinas displayed scattered *nr2e3* expression in the outer half of the INL and in a few cells of the ONL. However, in the remaining *insm1a* morphant retinas, expression of *nr2e3* was observed only in the ventro-nasal patch region of the retina (Figure 2.8B). Quantitative RT-PCR analysis confirmed that *nr2e3* expression was reduced (by 4.6-fold) in *insm1a* morphants relative to controls at 48 hpf (Figure 2.8C). By 72 hpf, *nr2e3* expression was confined to the photoreceptors in the ONL of controls retinas, as has been described previously [146, 171, 174]. Interestingly, *nr2e3* expression was also detectable in the ONL of i*nsm1a* morphant retinas at 72 hpf, although the expression pattern was less contiguous and not as intense as in controls (Figure 2.8B). Therefore, these data suggest that the loss of *insm1a* delays rod photoreceptor specification during retinal development. The partial recovery of *nr2e3* expression in *insm1a* morphants at 72 hpf could explain the small increase in rod photoreceptor number we observed at 4 dpf compared to 3 dpf. However, given that rod

photoreceptors remain significantly reduced relative to controls in 4 dpf *insm1a* morphants, it is likely that the increase in *nr2e3* expression is not sufficient to completely rescue rod photoreceptor development. Alternatively, the partial reduction in *nr2e3* expression at 72 hpf may be compounded by reductions in *nr2e3* interaction partners [172], producing an additive effect on rod photoreceptor differentiation in *insm1a* morphants.

2.4.8 Notch-Delta signaling negatively regulates insm1a

Finally, we sought to identify genetic pathways that lie upstream of Insm1a activity in the retina. The results of our knockdown experiments provide strong evidence that *insm1a* is required for proper differentiation of retinal neurons. Moreover, the developmental expression pattern of *insm1a* in the retina matches the pattern of retinal progenitor cell (RPC) exit from the cell cycle and the onset of neurogenesis. This suggests that Notch-Delta signaling may function as an upstream negative regulator of *insm1a* expression, since one well-known role of this pathway is to preserve a pool of undifferentiated proliferative RPCs during retinal development [153, 175, 176]. This hypothesis is supported by previous work demonstrating that inactivation of Notch-Delta signaling in mouse retinal explants caused an increase in Insm1 expression [177]. Therefore, we examined whether expression of *insm1a* was similarly affected by reducing Notch activity in vivo in the zebrafish.

We blocked all Notch signaling by exposing zebrafish embryos to the γ-secretase inhibitor DAPT from 10.5 to 28 hpf. This period of DAPT treatment allowed specification of the eye field to occur normally, but inhibited Notch activity during retinal neurogenesis. We then evaluated *insm1a* expression in control (DMSO-treated) and DAPT-treated embryos at 28 hpf by WISH. Whereas very little expression of *insm1a* was observed in the retinas of control embryos at this time (Figure 2.9A), strong expression of *insm1a* was observed throughout the retina and

lens of DAPT-treated embryos (Figure 2.9B). Expression was also increased in other tissues, including the brain. This result indicates that Notch-Delta signaling is an early negative regulator of *insm1a* expression.

2.4.9 Her4 interacts directly with the insm1a promoter in vitro

To further explore how Notch signaling regulates *insm1a* expression, we next investigated whether *insm1a* is a direct target of Notch effector genes. The transcriptional repressor *Her4* is a Notch target gene that is expressed throughout the developing nervous system [178, 179]. To determine whether Her4 directly interacts with the *insm1a* promoter, we carried out in vitro reporter assays using *her4* cDNA and a luciferase reporter driven by two different lengths of the *insm1a* promoter. Co-transfection of HEK293 cells using the *her4* expression vector and either a short *insm1a* regulatory sequence (-282 to +59) or long *insm1a* regulatory sequence (-2440/+59) demonstrated that Her4 is able to negatively regulate the *insm1a* promoter in a dose-dependent fashion (Figure 2.9C). In the absence of Her4, the 2.5kb *insm1a* promoter drove significantly greater luciferase activity than the 300bp promoter (t-test $p < 0.001$), indicating that important regulatory elements exist in both the distal and proximal promoter regions. Regardless of which promoter was used, co-expression of Her4 significantly decreased the luciferase activity, demonstrating that Her4 is a negative regulator of the *insm1a* gene (Figure 2.9 C). Taken together, these data suggest that Notch-Delta signaling inhibits *insm1a* expression, potentially via its effector Her4.

2.5 Discussion

The zinc-finger transcriptional regulator Insm1 has been primarily studied in the context of its roles in regulating neuroendocrine development and neurogenesis in various regions of

the brain and spinal cord [81, 89, 97, 99, 101]. Recently, we and others have demonstrated that Insm1 is expressed in embryonic retinal progenitor cells as well as adult rod progenitor cells [94, 177], suggesting that cellular differentiation in the retina is also subject to Insm1 regulatory control. In this study, we have directly tested this hypothesis, and indeed our results reveal a requirement for Insm1a in the differentiation of rod and cone photoreceptors. Thus, this study, in combination with a recent study showing that Insm1a is required for retinal regeneration following acute damage in the adult zebrafish [95], conclusively demonstrate that Insm1 is among the genes important for generating the diverse neuronal subtypes in the vertebrate retina.

In *insm1a*-deficient zebrafish embryos, we observed a decrease in retinal area, and a severe reduction of differentiated rod and cone photoreceptors at 3 dpf. Interestingly, cone photoreceptor cell number in *insm1a* morphants recovered significantly by 4 dpf, but rod photoreceptor cells did not. These data suggest that rod photoreceptors are more sensitive to perturbations in *insm1a* expression than cone progenitors or other retinal cell types, either inherently or as a consequence of their extended period of differentiation.

We also observed small reductions in the numbers of bipolar and ganglion cells and delayed maturation of bipolar and horizontal cell morphology in *insm1a* morphants. Thus, although loss of *insm1a* produced the most significant effects on the photoreceptors, it also resulted in changes to inner retinal neurons. The reduction in bipolar and ganglion cell number is unlikely to be the result of increased cell death, because the *insm1a* morpholino was co-injected with a morpholino targeting *tp53*, which is known to inhibit apoptotic cell death in morpholino injected embryos [71], and we did not observe an increase in TUNEL-positive cells in *insm1a* morphant retinas (data not shown). Instead, we propose that the smaller eye and reduced numbers of differentiated cells in the *insm1a* morphants are the result of delayed cell

cycle exit of at least a subset of RPCs, in combination with impaired terminal differentiation of photoreceptor precursors (and perhaps other subtypes as well). Additionally, we hypothesize that the delayed maturation observed for the bipolar and horizontal cells (as well as the disruptions in the OPL) are a secondary consequence of the lack of differentiated photoreceptors in the ONL, as these two classes of retinal neurons make direct synaptic contacts with photoreceptors and may require this interaction to complete their maturation. Interestingly, knockdown of *insm1a* did not affect either the number or maturation of the Müller glia, suggesting that this subtype does not require *insm1a* to properly differentiate.

The "breaching" phenotype observed in *insm1a* morphants, in which cells from the INL were observed in the ONL, is very interesting. The presence of these ectopic INL cells at 4 dpf was only observed in regions of *insm1a*-deficient retinas that also displayed gaps in the cone photoreceptors. This could suggest that the presence of cone photoreceptors (or their precursors) is needed to establish a physical boundary between the INL and ONL. A related possibility is that the loss of integrity in the OPL of *insm1a* morphants is caused by a lack of synaptic contacts between the missing cones and second order neurons in the INL. Interestingly, in mice, mosaic deletion of Rb (a tumor suppressor gene known to have cell cycle regulatory function) results in both a loss of rod photoreceptor cells and a breaching phenotype very similar to that observed following *insm1a* knockdown [180].

At 3 dpf, the ONL of *insm1a* morphants did contain cells visible by DAPI staining, but these cells did not immunolabel with markers of differentiated rod or cone photoreceptors. Therefore, it is possible that in the absence of *insm1a*, ONL cells are correctly specified as photoreceptor cells, but are either arrested or delayed in the final stages of differentiation. This hypothesis is supported by our WISH data showing that the photoreceptor specification genes *crx* and *nr2e3* are expressed similarly to controls in 3 dpf *insm1a* morphant retinas. In the

murine neuroendocrine pancreas, Insm1 is expressed in precursors of all pancreatic cell types. When Insm1 is absent, pancreatic precursor cells are specified, but terminal differentiation is impaired in α, δ and β-cells, as suggested by delayed onset of differentiation markers and reduced expression of genes involved in hormone secretion. Pancreatic β-cells are the most severely affected cell type in the Insm1-null pancreas, with β-cells precursors arresting completely prior to terminal differentiation [98]. In the mouse sympatho-adrenal lineage, differentiation of sympathetic neurons is delayed in the absence of Insm1, while chromaffin cell precursors are made in normal numbers, but fail to properly differentiate [101]. Additional studies are needed to determine if the loss of *insm1a* in the retina causes rod photoreceptor cell differentiation to be delayed, similar to sympathetic neurons and pancreatic α- and δ-cells, or if the rod photoreceptor progenitors are arresting prior to terminal differentiation, as is seen in chromaffin cells and pancreatic β-cells. The small increase in rod photoreceptor number from 3 to 4 dpf in *insm1a* morphants may indicate the former, but the latter has not been conclusively excluded.

In *insm1a* morphants, we observed a significant delay in the developmental expression of bHLH and other transcription factors that specify cell fate. For example, *ath5* expression in *insm1a* morphants at 33 hpf resembled controls at 25 hpf, and *ath5* expression in *insm1a* morphants at 48 hpf resembled the 33 hpf control expression pattern. Although *ath5* is known to be required for RGC differentiation [23, 157, 181], a recent study in the mouse retina demonstrated that *math5*-expressing progenitors also contribute significantly to the photoreceptor lineage [160]. Therefore, the delayed onset and progression of *ath5* expression in *insm1a* morphants may presage the delay in photoreceptor differentiation observed later in development. At this point it is unclear whether the delayed timing of *ath5* expression in *insm1a* morphants is due to altered transcriptional regulation of *ath5* by *insm1a* (or an *insm1a* target

gene, since *insm1a* is thought to function as a transcriptional repressor), or whether it is a secondary consequence of the delay in cell cycle progression (discussed below) that was also observed in *insm1a* morphants.

The bHLH transcription factor *neurod*, also displayed delayed expression in *insm1a* morphants. *Neurod* can be directly induced by *ath5* [161] and has been shown to be repressed by human INSM1 in vitro [127]. *Neurod* expression promotes photoreceptor differentiation, and regulates proliferation of RPCs [147, 162, 163]. Interestingly, although we observed delayed onset and progression of *neurod* expression in the retina of *insm1a*-deficient embryos, *neurod* expression was strongly induced in the developing olfactory epithelium. Therefore, the decreased retinal expression of *neurod* may be an indirect effect of the changes in *ath5* expression, whereas in the developing olfactory epithelium and elsewhere, *neurod* may be directly repressed by *insm1a*.

Similar to *ath5* and *neurod*, expression of the photoreceptor-specific transcription factors *crx and nr2e3* was also delayed in *insm1a* morphants. While expression of both genes was much lower than controls at 48 hpf, they recovered to near control levels by 72 hpf. However, recovery of *nr2e3* was less complete than *crx*, with patchier expression even at 72 hpf. The rebound of *crx* expression at 72 hpf may explain the recovery in cone photoreceptors observed between 3 and 4 dpf. However, the increase in *crx* and *nr2e3* expression is apparently not sufficient to permit recovery of rod photoreceptors in a similar window. It may be that the rods require higher expression of *nr2e3*, or that other factors required for rod photoreceptor differentiation remain reduced below a critical threshold in *insm1a* morphants.

Additionally, we have presented evidence that expression of *insm1a* is negatively regulated by Notch-Delta signaling, and have identified Her4 as a possible effector of Notch-mediated repression. Pharmacologic inhibition of Notch signaling resulted in increased

expression of *insm1a* in the retina and the brain. *Her4,* a known effector of Notch signaling [178, 179], repressed expression of a luciferase reporter gene driven by the *insm1a* promoter. While this evidence supports a role for Notch-Delta signaling in control of *insm1a* expression in the retina, other signaling cascades are likely to be involved. For example, in murine sympatho-adrenal development, BMPs have been implicated in regulating Insm1 expression [81].

In several Insm1-expressing tissues, including the hindbrain [99], spinal cord [89] and endocrine cells of the pancreas and intestines [101], Insm1 expression is observed mainly in postmitotic or terminally dividing cells which are undergoing differentiation, and no cell cycle regulatory role has been identified. In contrast, Insm1 has been shown to regulate cell cycle progression in the mouse neocortex [97] and sympathetic nervous system, where it also regulates differentiation [101], and *insm1a* regulates expression of cell cycle genes in the regenerating zebrafish retina [95]. In this study, we have shown that knockdown of *insm1a* caused a delay in cell cycle progression in the developing zebrafish retina. From 30 to 36 hpf, progression through S-phase and entry into late G2/M phase occurred more slowly in *insm1a* morphant retinas than in controls. In control retinal sections, nearly half of cells in late G2/M phase had been in S-phase in the preceding two hours, whereas in *insm1a* morphants, less than 10% of late G2/M phase cells had progressed from S-phase. While *insm1a* may directly regulate the transcription of cell cycle genes, previous studies suggest that Insm1 can also regulate the cell cycle independently from its transcriptional regulatory activity. For example, in *Medaka, insm1b* was shown to alter cell cycle progression without being localized to the nucleus [86], and murine Insm1 directly binds to CyclinD in cultured cells, interrupting CyclinD-CDK4 interaction and causing hypophosphorylation of the retinoblastoma protein (Rb), thereby inducing cell cycle arrest [132]. The interaction of Insm1 with Rb is particularly intriguing given that in the mouse Rb-deficient retinas have defects in rod photoreceptor differentiation, RPC proliferation, OPL

integrity, and horizontal cell maturation, phenotypes strikingly similar to those we observed in *insm1a* morphants [180, 182]. Therefore, it will be important to determine whether both the photoreceptor differentiation and cell cycle defects observed in *insm1a* morphants result from a downstream dysregulation of Rb.

What is the precise mechanism whereby Insm1a regulates photoreceptor differentiation? Several non-mutually exclusive functions can be imagined. One possibility is that Insm1a directly regulates the transcription of photoreceptor specification genes. This hypothesis seems less likely, because the expression pattern of *insm1a* does not match that of other known photoreceptor determination genes such as *neurod*, *crx* and *nr2e3* at later stages of retinal development (this study and [174]). However, we did observe that expression of all three genes initiated at approximately the same time and location, i.e. 28 hpf in the ventro-nasal patch (Figure 2.1D and data not shown). Therefore, it is possible that Insm1a protein is very stable and is retained in RPC lineages that produce photoreceptor progenitors. In contrast to *neurod*, *crx*, and *nr2e3*, we observed that the developmental expression pattern of *insm1a* was very similar spatially to that of *ath5* (this study, [94, 150]). As *math5*-expressing cells have been shown to contribute significantly to the photoreceptor lineage in the mouse retina [160], it is possible that expression of *insm1a* in *ath5*-positive RPCs influences photoreceptor competency. Yet another possibility is that Insm1a functions non-cell autonomously to promote photoreceptor differentiation by regulating expression of secreted regulatory factors. Finally, Insm1a may influence the timing of photoreceptor differentiation through its regulation of cell-cycle kinetics.

In summary, our results demonstrate that *insm1a* is required for photoreceptor differentiation, regulates cell cycle progression during retinal development, functions upstream of pro-neural bHLH transcription factors *neurod* and *ath5,* and is negatively regulated by Notch-Delta signaling. In addition to addressing gaps in our knowledge of the function of *insm1a* during

retinal development, our data provide another genetic link between cell cycle progression and progenitor differentiation in the vertebrate retina. Future studies will address the mechanisms of how Insm1 regulates cell cycle progression and transcription of retinal genes, as well as the identification of direct targets of Insm1 transcriptional control.

Chapter 2 Tables:

Table 2.1: Primer sequences used in this study.

Gene	Forward	Reverse	
Insm1a MOBS	AATTCAGGTGTGCCTCTGATT TCAACCCGAGGTAC	CTCGGGTTGAAATCAGAGGC ACACCTG	cloning
ath5	CCGGAGAAGTTTGAGAGTGC	GCTCAGAGCCATCTGTAGGG	qPCR
Crx	ATGCTGTGAACGGGTTAAC	AAGCTTCCAGAATGTCCAG	qPCR
insm1a	GGCACCACAGTAACCACCA	CGCTGGAAGTCTCCTCTTTCT	probe
Neurod	ATACAGCGAGGAAAGCATGA	CCGTTCGTGATGCGAGTG	qPCR
nr2e3	CCAGCAGTGGGAAACACTAT	ATGGGCTTTATCCACAGGAC	qPCR

Chapter 2 Figures:

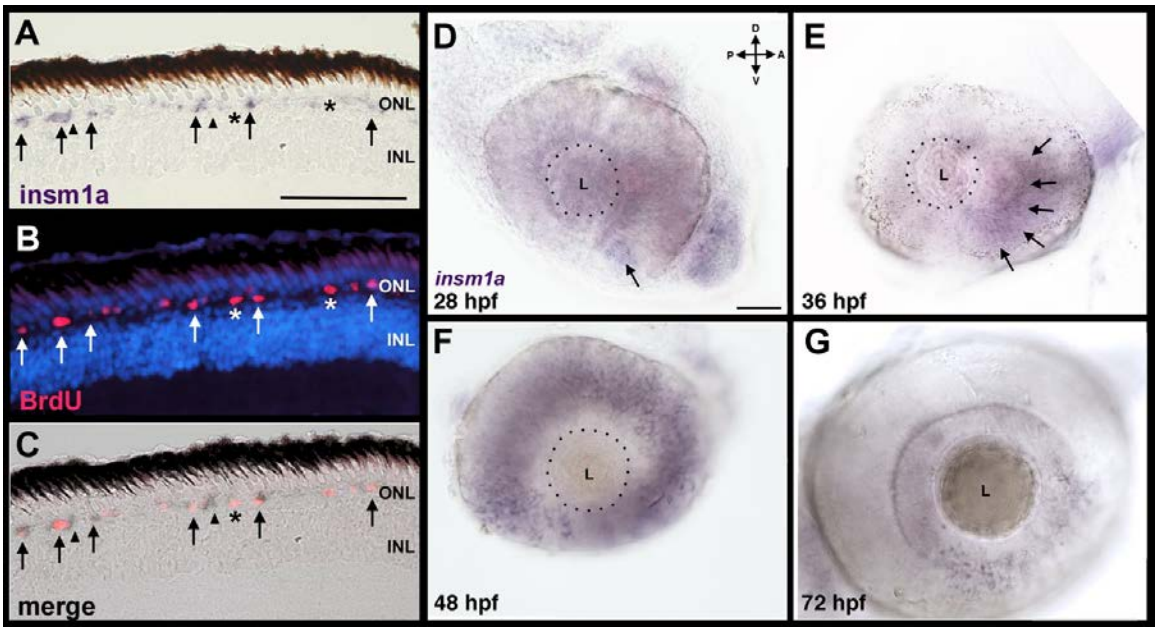

Figure 2.1: *Insm1a* is expressed in rod progenitor cells and in the developing retina.
(A-C) Expression of *insm1a* in XOPS-mCFP retinas. **(A)** In situ hybridization with an antisense probe for *insm1a* was performed on retinal cryosections of XOPS-mCFP retinas after a 4 hour exposure to BrdU. **(B)** Immunolabeling with anti-BrdU identified rod progenitor cells at the base of the ONL. **(C)** Overlay of in situ and immunolabeling demonstrates that many, but not all *insm1a*+ cells are also BrdU+. Arrows indicate *insm1a*+/BrdU+ cells; asterisks indicate *insm1a+*/BrdU- cells. **(D-G)** Whole mount in situ hybridization of wild-type embryos during development. **(D)** *Insm1a* expression was observed in the ventronasal patch between 24 and 28 hpf (arrow), **(E)** and *insm1a* expression expanded counterclockwise to the dorso-nasal retina at 36 hpf (arrows). **(F)** By 48 hpf, expression of *insm1a* had progressed to the dorso-temporal quadrant. **(G)** At 72 hpf, *insm1a* expression was only observed adjacent to the proliferative marginal zone at the retinal periphery. (**A** scale bar = 25µm; **D** scale bar = 50µm; D, dorsal; V, ventral; A, anterior; P, posterior; ONL, outer nuclear layer; INL, inner nuclear layer: L, lens; hpf, hours post fertilization)

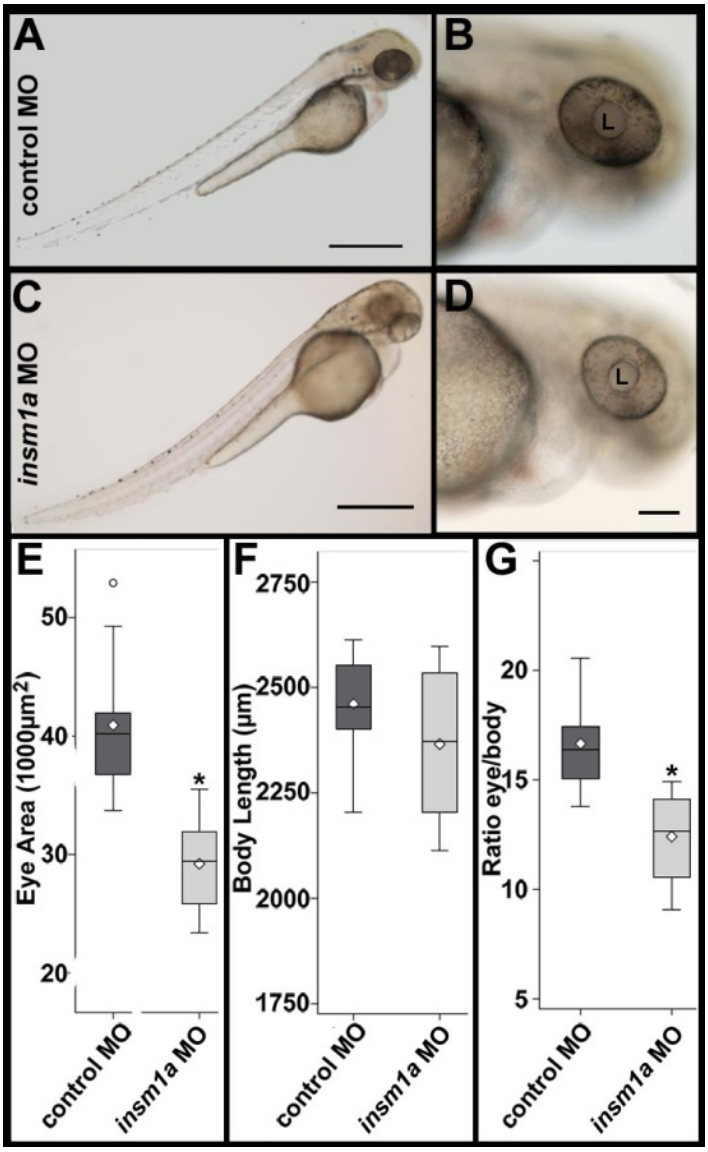

Figure 2.2: *Insm1a*-deficient embryos are microphthalmic.

Compared to embryos injected with a control morpholino **(A, B),** *insm1a* morphants **(C, D)** displayed mild body torqueing and smaller eyes at 48 hpf. Whereas the eye area was significantly smaller in *insm1a* morphants **(E)**, body lengths were not significantly different **(F)**, and eye areas remained significantly smaller after controlling for body length **(G)**. (**A, C** scale bar =500µm; **B, D** scale bar = 100µm; **E-G** ◊= mean; *p<0.0001, t-test; n > 12; L, lens; hpf, hours post fertilization; MO, morpholino)

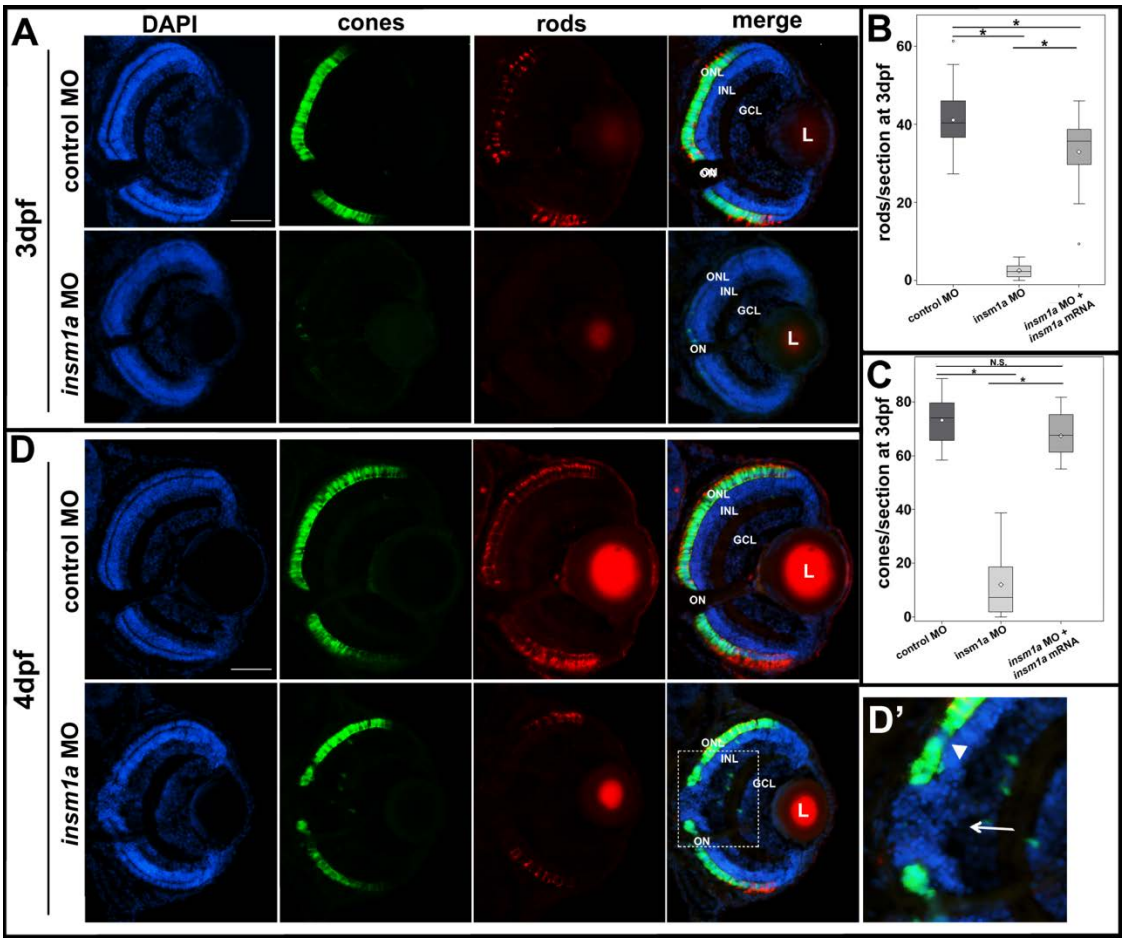

Figure 2.3: Photoreceptor cell differentiation is impaired in *insm1a* morphants.

(A) At 3 dpf cone (green) and rod (red) photoreceptor cells were severely reduced in *insm1a* morphants. **(B)** The reduction in rods was significant and could be partially rescued by co-injection of in vitro transcribed *insm1a* mRNA with the *insm1a* morpholino. (control: n= 31 eyes from 22 embryos; *insm1a* MO: n=24 eyes from 17 embryos; *insm1a* MO + *insm1a* mRNA: n=18 eyes from 10 embryos.) **(C)** The reduction in cones was significant and could be rescued by co-injection of in vitro transcribed *insm1a* mRNA with the *insm1a* morpholino**. (**control: n= 26 eyes from 17 embryos; *insm1a* MO: n=24 eyes from 17 embryos; *insm1a* MO+ *insm1a* mRNA n=18 eyes from 10 embryos.) **(D)** At 4 dpf, the rod photoreceptors remain significantly reduced. However, cone photoreceptors (green) significantly recovered, but were less dense and contained visible gaps (dotted box). **(D')** In regions lacking cones INL cells breached the OPL and extended into the ONL. Both small (arrowheads) and large (arrows) gaps were observed, accompanying the breached OPL. (**B, D:** ◊=mean, *p<0.0001; scale bars = 50µm; ONL, outer nuclear layer; INL, inner nuclear layer; GCL, ganglion cell layer; L, lens; ON, optic nerve; dpf, days post fertilization; MO, morpholino)

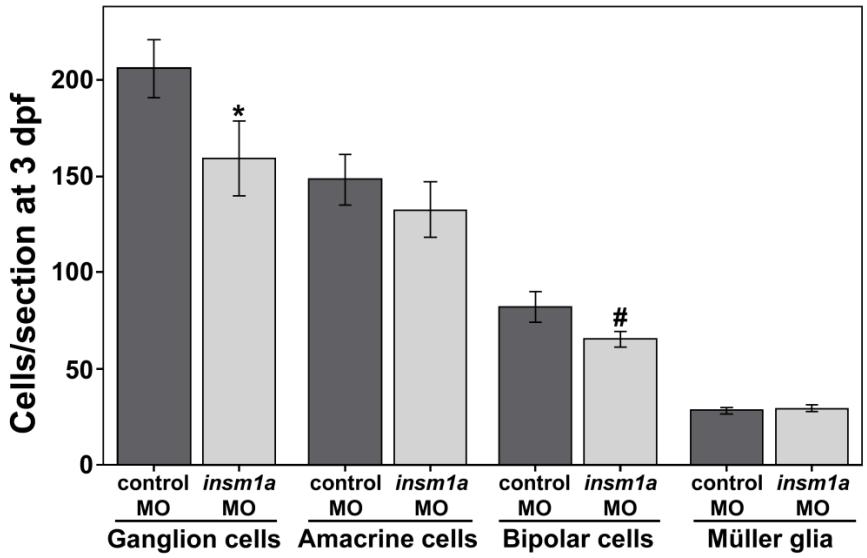

Figure 2.4: Knockdown of *insm1a* causes modest changes in cell number for some non-photoreceptor cell types.

At 3 dpf the numbers of ganglion cells and bipolar cells were slightly reduced in *insm1a* morphant retinas, whereas the numbers of amacrine cells and Müller glia were not significantly affected. (*p<0.005; #p<0.003; mean±stdev for all; n=6 embryos each for ganglion and amacrine cells, 5 each for bipolar cells and 18 eyes from 10 embryos each for Müller glia).

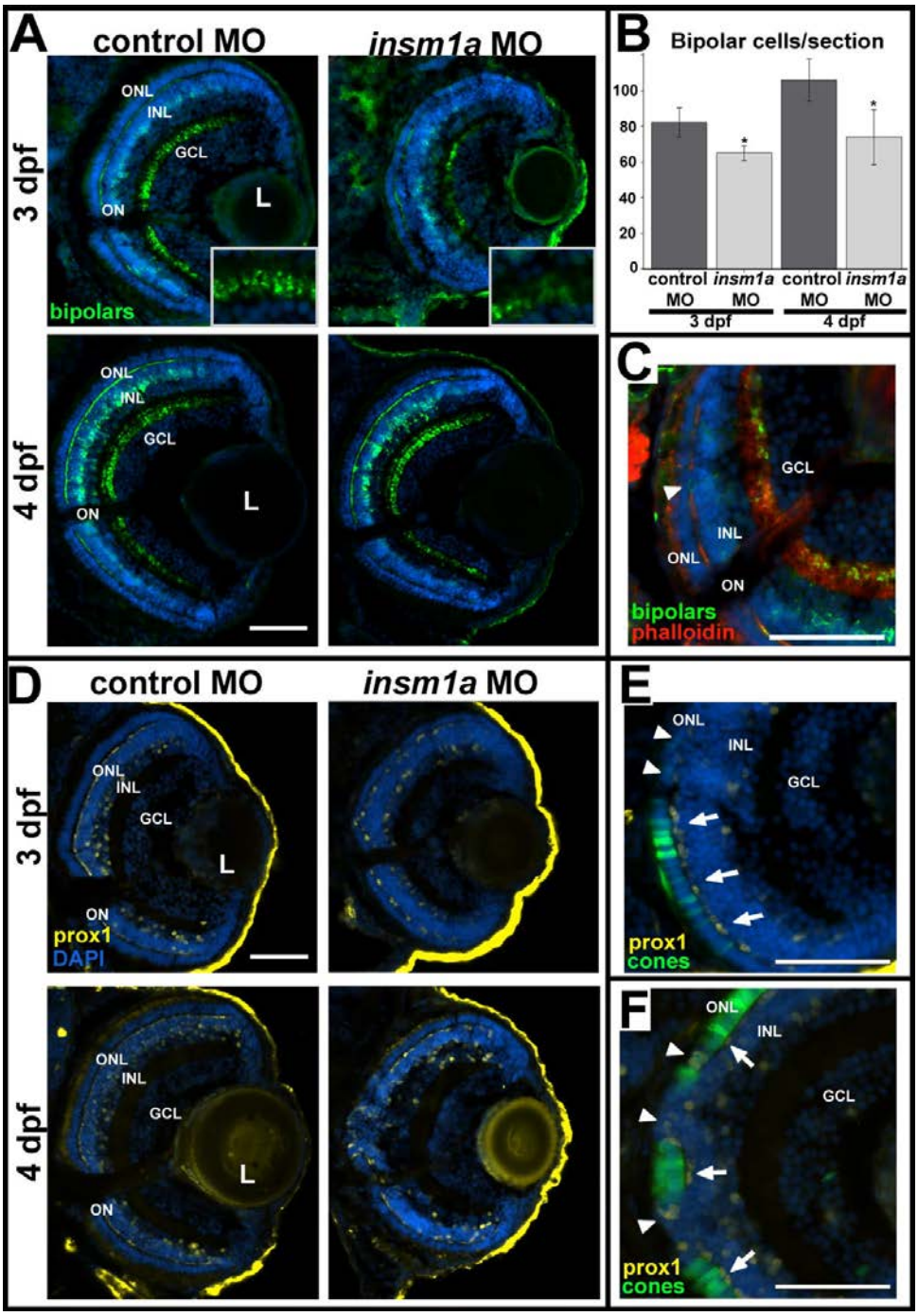

Figure 2.5: Bipolar and horizontal cell maturation is delayed in *insm1a* morphants.

(A) At 4 dpf, bipolar cell morphology and labeling intensity in *insm1a* morphants appeared similar to controls. However, some breaches in the OPL were observed **(C)** and these regions (shown by an absence of phalloidin staining) occasionally contained bipolar cell bodies (white arrowhead). **(D)** At 4 dpf, Prox1+ cells were present in the INL adjacent to the OPL in *insm1a* morphant retinas; however, they were rounder and more widely spaced than in controls. **(F)** In

Figure 2.5: Bipolar and horizontal cell maturation is delayed in *insm1a* morphants (continued).

regions of 4 dpf *insm1a* morphant retinas that contained cones, the adjacent Prox1+ horizontal cells displayed a more mature morphology (white arrows); however, in regions devoid of cones, the Prox1+ cells were absent or appeared less mature (white arrowheads). Prox1+ cells were also observed in the regions where cells from the INL had breached the ONL (white arrowheads). Scale bars = 50µm; ONL, outer nuclear layer; INL, inner nuclear layer; GCL, ganglion cell layer; IPL, inner plexiform layer; OPL, outer plexiform layer; L, lens; ON, optic nerve; dpf, days post fertilization; MO, morpholino.

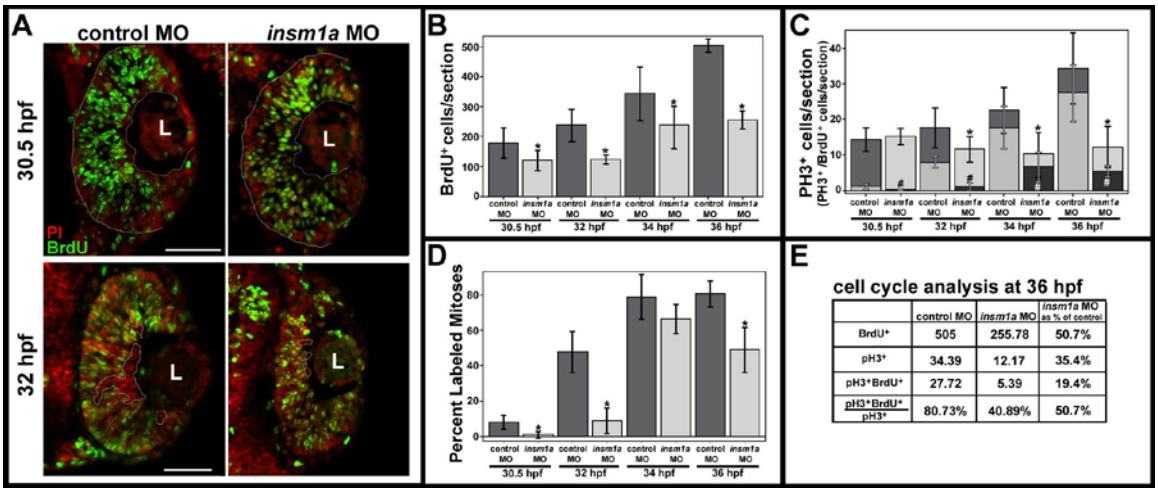

Figure 2.6: Cell cycle progression is delayed after *insm1a* knockdown:.

(A) At 30.5 hpf (0.5 hpi, top panels), BrdU+ cells (green) spanned the retina from basal to apical (dotted lines) in control retinas. However, in *insm1a* morphant retinas, the BrdU+ cells did not extend to the apical edge of the retina. At 32 hpf (2 hpi, bottom panels), fewer post-mitotic BrdU- cells were observed at the basal surface (dotted circles) in *insm1a* morphants compared with controls, indicating a delay in cell cycle exit in *insm1a* morphant retinas. **(B)** Quantitation of BrdU+ cells revealed a decrease in *insm1a* morphant retinas at all time points (*p<0.05). **(C)** The numbers of PH3+ cells were reduced at 2, 4 and 6 hpi in *insm1a* morphant retinas (*p<0.04). The number of cells double-positive for PH3 and BrdU was also reduced at all time points (#p<0.007). **(D)** The percent labeled mitoses (see Results for explanation) was significantly reduced in *insm1a* morphants at 0.5, 2 and 6 hpi, indicating that *insm1a* morphants took longer to progress from S phase into late G2/M phase compared with controls. **(E)** Summary of cell count analysis at 36 hpf (6 hpi); cell counts for *insm1a* morphants are expressed as a percentage of controls in the last column (for both controls and morphants: n=6 at 30.5, 32, and 34 hpf and n=3 at 36 hpf; mean ± st.dev). Scale bars = 50µm; L, lens; PI, Propidium iodide; hpf, hours post fertilization; hpi, hours post BrdU injection; MO, morpholino.

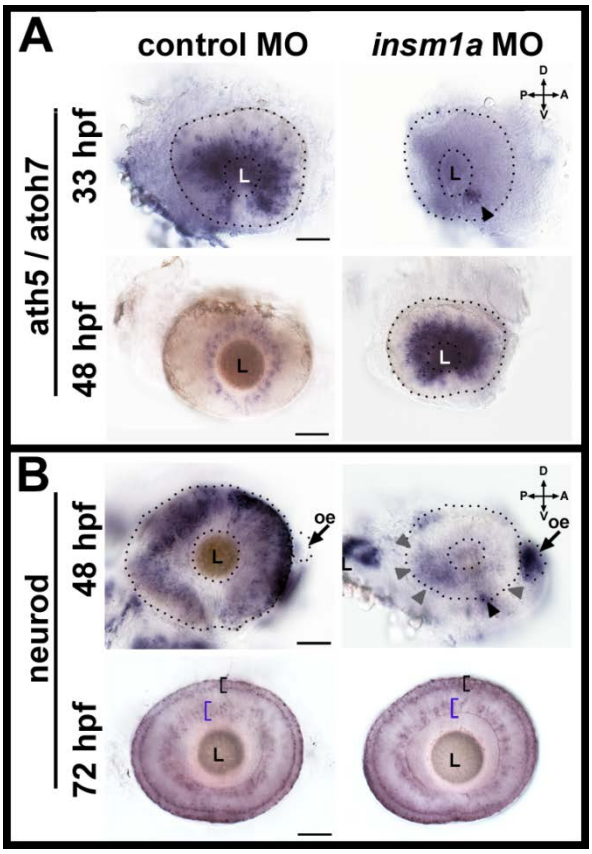

Figure 2.7: *Insm1a* acts upstream of pro-neural TFs *ath5* and *neurod.*

(A) At 33 hpf *ath5* was expressed throughout the developing retina in controls; in contrast *ath5* expression was detectable only in the ventro-nasal patch of *insm1a* morphants (arrowhead). At 48 hpf, *ath5* expression in control retinas was restricted to the GCL; in *insm1a* morphant retinas, expression had expanded throughout the retina, in a pattern that closely resembled that of 33 hpf controls. **(B)** *Neurod* expression at 48 hpf was observed strongly in the developing photoreceptors and in the adjacent INL of control retinas. In *insm1a* morphants, however, *neurod* expression was mostly confined to the ventro-nasal retina (black arrowhead), with some expression throughout the central retina (gray arrowheads). In contrast, strong expression of *neurod* was observed in the olfactory epithelium (arrows) of *insm1a* morphants, which was absent in controls. By 72 hpf, *neurod* expression in the ONL (black bracket) and inner portion of the INL (blue bracket) was qualitatively similar in both controls and *insm1a* morphants. Scale bars = 50µm; D, dorsal; V, ventral; A, anterior; P, posterior; GCL, ganglion cell layer; oe, olfactory epithelium; ONL, outer nuclear layer INL, inner nuclear layer; hpf, hours post fertilization.

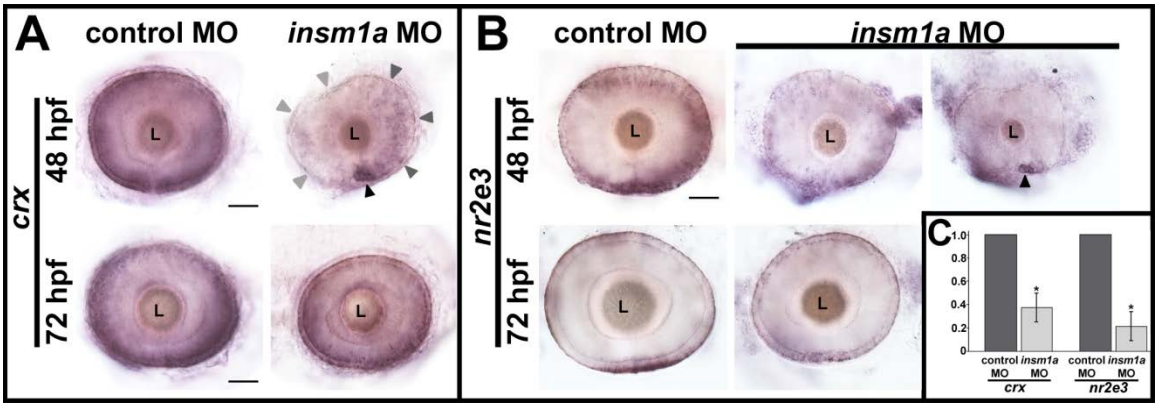

Figure 2.8: Expression of *crx* and *nr2e3* is reduced at 48 hpf in *insm1a* morphants.

(A) At 48 hpf, *crx* was expressed strongly in the developing ONL and weakly in some cells of the INL in control retinas. In *insm1a* morphant retinas *crx* was expressed in the ventro-nasal retina (black arrowhead), and expression decreased in a counterclockwise fashion across the retina (gray arrowheads). At 72 hpf, *crx* expression appeared similar between *insm1a* morphants and controls, and was observed primarily in the ONL. **(B)** At 48 hpf, *nr2e3* was expressed strongly in nascent photoreceptor cells in the ONL, and in scattered cells in the distal half of INL in control retinas. *Insm1a* morphants displayed varying degrees of reduction in *nr2e3* expression. In approximately half of the *insm1a* morphant retinas the *nr2e3* expression pattern was only slightly less intense than controls (left panel), whereas the remaining half expressed *nr2e3* only in the ventro-nasal retina (right, black arrowhead). At 72 hpf, *nr2e3* expression had recovered greatly in *insm1a* morphants; however, *nr2e3* staining did appear less dense and more discontinuous in *insm1a* morphants than in controls. **(C)** qPCR confirmed a 2.7-fold reduction in *crx* transcripts (*p<0.0128), and a 4.6-fold reduction in *nr2e3* (*p<0.0084) at 48 hpf. Scale bar = 50µm; ONL, outer nuclear layer; INL, inner nuclear layer; L, lens; hpf, hours post fertilization; MO, morpholino.

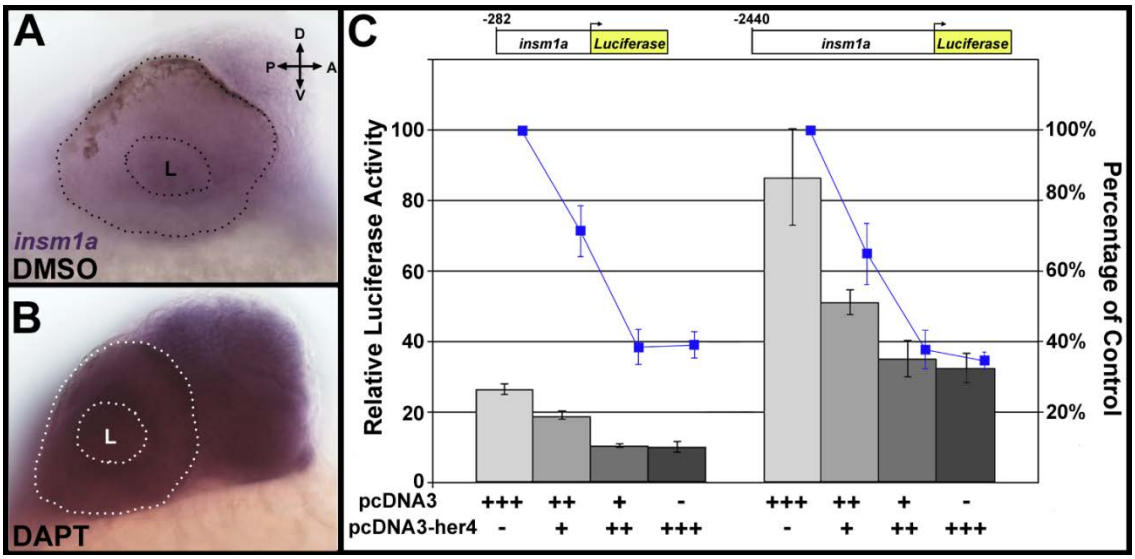

Figure 2.9: Notch-Delta and her4 negatively regulate *insm1a* expression.

(A, B) Pharmacologic inhibition of Notch signaling with DAPT resulted in an upregulation of *insm1a* expression in the developing eye and brain **(B)**, compared to control (DMSO) treated embryos **(A)**. **(C)** Co-transfection of HEK293 cells with a *her4* cDNA expression vector repressed a luciferase reporter gene driven by either 300bp (left) or 2.5kb (right) of the *insm1a* promoter. D, dorsal; V, ventral; A, anterior; P, posterior; L, lens; hpf, hours post fertilization.

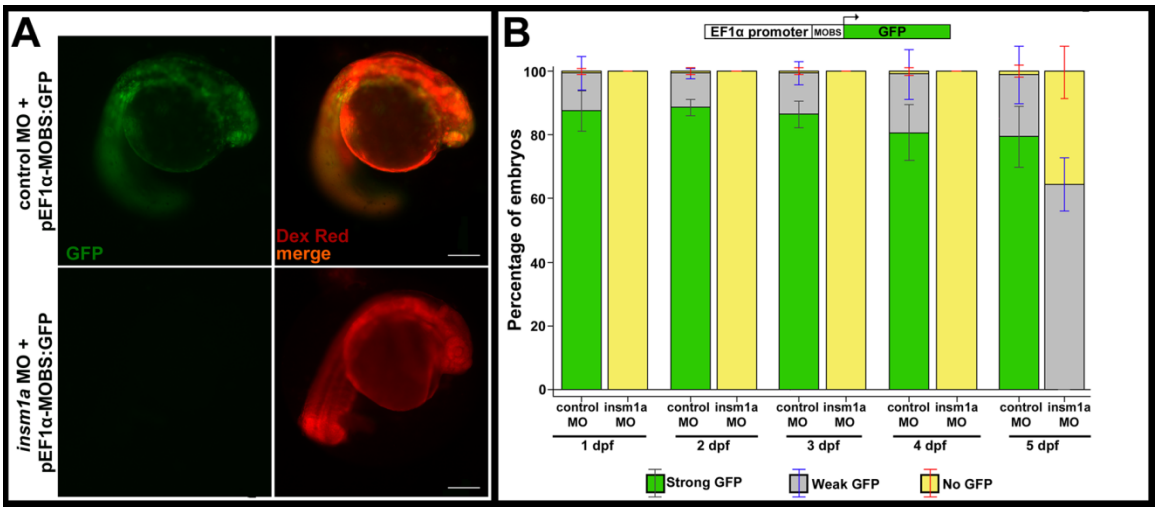

Supplemental Figure 2.S1. The *insm1a* MO is highly effective through 4 dpf.

Embryos were co-injected with either standard control or *insm1a* MO and an *eF1 -GFP* plasmid containing the *insm1a* MO binding site (pEF1 -MOBS:GFP; n>40 embryos for each group). (**A)** At 1 dpf, control MO injected embryos showed robust, ubiquitous expression of GFP (top panels), whereas *insm1a* MO injected embryos showed no expression of GFP (bottom panels). Tetramethylrhodamine dextran (Dex Red) was used as an internal injection control. (**B)** Quantitation of the numbers of injected embryos showing GFP expression from 1 dpf through 5 dpf. GFP expression similar to that shown in (A) (top panel) was categorized as "strong GFP". GFP expression that was limited to just a few cells in the embryo was categorized as "weak GFP" expression. "No GFP" required the complete absence of any identifiable GFP signal. From 1 dpf through 4 dpf, no *insm1a* morphants exhibited any GFP expression. In contrast, nearly all embryos co-injected with the standard control MO were GFP-positive, with over 90% strongly expressing GFP. By 5 dpf, nearly half of the *insm1a* morphants showed low levels of GFP expression, indicating a decline in the effectiveness of the *insm1a* MO. Scale bar = 200µm; MOBS, *insm1a* morpholino binding site; MO, morpholino; dpf, days post fertilization.

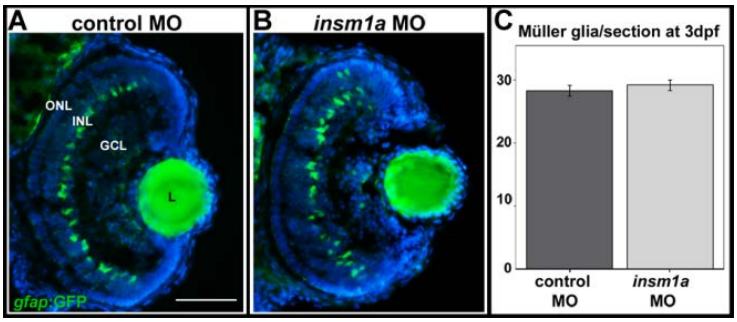

Supplemental Figure 2.S2: Muller glia differentiation is not affected by *insm1a* knockdown.
(A-B) At 3 dpf, Müller glia cells were counted using the *gfap*:GFP transgene (green). Although the cell bodies were slightly less well organized in *insm1a* morphants compared to controls, the number of Müller glia cells was not significantly different **(C)**. (n=18 eyes from 10 embryos for each, mean ± stdev; scale bar = 50µm; ONL, outer nuclear layer; INL, inner nuclear layer; GCL, ganglion cell layer; L, lens; dpf, days post fertilization)

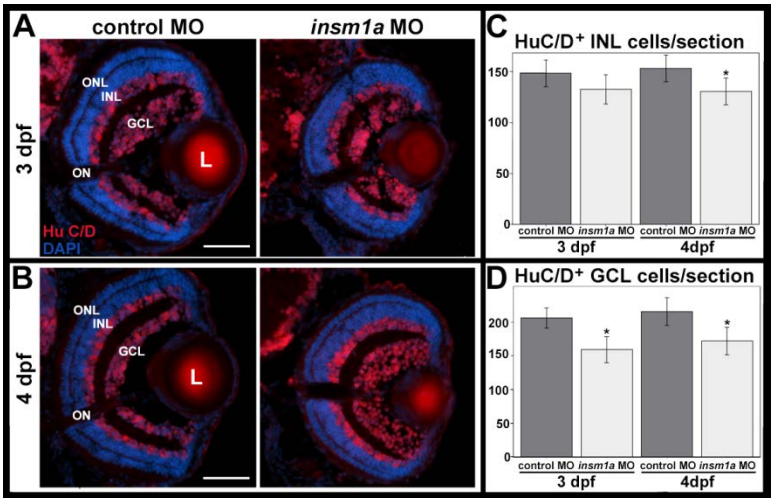

Supplemental Figure 2.S3: Amacrine and ganglion cell number is slightly reduced in *insm1a* morphants.
(A, B) HuC/D labels amacrine cells in the INL and ganglion cells in the GCL. **(C)** Amacrine cell number is slightly reduced at both 3 and 4 dpf. **(D)** Ganglion cells are reduced at both 3 and 4 dpf. (**C, D.** 3 dpf: controls n=6, *insm1a* morphants n=5; 4 dpf; **C:** *p<0.0274; **D:** *p<0.005; scale bars = 50µm; ONL, outer nuclear layer; INL, inner nuclear layer; L, GCL, ganglion cell layer; lens; ON, optic nerve; dpf, days post fertilization)

CHAPTER 3: FUNCTIONAL ANALYSIS OF A ZEBRAFISH INSM1 MUTANT

Marie Forbes-Osborne[1], Sana Aslam[2], Ann C. Morris

[1]Department of Biology, University of Kentucky, Lexington, Kentucky 40506-0225

[2]The Sayre School, Lexington, Kentucky, 40507

3.1 Introduction

Previous studies have shown that *insm1a* expression is required during retinal development, with both cell cycle progression and photoreceptor differentiation defects observed when *insm1a* expression was reduced. The effect of *insm1a* on cone PRC development appears to largely be in controlling the timing of cone PRC differentiation; with cone PRC differentiation delayed when *insm1a* is knocked down [88]. However, due to the limitations of the *insm1a* MO, which is effective only until 4 dpf, we have been unable to determine whether the effect on rod RPCs was a similar delay or instead a failure to differentiate. To separate these required the use of an *insm1a* mutant.

Undertaken by the Sanger Wellcome Trust, the Zebrafish Mutation Project is an effort to produce zebrafish lines with mutations in every protein-coding gene in the genome. Male fish were exposed to N-ethyl-N-nitrosourea (ENU, an alkylating agent known to induce point mutations), before being bred to produce potential (F_1) mutant offspring. Whole exome sequencing of the sperm from male F_1 offspring was completed to identify individual F_1 males with significant mutation load. These males were crossed to wild-type females to produce F_2 lines. Male and female F_2 fish from a single male F_1 were incrossed and assayed both phenotypically and genotypically for the mutant alleles identified in the F_1. After determining the presence of individual gene mutations, animals from the F_2 generation were made available to the community. As a result of the high efficiency of ENU mutagenesis, these F_2 fish often

harbored more than one mutation in their genomes, with an average of 7.55 nonsense and 3.36 essential splice-site mutations per animal [183].

An *insm1a* mutant was identified with a single A to T transversion at base pair 421, which results in the lysine (AAG) at amino acid position 141 being converted to a stop codon (TAG). This is expected to result in an early truncation of the *insm1a* protein; occurring within the NLS and upstream of the ZF DNA binding domains (Figure 3.1). Lysine 141 is the fourth of four dibasic residues within the NLS, which are hypothesized to be essential for nuclear import. No alternative start site could be identified that might permit in-frame translation of a longer form of the protein. As both the ability to enter the nucleus and bind DNA are expected to be impaired or lost, we hypothesized that *insm1_K141X* would be a null allele.

3.2 Materials and Methods

3.2.1 Zebrafish lines and maintenance

Zebrafish were bred, raised and maintained in accordance with established protocols for zebrafish husbandry [138]. Embryos and larvae were housed at 28°C, on a 14 h light:10 h dark cycle. Fish were anaesthetized with Ethyl 3-aminobenzoate methanesulfonate salt (MS-222, Tricaine, Sigma-Aldrich, St. Louis, MO). Embryos were staged as previously described [62]. Wild-type strains included the Ekwill strain (Ekwill Fish Farm, Gibsonton, FL), the AB strain obtained from the Zebrafish International Research Center (ZIRC, Eugene, OR) and hybrids produced by crossing the Ekwill and AB strains. The insm1a^{sa0195} line (hereafter insm1a_K141X) was obtained from the Wellcome Trust Sanger Institute (Hinxton, United Kingdom). The Tg (XlRho:EGFP)fl1 transgenic line (hereafter called XOPS-GFP) has been previously described [77, 141], and was obtained from James Fadool (Florida State University, Tallahassee, FL). All animal procedures were carried out in accordance with guidelines established by the University of Kentucky Institutional Animal Care and Use Committee.

3.2.2 Microinjections of morpholinos and mRNA

A translation-blocking antisense morpholino (MO1: 5'-GGTTGAAATCAGAGGCACACCT-3') designed against *insm1a* was injected into fertilized embryos prior to the second cell division The *insm1a* MO1 was injected at 6.0-ng/embryo. Since injection of MO1 caused some toxicity to the embryos, an antisense *tp53* morpholino (p53MO) was co-injected to suppress cell death [143]. The p53MO (5'-GCGCCATTGCTTTGCAAGAATTG-3') was injected at 1.5-fold the amount of the *insm1a* MO. A standard control MO, targeting a mutant variant of the human β-globin gene (5'-CCTCTTACCTCAGTTACAATTTATA-3'), was injected similarly to the *insm1a* MO. All morpholinos were synthesized by GeneTools, LLC (Philomath, OR) and have been previously described (Chapter 2 and [88].

Capped mRNA was synthesized from cloned *insm1a* coding sequences lacking the morpholino binding site using the mMessage (T7 or Sp6) Kit (Ambion, Austin, TX) according to the manufacturer's instructions. The 4 mRNAs are described in Figure 3.4, and include a full length (1152 bp) *insm1a* mRNA, a full length (1152 bp) *insm1a* mRNA containing an early stop codon at nucleotides 421-423, a 423 bp N-terminal only truncation with the stop codon placed at the same location, and a 732 bp C-terminal only truncation that has a start codon at the wild-type nucleotides 421-423. mRNA was cleaned by phenol-chloroform extraction and ethanol precipitation, and injected at 450 pg per embryo.

All injected embryos were transferred to 1x E3 media with 4x calcium containing 0.003% 1-phenyl-2-thiourea (PTU) at 24 hours post fertilization (hpf) to inhibit pigmentation and 0.1% methylene blue to inhibit fungal growth.

3.2.3 Sample Collection

At selected time points, embryos and larvae were killed using either Ethyl 3-aminobenzoate methanesulfonate salt (MS-222, Tricaine, Sigma-Aldrich, St. Louis, MO) or rapid

cooling as previously described, collected, and washed in ice cold PBS. Tissues were fixed overnight at 4°C in freshly prepared 4% Paraformaldehyde (PFA) for immunohistochemistry. Fixed tissues were cryoprotected in 10% sucrose in 0.8XPBS for at least 3 hours and in 30% sucrose overnight at 4°C. Samples were mounted in OCT Medium (Ted Pella, Redding, CA) and frozen at -80°C. Ten micron Sections were cut on a cryostat (Leica CM 1850, Leica Biosystems, Buffalo Grove, IL), mounted on gelatin-coated slides, and dried overnight at room temperature before storing at -20°C until ready to use.

3.2.4 Immunohistochemistry

Slides were warmed to room temperature and sections were rehydrated and postfixed in 1% PFA for 10 minutes. After 2 washes in PBS, and 2 washes in PBST, sections were blocked in PBST containing 1% BSA for at least 30 minutes at room temperature. Slides were incubated with primary antibody in PBST/BSA with 5% Normal Goat serum, overnight at 4°C in a humidified chamber. The following day, slides were washed 3 times in PBST, and incubated with secondary antibody in PBST/BSA for 1 hour at room temperature in the dark. Slides were washed 2 times with PBST, counterstained with DAPI (4', 6-diamidino-2-phenylindole, 1:10,000 dilution; Sigma-Aldrich) in PBS, and mounted in 40% glycerol in PBS. Images were obtained on an inverted fluorescent microscope (Eclipse Ti-U; Nikon Instruments), using a 40X objective.

The following antibodies were used: 4C12 (1:100 dilution), a monoclonal antibody that recognizes an unknown epitope on rods (Fadool J, Linser, P unpublished; a generous gift of James Fadool, FSU, Tallahassee, FL), Zpr-1 (1:20 dilution), a monoclonal antibody that recognizes red and green cones (ZIRC). Alexa Fluor 488 goat anti-mouse, 546 goat anti-mouse (Molecular Probes, Invitrogen), and Cy5 conjugated goat anti-mouse (Jackson ImmunoResearch, West Grove, PA) secondary antibodies were all used at 1:150-200 dilution.

3.2.5 Cell counts

Immunolabeled cryosections from the central retina containing three distinct cell layers and a lens were used for cell counts. Cells were counted a minimum of 3 times, and counts were averaged for statistical analysis. SAS 9.3 was used for all statistical analyses. ANOVA and MANOVA were used for analysis with greater than 3 treatment groups or multiple analyses from individual treatments.

3.3 Results

3.3.1 Isolation of the insm1a_K141X mutant

Embryos produced by F_2 incross were obtained from the Wellcome Trust Sanger Institute, and raised to adulthood. Adults were fin-clipped and genomic DNA was extracted. A piece of the *insm1a* gene spanning the mutant locus was amplified by PCR and used as a template for sequencing. Genotype determination was completed using both sequencing data and histograms (Figure 3.2A). To remove potentially confounding mutations in genes other than *insm1a*, *insm1a_K141X* mutant animals were outcrossed to XOPS:GFP zebrafish three times; with heterozygous *insm1a_K141X* mutants identified by tail clip and sequencing at each stage. Three outcrosses were chosen as each F_2 was determined to harbor approximately 10 total mutations [183]. Thus, if the *insm1a_K141X* mutation was being isolated in each outcross and assuming no mutations in linked genes, 3 generations of outcrosses should remove all other background mutations. After outcrossing, the F_5 heterozygotes were incrossed to produce homozygous *insm1a_K141X* mutants, heterozygous *insm1a_K141X*, and *insm1a_WT* animals for use in future comparative studies. The animals obtained from the Wellcome Trust Sanger Institute were produced on a genetic background that was different from our commonly used laboratory strains. Therefore, *insm1a_WT* lines generated from the F_5 incross were also

maintained with the *insm1a_WT* designation, to ensure a proper control population for use in these studies.

3.3.2 Homozygous Insm1a_K141X mutation does not affect viability, survival or fertility

When F_5 or later generation adults heterozygous for the *insm1a_K141X* allele were bred, offspring homozygous for the *insm1a_K141X* allele were recovered at expected frequencies at all-time points assayed. There was no apparent effect on survival at 3, 5, 10, and 14 dpf, or at adulthood. Fecundity was also similar in both homozygous *insm1a_K141X* and *insm1a_WT* animals, with no discernable effect of *insm1a* mutation on success of mating, including egg quality and production, fertilization percentages and survival of embryos.

The survival data for the homozygous *insm1a_K141X* mutant directly contrasts with the mouse, where 2 independently generated global knockouts of Insm1 are embryonic lethal. It is probable that the presence of the second zebrafish co-ortholog of Insm1, *insm1b,* is the reason no lethality is observed in the homozygous *insm1a_K141X* mutant. Although *insm1b* expression overlaps with *insm1a* expression in many tissues, including pancreas and brain, *insm1b* is excluded from the eye [88, 94] and is not expected to affect retinal development in these mutants.

3.3.3 Photoreceptor development is not altered in the insm1a_K141X mutant

Homozygous *insm1a_K141X* and *insm1a_WT* animals were incrossed, and embryonic or juvenile animals were collected at 3, 5, and 10 dpf. Retinal cryosections were prepared at each time point, and the number of rod and cone PRCs was counted using immunohistochemistry with either a rod or cone photoreceptor specific antibody (4C12 and Zpr-1 respectively). At all time points assayed, neither rod nor cone PRC number was significantly different between the homozygous *insm1a_K141X* mutant and the *insm1a_WT* animals (Figure 3.3C-D). A slight though not significant decrease was observed in the rod PRCs of the *insm1a_K141X* mutants only at 3

dpf ($p < 0.35$). The retinas appeared normal throughout, with no apparent lamination defects or changes in cellular morphology (Figure 3.3A-B).

The lack of a developmental retinal phenotype in what was expected to be a null mutant was unexpected and perplexing. The *insm1a_K141X* allele is expected to lack both the ZF DNA binding domains and the bulk of the NLS, and yet no deficit in PRC differentiation was observed. It is possible that the *insm1a_K141X* mutant is a null allele, but fails to phenocopy the morpholino because the morpholino phenotype is either non-specific or the result of off-target binding of the morpholino. An additional possibility, recently shown for another gene by Rossi et al. [184] is that the mutant may make use of a compensatory pathway, which is absent in the morpholino-treated embryos, to replace the activity of the mutated gene. Alternatively, it is possible that the morpholino phenotype is correct, and the mutant Insm1a protein retains some or all wild-type function. There are multiple potential ways that this could occur. First, perhaps the stop codon is subject to translational read-through, resulting in a functional protein, nearly identical to the wild-type protein. Second, the truncated form of the protein could remain stable after translation, and retain at least partial functionality. We have used several mRNA rescue experiments to determine which of these possibilities is more likely.

First, if translational read-through is occurring, then co-injection of a full length mRNA containing the mutation should rescue the morphant phenotype, while injection of a truncated mRNA cannot. Second, if the truncated protein retains function and translational read-through is unnecessary or absent, then co-injection of a truncated *insm1a_K141X* mRNA should rescue the morphant phenotype. Lastly, if rescue of the morphant phenotype is independent of the identity of the zebrafish sequence injected, then co-injection of a C-terminal *insm1a* truncation, where the lysine at amino acid 141 has been mutated to produce an in-frame start codon,

should also rescue the morphant phenotype. In order to test these predictions, three *insm1a* variants were cloned and used to produce mRNA for injection (Figure 3.4).

3.3.4 Truncation variant testing indicates residual function of the insm1a_K141X mutant sequence

To test whether the lack of discernable phenotype in the *insm1a_K141X* mutant, could be explained by retained functionality of the mutant sequence, we assayed the ability of the truncated *insm1a* alleles to rescue the previously observed *insm1a* morphant photoreceptor specific phenotype. The full length *insm1a_K141X* cDNA (hereafter *insm1a_K141X)*, a 423 bp fragment of *insm1a* coding the first 140 amino acids (hereafter *insm1a_Nterm),* and a 732 bp fragment of *insm1a* coding for the final 265 amino acids (hereafter *insm1a_Cterm*) were cloned (Figure 3.4). Capped mRNA was prepared as previously described (2.3.2) for each variant. Embryos were injected at the one cell stage with either a control MO, the *insm1a* MO1 alone, or the *insm1a* MO1 with either the wild-type or mutant full length *insm1a* mRNA or one of the truncation variants. Injection volumes (4.2 nL per embryo) and injection quantities were kept constant throughout for both control and *insm1a* morpholinos (6.07 ng per embryo), p53 morpholino (9.11 ng/embryo), and for the mRNAs (450 ng). At 3 dpf, embryos were collected and processed for IHC. Retinal morphology and rod and cone PRC counts were compared amongst the conditions (as in 2.3.8 and 2.3.10).

3.3.4.1 Overall survival and morphology were unchanged for insm1a_K141X and insm1a_Nterm mRNA rescues

No new morphological changes in body shape, brain morphology or whole embryo development were observed in the *insm1a_K141X* and *insm1a_Nterm mRNA rescue categories.* Survival was similar to that observed in the original morpholino studies (Chapter 2) [88]. Upon sectioning, the overall morphology of the retina in all categories was similar, and no defects in

lamination were observed in either group (Figure 3.5A). The *insm1a_Cterm* mRNA rescue showed severe defects in embryogenesis, beginning as early as 8 hpf. These included disorganization of cells in the early embryo, followed by necrosis and increased embryonic death. Few embryos survived beyond 36 hpf, and by 3 dpf, the surviving embryos were highly dysmorphic, with strong body curvature, truncated tails, and brain abnormalities. After sectioning, no retinal lamination could be seen in the *insm1a_Cterm* rescue retinas (data not shown). Reducing the *insm1a_Cterm* mRNA to half dosage slightly increased the survival rate, but embryos remained highly abnormal. As a result, only the *insm1_K141X* and *insm1a_Nterm* mRNA rescues were used for additional testing.

3.3.4.2 Cone PRC number was significantly but unequally rescued by all insm1a mRNA variants

The number of cone PRCs per retinal section was determined by counting cells after IHC with the cone specific antibody Zpr-1. The *insm1a* morphants displayed a significant reduction in cone PRCs, with an average of 13.9 cone PRCs per section compared to an average 73 in the control morphants. The *insm1a_WT mRNA,* the *insm1a_K141X* mRNA, and the *insm1a_Nterm mRNA* were able to significantly rescue the *insm1a* morphant phenotype, with an average of 67, 64, and 26.3 cone PRCs per retinal section, respectively. Statistical analysis showed that the rescue of the morpholino-induced cone PRC deficit was equivalent for the *insm1a_WT* and *Insm1_K141X* rescue constructs, and that the cone PRC numbers were not significantly different between the control MO, the *insm1a_WT* rescue and the *insm1a_K141X* rescue. The cone PRC number in the *insm1a_Nterm* mRNA rescue was significantly different from both the control and *insm1a* morphants. (Figure 3.5C).

3.3.4.3 Rod PRC number was significantly rescued by all insm1a mRNA variants

The number of rod PRCs per retinal section was counted after IHC with the rod PRC specific antibody 4C12. Similar to the previous morpholino studies, rod PRCs were significantly

reduced in the *insm1a* morphants compared to control morphants, with 2.7 and 40.3 rod PRCs per retinal section, respectively. The *insm1a_WT, insm1a_K141X,* and *insm1a_Nterm* mRNAs all provided significant rescue of the *insm1a* MO after co-injection, with an average of 29.6, 14.2, and 10.7 rods per retinal section, respectively. Statistical analysis determined that the rod PRC rescue was similar for both the *insm1a_K141X* and *insm1a_Nterm* mRNA sequences (Figure 3.5), while remaining significantly reduced compared to both control morpholino and *insm1a_WT* mRNA rescue.

3.4 Discussion

The failure of a mutant to phenocopy a morphant phenotype is not an uncommon situation, with a recent study describing this failure rate at between 50 and 80% [185]. However, before discounting the *insm1a* morpholino results it is important to look closely at the studies used to produce this estimate of morpholino quality, and to explore additional potential confounding variables in the analysis of the mutant.

A recent paper by Kok et al., showed a low correlation between published morphant phenotypes and the phenotypes observed in later generated mutants of the same gene. Using a literature search of the studies in question, revealed that while some of the phenotypes observed in the morpholino experiments may have been spurious, the vast majority of the morpholino studies for which this is true were not adequately controlled (Table 4.1). Among the 31 mutants for which literature search produced a full experimental design, only 5 mutants (16.1%) phenocopied the morpholino experiment. However, only 12 morpholino experiments included any mRNA rescue of the morphant phenotype (38.7%) to attempt to show specificity, and only 5 (16.1%) used a zebrafish mRNA. This is important, as our lab and others have shown that the ability of a human mRNA ortholog to rescue the zebrafish morphant phenotype is not equivalent to the level of rescue observed with the zebrafish mRNA [186]. Additionally, only 9

experiments (29%) used two independent morpholinos and had adequate controls (either a mismatch morpholino or standard control morpholino). In total, only 3 of 31 experiments (9.6%) contained the minimum controls for morpholino experiments as described in [71, 72, 187]. The previously completed *insm1a* morpholino experiments, however, were properly controlled, with 2 separate morpholinos, a standard control morpholino, and mRNA rescue included; thus reducing the chances that the effect of *insm1a* knockdown was non-specific. One remaining possibility is that the morpholino rescue was non-specific. Although we did not observe any rescue when co-injecting a GFP mRNA, it could be possible that injection of any zebrafish mRNA would be sufficient to rescue the morphant phenotype.

The additional rescue experiments described here provide additional evidence that the mutant sequence retains at least some wild-type function. However, these experiments were unable completely separate which mechanism underlies this function. The rescue of the cone PRCs was nearly equivalent for the 2 full length mRNAs, while being significantly lower for the N-terminal truncation. This result could indicate that translational readthrough is occurring in the *insm1a_K141X* mutant, and that this readthrough underlies the observed lack of a retinal phenotype. However, the rescue of the rod PRCs was reduced in both the full length *insm1a_K141X* and in the truncated *insm1a_Nterm* mRNA rescues compared to the wild-type rescue. Additionally, both full length and the N-terminal rescues had significantly increased numbers of both rod and cone PRCs compared to the *insm1a* morpholino alone, clearly indicating at least partial functionality in all 3 mRNA variants containing the N-terminal portion of the *insm1a* sequence. This maintenance of Insm1 function with only the N-terminal portion of the protein is not without precedence. Similar N-terminal truncations of INSM1 have been shown to maintain the ability to bind RACK1 and enhance the insulin receptor signaling pathway [133] and to bind CyclinD1 and induce cell cycle arrest [132].

The attempted rescue of the morphant phenotype with a C-terminal truncation variant resulted in additional, more severe developmental defects. Because the C-terminal portion contains the zinc-finger DNA binding domains, it is possible that any protein produced, which folds properly, is acting as a sink for sequences or factors bound by the Insm1a zinc finger domains. Alternatively, the absence of the N-terminal portion could cause misfolding resulting in other unexpected interactions.

In the previously discussed rescue experiments, mRNA injection is assumed to result in protein translation and folding. In the absence of an Insm1a antibody, mRNA stability, the extent of non-sense mediated decay, rates of protein translation and degradation are unknown. Potential explanation for the differences in the ability of the full length and N-terminal truncations to rescue the two PRC-specific morpholino phenotypes could be that the longer mRNA is more stable, that the N-terminal truncation product folds less well or improperly, or that the resulting protein is more likely to be targeted for degradation. Repeating the rescue experiments with tagged mRNA (HA or FLAG for example) might permit the mechanism to be examined more closely at the protein level. This approach could prove problematic, as the N-terminal most amino acids are known to possess the bulk of the transcriptional regulatory activity [79], and the site of the truncation mutation is within the dibasic motif required for nuclear localization [81].

Chapter 3 Figures:

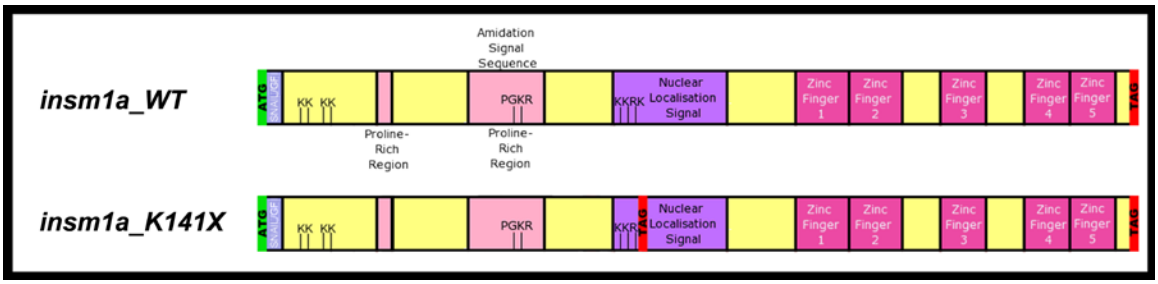

Figure 3.1: Schematic of *insm1a* wild-type and mutant alleles

The wild-type *insm1a* allele encodes a 384 amino acid peptide, with an N-terminal SNAIL/GFI domain, which has homology with the SNAIL/GFI superfamily of transcriptional repressors. The N-terminal domain additionally contains 2 proline-rich regions that have been implicated in protein-protein interactions, and a putative nuclear localization signal sequence. The C-terminal portion of the protein contains 5 zinc-finger DNA binding motifs. In the *insm1a* mutant, a single A to T transversion results in the conversion of the Lysine at amino acid position 141 to a premature stop codon. The resulting protein should lack both the zinc finger DNA binding domains and the bulk of the nuclear localization signal sequence.

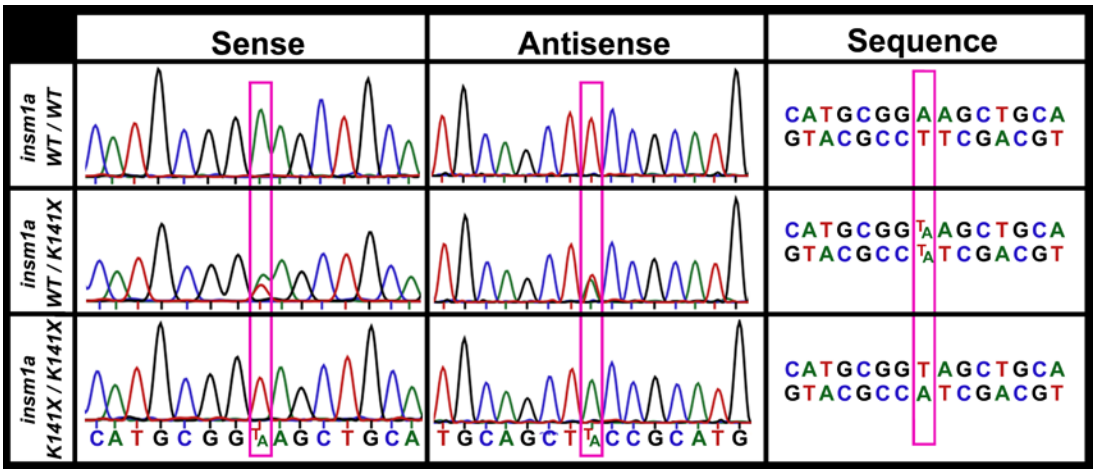

Figure 3.2: Genotyping analysis of *insm1a* alleles

Histograms and sequences of genotyping from *insm1a* variants. Pink boxes indicate the single nucleotide that is changed between the wild-type and mutant *insm1a* alleles. The coding strand A is changed to a T in the mutant sequence. Heterozygotes are identified primarily using the histogram, which shows a characteristic double peak at the mutation site.

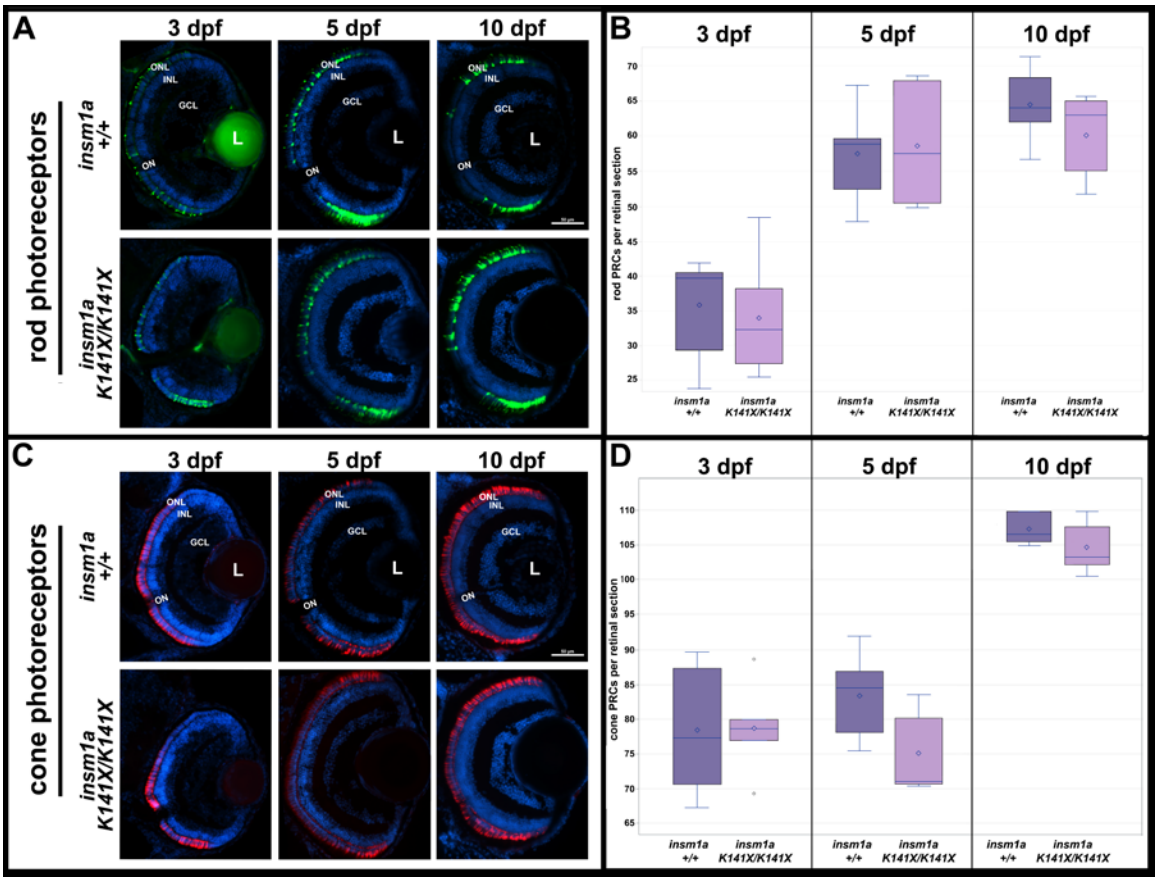

Figure 3.3: The insm1a_K141X mutants have no changes in retinal development.

A,C: Retinal sections at 3, 5, and 10 dpf show no changes in retinal organization and lamination between wildtype *insm1a* and *insm1_K141X* mutants. **B,D:** Cell counts revealed no statistically significant changes in either rod or cone cells at any time point. (rod PRCs: n=6 retinal sections from 6 animals, cones PRCs n=5 retinal sections from 5 embryos; ◊=mean; scale bars = 50µm; ONL, outer nuclear layer; INL, inner nuclear layer; GCL, ganglion cell layer; L, lens; ON, optic nerve; dpf, days post fertilization; PRCs, photoreceptor cells).

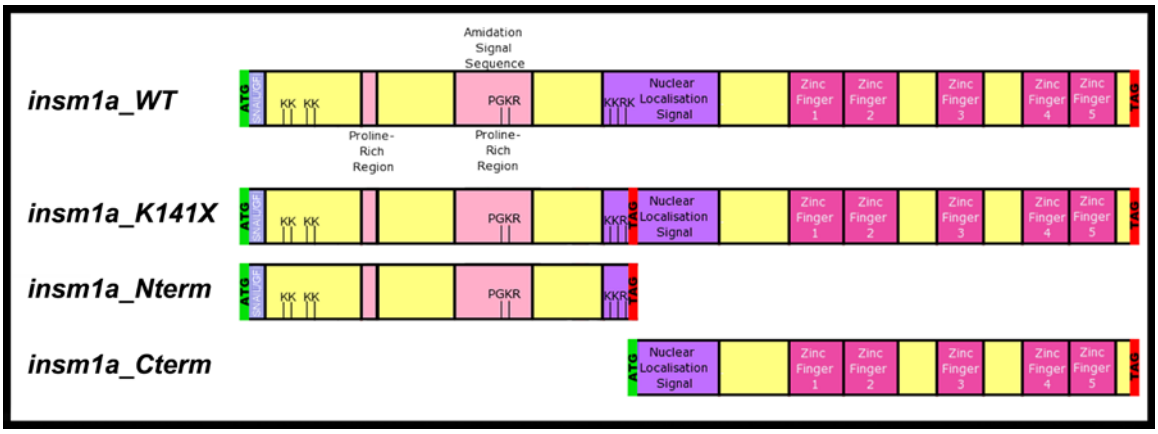

Figure 3.4: Schematics of insm1a variants for analysis of truncated protein function

Both the *insm1a_WT* and *insm1a_K141X* mRNAs include the entire 1152 bp coding region with a stop codon at the terminal end of the mRNA, the K141X allele has an additional stop codon replacing the lysine at amino acid position 141. The *insm1a_Nterm* mRNA is a 423 bp truncation variant that includes the sequence from the start codon through the stop produced by the A-to-T mutation at nucleotide 421. This N-terminal truncation includes the SNAIL/GFI domain and the proline-rich protein-protein interacting domains, but lacks the bulk of the nuclear localization signal sequence, and has no zinc-finger DNA binding domains. The *insm1a_Cterm* mRNA is a 732 bp truncation variant that results in the lysine at amino acid position 141 being converted to a start codon. This C-terminal only truncation contains the zinc-finger DNA binding domains and a portion of the putative nuclear localization signal sequence, but none of the protein-protein interacting domains, and no SNAIL/GFI domain.

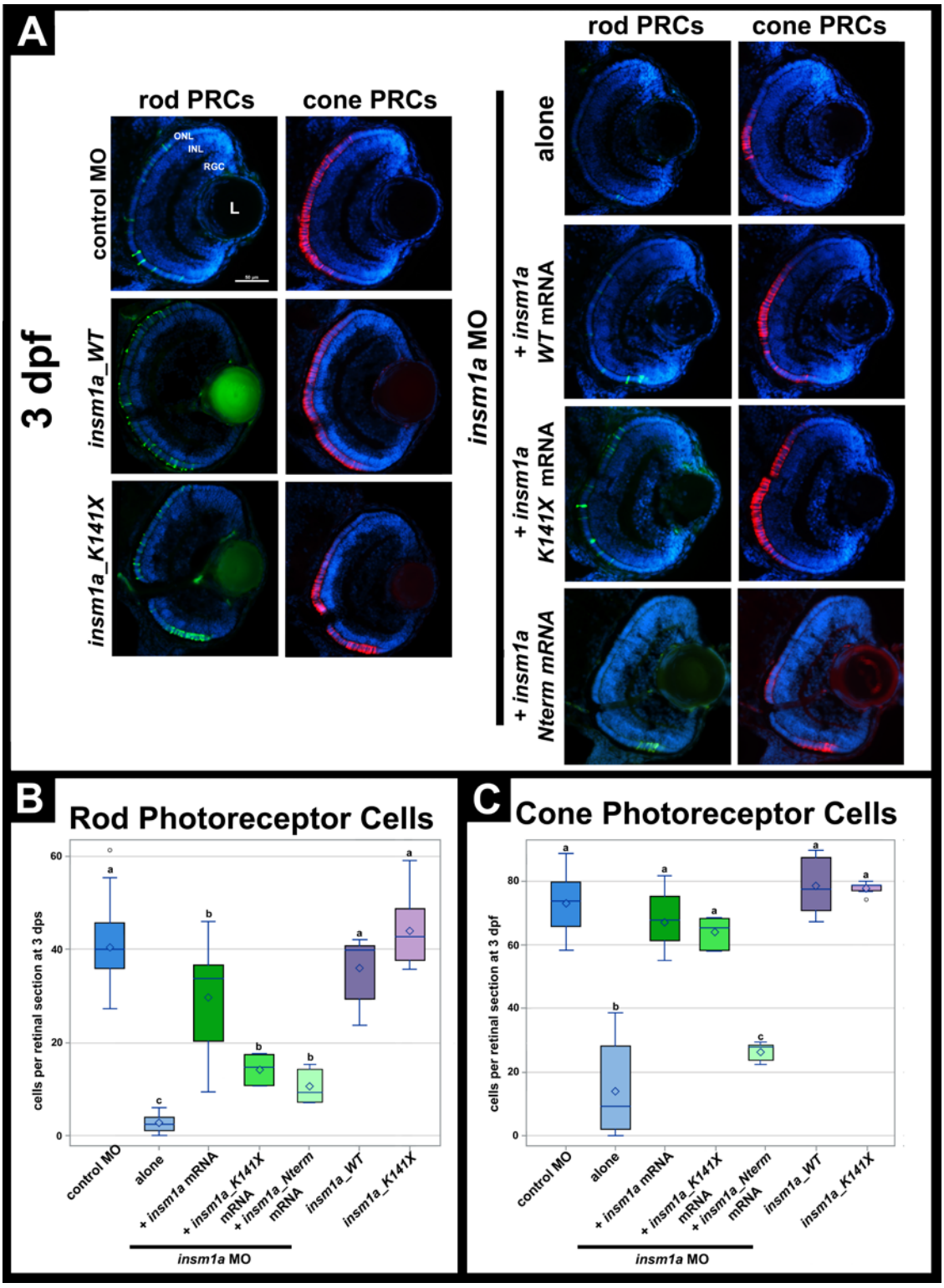

Figure 3.5: *Insm1a_K141X* and *insm1_Nterm* mRNAs rescue the *insm1a* morpholino phenotype.

Figure 3.5: *Insm1a_K141X* and insm1_Nterm mRNAs rescue the *insm1a* morpholino phenotype (continued).

A: Comparison of retinal sections at 3 dpf from control morphants, *insm1a_WT* and *insm1a_K141X* mutants, *insm1a* morphants, *insm1a* morphants with wild *insm1a_WT*, *insm1a_K141X,* and *insm1a_Nterm* mRNA rescues. Retinal lamination is consistent throughout all groups. **B:** Counts of rod photoreceptor cells in each group. The *insm1a_K141X* and *insm1a_Nterm* mutant mRNAs were able to rescue the *insm1a* morpholino as well as the wild-type *insm1a* mRNA, which is evidence of residual function of the mutant sequence, which does not rely on translational read through. Statistical analysis grouped: (a) control morphants, *insm1a_WT* and *insm1a_K141X* mutants; (b)*insm1a* morphants *with insm1a_WT mRNA, insm1a* morphants with *insm1a_K141* mRNA, and *, insm1a* morphants with *insm1a_Nterm* mRNA; (c) *insm1a* morphants. **C:** Counts of cone photoreceptor cells in each group. The *insm1a_K141X* mutant mRNA is able to rescue the *insm1a* morpholino as well as the wild-type *insm1a* mRNA, while the *insm1a_Nterm* mRNA provides lesser though still significant rescue of the *insm1a* morphant. Statistical analysis grouped: (a) control morphants, *insm1a_WT, insm1a_K141X* mutants; *insm1a* morphants *with insm1a_WT mRNA,* and *insm1a* morphants with *insm1a_K141* mRNA; (b) *insm1a* morphants, (c) *insm1a* morphants with *insm1a_Nterm* rescue. (Control MO: n=34 retinal sections from 34 embryos for rods and n=29 retinal sections from 29 embryos for cones. *Insm1a* MO: n= 27 retinal sections from 27 embryos for both rods and cones. *Insm1a* MO + *insm1a_WT* mRNA: n=19 retinal sections from 19 embryos for both rods and cones. *Insm1a* MO + *insm1a_K141X* mRNA: n= 6 retinal sections from 6 embryos for both rods and cones. *Insm1a* MO + *insm1a_Nterm* mRNA: n = 5 retinal sections from 5 embryos for both rods and cones. *Insm1a_WT*: n=6 retinal sections from 6 embryos for rods, and n=5 retinal sections from 5 embryos for cones. *Insm1a_K141X*: n=6 retinal sections from 6 embryos for rods, and n=5 retinal sections from 5 embryos for cones. ANOVA, rods: $F = 77.44$, $Prob > F < 0.001$, cones: $F = 119.16$, $Prob > F < 0.0001$; ◊=mean; scale bars = 50µm; ONL, outer nuclear layer; INL, inner nuclear layer; GCL, ganglion cell layer; L, lens; ON, optic nerve; dpf, days post fertilization; PRCs, photoreceptor cells).

CHAPTER 4: EXAMINING INSM1 FUNCTION IN THE MOUSE RETINA USING AN INSM1 KNOCKOUT MOUSE

Marie A. Forbes-Osborne[1], Sarah M. Lorenzen[2], Jaime Garcia-Anoveros[2], Ann C. Morris[1]
[1]Department of Biology, University of Kentucky, Lexington, Kentucky 40506-0225
[2]Feinberg School of Medicine, Northwestern University, Chicago, Illinois 60611
Key words: Insm1, mouse, eye, retina, RNA-seq

4.1 Introduction

Proper retinogenesis is built upon a highly interconnected network of transcriptional regulatory machinery. Misexpression of any player can have far reaching effects. Understanding the interactions between factors is essential to understanding both normal retinal development and the development of retinal malformations. Insm1 is known to act within several different developmental regulatory pathways. However, the pathway involved varies between tissues (see Figure 1.3). For example, Insm1 is downstream of BMP signaling, Ascl1, and Phox2b in sympatho-adrenal development, but downstream of Notch signaling, Pdx1, and Ngn3 in endocrine pancreas development. Additionally, Insm1 is a regulator, perhaps indirectly, of Phox2a and Gata3 in the sympatho-adrenal system and of NeuroD and Insulin in endocrine pancreas. This, together with the tendency of Insm1 to be involved in self and feedback regulatory loops and the paucity of genes known to be regulated by *Insm1* supports the use of an unbiased approach to identify genes downstream of *Insm1* in the retina.

Gene expression analysis by RNA-seq uses next generation sequencing technology to provide a snapshot of transcription levels within a set of samples. This permits computational identification of changes in gene expression between samples. RNA is extracted from matched tissues and mRNA is enriched, either by Poly(A) hybridization or rRNA depletion. Strand synthesis produces cDNAs, which are ligated to identification adaptors. After adaptor ligation, samples may be amplified by PCR. The samples are then pooled and sequenced using one of the

next generation sequencing platforms, for example, Illumina HiSeq 2000/2500 or GS FLX+. These experiments can generate hundreds of millions of 40-400 base pair reads depending on the platform used. The reads are then checked for quality, trimmed to remove adaptors and low quality reads, and mapped to either an existing genome or transcriptome. After mapping, transcript abundance is estimated and used to identify genes which are differentially expressed between samples [188]. Using RNA-seq will allow us to identify genes which are altered in the retina when *Insm1* expression is ablated during development.

Although we had initially planned to complete these experiments using the zebrafish, we chose to move into the mouse for several reasons. First, we wanted to use a knockout or a mutant and not a morphant. The limitations of the morpholino, most importantly potential questions about specificity and off target effects of morpholinos (further discussed in Chapters 3 and 5) were an important consideration. While we had characterized an *insm1a* mutant in the zebrafish, we could not identify any pathogenic effects of that mutation (See Chapter 4 and 5), and the generation and characterization of additional mutants would delay the experiments extensively. Second, we needed to consider the amount of tissue which would be required for the RNA-seq analysis and for the subsequent experimental validation, as well as our ability to faithfully dissect away all the surrounding brain tissue, which also expresses *insm1a.* These were serious obstacles given the small size of the developing zebrafish embryo and eye, especially with the very close association of the highly *insm1a* expressing olfactory epithelium. As a result, we collaborated with the lab of Dr. Jaime Garcia-Anoveros at The Northwestern University Feinberg School of Medicine, where a mouse *Insm1* knockout had been previously generated [189], to perform RNA-seq analysis of wild-type and Insm1 knock out eyes during development.

A 3.4 kb genomic locus, containing the entire 2.9kb single exon *Insm1* gene, was replaced by homologous recombination with a neomycin resistance cassette flanked by *loxP*

sites using Sv129 mouse-derived HM1-M embryonic stem cells. The recombined stem cells were injected into C57BL/6 blastocysts to generate chimeras. Chimeras that transmitted the knockout cassette were crossed to a ubiquitously expressed E2a-Cre transgenic mouse to remove the neomycin cassette. The resulting mouse retained a single *loxP* site in place of the *Insm1* locus (hereafter this locus will be referred to as *Insm1^{-})*. The generation and validation of this mouse has been previously described in [189].

Insm1$^{-/-}$ is embryonic lethal, with decreased survival of pups observed after E16 and no *Insm1$^{-/-}$* animals recovered at P0. Backcrosses into the CD1 outbred line permitted *Insm1$^{-/-}$* embryos to be reliably obtained up to E18.5, and occasionally obtained as late as E20.5 though at reduced percentages. As a result, *Insm1$^{+/-}$* animals were used to generate timed pregnancies, and tissues were collected for RNA preparation, histology, and genotyping.

Based on the morpholino experiments outlined in Chapter 2, and previous *Insm1* expression studies in the mouse, we chose to focus on two distinct periods of retinal development. The first was the proliferative phase, when most retinal cells remain in the cell cycle. The morpholino experiments showed a delay in cell cycle progression between 30 and 36 hpf, when *insm1a* expression was reduced, suggesting a role for *Insm1* in regulating retinal cell proliferation. The similar period of retinal development in the mouse is E14.5, when most of the retinal cells remain undifferentiated progenitors[190] . Specification of these cells has already begun, however, and differentiation is beginning to occur in some cell subtypes [191].

The second period of interest was the window of photoreceptor specification and differentiation. Cone photoreceptors are generated earlier than rod photoreceptors, with the bulk of cone differentiation occurring by birth. Although the bulk of rod photoreceptor genesis in the mouse occurs in the early postnatal period, and the peak is at P0, the onset of differentiation occurs much earlier, with significant numbers of rod photoreceptors

differentiating beginning at E16 [191]. In light of the largely non-overlapping periods of rod and cone genesis, and the embryonic lethality in the *Insm1*$^{-/-}$ mouse, we opted to use the latest embryonic stage at which we could reliably obtain embryos, E18.5.

4.2 Materials and Methods

4.2.1 Mouse breeding and maintenance

Insm1 knockout mice were generated and maintained by the Garcia-Anoveros laboratory at the Northwestern University Feinberg School of Medicine. All procedures were carried out in accordance with guidelines established by the Northwestern University Institutional Care and Use Committee.

4.2.2 Generation of homozygous knockout embryos

Heterozygous mice were used to generate timed pregnancies, with males and females being co-housed for a single overnight period. The presence of a plug along with consistent weight gain were used as indicators of pregnancy. Midnight of the mating period was considered E0. At the desired developmental stage, dams were sacrificed by isoflurane overdose and cervical dislocation.

Embryos were harvested at E12.5, E14.5 and E18.5. For RNA preparation, E14.5 and E18.5 eyes were dissected in PBS, rinsed and transferred to Trizol before being stored at -80°C. For histology, embryos were decapitated, and fixed in 4% PFA . Tissues for genotyping were also collected from each embryo and flash frozen. All samples were shipped overnight with frozen samples on dry ice and PFA samples on cold packs. Upon receiving, Trizol-stored tissues were stored at -80°C, tissues for histology were cryoprotected in 15% sucrose and embedded in OCT for sectioning, and genotyping samples were used for genomic DNA prep using the Qiagen Blood and Tissue Prep Kit according to the manufacturer's instructions.

4.2.3 Genotyping PCR

PCR genotyping for the both the *Insm1*$^{-}$ and *Insm1*^{WT} alleles used the forward primer 5'-TTTGGAAGCCAGCCAGCA-3'. PCR genotyping for the *Insm1*$^{-}$ allele used the reverse primer 5'-CCCGATTCTTGTGAGAGAGGAGGA-3', while PCR for the *Insm1*^{WT} allele used the reverse primer 5'-GGGAACGCGCAACTCAACTC-3'. Primers were synthesized by Eurofins Operon MWG, LLC (Huntsville, AL). Because of the high GC content of the amplicons, all PCR reactions used Invitrogen recombinant Taq DNA polymerase (Item: 10342; ThermoFisher Scientific, Grand Island, NY) supplemented with 5M Betaine (Item: B0300, Sigma-Aldrich, Saint Louis, MO).

For each time point, E14.5 and E18.5, samples were generated from single embryos, across multiple litters. For RNA, both eyes were dissected from individual embryos. Additional tissue was collected and frozen for genotyping. After extracting genomic DNA (gDNA) from the frozen tissue, paired PCR experiments were completed to determine the status of the *Insm1* locus in each animal (Figure 3.1). PCR was repeated as necessary to ensure correct genotypic identification.

4.2.4 RNA preparation and quality analysis

For the RNA-seq experiment, all RNA samples for a given time point were prepared simultaneously. RNA was extracted from samples frozen in TRIzol Reagent (Life Technologies, Invitrogen), following the manufacturer's protocol. RNA was treated with RNAse-Free DNAse I (Roche, Indianapolis, IN) to remove genomic DNA. RNA concentration and quality were determined by spectrophotometric analysis (NanoDrop, Wilmington, DE) and by microfluidic chip using the Bioanalyzer 2100 and RNA 6000 Nano Kit (Item: 5067, Agilent Technologies, Santa Clara, CA), following manufacturer instructions. Only RNA samples with RIN >8, A260/230 >1.5, and A260/280 >1.5 were used for RNA-seq and quantitative PCR experiments.

4.2.5 Library prep and sequencing

RNA samples for RNA-seq were shipped overnight on dry ice to the Next Generation Sequencing Lab (Eurofins Operon MWG, LLC, Huntsville, AL), where 3'Fragment Library prep was completed. This library prep uses a proprietary technology to produce a next generation sequencing library. Samples were tested for quality both before and after library prep. Libraries were sequenced on an Illumina HiSeq 2500, using standard chemistry.

4.2.6 RNA-Seq analysis

Fastqillumina sequence files generated from the library sequencing were uploaded to the Galaxy Browser (usegalaxy.org) [192-194]. Initial quality checking was completed using FastQC [195] to examine the per base and per sequence quality. Sequence files were converted from Fastqillumina to Fastqsanger using FastQ Groomer, and used to generate summary statistics and boxplots of quality scores. Sequences were trimmed to remove any bases with quality scores of less than 20 using FastQ Trimmer [196]. Tophat2 was used to map trimmed reads to the Mus musculus genome (mm10). Standard parameters were used, except that junction data and gene annotation models were provided using gene and gene prediction tables downloaded from the USC main table browser (available at genome.uscs.edu). After alignment, raw counts were calculated for each sample, using Cufflinks [197]. As the 3' fragment library used in these experiments produces a single read for each transcript, no length correction was applied. Assembled and skipped transcripts for each experimental condition were merged using Cuffmerge to produce a single assembly for each sample at each time point. The mouse genome assembly from above was used as a guide. Expression changes were identified from merged datasets using Cuffdiff2, with classic (non-scaling) normalization, a false discovery rate of 0.05, pooled estimates of dispersion, and no length correction. Length correction was not required due to the use of the 3' fragment library prep as discussed previously. Transcript IDs were

converted to gene symbol lists, and gene names were added using the Database for Annotation, Visualization and Integrated Discovery (DAVID) (available at: david.ncifcrf.gov/) [198], the Ensembl Mouse Genome Browser (available at: useast.ensembl.org/Mus_musculus/Info/Index), and BioGPS (available at: biogps.org/) [199-201].

4.2.7 Pathway and GO Term based analyses

For each condition, differentially expressed genes (DEGs) with an absolute fold change of 1.5 or greater were uploaded to Enrichr (available at amp.pharm.mssm.edu/Enrichr/)[202]. For each category of DEGs (E14.5 increased in *Insm1a*$^{-/-}$, E14.5 decreased in *Insm1a*$^{-/}$, E18.5 increased in *Insm1a*$^{-/-}$, and E18.5 decreased in *Insm1a*$^{-/-}$), Pathway based analyses were generated using the National Cancer Institute Pathway Database and the Panther classification system.

4.2.8 Histology and Immunohistochemistry

Ten micron sections were cut on a cryostat (Leica CM 1850, Leica Biosystems, Buffalo Grove, IL), mounted on poly-lysine coated slides, and stored at -20°C. Slides were pre-warmed, and sections were rehydrated and postfixed in 3.7% PFA for 30 minutes at room temperature. After 3x 10 minute washes in Dulbecco's PBS containing Calcium and Magnesium (hereafter DPBS+ions), sections were permeabilized for 2 hours with 0.2% Triton X-100 in DPBS+ions at room temperature. After 3x10 minute washes in DPBS+ions with 0.05% Trition X-100 (hereafter Wash Buffer), sections were blocked for at least 2 hours in Wash Buffer containing 10% Normal Goat Serum at 37°C. Slides were incubated with primary antibodies in Wash Buffer with 5% Normal Goat serum, overnight at 4°C in a humidified chamber. The following day, slides were transferred to 37°C and incubated, still in primary antibody, for a minimum of 3 hours. Slides were rinsed in DPBS+ions, then washed 3x30 minutes in Wash buffer, then incubated with secondary antibody in Wash Buffer for 2 hour at 37°C in the dark. Slides were washed 3x30

minutes with Wash Buffer, 3x5 minutes with DPBS+ions, counterstained 10 minutes with DAPI (4', 6-diamidino-2-phenylindole, 1:10,000 dilution; Sigma-Aldrich) in DPBS+ions, and washed 3x5 minutes with DPBS+ions. Prior to mounting, slides were moved through a DPBS pH gradient (down to pH6.2) to reduce background, with a minimum of 2 hours and a maximum of 0.2 pH change per step. Before imaging, slides were mounted in 40% glycerol in PBS. Images were obtained on an inverted fluorescent microscope (Eclipse Ti-U; Nikon Instruments), using a 40X objective. All steps except for antibody incubations were performed under constant slow rotation. The following antibodies were used: Tuj1 (1:500 dilution), a monoclonal antibody that recognizes neuron specific Class III ß-tubulin (Covance Inc., Princeton, NJ); Alexa Fluor 488 goat anti-mouse, 488 goat anti-rabbit, 546 goat anti-rabbit, 546 goat anti-mouse (Molecular Probes, Invitrogen), 647 goat anti-rabbit and Cy5 conjugated goat anti-mouse (Jackson ImmunoResearch, West Grove, PA). Alexa 488 and 546 secondary antibodies were all used at 1:200 dilution, 647 and Cy5 secondary antibodies were used at 1:150 dilution.

4.3 Results

4.3.1 RNA-seq Analysis of wild-type and Insm1 knockout mouse eyes in embryonic development

To identify gene expression changes associated with *Insm1* ablation, RNA was isolated from pairs of E14.5 or E18.5 eyes (6 embryos, 12 eyes at each time point, 3 each from WT and *Insm1*$^{-/-}$). Twelve 3' fragment libraries were produced by Eurofins Operon MWG, LLC. A single Illumina HiSeq lane produced a total of nearly 209 million reads across the 12 samples (Table 4.1). Mean quality scores exceeded 35 (35.6-36.3), with more than 93% of reads having a minimum quality score greater than or equal to 30 (92.1%-94%). Using Tophat, 172.8 million reads could be aligned to the mouse genome, representing more than 82% of the total reads. After Cufflinks analysis of merged data sets for each time point, we were able to detect 23,130 transcripts at E14.5 and 23,795 transcripts at E18.5, of which 20,911 at E14.5 and 21,293 at E18.5 had an FPKM value greater than 1.0 in any of the samples.

At E14.5, 1158 transcripts were determined to be differentially expressed (DETs), with at least a 2 fold change in expression between WT and *Insm1*$^{-/-}$, and a p-value ≤0.05. Of these, 377 were increased in the *Insm1*$^{-/-}$, while 781 were decreased. We were able to identify a single known or predicted gene for 1029 of these transcripts (288 with increased and 741 decreased expression in the *Insm1*$^{-/-}$). At E18.5, 1332 DETs were identified (771 with increased expression and 561 with decreased expression in the *Insm1*$^{-/-}$), representing 1008 unique known or predicted protein coding genes (644 increased and 364 decreased) (Table 4.2). The Top 25 differentially expressed, annotated genes (DEGs) for each time point are listed in Table 4.3 and 3.4. A comprehensive list of all transcripts is included as Appendix II, as the data set has not yet been uploaded to the NCBI Gene Expression Omnibus.

Pathway analysis of the DEGs at each time point was completed using Enrichr. Enrichr is a web-based platform for identifying biologically related or connected pathways and other

networks which demonstrate a significant association with the DEGs identified in the experimental data set. Using the NCI Pathway databases, more than 175 pathways were determined to be enriched in the E14.5 DEGs, and more than 225 were identified from the E18.5 DEGs. The top 15 up- and downregulated pathways (using the combined statistic) are in Table 4.5A-B and Table 4.6A-B.

4.3.2 At E14.5 and E18.5 eyes from Insm1 knockout mice have altered cell survival and cell death pathways

At E14.5, multiple pathways normally involved in cell survival, either through inhibition of apoptosis promoting factors or through increased cell survival, were identified in the downregulated pathways. This includes direct p53 effectors and Integrin-Linked kinase (ILK) signaling. Pathways with dual survival/cell death roles were also identified, including the p53 pathway, p38-gamma and p38-delta pathway, and mTOR signaling. Some genes associated with these pathways are known to be anti-apoptotic, while others are dual use acting in both cell survival and cell death. Fewer upregulated genes were associated with these pathways. The pathways identified include several cell death associated pathways, including 2 different p63 isoform target pathways and the p73 pathway. The p53 pathway was also identified. At E18.5, pro-apoptotic pathways, including the Caspase Cascade in Apoptosis, the p73 pathway, and Regulation of Retinoblastoma protein were overrepresented in the upregulated pathways category. The ILK signaling pathway remained downregulated as well.

The downregulation of cell survival and anti-apoptotic pathways along with the upregulation of pro-apoptotic pathways could indicate an increase in cell death. Alternatively, they could indicate an increase in cell stress, which has not yet begun to cause cell death at E14.5. Preliminary immunohistochemistry at this time point showed no gross changes in retinal thickness or structure (Figure 3.2) that might indicate cell death is occurring, but additional

experiments will be required to determine whether there is a significant change in cell death at either E14.5 or E18.5 in the *Insm1* knockout.

3.3.2 At E14.5 Cell cycle regulatory pathways were enriched in *Insm1* knockouts

Several cell cycle regulatory pathways were also over-represented at E14.5. At E14.5 down regulated pathways included the Aurora A signaling, CDC42 mediated signaling and Regulation of Retinoblastoma Protein pathways. All are required for normal cell cycle progression in healthy cells, and decreased signaling could indicate either unregulated cell division or cell cycle arrest. At E18.5 upregulated pathways included: the Regulation of Retinoblastoma Protein pathway, the Fanconi Anemia pathway, the Aurora B pathway, and the E2F Transcription factor network. These all contain genes involved in cell cycle regulation or proliferation, though the Fanconi Anemia pathway also includes DNA repair genes in addition to cell cycle checkpoint genes.

While cell cycle dysregulation is the likely outcome of changes in these pathways, we have not determined the functional changes associated with the gene changes. Many of the factors involved in cell cycle regulatory pathways are capable of both negatively and positively regulating cell cycle, with the direction of regulation determined by cellular context and post-translational modifications. The absence of expression changes in genes like *Rb1*, which is known to be modulated by phosphorylation state [203], should be noted. However, it is possible that post-translational modifications are present, and that these modifications are essential to retinal development. This possibility is especially interesting, given the number of kinase genes whose expression is altered in the *Insm1* knockout (19 down and 2 up at E14.5, and 6 down and 22 up at E18.5).

4.3.3 Chromatin modification genes are differentially expressed in the Insm1 knockout eye

At E14.5, a number of genes with known chromatin modification functions were identified. These included the downregulated expression of genes with acetylation and acetyltransferase activity (*Ep300, Myst2, Sirt6*); as well as a number of genes which regulate chromosome condensation (*Suv39h1*, *Chd4*), sometimes in a cell cycle specific manner (*Nacph, Smc1, Ppp2r1a*). Upregulated genes include genes that act in maintaining chromatin in actively dividing cells (*Smc1b*, *Zfp42*), and factors involved in chromosome remodeling and de-novo chromatin assembly (*Smarca1*, *Chrac1*).

At E18.5, fewer differentially expressed genes are associated with chromatin modification, but a trio of upregulated factors all act in chromatin modification during the cell cycle (*Brd2, Sirt6, Smc2*). The increase in cell cycle positive factors could indicate an increase in the number of cells which have remained in the cell cycle, at the expense of cell cycle exit and differentiation. Alternatively, it could be indicative of an overall delay in retinal development or an increase in cell cycle length. That each overexpressed gene acts in a different phase of the cell cycle, with Brd2 regulating CyclinD1, Sirt6 acting to de-condense chromatin for S phase entry, and Smc2 required for chromatin condensation prior to M-phase entry [204], makes it unlikely that an increase in cell cycle length alone could account for these changes. Analysis of numbers of dividing cells in the knockout and wild-type retinas could provide additional information concerning cell cycle exit timing and determine if aberrant cell division or maintenance of proliferative state occurs the absence of *Insm1.*

4.3.4 Photoreceptor cell specification and maturation genes are differentially expressed in the Insm1 knockout

The Visual Signal Transduction: Cones pathway was upregulated at E18.5. This pathway includes an activator of guanylate cyclase in the absence of free calcium (*Guca1b*), which is

required for rod PRCs to return to the dark state after light exposure, and a guanine nucleotide binding protein (*Gnb3*), which modulated signal transduction.

Although the individual genes were not identified by the pathway analysis, clear differences in other photoreceptor associated genes were identified using a candidate gene approach. As mitotic retinal progenitors begin to leave the cell cycle and become post-mitotic, they express *Rb1* and *Otx2*. Induction of *Crx* and *Nrl* push the cells towards the photoreceptor lineage. If *Nrl* and *Crx* expression are maintained, and *Nr2e3* expression is added, the post-mitotic cells become rod precursors, and begin to express rhodopsin. If *Crx* expression is maintained, but *Nrl* expression lapses, the post-mitotic cells become cone precursors. The addition of *Rorb* specifies the S-cones, which will express *Opn1sw*; *Trb2* (also known as *Thrb*) specifies M-cones, which will express *Opn1mw*. Additional phototransduction pathway genes are expressed during photoreceptor cell maturation. These genes differ between rod and cone photoreceptors, and include the transducin subunit gene *Gnat1*, and the phosphodiesterase genes *Pde6a* and *Pde6g* in the rod photoreceptors, and the cone photoreceptor specific *Gnat2* and *Pde6c*.

In the *Insm1 KO, Rb1* expression is unchanged at both E14.5 and E18.5 when compared to the wild-type. At E14.5, *Otx2 and Crx* were downregulated in the *Insm1* knockout eyes, and both genes met the fold change and p-value cutoffs previously described. *Nrl, Nr2e3, Trb2* and *Ops1sw* are altered at E14.5, but unchanged at E18.5, with only N*r2e3* and *Opn1sw* unregulated, while the remainder were all downregulated in the *Insm1* knock out. *Rorb* was downregulated at E14.5, but upregulated at E18.5. Although these genes failed to meet the fold change or p-value cutoffs, they were consistently differentially expressed. Additional genes with known roles in photoreceptor cell specification, maturation, or function were also differentially expressed, including *Pouf4f1, Prdm1, Tulp1* and *Pde6g,* all of which met out cutoff values, as well as *Atoh7,*

Gnat1, Gnat2, Mab21l2, Nr1d1, Pde6d, and *Pou4f3,* all of which just missed the cutoff values despite being consistently differentially expressed. Rhodopsin was not expressed at E14.5 in either wild-type or *Insm1* knockout retinas, and was unchanged between the *Insm1* knockout and the wild-type at E18.5. However, this was not necessarily unexpected, as even at E18.5 rhodopsin expression is very low. Ops1mw was not detected in any sample at either time point. These results are summarized in Figure 3.3, for both time points.

4.4 Discussion

In this study, we used RNA-seq analysis to identify changes in gene expression resulting from the knockout of *Insm1.* Using RNA from E14.5 and E18.5 eyes, we have identified numerous genes with altered expression by comparing *Insm1* knockout to the wild-type. The use of E14.5 eyes was intended to capture changes in gene expression at a time when many retinal progenitor cells remained in the cell cycle, and retinal cell differentiation was relatively scarce. In light of the photoreceptor specific phenotype of the *insm1a* morphant zebrafish, photoreceptor specification, maturation and maintenance genes were clear targets. The bulk of rod photoreceptor differentiation occurs postnatally. However, the embryonic lethality of the *Insm1* knockout precluded analysis at time points beyond E18.5. Many general photoreceptor specification genes and rod photoreceptor specification genes are expressed prior to E18.5, which permitted the analysis of rod specification factors, though not mature rod markers, like rhodopsin.

The use of pathway analysis allowed us to examine the changes in gene expression in a biologically relevant context. Rather than relying on Gene Ontology (GO) Terms to individually place genes into categorical groups, pathways analysis uses context and sample dependent cues (including other differentially expressed genes) to place genes in biologically meaningful networks. This allowed us to identify developmental pathways and genetic cascades involved in

cell cycle regulation, pro- and anti-apoptotic signaling, axon and neurogenesis, intrinsic and extrinsic signaling pathways, protein and chromosome modification, and others that are significantly altered in the *Insm1* knock out eyes. Additional analysis and validation of RNA-seq results will allow us to further refine the pathway analysis.

Genes associated with cell death, cell cycle regulation, and chromatin condensation were differentially expressed at both E14.5 and E18.5, suggesting a lasting impact of *Insm1* ablation on retinal development. The downregulation of cell survival factors and cell death inhibitors at E14.5 indicate an increase in cell death during this proliferative phase. Additionally, the downregulation of factors involved in normal cell cycle progression and increases in chromatin modifications associated with cell cycle entry and progression might suggest aberrant or unregulated cell division. Together these could indicate an increase in proliferation which results in death of excess cells or cells which are damaged by rapid cell cycling. Additionally, at E18.5, cell cycle factors associate with increased cell division were upregulated, which could indicate the failure of cells to leave the cell cycle and begin differentiating. Immunohistochemical analysis of retinal sections using markers of cell proliferation, cell cycle phase, and cell death will be necessary to determine if the number of proliferative cells is altered in the *Insm1* knockout. Additional experiments to determine relative cell cycle length, through for example BrdU pulse experiments, may also be required.

The identification of a number of factors involved in post-translational modification of proteins is also interesting. Using a candidate gene approach, analysis of phosphorylation states of specific proteins should be undertaken. For example, the phosphorylation state of Rb1 or CDK4 are known to regulate their activity. Their transcription appears to be consistent in the mutant eyes, but we currently do not have information concerning the phosphorylation or activity of these genes. Insm1 is known to bind factors like CyclinD and HDACs. This interaction

leads to changes in phosphorylation state of other proteins which interact with the these factors in the absence of Insm1. It is possible, that the changes in gene expression are underrepresenting the effect of Insm1 ablation on the cellular environment. By examining protein modification, we may uncover additional mechanisms by which Insm1 is affecting retinal proliferation and development.

While the changes in expression of photoreceptor specification, differentiation, and maintenance genes may have been expected, especially in light of the *insm1a* morphant phenotype in the zebrafish, they are also very interesting. The differential expression of these genes in the *Insm1* knockout mouse suggests that the retinal function of *Insm1* described in the zebrafish may be conserved in mammalian retinal development. Additionally, these findings bolster the previously observed morphant phenotypes, providing additional evidence of the specific effect of *Insm1* during photoreceptor cell specification and maturation.

While only a subset of photoreceptor-associated genes, including *Otx2*, *Crx*, *Pde6g, Prdm1, Pou4f1, and Tulp1,* displayed a 1.5-or greater expression change in the *Insm1* knockout retinas, a number of additional genes with known roles in photoreceptor specification, maturation and function, such as *Opn1sw, Rorb, Nrl, Nr2e3, Trb2, Gnat1, Gnat2, Pde6d, Mab21l2, Pou4f3, and Ascl1* were consistently differentially expressed. For many of these genes, either the fold-change or p-value numbers just missed our cutoffs; for a smaller number, their very low expression values or highly variable, though greatly reduced expression in the *Insm1* knockout led their exclusion. Genes known to be involved in the specification of other retinal subtypes but not in the specification of PRCs were not observed to have differential expression (Figure 4.4).

When taken cumulatively, the changes in gene expression observed in the *Insm1* knockout eyes strongly suggests that *Insm1* affects the development of the photoreceptor cell

lineage specifically. Modest changes in the expression of genes that require tightly controlled expression, either temporally or spatially, for proper activity may prove to be important for cell fate determination or for cell maturation. For example, the relative abundance of *Crx* to *Nrl* is essential in specifying the rod or cone photoreceptor lineage [205]. We may be able to isolate functional consequences of some of these changes by examining the E18.5 cell types. For example, if there is a shift to cone cell fate in the absence of *Insm1*, as might be suggested by the upregulation of Rorb at E18.5, immunohistochemical analysis for early markers of cone cells should show this.

In summary, ablation of *Insm1* results in significant changes in gene expression in E14.5 and E18.5 eyes. This study provides new information concerning the potential targets of Insm1 regulation and the effect of Insm1 on eye development. This study bolsters the previous work of our lab and others showing a role for insm1 in cell cycle progression, cell survival and death, and transcriptional regulation of cell fate specification genes. The ability of Insm1 to directly regulate transcription of most of these genes has not been examined previously, as few targets have been identified. Additional targets of Insm1 interaction outside transcriptional regulation might also be inferred from this data. While identifying these potential interactors would require a less targeted approach, we can use the pathways analysis in conjunction with previously identified partners to select potential interactors more scientifically.

Chapter 4 Tables

Table 4.1: RNA-seq data read and quality analysis

ID	Yield (Mbp)	#Cluster	%Q30	MeanQ	Tophat Aligned	Percent Aligned
E14.5_WT.1	1,717	17,165,507	92.07%	35.6	11,588,635	67.51%
E14.5_WT.2	1,588	15,881,372	93.87%	36.27	13,337,753	83.98%
E14.5_WT.3	1,582	15,819,469	93.56%	36.15	13,261,122	83.83%
E14.5_KO.1	1,865	18,646,626	93.01%	35.97	15,089,928	80.93%
E14.5_KO.2	1,794	17,938,375	93.58%	36.17	15,094,250	84.15%
E14.5_KO.3	1,705	17,047,531	93.98%	36.29	14,564,599	85.44%
E18.5_WT.1	1,757	17,569,862	93.32%	36.04	14,095,495	80.23%
E18.5_WT.2	1,945	19,449,136	93.77%	36.2	16,438,639	84.52%
E18.5_WT.3	1,775	17,748,404	93.93%	36.27	15,398,294	86.76%
E18.5_KO.1	1,679	16,789,873	93.84%	36.24	14,587,667	86.88%
E18.5_KO.2	1,657	16,573,262	93.59%	36.15	13,866,609	83.67%
E18.5_KO.3	1,825	18,253,699	93.64%	36.16	15,460,233	84.70%
Average	**1,740.75**	**17,406,926.33**	**93.51%**	**36.13**	**14,398,602**	**82.72%**
Total	**20,889**	**208,883,116**	--	--	**172,783,224.00**	--

Table 4.2: Transcript and differentially expressed targets Identified

Time point	E14.5	E18.5
Transcripts Total	23,130	23,795
Transcripts with FPKM >1.0	20,911	21,293
DETs Total	1158	1332
DETs Up Regulated	377	774
DETs Down Regulated	781	561
DEGs Total	1029	1008
DEGs Up Regulated	288	644
DEGs Down Regulated	741	364

Table 4.3A: Top Upregulated DEGs at E14.5

Gene Symbol	Gene Name	Log2 fold Change	P-Value
Grik2	Glutamate receptor, ionotropic, kainate 2 (beta 2)	3.2232	0.0438
Col19a1	Collagen, type XIX, alpha 1	2.8686	0.0451
Galntl6	UDP-N-acetyl-alpha-D-galactosamine polypeptide N-acetylgalactosaminyltransferase-like 6	2.7790	0.0403
Tmc8	Transmembrane channel-like gene family 8	2.3218	0.0215
Meis2	Meis homeobox 2	2.3088	0.0367
Tnfrsf13c	Tumor necrosis factor receptor superfamily, member 13c	2.2638	0.0419
Zkscan2	Zinc finger with KRAB and SCAN domains 2	2.2253	0.0284
Mas1	MAS1 oncogene	2.2167	0.0188
Tulp2	Tubby-like protein 2	2.1464	0.0352
Ccl7	Chemokine (C-C motif) ligand 7	2.1450	0.0336
CD59a	CD59a antigen	2.0273	0.0348
Smarca1	SWI/SNF related matrix associated, actin dependent regulator of chromatin, subfamily a-like 1	2.0136	0.0499
Usp29	Ubiquitin specific peptidase 29	2.0115	0.0377
Pzp	Pregnancy zone protein	1.9486	0.0474
Tg	Thyroglobulin	1.9201	0.0292
Fat3	FAT tumor suppressor homolog 3	1.7335	0.0062
Ddx43	DEAD (Asp-Glu-Ala-Asp) box polypeptide 43	1.6727	0.0424
Fbxo48	F-box protein 48	1.6593	0.0376
Rnf112	Ring finger protein 112	1.6310	0.0276
Robo1	Roundabout homolog 1	1.5720	0.0125
Kcnb2	Potassium voltage gated channel, Shab-related subfamily, member 2	1.4323	0.0253
Camp	Cathelicidin antimicrobial peptide	1.3728	0.0200
Lrrc7	Leucine rich repeat containing 7	1.3457	0.0242
Nr2c2	Nuclear receptor subfamily 2, group C, member 2	1.3386	0.0191
Erdr1	Erythroid differentiation regulator 1	1.3160	0.0251

Table 4.3B: Top Downregulated DEGs at E14.5

Gene Symbol	Gene Name	Log2 fold Change	P-Value
Bst1	Bone Marrow stromal cell antigen 1	-4.6091	0.0215
Insm1	Insulinoma-associated 1	-3.9265	0.0001
Mst1	Macrophage stimulating 1	-3.5478	0.0047
Cyp2s1	Cytochrome P450, family 2, subfamily s, polypeptide 1	-3.2552	0.0426
Tmem178	Transmembrane protein 178	-3.1685	0.0070
Sytl3	Synaptogamin-like 3	-3.0626	0.0294
Sash1	SAM and SH3 domain containing 1	-2.8631	0.0246
Rfx5	Regulatory Factor X, 5	-2.2711	0.0001
Slc10a1	Solute carrier family 20, member 1	-2.2455	0.0402
Eps8l1	Epidermal growth factor receptor kinase substrate 8-like 1	-2.2400	0.0151
Rims1	Regulating synaptic membrane exocytosis1	-2.2242	0.0119
Ybx1-ps2	Y box protein 1, pseudogene 2	-2.2123	0.0188
Pdzk1	PDZ domain containing 1	-2.1513	0.0238
Tinagl1	Tubulointerstital nephritis antigen-like 1	-2.1489	0.0061
Pmfbp1	Polyamine modulated factor 1 binding protein 1	-2.1100	0.0399
Mybl2	Myeloblastosis oncogene-like 2	-2.1040	0.0001
Igfals	Insulin-like growth factor binding protein, acid labile subunit	-2.0784	0.0358
Scube2	Signal peptide, CUB domain, EGF-like 2	-2.0238	0.0266
Srp54c	Signal recognition particle 54B	-1.9885	0.0324
Irf7	Interferon regulatory factor 7	-1.9770	0.0237
Plk3	Polo-like kinase 3	-1.9639	0.0074
Tdg	Thymine DNA glycosylase	-1.9445	0.0219
Rpl31-ps10	Ribosomal protein L31, pseudogene 10	-1.8681	0.0048
Cebpa	CCAAT/enhancer binding protein (C/EBP), alpha	-1.8597	0.0499
Lrp2bp	Lrp2 binding protein	-1.8483	0.0270

Table 4.4A: Top Upregulated DEGs at E18.5

Gene Symbol	Gene Name	Log2 fold Change	P-Value
Cd247	CD247 antigen	5.0023	0.0443
Gjb4	Gap junction protein, beta 4	4.1486	0.0427
Car9	Carbonic anhydrase 9	3.7022	0.0002
Ciz1	CDKN1A interacting zinc finger protein 1	3.3299	0.0001
Cdc37l1	Cell division cycle 37-like 1	3.3136	0.0440
Dusp27	Dual specificity phosphatase 27	3.2335	0.0469
Smpd5	Sphingomyelin phosphodiesterase 5	2.8257	0.0482
Cacna1c	Calcium channel, voltage-dependent, L type, alpha 1C subunit	2.7680	0.0068
Grp	Gastrin releasing peptide	2.7425	0.0457
Atg9b	Autophagy related 9B	2.6286	0.0297
Thada	Thyroid adenoma associated	2.5969	0.0144
Atad2b	ATPase family, AAA domain containing 2B	2.4983	0.0141
Paox	Polyamine oxidase (exo-N4-amino)	2.4489	0.0090
Afap1l2	Actin filament associated protein 1-like 2	2.4119	0.0085
Lcor	Ligand dependent nuclear receptor corepressor	2.3979	0.0122
Il1rapl2	Interleukin 1 receptor accessory protein-like 2	2.3932	0.0037
Ptk2b	PTK2 protein tyrosine kinase 2 beta	2.3910	0.0081
Sp110	Sp110 nuclear body protein	2.3768	0.0060
Cdk6	Cyclin-dependent kinase 6	2.2562	0.0190
Ccr9	Chemokine (C-C motif) receptor 9	2.1759	0.0282
Robo2	Roundabout homolog 2	2.0246	0.0289
Sst	Somatostatin	1.9997	0.0362
Wdr78	WD repeat domain 78	1.9916	0.0425
Fibcd1	Fibrinogen C domain containing 1	1.9079	0.0371
Usp35	Ubiquitin specific peptidase 35	1.9058	0.0064

Table 4.4B: Top Downregulated DEGs at E18.5

Gene Symbol	Gene Name	Log2 fold Change	P-Value
Dbp	D site albumin promoter binding protein	-4.33669	0.0438
Slc2a2	Solute carrier family 2 (facilitated glucose transporter); member 2	-3.70268	0.03325
Abhd15	Abhydrolase domain containing 15	-3.52131	0.0279
Rpl31-ps16	Ribosomal protein L31; pseudogene 16	-3.01999	0.03445
Cst3	Cystatin C	-2.72252	0.0418
Camp	Cathelicidin antimicrobial peptide	-2.69184	0.00675
Apoh	Apolipoprotein H	-2.59039	0.0126
Aldh1a7	aldehyde dehydrogenase family 1; subfamily A7	-2.25423	5.00E-05
Pank3	Pantothenate kinase 3	-2.02142	0.03295
ifi2712a	Interferon; alpha-inducible protein 27 like 2A	-2.00811	0.0296
Hist1h2ae	histone cluster 1; H2ae	-1.85609	0.005
Rasl2-9	RAS-like; family 2; locus 9	-1.79552	0.04655
Trp63	Transformation related protein 63	-1.73333	0.0009
Gaint3	UDP-N-acetyl-alpha-D-galactosamine:polypeptide N-acetylgalactosaminyltransferase 3	-1.6682	0.0416
Rem1	RAD and GEM related GTP binding protein 1	-1.65933	0.0382
Acmsd	Amino carboxymuconate semialdehyde decarboxylase	-1.58188	0.01975
Tdh	L-threonine dehydrogenase	-1.5453	0.03775
Pex5l	Peroxisomal biogenesis factor 5-like	-1.44106	0.03995
Podxl2	Podocalyxin-like 2	-1.43129	0.02245
Hspe1-rs1	Heat shock protein 1 (chaperonin 10); related sequence 1	-1.42744	0.0078
Smim24	Small integral membrane protein 2	-1.32785	0.0279
Slc15a2	Solute carrier family 15 (H+/ peptide transporter); member 2	-1.23444	0.00045
Cntnap5a	Contactin associated protein-like 5A	-1.18724	0.01325
Gpihbp1	GPI-anchored HDL-binding protein 1	-1.17597	0.03365
Pitx1	Paired-like homeodomain transcription factor 1	-1.15206	0.0306

Table 4.5A: Top 15 Upregulated Pathways at E14.5

Term	Fisher's Exact Value	Deviation from Expected Rank	Combined Score
Validated transcriptional targets of deltaNp63 isoforms	0.0554	-1.6107	1.1718
Validated transcriptional targets of TAp63 isoforms	0.0686	-1.5889	1.1560
Regulation of RhoA activity	0.0576	-1.5083	1.0973
C-MYB transcription factor network	0.1466	-1.4960	1.0884
Urokinase-type plasminogen activator (uPA) and uPAR-mediated signaling	0.3001	-1.0009	0.7282
Posttranslational regulation of adherens junction stability and disassembly	0.3344	-0.9480	0.6897
Integrin family cell surface interactions	0.2002	-0.9466	0.6887
Plexin-D1 Signaling	0.1800	-0.9174	0.6674
Signaling events mediated by HDAC Class II	0.2517	-0.8791	0.6396
Glypican 1 network	0.2068	-0.8677	0.6313
Regulation of Androgen receptor activity	0.3564	-0.8458	0.6153
BMP receptor signaling	0.3001	-0.8386	0.6101
TCR signaling in naive CD8+ T cells	0.3510	-0.8369	0.6088
RAC1 signaling pathway	0.3618	-0.8089	0.5885
FOXA2 and FOXA3 transcription factor networks	0.3175	-0.8047	0.5854

Table 4.5B: Top 15 Downregulated Pathways at E14.5

Term	Fisher's Exact Value	Deviation from Expected Rank	Combined Score
Direct p53 effectors	0.0084	-1.6841	0.2473
PAR1-mediated thrombin signaling events	0.0306	-1.5945	0.2342
Integrin-linked kinase signaling	0.0387	-1.4590	0.2143
Notch signaling pathway	0.0589	-1.4557	0.2138
Validated nuclear estrogen receptor alpha network	0.0417	-1.4462	0.2124
p73 transcription factor network	0.0761	-1.3371	0.1964
ATF-2 transcription factor network	0.0877	-1.2674	0.1861
BCR signaling pathway	0.1125	-1.2032	0.1767
C-MYB transcription factor network	0.1090	-1.1973	0.1759
IFN-gamma pathway	0.0774	-1.1865	0.1743
E-cadherin signaling in keratinocytes	0.0599	-0.9540	0.1401
Posttranslational regulation of adherens junction stability and disassembly	0.1318	-0.9480	0.1392
FOXA2 and FOXA3 transcription factor networks	0.1122	-0.9240	0.1357
Signaling events mediated by Hepatocyte Growth Factor Receptor (c-Met)	0.1837	-0.8655	0.1271
Regulation of Androgen receptor activity	0.1600	-0.7919	0.1163

Table 4.6A: Top 15 Upregulated Pathways at E18.5

Term	Fisher's Exact Value	Deviation from Expected Rank	Combined Score
Class I PI3K signaling events	0.0665	-1.6471	0.1174
Coregulation of Androgen receptor activity	0.0406	-1.6069	0.1145
Regulation of RhoA activity	0.0665	-1.4503	0.1034
TCR signaling in naive CD4+ T cells	0.1448	-1.4158	0.1009
HIV-1 Nef: Negative effector of Fas and TNF-alpha	0.1108	-1.3916	0.0992
Aurora B signaling	0.1384	-1.2921	0.0921
Fanconi anemia pathway	0.1914	-1.1273	0.0803
E2F transcription factor network	0.2062	-1.1157	0.0795
Posttranslational regulation of adherens junction stability and disassembly	0.2074	-1.0578	0.0754
S1P2 pathway	0.1908	-0.9474	0.0675
TCR signaling in naive CD8+ T cells	0.2320	-0.9411	0.0671
RAC1 signaling pathway	0.2487	-0.9107	0.0649
C-MYB transcription factor network	0.2668	-0.8132	0.0580
Fc-epsilon receptor I signaling in mast cells	0.2825	-0.8053	0.0574
Caspase Cascade in Apoptosis	0.2655	-0.7328	0.0522

Table 4.6B: Top 15 Downregulated Pathways at E18.5

Term	Fisher's Exact Value	Deviation from Expected Rank	Combined Score
FOXA2 and FOXA3 transcription factor networks	0.0118	-1.5207	1.6843
Signaling mediated by p38-alpha and p38-beta	0.0076	-1.5090	1.6713
ATF-2 transcription factor network	0.0225	-1.6313	1.5920
FGF signaling pathway	0.0531	-1.5814	1.5433
Validated targets of C-MYC transcriptional activation	0.0453	-1.4153	1.3812
Class I PI3K signaling events mediated by Akt	0.0503	-1.1942	1.1654
Stabilization and expansion of the E-cadherin adherens junction	0.0663	-1.1502	1.1224
Urokinase-type plasminogen activator (uPA) and uPAR-mediated signaling	0.0720	-1.1258	1.0987
Endogenous TLR signaling	0.0276	-1.0639	1.0382
Integrin-linked kinase signaling	0.0808	-1.0568	1.0313
LKB1 signaling events	0.0808	-1.0007	0.9765
Validated transcriptional targets of deltaNp63 isoforms	0.0808	-0.9820	0.9583
mTOR signaling pathway	0.1534	-1.1660	0.7559
Regulation of nuclear beta catenin signaling and target gene transcription	0.1971	-1.0646	0.6901
Signaling events mediated by Hepatocyte Growth Factor Receptor (c-Met)	0.5440	0.4030	-0.2076

Chapter 4 Figures:

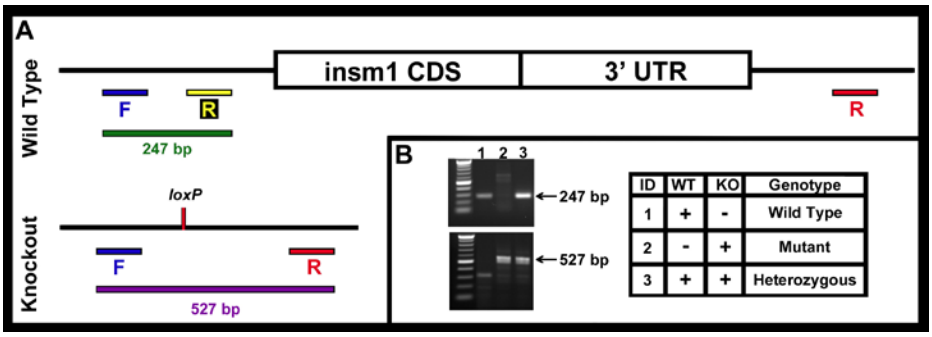

Figure 4.1: Genotyping embryos produced by heterozygous *Insm1* knockout incross

A. Schematic representation of the wild-type Insm1 locus and the same location after gene knockout. The forward genotyping primer (blue) remains intact in both the wild-type and the knockout. Used with the forward primer, the reverse primer (yellow) produces a 247 bp PCR product from the wild-type chromosome. The binding site for this primer is lost in the knockout, but the reverse primer (red) when used with the forward primer produces a 527 bp product from the knockout chromosome. This product would be more than 5 kb on the wt chromosome, and is not amplified under the conditions used for genotyping. **B.** Example PCR products for each genotype.

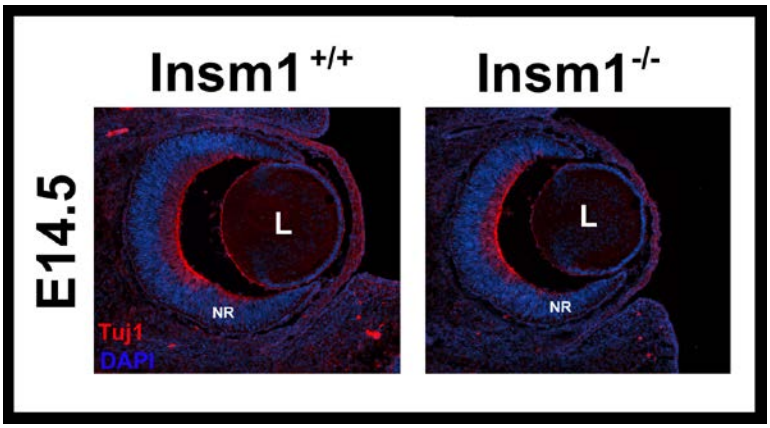

Figure 4.2: No gross changes in morphology were observed between Insm1 wild-type and knockout eyes at E14.5.

At E14.5, retinal thickness and structure appeared consistent between Insm1 wild-type and knockout animals. Immunohistochemistry with Tuj1, which recognized neuronal ß-III tubulin, was similar as well. (L, lens; NR, neural retina)

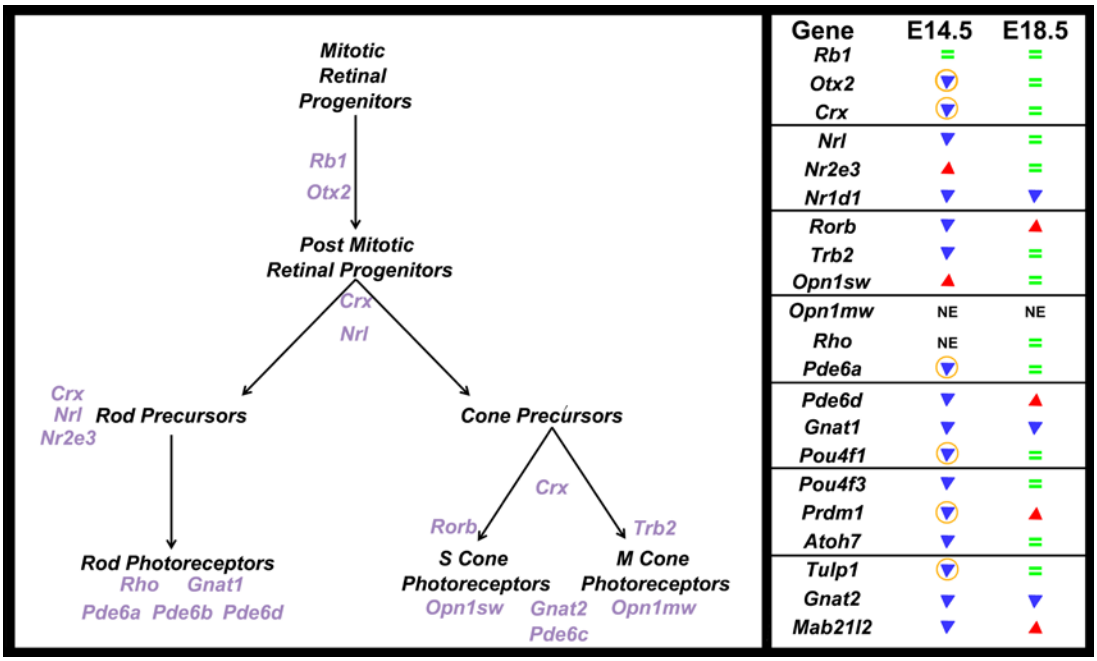

Figure 4.3 Expression of photoreceptor cell genes is altered in the *Insm1* KO mouse when compared with the wild-type.

Key regulators of photoreceptor cell specification and identity are differentially expressed in the *Insm1* knockout mouse eye. Expression of the cell cycle regulatory factor *Rb1* unchanged at both E14.5 and E18.5. *Otx2*, required for photoreceptor cell fate specification is decreased at E14.5, but recovers to wild-type levels at E18.5. A similar pattern is observed in the expression of *Crx*, which acts in both differentiation and maintenance of photoreceptor cells; *Nrl*, which is required for rod cell fate; and *Trb2*, which is an inducer of M-cone differentiation. *Nr2e3*, which directs cone cell fate, and *Opsn1sw*, which is expressed in S-cones, are upregulated at E14.5, but return to the wild-type level at E18.5. The S-cone induction gene, *Rorb*, is downregulated at E14.5 and upregulated at E18.5. Rhodopsin (*Rho*), the visual pigment in rod photoreceptor cells is not expressed at E14.5, and expression is similar between *Insm1* knockouts and wild-types at E185.5. However, *Rho* expression is very low at E18.5, as relatively few mature rods exist prior to birth. The M-cone opsin (*Opn1mw*) is not expressed in any samples at either time point. Additional genes implicated in specification, maturation and activity of the photoreceptor cells, are shown in to the right. Up or downregulation of expression in *Insm1* knockout mouse eyes is shown by blue or red arrow heads, respectively. Changes that met both the 1.5-fold change and p-vale cut off are circled. (NE, no expression)

CHAPTER 5: SUMMARY AND DISCUSSION: EXPRESSION OF INSM1 REGULATES CELL CYCLE PROGRESSION AND PHOTORECEPTOR DIFFERENTIATION IN THE DEVELOPING RETINA

Marie Forbes-Osborne

Department of Biology, University of Kentucky, Lexington, Kentucky 40506-0225

5.1 Summary and Discussion

High fidelity vision requires proper retinal development and integration, which can only occur through tightly controlled retinal stem cell proliferation, specification, and differentiation; followed by maintenance of the retinal neurons, glia, and their connections. The intrinsic and extrinsic signals required for these processes have been and continue to be the objects of significant study. To date, dozens of factors have been identified and the mechanism by which they affect retinal development have been described. Many other factors have been identified, but nothing is known about their function; many additional factors remain unknown.

As a part of the central nervous system, the retina is unable to repair damage from trauma or disease. Few strategies have been developed to attempt clinical repair of retinal cell loss, and those tested have been largely unsuccessful. Our current understanding of retinal development and the mechanisms underlying retinal cell integration are, simply, too incomplete to intelligently design cell-based therapeutics. This is beginning to change, however. First, a great deal of data are being produced concerning the signaling required for retinal cell specification, differentiation, and maturation during development. These data are essential to the successful generation of retinal neurons for transplantation-based therapies. Secondly, a growing number of laboratories are also focusing on the underlying mechanisms of retinal regeneration in animals that naturally perform retinal repair. These experiments are producing a catalog of genes which are essential for the integration of newly born retinal neurons. Together

these experiments can provide a recipe of genetic factors and interactions, which will enhance future therapeutic efforts to restore lost vision.

In this dissertation, the goal was to determine the function of Insm1 in retinal development, as well as to identify potential interacting factors and the pathways underlying the activity of Insm1 (summarized in Figure 5.1). Initially, we knew only that *insm1a* was expressed during eye development and that *insm1a* expression was upregulated in response to chronic rod photoreceptor degeneration. This led to the initial hypothesis that *insm1a* was required, in general, for proper retinal development, and more specifically for rod photoreceptor differentiation. The data supporting this hypothesis are presented in Chapters 2.

Developmentally, retinal expression of *insm1a* is observed in a subset of cells, which are neither rapidly proliferating progenitor cells nor mature neurons. Onset of expression precedes the onset of cellular differentiation, and *insm1a* is excluded from regions where differentiation is largely complete. This suggests that any role *insm1a* plays in the specification of retinal neurons occurs during a narrow developmental window near the time of the terminal cell division. The absence of *insm1a* in mature retinal neurons suggests that *insm1a* is not involved in the maintenance of cell fate after differentiation.

Reduced expression of *insm1a* during development resulted in a specific defect in photoreceptor differentiation, and rod photoreceptors were more affected than cone photoreceptors. The re-activation of *insm1a* after rod photoreceptor degeneration, especially when coupled with the developmental defects in rod photoreceptor genesis when *insm1a* expression is perturbed, indicate a specific function for Insm1 in rod photoreceptor development. The experiments contained in Chapter 2 placed *insm1a* upstream of the photoreceptor specific factors *crx* and *nr2e3*. Additionally, *insm1a* was shown to be upstream of specification factors, including *ath5* and *neurod*, which are associated with differentiation of

both rod and cone photoreceptor cells as well as other retinal neurons, thus suggesting a potential wider function for *insm1a* in the retina. The identification of additional genes in the *insm1a* pathway will be required to determine the exact mechanism by which *insm1a* affects retinal development.

To increase our understanding of the transcriptional changes mediated by Insm1, we completed a RNA-seq based, differential expression analysis, comparing *Insm1* knockout and wild-type eyes at 2 developmental time points. These experiments, contained in Chapter 4, revealed over 2000 differentially expressed genes. Bioinformatics based pathways analyses showed an enrichment of cell cycle, cell death and survival, protein and chromosomal modification, and photoreceptor cell fate specification genes. Although validation of these genes is ongoing, and the data remains incomplete, the patterns of expression changes are intriguing, providing evidence of altered proliferation, homeostasis, cellular metabolism, and neuronal maturation. Careful analysis and additional experiments will be necessary to tease out the direct and indirect actions of *Insm1* from these data.

Additional experiments contained in Chapter 2 showed a role for *insm1a* in cell cycle regulation in the developing retina. Reduced *insm1a* expression slowed cell cycle progression at the time when the first progenitor cells were preparing to leave the cell cycle and differentiate. This corresponds to the time period when *insm1a* expression is observed throughout the developing retina, and precedes the restriction of *insm1a* to areas adjacent to the proliferative cells at the retinal margin. This led to a second hypothesis that *Insm1* may regulate the expression of cell cycle progression genes as well as cell fate specification genes. When taken together with the expression patterns, this suggests that *insm1a* may have a role in driving cells towards their terminal division, perhaps affecting cell cycle exit rather than acting to maintain a stem cell-like state. This hypothesis is additionally supported by the reactivation of *insm1a* in

the rod progenitor cells, at the base of the outer nuclear layer, in response to rod photoreceptor degeneration. These cells are known to divide and produce additional rod photoreceptors upon rod photoreceptor cell loss and in response to normal increases in eye size during the zebrafish lifespan. The rod progenitor cells arise from a pool of stem cells in the INL, and might be likened to a transit amplifying cell. If *insm1a* expression was required to maintain the stem cell-like state of the progenitor population we would expect to see expression in the INL stem cell pool in this degeneration model. However, expression in cells of the INL is rare, while the ONL expression in the rod progenitors is significantly upregulated.

The effects of Insm1 on cell cycle length, much like its action in cell fate specification or differentiation, may be mediated through the direct binding of Insm1 to transcriptional regulatory targets. However, in light of the evidence that Insm1 protein is able to bind and sequester cell cycle regulatory factors (including CyclinD1), as well as bind with protein complexes known to be involved in protein modification and degradation (including SORBS1 and RACK1), we hypothesize that Insm1 is involved in non-nuclear regulation of cell cycle progression and retinal cell fate specification or differentiation instead of or, more likely, in addition to acting in direct transcriptional regulation of target genes.

This third hypothesis was bolstered by experiments presented in Chapter 3; principally the analysis of a zebrafish *insm1a* mutant. This mutation leads to an early stop codon, and the truncation product lacks the zinc-finger DNA binding domains and the bulk of the nuclear localization signal sequence. As a result, this was expected to be a null mutation. However, the homozygous mutant embryos showed normal retinal development. To attempt to understand this lack of retinal phenotype, several experiments were completed to test the functionality of the mutant protein. Both a full-length *insm1a* mRNA containing the mutation and an N-terminal truncation variant were able to significantly rescue the rod photoreceptor defect observed with

the *insm1a* morpholino. This suggests either that Insm1 is entering the nucleus through some alternative means and is associated with transcriptional regulatory targets in an indirect manner (such as through cofactor or complex binding), or that the nuclear activity (presumably regulating transcription) is not essential to retinal development. The reality likely lies between these options. Insm1 localization and association to the chromosome by HDAC binding has been previously shown [127]. Identification of additional binding partners and interacting complexes will be required to determine the extent to which Insm1 import into the nucleus via these interactions is occurring.

Separately, the specific mechanism by which Insm1 is affecting cell cycle remains to be explored as well. Previously, Insm1 was shown to affect cell cycle progression by interfering with the CyclinD/CDK4 association. The binding of Insm1 and CyclinD interrupts the activation of CDK4, leading to decreased phosphorylation of Rb1and cell cycle arrest. This effect appears to be mediated through the interaction with CyclinD, and does not change expression levels of *CyclinD*, *CDK4* or *Rb1* [132]. This is in opposition to what was observed in tumor cells, where inappropriate activation of *Insm1* occurs alongside rampant cell proliferation. It has been suggested that the cell cycle regulatory machinery is damaged in tumor cells, resulting in an inability of the cell to respond to the anti-proliferative signals of genes like Insm1 [132]. While this may be true, especially in tumors, our data also suggests that the effect of Insm1 on cell cycle may be context or tissue dependent. For example, in our *insm1a* knockdown, decreased *insm1a* resulted in cell cycle elongation. These experiments might suggest that the mechanism by which *insm1a* is affecting cell cycle progression in the developing retina and in tumors is not mediated by CyclinD/CDK4 and Rb1. However, our RNA-seq analysis revealed a reduction in *CyclinD1* expression at E14.5 in the *Insm1* knockout mouse, albeit with no change in either *Cdk4* or *Rb1* expression. In previous experiments, when Insm1 was overexpressed causing cell cycle

arrest through CyclinD1 binding, overexpression of both CyclinD1 and CDK4 were required to rescue the cell cycle arrest[132], suggesting that the observed change in CyclinD1 may not be sufficient to perturb the cell cycle. Additionally, there may be other interacting factors, which when bound by Insm1 affect cell cycle progression in a positive manner. Alternatively, perhaps the cell cycle progression defect observed when Insm1 is perturbed results from a changes in transcription of additional factors beyond *Rb1*, *CyclinD* and *CDK4*. Lastly, it is possible that the mechanism of this change lies not in Insm1 directly regulating transcription, but rather regulating modification of factors like Rb1. For example, in our RNA-seq experiments using the *Insm1* knockout, *Rb1* expression is unchanged, but cell cycle regulatory factors downstream of *Rb1* are differentially expressed. This in conjunction with the altered expression of numerous kinases might suggest that Insm1 is regulating cell cycle progression through the phosphorylation state of Rb1. Whether this is through the control of protein modification gene transcription or through the extra-nuclear binding of Insm1 to protein modifiers or the regulators of protein modifiers is still unknown.

In summary, the work described in this dissertation, provides a detailed examination of the function and mechanism of action of Insm1 during retinal development. It includes a detailed description of Insm1 expression during zebrafish retinal development, and the consequence of Insm1 reduction and ablation on retinal development in the zebrafish and mouse, respectively. The results of these experiments have demonstrated a specific role for Insm1 in photoreceptor specification and differentiation. Insm1 was also shown to regulate cell cycle progression and is suggested to have roles in neuronal maturation and connectivity. Additional work remains to identify the mediators through which Insm1 acts in these various pathways. Specifically, it will be important to determine if Insm1 activity is occurring through

DNA binding and regulation of transcription, through extranuclear association with regulatory factors, inclusion in complexes of regulators, or some combination of all of these.

Chapter 5 Figures:

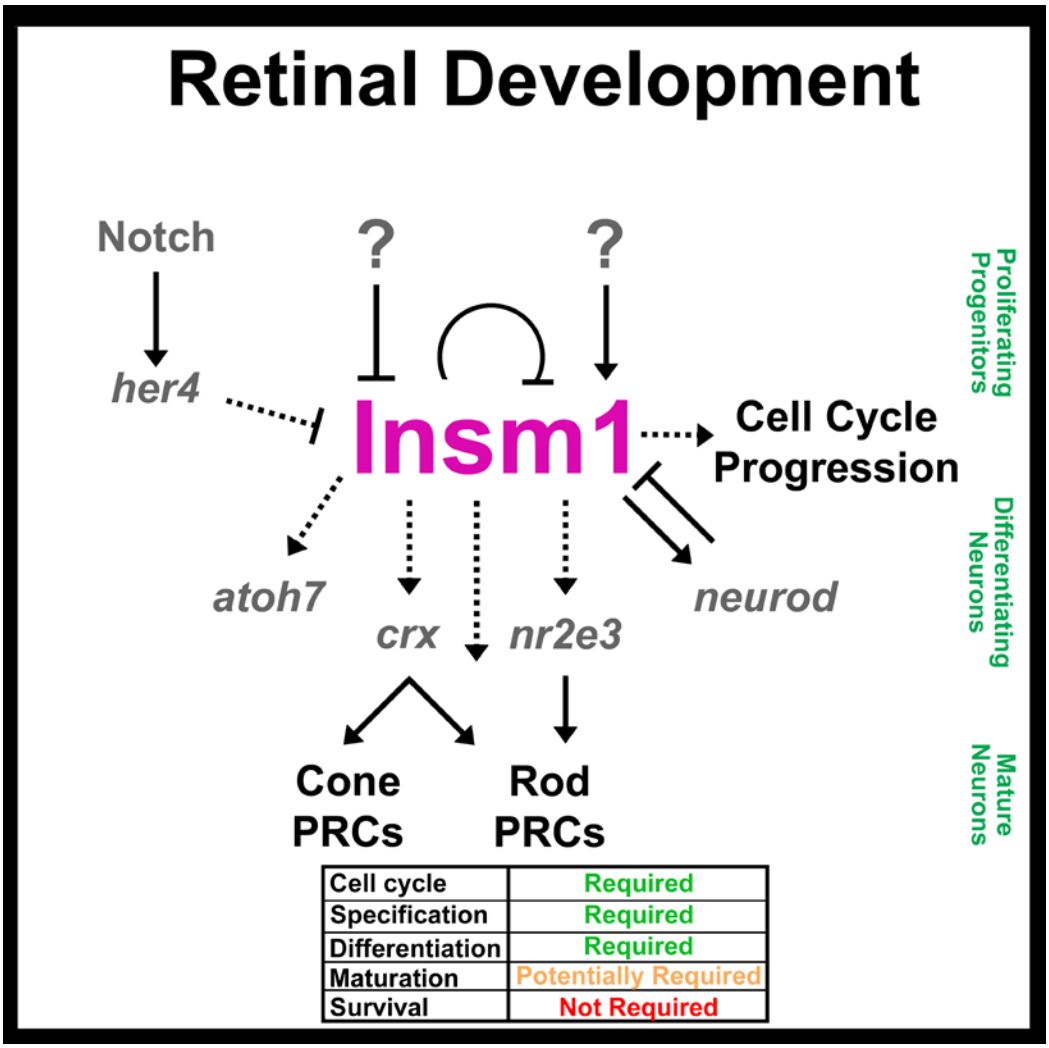

Figure 5.1: Insm1 affects cell cycle progression and photoreceptor specification in the developing retina.

Notch signaling regulates Insm1 expression, through regulation of *hairy-enhancer split related* genes, like *her4*. Additional regulatory pathways have been suggested, but remain to be identified. *Insm1* regulates cell cycle progression and the specification and differentiation of photoreceptor cells in the retina. Maturation of retinal neurons may be affected by Insm1, as was suggested by maturation defects described in Chapter 2, but these may be secondary effects of the loss of rod and cone photoreceptor cells when *Insm1* expression is perturbed. *Insm1* expression is absent from mature retinal neurons, and does not function to maintain their survival.

APPENDIX I: ADDITIONAL PROJECTS: MODELING RETINITIS PIGMENTOSA IN THE ZEBRAFISH

Marie Forbes-Osborne[1], Hannah E. Henson[1], Sara Perkins[1], Kayla Swiatek[2] Ann C. Morris[1]
[1]Department of Biology, University of Kentucky, Lexington, Kentucky 40506-0225
[2]Washington University in St. Louis, St. Louis, Missouri, 63130

A1.1 Introduction

A1.1.1 Retinitis Pigmentosa

Retinitis Pigmentosa (RP) is a heterogeneous group of related eye conditions that share a common clinical symptomatology. Affected individuals experience bilateral progressive degeneration of the photoreceptor cells followed by subsequent degeneration of the retinal pigmented epithelium (RPE). RP often presents clinically as nyctalopia, resulting from a primary degeneration of the rod photoreceptor cells. As the disease progresses, additional visual field deficits develop, including photophobia, patchy loss of peripheral vision, and tunnel vision. For many, RP carries a high probability of devastating vision loss, with legal or clinical blindness being frequent disease endpoints [206, 207].

Age of disease onset is highly variable, ranging from infancy to late in life, though a majority of cases present in late adolescence and early adulthood [42, 43, 206]. In the early disease stage, visual acuity is often normal and examination of the fundus shows none of the clinical signs of RP (bone spicule-shaped pigment deposition, blood vessel attenuation, or waxy pallor of the optic disk). However, in many cases electroretinogram (ERG) studies show decreased b-wave amplitudes, especially in scotopic conditions. As the disease progresses, the nyctalopia worsens, and is accompanied by dyschromatopsia, losses in peripheral visual field, and decreased visual acuity. Many patients become photophobic, especially in diffuse lighting conditions. Macular involvement occurs in a subset of patients, and may include macular edema or atrophy. Development of cataracts may also worsen visual acuity. Fundus examination shows

distinct narrowing of the retinal vasculature, accompanied by pigmentary changes with depigmentation peripheral to the macula and bone spicule-shaped pigment deposition peripheral to the depigmentation. Photopic ERG often shows reduced a- and b-waves, while scotopic ERGs are often not recordable. In late stage RP, patients may retain a narrow window of very low acuity central vison or may have no remaining vision at all. However, many patients may continue to perceive light even at this advanced disease stage. Fundoscopic examination reveals very sparse and thin retinal vessels, and clear pigment deposition throughout. The optic disk is pale, indicating optic nerve atrophy [41, 208], and no responses are recordable on ERG.

The genetic basis of RP is moderately well understood, with between one third and half of known cases being linked to a causative locus[42, 209]. Most of these defined cases are in families where the disease is observed in several people across multiple generations; this is especially true in dominant disease mutants and within closed reproductive communities (e.g. Ashkenazi Jews[210], several isolated populations in the northern Netherlands[211], and several families known to practice consanguineous marriage in Pakistan[212]). However, more than 40% of RP cases in the US are isolated, with no known family history of either RP or other retinal degenerative diseases [42]. Currently, unless these sporadic cases occur due to a mutation in one of the more common of the 60 known loci, there is little chance that the causative gene will be uncovered without considerable effort, potentially requiring whole exome or even whole genome level evaluation[209].

Of the 75 genes linked to retinal degenerative diseases, only 39% are expressed exclusively in the retina, an additional 3 are expressed only in the RPE and 5 are within or linked to the mitochondrial genome. Fifteen are phototransduction genes, 7 are involved in the retinol cycle, 3 are transcription factors, 3 are mRNA splicing factors, 9 are structural or cytoskeletal proteins, and 20 produce proteins with unknown functions [209]. An additional 45 loci have

been linked to RP or one of its allied conditions, but the identity of the gene involved remains unknown.

In addition to the more common autosomal dominant (adRP), autosomal recessive (arRP), and X-linked (xlRP), a potential Y-linked RP has been described, as well as digenic-diallelic, digenic-triallelic, and tetraallelic modes of inheritance. Numerous modifier alleles have been described, though their effect size remains largely unknown [209]. The estimated "aggregate carrier frequency " for arRP is thought to be as high as 10%; much higher than cystic fibrosis, which is often cited as having the highest "aggregate carrier frequency" [209]. Despite the high aggregate carrier frequency, the high number of genes involved in arRP means that the chances of 2 unrelated individuals transmitting mutations in the same gene is very low. The highly variable genetics of RP is further compounded by rare incomplete penetrance and variability in severity. For example, the adRP P23H mutation in rhodopsin is highly variable, with over 100 fold-difference in photoreceptor function observed between 2 closely related individuals [209, 213].

There has been much discussion concerning the pathogenicity underlying RP. Some groups believe that RP should be considered a continuum of metabolic disorders of the eye [42], especially in light of the number of metabolic diseases which have an RP-like component [41]. Others postulate that RP is a disease of signal dysregulation, aberrant protein trafficking, or improper maintenance of cell specification or connections [42, 213, 214]. It is probable that these occur in various combinations and at differing levels in the different mutations, and only careful examination of both quality animal models and affected human patients will suffice to determine how these retinal degenerations progress.

A1.1.2 Current Treatments

Current treatments are extremely limited. Treatment of eye related complications such as cataracts and macular edema can aid in preserving vision for some patients. Some evidence exists that high doses of vitamin A may slow degeneration [215, 216], though other studies found no benefits to vitamin A supplementation [217, 218]. Lutein supplementation appeared to have a positive effect in one short duration study [219], but had no effect in a second longer duration study [220]. Other treatments including docosahexaenoic acid (DHA) and hyperbaric oxygen have largely showed no effect on visual field or acuity [221-224], while high dose vitamin E supplementation was associated with increased disease progression [215, 217]. Ciliary neurotrophic factor (CNTF) was determined to have no effect at low doses, and to be detrimental at high doses; though removal of the CNTF secreting implant reversed the change in sensitivity [225]. Two small unmasked studies (n=33 and n =41) of nilvadapine, a calcium channel blocker currently being tested as a treatment for Alzheimer's disease, showed significantly slowed progression of central visual field loss using one measurement (MD slope), but no change by an alternative measurement (ΔCENT4) [226, 227]. Another small unmasked study (n=30) of valproic acid, showed both improvements in best corrected visual acuity and amplitude and latency in ERG [228]. This trial was the first to show a clear benefit on outcomes that would be relevant for patients, like visual acuity, but additional trials will be required to determine the true value of valproic acid in RP. The first placebo controlled, randomized, double blinded trial of valproic acid began in 2010 and will be completed in December of 2015 (ClinicalTrials.gov Identifier: NCT01233609).

Gene therapy, which was once seen as the light at the end of the tunnel for genetic conditions, has not yet come to fruition in RP. The large number of disease-associated genes and the large percentage of patients without a known causative mutation increases the difficulty, as

gene therapies must be designed specifically for each gene. The high percentage of adRP also increases the difficulty of gene therapeutics, as it may be necessary to replace the faulty gene rather than to simply provide an additional wild-type copy of the gene as may be possible in arRP and xlRP. Dominant negative mutations especially would require inactivation of the mutated gene copy. Considerable work is also required to produce a safe and effective means of gene replacement; one that does not cause treatment-induced malignancies (as has been seen in other gene therapy trials [229-231], but is highly efficient at transforming the desired tissue.

Similarly, cell based transplantation therapies remain far from successful implementation. Generation of retinal cells for transplantation requires either the use of induced pluripotent stem cells (iPSCs) or embryonic stem cells (ESC), both of which have their difficulties. The use of iPSCs carries with it a risk of oncogenic transformation [232, 233], which has raised ethical concerns especially as vision loss is not a life-threatening condition. The use of embryonic stem cells also presents a potential moral dilemma, and might act as a deterrent to treatment. Even outside these fundamental concerns, there are additional difficulties to be overcome to permit cell based transplantation therapies. First, we must be able to generate significant numbers of specified, differentiated photoreceptor cells in culture, transplant those cells into the damaged retina, and facilitate their integration and survival. This is especially difficult in the context of a disease like RP, where the loss of the photoreceptor cells is often compounded by significant remodeling of the second order neurons[234]. This remodeling may further limit the window during which cell based transplantation is appropriate. Similarly, the ability of implantable devices to rescue visual function is also likely to be negatively affected by the retinal reorganization.

Taking into account all the current roadblocks to treating RP, one of the best remaining options is to identify new compounds that can help maintain vision by reducing the

degenerative effects of the mutation. The ability to do large scale screens of small molecules is one of the strongest advantages of the zebrafish. If embryos or early larvae are being used, screening can be completed using 96 well plates. The high fecundity of the zebrafish makes generating thousands of embryos quick and easy. Alternatively, larval animals can be treated in 6 or 24 well plates depending on the age, and even adults can be maintained in relatively small volumes (40 animals in a 4 liter tank). The Molecular Libraries Small Molecule Repository (MLSMR) at the NIH has over 300,000 small molecules available, and numerous companies and research groups have countless others. The creation of a panel of high quality RP models in the zebrafish would allow the screening of hundreds to thousands of compounds with relative ease. Additionally, because we have included a fluorescent reporter in the rod photoreceptors, it is possible that efficacy of treatment could be discerned in live animals, through simple fluorescent microscopy.

A1.1.3 Design and rationale

To overcome the limitations of other systems (including long generation times, difficulties in producing transgenics, and the rod-dominated nature of some model organisms compared to the human) we have begun to produce zebrafish expressing dominant human RP mutations. As a diurnal vertebrate, the zebrafish retina shares a high degree of similarity with the human retina. This includes a rich complement of cone photoreceptor cells, in addition to the rod photoreceptor cells.

A1.1.3.1 Two systems of degeneration

To provide additional information on the pathogenicity of these disease associated mutations, we are interested in examining developing, juvenile and adult retinas. We also would like to be able to separate the retinal degeneration from the intrinsic regeneration of the

zebrafish retina. To do this, we have designed both constitutively active and chemically-inducible gene expression systems.

The constitutively active lines express the RP-associated RHO mutations under the control of the rod PRC-specific promoter XOPS5.5. This promoter has been previously used to generate the rod PRC reporter line, XOPS:GFP (previously described in Chapter 2 and [77, 141]). In these lines, separate constructs were produced carrying one of five dominant RP-associate mutations in human rhodopsin, or a wild-type rhodopsin, as well as a fluorescent transgenesis marker, flanked by inverted transgenesis repeats (Figure A1.1). The mutations range in their RP-associated phenotypes (from mild, regional degeneration to severe degeneration with early onset) (Table A1.2).

The chemically inducible lines that will allow spatiotemporal control of transgene expression have been designed using the TetON system. TetON combines two elements: a reverse tetracycline-controlled transactivator (rtTA) and a cis-acting operator-promoter to which the rtTA binds (the Tet-responsive element, TRE). In the presence of doxycycline, the rtTA is activated and binds to the TRE, driving transcription of downstream genes. In these experiments, two downstream genes are driven by a bidirectional TRE (biTRE), which permits the production of the RHO transgene and a fluorescent marker, mCherry. A rod PRC specific rtTA line was previously generated [235], and was obtained for use in these experiments. For the biTRE lines, zebrafish embryos have been injected with the biTRE constructs (Figure A1.2) to create the inducible transgenic lines. Founder zebrafish carrying genomic integrations will be identified by outcrossing and PCR genotyping of embryos. The F1 embryos will be tested by RT-PCR and fluorescence imaging for proper expression and induction of each of the transgenes. If the transgenes work as expected, we will then induce expression of mutant rhodopsin and characterize the time-course of rod photoreceptor degeneration in each line using a

combination of molecular, biochemical, and immunohistochemical methods. We will subsequently wash out the chemical inducer to quench expression of the transgene and determine the time course and extend of photoreceptor regeneration by similar methods.

A1.2 Materials and Methods

A1.2.1 Zebrafish lines and maintenance

Zebrafish were bred, raised and maintained in accordance with established protocols for zebrafish husbandry [138]. Embryos and larvae were housed at 28°C, on a 14 h light:10 h dark cycle. Wild-type strains included the Ekwill strain (Ekwill Fish Farm, Gibsonton, FL), the AB strain obtained from the Zebrafish International Research Center (ZIRC, Eugene, OR) and hybrids produced by crossing the Ekwill and AB strains. The Tg (XlRho:EGFP)fl1 transgenic line (hereafter called XOPS-GFP) has been previously described [77, 141], and was obtained from James Fadool (Florida State University, Tallahassee, FL). All animal procedures were carried out in accordance with guidelines established by the University of Kentucky Institutional Animal Care and Use Committee.

A1.2.2 Creation of RP-associated mutation in Rhodopsin

A plasmid containing a wild-type human Rhodopsin cDNA (Clone 832757) was obtained from Addgene. Phusion polymerase (Item# M0530, New England Biolabs), was used in nested primer PCRs (primers in Table A1.1), to introduce individual mutations at 5 locations (Table A1.2). Additionally, the final PCR for each construct incorporated an N-terminal super minimal flag (SMF) tag (DYKD, gACTACAAgCAT), that allows human rhodopsin to be distinguished from the endogenous zebrafish rhodopsin by Western blot using the M1 antibody (Item# F0304, Sigma-Aldrich). An SMF tagged wild-type human Rhodopsin was also produced for use as a control. PCR products were A-tailed and cloned into pGEM-T Easy vector (Promega). After sequencing to ensure incorporation of both the tag and the selected mutation, the tagged

rhodopsin mRNAs were subcloned into the pME-MCS vector from the Tol2kit (information available at: *http://tol2kit.genetics.utah.edu/index.php/PME-MCS*).

A1.2.3 Generation of constitutive transgenesis plasmids

A p5E(XOPS5.5) plasmid was generated by subcloning a 5.5 kb rhodopsin promoter from *X. laevis* from the pXOPS5.5-eGFP plasmid, kindly provided by Jim Fadool. Gateway cloning was used to generate plasmids for transgenesis using the pTol2CG2 Destination vector and a p3E(polyA) from the Tol2 Kit, along with the pME(smfRHO_variant) and p5E(XOPS5.5). Plasmids were tested by restriction digest and sequenced to ensure correct recombination of the vectors. Final plasmids were called pT2(XOPS5.5:AsRHO_variant). Plasmids for injection were isolated using column purification (Qiagen) followed by phenol chloroform extraction and ethanol precipitation.

A1.2.4 Generation of inducible transgenesis plasmids

The p5E (biTRE:nlsCherry-dA) and p3E(dA) plasmids previously described in [235], were provided by Abbie Jensen (University of Massachusetts Amherst, Amherst, MA). The previously described pDestTol2GC2 was used in Gateway cloning reactions with the pME(smfRHO_variant), p5E (biTRE:nlsCherry-dA), and p3E(dA) plasmids to generate transgenesis plasmids, called pT2(nlsCh:biTRE:AsRHO_variant). Plasmids were tested by restriction digest and sequenced to ensure correct recombination of the vectors. Plasmids for injection were isolated using column purification (Qiagen) followed by phenol chloroform extraction and ethanol precipitation.

A1.2.5 Preparation of transposase mRNA

Capped mRNA was synthesized from the pCs2(Tol2 transposase) plasmid (Tol2Kit) using the mMessage (Sp6) Kit (Ambion, Austin, TX) according to the manufacturer's instructions. mRNA was cleaned by phenol-chloroform extraction and ethanol precipitation.

A1.2.6 Tol2-mediated transgenesis

One cell stage wild-type or XOPS:GFP embryos were injected with 25-30 pg each of in vitro transcribed Tol2 transposase mRNA and one of the pT2(XOPS5.5:AsRHO_variant) or pT2(nlsCh:biTRE:AsRHO_variant) plasmids.

Embryos were transferred to 1xE3 media made with 4x Calcium at 24hpf, with 0.1% methylene blue added to inhibit fungal growth. Embryos were screened for successful injection between 12 and 72 hpf, and all injected embryos were raised to adulthood for screening.

A1.2.7 Founder Isolation

When injected animals reached sexual maturity, individual animals were either incrossed or outcrossed to wildtype or XOPS:GFP animals. Embryos produced from these crosses were screened at 24 to 96 hpf for green heart, indicating incorporation of the pT2 plasmid, which contained a CMLC:GFP transgene in addition to the sequences described above. Identified carriers were raised and founder parents maintained to produce individual lines for experiments. Screening and founder information can be found in Table A1.3.

A1.2.8 Sample Collection

At selected time points, embryonic, larval, and adult fish were anaesthetized with Ethyl 3-aminobenzoate methanesulfonate salt (MS-222, Tricaine, Sigma-Aldrich, St. Louis, MO), and sacrificed by ice immersion as previously described [144]. Whole embryos, larval heads, and adult eyes were collected and washed in ice cold PBS or Hank's Buffered Saline Solution. For immunohistochemistry, tissues were fixed overnight at 4°C in freshly prepared 4% Paraformaldehyde (PFA). Fixed tissues were cryoprotected in 10% sucrose in PBS for at least 3 hours and in 30% sucrose overnight at 4°C. Samples were mounted in OCT Medium (Ted Pella, Redding, CA) and frozen at -80°C. Ten micron Sections were cut on a cryostat (Leica CM 1850, Leica Biosystems, Buffalo Grove, IL), mounted on gelatin-coated slides, and dried overnight at

room temperature. For Western blot, collected tissues were frozen in RIPA buffer at -80°C, before being manually disrupted.

A1.2.9 Immunohistochemistry

Before immunolabeling, sections were rehydrated and postfixed in 1% PFA for 10 minutes at room temperature. After 2 washes in PBS, and 2 washes in PBST, sections were blocked in PBST containing 1% BSA for at least 30 minutes at room temperature. Slides were incubated with primary antibody in PBST/BSA with 5% Normal Goat serum, overnight at 4°C in a humidified chamber. The following day, slides were washed 3 times in PBST, and incubated with secondary antibody in PBST/BSA for 1 hour at room temperature in the dark. Slides were washed 2 times with PBST, counterstained with DAPI (4', 6-diamidino-2-phenylindole, 1:10,000 dilution; Sigma-Aldrich) in PBS, and mounted in 40% glycerol in PBS. Images were obtained on an inverted fluorescent microscope (Eclipse Ti-U; Nikon Instruments), using a 40X objective.

The following antibodies were used: 4C12 (1:100 dilution), a monoclonal antibody that recognizes an unknown epitope on rods (Fadool J, Linser, P unpublished; a generous gift of James Fadool, FSU, Tallahassee, FL), Alexa Fluor 488 goat anti-mouse, 488 goat anti-rabbit, 546 goat anti-rabbit, 546 goat anti-mouse (Molecular Probes, Invitrogen), 647 goat anti-rabbit and Cy5 conjugated goat anti-mouse (Jackson ImmunoResearch, West Grove, PA) secondary antibodies were all used at 1:100-200 dilution.

A1.3 Results

A1.3.1 Creation of founder lines

For each RP-associated mutation and the wild-type control, both constitutive and inducible constructs were injected into one-cell stage embryos. After injection, embryos were screened from 24 to 72 hpf, for expression of the cardiac GFP marker. All embryos were raised, irrespective of the presence or absence of this transient transgene expression. Once injected

animals reached sexual maturity, the potential founder animals were outcrossed, and their offspring screened for the presence of the marker gene. Identified germ-line transmitting founder fish (Table A1.3) were used to create independent lines for analysis.

A1.3.2 Preliminary analysis of a P23H mutant line

An early identified founder for the P23H mutation was determined to transmit the inserted allele at a rate of nearly 50%. This animal was outcrossed, and the offspring sorted by presence or absence of green hearts. All offspring were raised, and animals were collected at 3, 5, 7 and 10 dpf, as well as 4 weeks post fertilization. After fixing, 10 micron sections were cut, and used for immunohistochemistry to examine rod photoreceptor cells.

At all time points assayed, no clear signature of rod photoreceptor loss could be identified. Retinas appeared well organized, with no lamination defects observed (data not shown). Although P23H mutation is not a severe mutation, we expected to observe signs of degeneration in the individuals carrying this mutation. Analysis of offspring from this individual determined that the founder was transmitting multiple insertions, which might suggest an increased risk of insertion site silencing. Careful analysis of this line, including rod photoreceptor cell counts will be required to determine if any degeneration is occurring.

A1.4 Discussion

Retinitis Pigmentosa is a progressive, genetic disease, which is the leading cause of inherited blindness among working aged individuals world-wide. Here, I outline the first steps in our efforts to create inducible and constitutive zebrafish lines to model this disease.

Currently, we have produced potential founders for 10 of 12 planned lines. For 4 lines, 1 or more founder animals with demonstrated germ line transmission have been identified. Screening is continuing for the remaining lines. Once single insertion site integration has been determined, analysis of the retinal phenotypes can begin. We plan to collect animals and use

immunohistochemistry to assay the rod photoreceptor cell number and to determine the presence of dying cells.

We predict that we will see significant cell death in the mutant Rhodopsin lines, but do not expect to observe any ectopic cell death in the wild-type lines. However, these lines are effectively over-expressing rhodopsin as they have the normal zebrafish rhodopsin genes as well as the human Rhodopsin transgene. It is possible that the presence of the additional Rhodopsin gene might be detrimental to rod photoreceptor cell health. If this is the case, it may be necessary to inactivate the zebrafish rhodopsin genes, using CRISPR/Cas9 or TALEN-mediated mutagenesis, before continuing. If no cell death is observed in the wild-type Rhodopsin lines, analysis of the mutant lines can proceed.

We expect the different mutations to produce different disease patterns. For example, in human patients the K296E mutation is extremely severe compared to the T58R mutation. We would therefore expect to see this relative severity mirrored in the zebrafish lines, with the K296E animals displaying earlier onset and faster progression of rod cell loss. Careful examination of photoreceptor cell number, cell morphology, and ultrastructural analysis will be required to determine the extent and pattern of degeneration. Comparison of constitutive and inducible lines may help to identify cellular consequences of mutant Rhodopsin expression as well.

The generation of these zebrafish models of Retinitis Pigmentosa are a necessary first step to help increase our understanding of how these mutations lead to a retinal pathology, and to then identify potential methods to reduce the disease burden associated with them. While this project remains in its early stages, there is a clear value in creating these models. The constitutive lines will be invaluable in screening small molecule libraries to identify novel potential treatments. The inducible lines will permit us to separate the intrinsic regeneration

capacity of the zebrafish retina from the induced degeneration. This will allow us to identify genetic factors underlying this regenerative ability, and may help us to determine what factors might permit regeneration in the mammalian retina.

Appendix I Tables:

Table A1.1: Primers used for nested-primer PCR mutagenesis

Primer ID	Sequence 5'→3'	Used with
P1	TTCGCAGCATTCTTGGGTGG	P3 to introduce mutation
P2	CGGTTTAAACGTCGACATGGACTACA AGGATAATGGCACAGAAGGCCCTAAC TTCTACGTGCCCTTCTCCAATGCGAC	P5 to stitch P1/P3 and P4/P6 PCR products together; add SMF tag
P5.1	CGCCCGGGCCGCGGTTAGGCCGGGG CCACCTGGCTCGTCTCCGT	P2 to stitch P1/P3 and P4/P6 PCR products together; add subcloning digest sites
P5.2	CGCCCGGGCCGCGGTTAGGCCGAGG CCACCTGGCTCGTCTCCGT	P2 to create P347S mutation, add subcloning digest sites
P6	GTAGGGGATGGGAGACGCCTAT	P4 to introduce mutations
P3_P23H	GTACTCGAAGTGGCTGCGTACC	P1 to introduce P23H mutation
P4_P23H	GGTACGCAGCCACTTCGAGTAC	P6 to introduce P23H mutation
P3_T58R	GACGTAGAGCCTGAGGAAGTT	P1 to introduce T58R mutation
P4_T58R	AACTTCCTCAGGCTCTACGTC	P6 to introduce T58R mutation
P3_R135L	CACCACGTACAGCTCGATGGC	P1 to introduce R135L mutation
P4_R135L	GCCATCGAGCTGTACGTGGTG	P6 to introduce R135L mutation
P3_K296E	GGCGGCGCTCTCGGCAAAGAA	P1 to introduce K296E mutation
P4_K296E	TTCTTTGCCGAGAGCGCCGCC	P6 to introduce K296E mutation

Table A1.2: RP-associated Rhodopsin mutations created in this study

Allele	Clinical Data and Significance	Pathogenicity	Citations
P23H; Pro23-to-His	**Canonical adRP mutations** **Most common adRP mutation in the US, absent in Europe** **High phenotypic variability even in closely related individuals** **Light exposure affects severity- potential phototoxicity**	**(Cell culture) retained in the ER, unmodified, forms insoluble multimers due to non-native conformation**	**[236-241]**
T58R; Thr58-to-Arg	**Regional pigmentary changes, greater in inferior and inferionasal retina** **Impairment is primarily in the superior visual field** **Less severe, with complete blindness rarely observed**		**[237, 242-244]**
R135L; Arg135-to-Leu	**Very early onset** **Highly progressive- substantial visual field loss by early teens** **Severe retinal vessel attenuation** **Addition of modifier loci leads to retinitis punctata albescens**	**(Cell culture) Hyper-phosphorylated, high affinity arrestin binding leads to arrestin endocytosis and damage to the endocytic pathway**	**[245-249]**
K296E; Lys296-to-Glu	**Early onset** **Cataracts develop between ages 30 and 50** **Degeneration may result from persistent stimulation**	**(Cell culture) Constitutively active Rhodopsin, mutation interrupts K296-E113 salt bridge that maintains inactive conformation**	**[250, 251]**
P347S; Pro347-to-Ser	**Dosage dependent**	**(Mouse) accumulation of single membrane-bound vesicles at IS/OS junction containing RHO_P347S**	**[237, 252]**

Table A1.3 Founder screening

System	Rhodopsin Allele	Screened, n	Founders Identified
Constitutive	**WT**	**36**	**0**
Constitutive	**P23H**	**11**	**7**
Constitutive	**T58R**	**11**	**0**
Constitutive	**R135L**	**46**	**0**
Constitutive	**K296E**	**13**	**3**
Constitutive	**P347S**		
Inducible	**WT**	**33**	**0**
Inducible	**P23H**	**21**	
Inducible	**T58R**	**24**	**1**
Inducible	**R135L**	**22**	**2**
Inducible	**K296E**	**27**	**0**
Inducible	**P347S**		

Appendix I Figures:

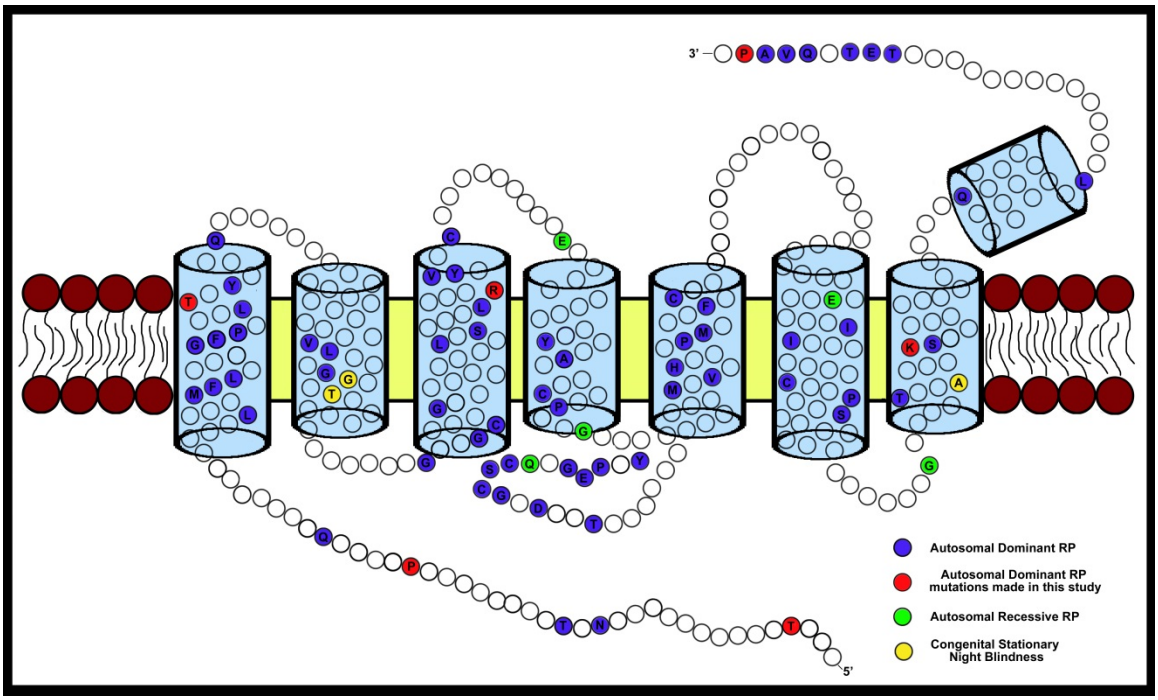

Figure A1.1: Schematic representation of the human Rhodopsin protein

Rhodopsin is a 7 transmembrane domain G-coupled protein, with a cytoplasmic N-terminal domain. Individual RP- associated mutations are shown, with Autosomal Dominant mutations shown in blue, Autosomal Recessive mutations in green, and Congenital Stationary Night Blindness mutations in Yellow. Mutations produced for this study are denoted in red.

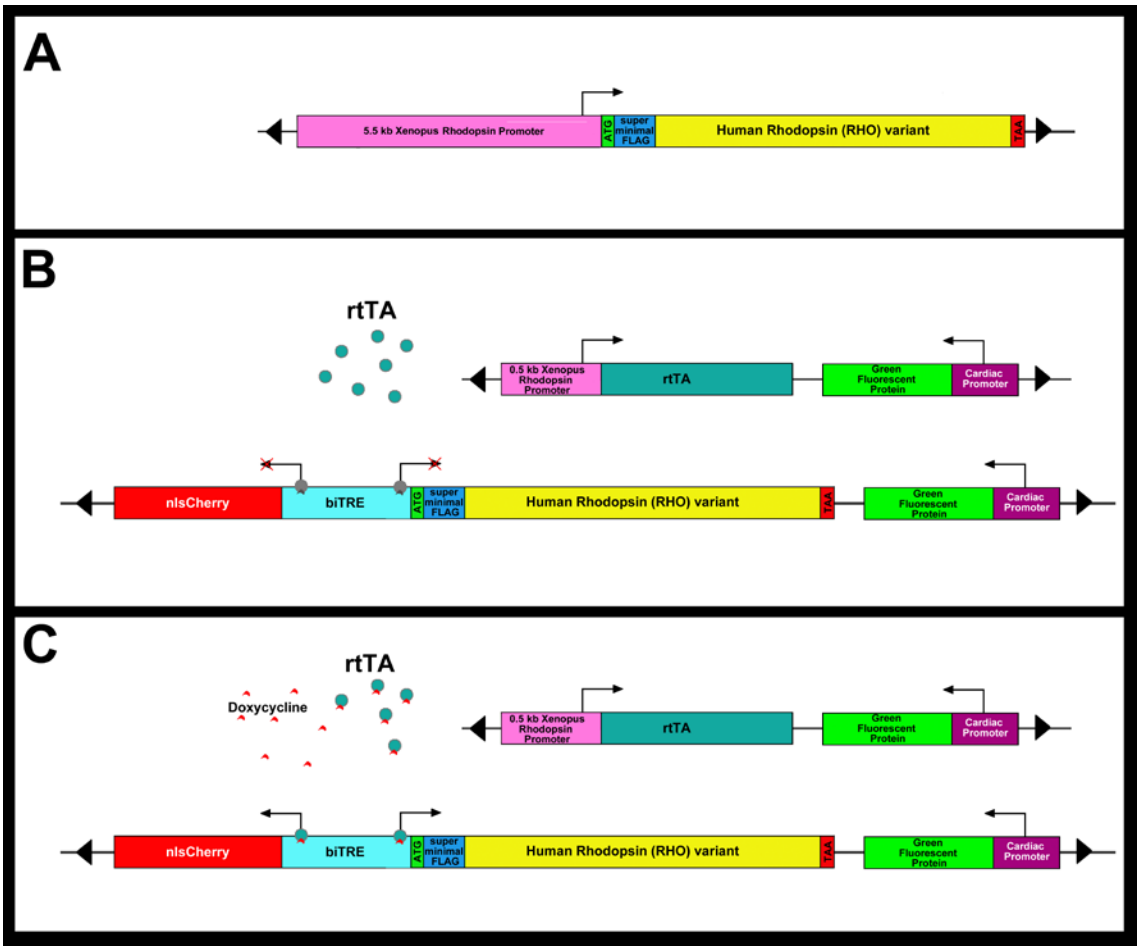

Figure A1.2 Constitutive and Inducible Transgenesis Constructs

All transgenesis constructs are flanked by inverted Tol2 repeat elements to permit integration into the chromosome. **A.** The constitutive lines are produced using a transgenesis construct containing a 5.5 kb Xenopus rhodopsin promoter driving expression of a tagged human Rhodopsin gene. These constructs also contain a cardiac myosin light chain (cmlc) promoter driving GFP, which acts as a transgenesis marker. **B-C.** The inducible lines use the TetON expression system to permit inducible expression of the human Rhodopsin variants. The reverse tetracycline-controlled transactivator (rtTA) is produced in rod photoreceptors under the control of a 0.5kb Xenopus rhodopsin promoter. The inactive rtTA is unable to bind the bidirectional Tet-responsive element (biTRE) in the absence of the ligand, doxycycline. In the presence of doxycycline, the rtTA is activated and binds to the biTRE, driving transcription of two downstream genes, the RHO variants and a fluorescent marker, mCherry. These constructs also contain the cardiac GFP marker.

APPENDIX II: COMPARISON OF RETINAL GENE EXPRESSION IN WILD-TYPE AND INSM1 KNOCKOUT MOUSE EMBRYOS AT E14.5 AND E18.5

Overall Design: Whole eyes from E14.5 and E18.5 *Insm1* knockout mice and wild-type litter mates were used to generate RNA for RNA-seq analysis. Three samples of each genotype at each time point were generated. After 3-prime fragment library preps, samples were run on an Illumina HiSeq2500 using standard chemistry. These tables contain transcripts with FPKM values greater than 50 for at least one experimental condition, with a minimum 1.5-fold change and $p>0.05$.

Appendix II Tables:

Table A2.1: EE14.5 Differentially Expressed Genes

Time point	Direction	WT	KO	log2(fold change)	p value	q value	Gene symbol	Gene Name
E14	Up in KO	3013.55	13796.8	2.19479	5.00E-05	0.024453	Gm10320	Predicted pseudogene 10320, known protein coding
E14	Up in KO	0	383.817	infinity	5.00E-05	0.024453	Ehfb	EF hand domain family, member B
E14	Up in KO	0	78.1718	infinity	5.00E-05	0.024453	4631405J19Rik	RIKEN cDNA 4631405J19 gene, known processed transcript
E14	Up in KO	0	617.275	infinity	5.00E-05	0.024453	Mm.394402	Transcribed locus
E14	Up in KO	0	567.425	infinity	5.00E-05	0.024453	Mm.98299	Transcribed locus
E14	Up in KO	0	103.797	infinity	5.00E-05	0.024453	Trim14	Tripartite motif-containing 14
E14	Up in KO	0	447.925	infinity	5.00E-05	0.024453	Gm35631	Predicted gene 35631, ncRNA
E14	Up in KO	0	415.451	infinity	5.00E-05	0.024453	Gm9534	Predicted gene 9534, pseudo
E14	Up in KO	0	633.555	infinity	5.00E-05	0.024453	Gpr125	G protein-coupled receptor 125
E14	Up in KO	0	230.691	infinity	5.00E-05	0.024453	Acsm3	Acyl-CoA synthetase medium-chain family member 3
E14	Up in KO	0	458.673	infinity	5.00E-05	0.024453	Nrg1	neuregulin 1
E14	Up in KO	0	98.7297	infinity	5.00E-05	0.024453	4930519F16Rik	RIKEN cDNA 4930519F16 gene, known processed transcript
E14	Up in KO	0	102.853	infinity	0.0001	0.038611	4930404N11Rik	RIKEN4930404N11 gene, known protein coding
E14	Up in KO	0	25.5575	infinity	0.0001	0.038611	Coro6	Coronin 6
E14	Up in KO	0	337.281	infinity	0.0001	0.038611	Rarb	Retinoic acid receptor, beta
E14	Up in KO	0	385.514	infinity	0.0001	0.038611	Pdzd2	PDZ domain containing 2
E14	Up in KO	0	300.233	infinity	0.0001	0.038611	Slc25a41	Solute carrier family 25 member 41
E14	Up in KO	0	333.886	infinity	0.0001	0.038611	Glce	Glucuronyl C5-epimerase
E14	Up in KO	0	359.942	infinity	0.00015	0.048547	Hnrnpu	Heterogeneous nuclear riboprotein U
E14	Up in KO	0	330.653	infinity	0.00015	0.048547	Ppp2r5c	Protein phosphatase 2, regulatory subunit B (B56), gamma isoform
E14	Up in KO	0	347.821	infinity	0.00015	0.048547	RPs27 Gpd1	Ribosomal protein subunit 27, Glycerol-3-phosphate dehydrogenase 1
E14	Up in KO	0	389.879	infinity	0.00015	0.048547	LOC10524459	uncharacterized ncRNA Locus
E14	Up in KO	0	337.766	infinity	0.00015	0.048547	Usp29	Ubiquitin specific protease 29
E14	Up in KO	0	322.653	infinity	0.0002	0.060296	Chrac1	Chromatin accessibility complex 1
E14	Up in KO	0	348.224	infinity	0.0002	0.060296	Mm.367605	Transcribed locus
E14	Up in KO	0	358.972	infinity	0.00025	0.069646	3830408C21Rik	RIKEN 3830408C21 gene, known protein coding
E14	Up in KO	0	323.623	infinity	0.00025	0.069646	Tuba1c	Tubulin, alpha 1C
E14	Up in KO	0	324.027	infinity	0.0003	0.0786	Gm6712	Predicted gene 6712, known lincRNA
E14	Up in KO	336598	574434	0.771116	0.00035	0.086548	Malat1	Metastasis associated lung adenocarcinoma transcript 1
E14	Up in KO	0	323.138	infinity	0.00035	0.086548	Dpp10	dipeptidylpeptidase 10
E14	Up in KO	0	374.685	infinity	0.0004	0.093651	Clul1	clusterin-like 1, Gm41522
E14	Up in KO	0	349.598	infinity	0.00045	0.103162	Jmjd1c	jumonji domain containing 1C
E14	Up in KO	0	302.415	infinity	0.0005	0.113443	Timd4	T cell immunoglobulin and mucin domain containing 4
E14	Up in KO	0	355.82	infinity	0.00055	0.122267	Sash1	SAM and SH3 domain containing 1
E14	Up in KO	1092.39	5162.58	2.2406	0.00085	0.1834	Mm.426323	Transcribed locus, embryonic and reproductive
E14	Up in KO	27078.6	62179.5	1.19929	0.0009	0.192303	Xist	Inactive X specific transcripts
E14	Up in KO	299845	490689	0.71059	0.001	0.207623	Snrnpb2	U2 small nuclear ribonuclearprotein B
E14	Up in KO	0	329.037	infinity	0.001	0.207623	Nat1	N-acetyl transferase 1
E14	Up in KO	0	232.569	infinity	0.00115	0.234344	Gm23502	Predicted gene 23502, known snRNA
E14	Up in KO	0	257.656	infinity	0.0012	0.24229	Kcnv2	Potassium channel, subfamily V, member 2
E14	Up in KO	0	76.3109	infinity	0.0013	0.253189	Btnl10	butyrophilin-like 10
E14	Up in KO	0	255.959	infinity	0.00135	0.256128	Trpc4	transient receptor potential cation channel, subfamily C, member 4
E14	Up in KO	0	51.6282	infinity	0.0014	0.263344	Itgad	integrin, alpha D
E14	Up in KO	0	276.439	infinity	0.00145	0.26593	Rpl27-ps1	ribosomal protein L27, pseudogene 1
E14	Up in KO	0	257.252	infinity	0.00165	0.285959	Gm20483	Predicted gene 20483, known antisense
E14	Up in KO	0	252.241	infinity	0.00165	0.285959	Acer1	Lkline ceramidase 1
E14	Up in KO	0	280.965	infinity	0.00165	0.285959	Mm.478165	Transcribed locus, embryonic, liver, mammary, thymus, bone marrow
E14	Up in KO	0	77.7186	infinity	0.0019	0.285959	1700011I03Rik	RIKEN cDNA 1700011I03 gene, known protein coding
E14	Up in KO	0	230.307	infinity	0.0021	0.285959	Rasgef1a	RasGEF domain family, member 1A
E14	Up in KO	13455.6	26270.5	0.96523	0.00215	0.285959	Polr1d	Polymerase (RNA) I polypeptide D
E14	Up in KO	0	253.615	infinity	0.00215	0.285959	Gm11851	Predicted gene 11851, known lincRNA
E14	Up in KO	0	345.558	infinity	0.0022	0.285959	Gm20139	Predicted gene 2-139, ncRNA
E14	Up in KO	0	358.002	infinity	0.0022	0.285959	4930553C11Rik	RIKEN cDNA 4930553C11 gene, ncRNA
E14	Up in KO	0	358.002	infinity	0.0022	0.285959	Mm.246927	Transcribed locus, embryonic head/brain
E14	Up in KO	0	286.623	infinity	0.00235	0.285959	Mm.134273	Transcribed locus, eye
E14	Up in KO	0	286.623	infinity	0.00235	0.285959	Mm.419872	Transcribed locus, eye
E14	Up in KO	0	230.307	infinity	0.0024	0.285959	Gm10490	Predicted gene 10490, known protein coding
E14	Up in KO	0	338.736	infinity	0.00245	0.285959	Tox3	TOX high mobility group box family member 3
E14	Up in KO	0	338.736	infinity	0.00245	0.285959	Mm.447396	Transcribed locus, brain
E14	Up in KO	0	200.613	infinity	0.003	0.285959	Cd5	CD5 antigen
E14	Up in KO	0	260.566	infinity	0.00305	0.285959	Gm34489	Predicted gene 34489, ncRNA

Table A2.1 E14.5 Differentially Expressed Genes (continued)

Time point	Direction	WT	KO	log2(fold change)	p value	q value	Gene symbol	Gene Name
E14	Up in KO	0	260.566	infinity	0.00305	0.285959	Mm.382125	Transcribe locus, pattern unknown
E14	Up in KO	0	260.566	infinity	0.00305	0.285959	Gm42042	Predicted gene 42042, ncRNA
E14	Up in KO	17371.7	31657.8	0.865822	0.0031	0.285959	Robo1	Roundabout homolog 1
E14	Up in KO	24599.6	43227	0.813295	0.00315	0.285959	Perp	PERP, TP53 apoptosis effector
E14	Up in KO	0	332.43	infinity	0.00335	0.285959	Gm30624	Predicted gene 36024, ncRNA
E14	Up in KO	0	338.251	infinity	0.00345	0.285959	Gm35835	Predicted gene 35835, ncRNA
E14	Up in KO	0	271.51	infinity	0.0035	0.285959	Gm30145	Predicted gene 30145, ncRNA
E14	Up in KO	0	271.51	infinity	0.0035	0.285959	Mm.55347	Transcribed locus, expression pattern unknown
E14	Up in KO	0	271.51	infinity	0.0035	0.285959	Rad51b	RAD 51 homolog B
E14	Up in KO	0	271.51	infinity	0.0035	0.285959	Dmrt2	doublesex and mab-3 related transcription factor 2
E14	Up in KO	0	271.51	infinity	0.0035	0.285959	Gm11820	Predicted gene 11820, ncRNA
E14	Up in KO	0	296.192	infinity	0.00355	0.285959	4930547E14Rik	RIKEN cDNA 4930547E14 gene, miscRNA
E14	Up in KO	0	296.192	infinity	0.00355	0.285959	Gabrb1	gamma-aminobutyric acid (GABA) A receptor, subunit beta 1
E14	Up in KO	0	296.192	infinity	0.00355	0.285959	Ankle2	Ankyrin repeat and LEM domain containing 2
E14	Up in KO	0	296.192	infinity	0.00355	0.285959	Gm30149	Predicted gene 30419, ncRNA
E14	Up in KO	0	321.764	infinity	0.00365	0.285959	Aim1	Absent in melanoma 1
E14	Up in KO	0	246.827	infinity	0.0039	0.285959	LOC432742	Hypothetical locus LOC432742
E14	Up in KO	0	246.827	infinity	0.0039	0.285959	Rnase4	Ribonuclease, RNAse A family 4
E14	Up in KO	0	246.827	infinity	0.0039	0.285959	2310069G16Rik	RIKEN cDNA 2310069G16 gene, known lincRNA
E14	Up in KO	0	246.827	infinity	0.0039	0.285959	Tmem156	Transmembrane protein 15
E14	Up in KO	0	246.827	infinity	0.0039	0.285959	Noxp20	Aka Fam114a1
E14	Up in KO	0	246.827	infinity	0.0039	0.285959	Gm31746	Predicted gene 31746, ncRNA
E14	Up in KO	0	281.287	infinity	0.0039	0.285959	Rasgef1	RasGEF domain family member 1A
E14	Up in KO	0	281.287	infinity	0.0039	0.285959	Gm32647	Predicted gene 32647, ncRNA
E14	Up in KO	0	255.716	infinity	0.00395	0.285959	Gm41062	Predicted gene 41062, ncRNA
E14	Up in KO	0	255.716	infinity	0.00395	0.285959	Card6	caspase recruitment domain family, member 6
E14	Up in KO	0	255.716	infinity	0.00395	0.285959	Mm.308998	Transcribe locus, pattern unknown
E14	Up in KO	0	255.716	infinity	0.00395	0.285959	Gm10250	Atp5h pseudogene
E14	Up in KO	0	255.716	infinity	0.00395	0.285959	Gm13826	ribosomal protein L37-like
E14	Up in KO	0	286.138	infinity	0.0041	0.293918	Ophn1	oligophrenin 1
E14	Up in KO	0	272.884	infinity	0.0042	0.295315	Slc2a35	Solute carrier family 25, member 35
E14	Up in KO	0	272.884	infinity	0.0042	0.295315	Pfas	Phosphoribosylformylglycinamidine synthase (FGAR amidotransferase)
E14	Up in KO	0	297.97	infinity	0.00435	0.300109	Klf12	Kruppel-like factor 12
E14	Up in KO	0	297.97	infinity	0.00435	0.300109	Gm19462	Predicted gene 19462, unknown
E14	Up in KO	53456.3	85870.4	0.6838	0.0045	0.306613	Epcam	Epithelial cell adhesion molecule
E14	Up in KO	0	272.399	infinity	0.0047	0.313447	Mm.158892	Transcribed locus 158892, brain, mammary gland
E14	Up in KO	0	51.6422	infinity	0.0047	0.313447	Gm15658	Predicted gene 15658, known antisense
E14	Up in KO	0	637.433	infinity	0.0047	0.313447	Zfp133-ps	zinc finger protein 133, pseudogene
E14	Up in KO	0	126.565	infinity	0.00485	0.319577	4933406C10Rik	RIKEN cDNA 4933406C10, known lincRNA
E14	Up in KO	0	285.168	infinity	0.00485	0.319577	Fam227b	Family with sequence similarity 227, member b
E14	Up in KO	0	177.79	infinity	0.005	0.324602	Smc1b	Structural maintenance of chromosomes 1B
E14	Up in KO	0	281.772	infinity	0.00515	0.328525	Slc25a3	solute carrier family 25, member 3
E14	Up in KO	0	281.772	infinity	0.00515	0.328525	Mm.247153	Transcribed locus, eye expressed
E14	Up in KO	0	223.518	infinity	0.00565	0.355272	MMp13	Matrix mellopeptidase 13
E14	Up in KO	16671.7	28312	0.764015	0.00575	0.359506	Bmpr1b	Bone morphogenic protein receptor, type 1B
E14	Up in KO	1121.57	3729.63	1.73351	0.00615	0.37082	Fat3	FAT tumor suppressor homolog 3
E14	Up in KO	0	234.025	infinity	0.00625	0.37582	Gm9143	Predicted gene 9143, known processed pseudogene
E14	Up in KO	0	127.05	infinity	0.00655	0.390657	Prss45	protease, serine 45
E14	Up in KO	0	182.396	infinity	0.0068	0.402297	Phf2os1	PHD finger protein 2, opposite strand 1
E14	Up in KO	4544.46	9217.76	1.02031	0.00695	0.408972	Gm10754	lincRNA
E14	Up in KO	0	124.303	infinity	0.0078	0.441292	A730036I17Rik	RIKEN cDNA A730036I17 gene, known lincRNA
E14	Up in KO	0	224.892	infinity	0.008	0.450292	Rbmxl2	RNA binding motif protein, X-linked-like 2
E14	Up in KO	0	148.982	infinity	0.0081	0.4536	Gm11978	Predicted gene 11978, known transcribed processed pseudogene
E14	Up in KO	0	198.836	infinity	0.00835	0.465232	Zfp14	zinc finger protein 14
E14	Up in KO	0	153.511	infinity	0.00855	0.472785	Hist1h1t	histone cluster 1, H1t
E14	Up in KO	0	151.248	infinity	0.0088	0.481767	Gm27224	Predicted gene 27224, known lincRNA
E14	Up in KO	11658.9	19960.1	0.775694	0.00975	0.514576	Sltrk6	SLIT and NTRK-like family, member 6
E14	Up in KO	14005.5	23328.7	0.736115	0.0098	0.514746	Tasp1	taspase, threonine aspartase 1
E14	Up in KO	0	199.239	infinity	0.01025	0.534555	Hoxd13	homeobox D13
E14	Up in KO	0	205.705	infinity	0.0104	0.537285	Kcnk7	potassium channel, subfamily K, member 7
E14	Up in KO	0	200.128	infinity	0.0104	0.537284	Tnfsf15	tumor necrosis factor ligand superfamily, member 15
E14	Up in KO	0	206.513	infinity	0.01055	0.542487	Gm26583	Predicted gene 26583, known lincRNA
E14	Up in KO	0	74.0481	infinity	0.0106	0.543787	Rapgef3os2	Pas guanine nucleotide exchange factor 3, opposite strand 2
E14	Up in KO	0	181.911	infinity	0.01065	0.543817	Gm14664	Predicted gene 14664, known lincRNA
E14	Up in KO	3132.31	6647.34	1.08555	0.01085	0.552747	Rbbp9	retinoblastoma binding protein 9
E14	Up in KO	3032.25	6357.17	1.068	0.01155	0.574873	Gm30340	lincRNA
E14	Up in KO	4381.64	8566.19	0.967182	0.01155	0.574873	Cdcp1	CUB domain containing protein 1
E14	Up in KO	0	153.429	infinity	0.01165	0.574873	Slurp1	secreted Ly6/Plaur domain containing 1
E14	Up in KO	0	153.429	infinity	0.01165	0.574873	Lrriq3	leucine-rich repeats and IQ motif containing 3
E14	Up in KO	320055	466189	0.542594	0.01185	0.579544	Cnpy2	canopy 2 homolog
E14	Up in KO	0	104.226	infinity	0.0126	0.591085	Serpinb1b	serine (or cysteine)peptidase inhibitor, clade B,

Table A2.1 E14.5 Differentially Expressed Genes (continued)

Time point	Direction	WT	KO	log2(fold change)	p value	q value	Gene symbol	Gene Name
								member 1b
E14	Up in KO	0	104.226	infinity	0.0126	0.591085	Hist1h4k	Histone cluster 1, H4k
E14	Up in KO	0	104.226	infinity	0.0126	0.591085	Cebpe	CCAAT/enhance binding protein (C/EBP), epsilon
E14	Up in KO	0	104.226	infinity	0.0126	0.591085	Gm26621	predicted gene 26621, known processed transcript
E14	Up in KO	0	104.226	infinity	0.0126	0.591085	E330017ARik	RIKEN cDNA E330017A01 gene, known protein coding
E14	Up in KO	0	104.226	infinity	0.0126	0.591085	Ms4a3	membrane-spanning 4-domains, subfamily A member 3
E14	Up in KO	0	104.226	infinity	0.0126	0.591085	Gm12469	Predicted gene 12469, known processed pseudogene
E14	Up in KO	0	104.226	infinity	0.0126	0.591085	1700021N21Rik	RIKEN cDNA 1700021N21 gene, known antisense
E14	Up in KO	0	104.226	infinity	0.0126	0.591085	Gm15631	Predicted gene 15631, known lincRNA
E14	Up in KO	0	104.226	infinity	0.0126	0.591085	Gm10160	Predicted gene 10160, known protein coding
E14	Up in KO	0	103.256	infinity	0.01305	0.600846	Tcte3	T-complex-associated testis expressed 3
E14	Up in KO	6360.15	14734.1	1.21203	0.0133	0.604765	Arl16	ADP-ribosylation factor-like 16
E14	Up in KO	3343.27	6716.69	1.00649	0.0138	0.621085	Aldh1	alcohol dehydrogenase 1 (class I)
E14	Up in KO	0	148.096	infinity	0.014	0.623708	Gm3526	Predicted gene 3526, known protein coding
E14	Up in KO	0	148.096	infinity	0.014	0.623708	Glod5	glyoxalase domain containing 5
E14	Up in KO	0	153.914	infinity	0.01435	0.630369	Gm5544	Predicted gene 5544, known lincRNA
E14	Up in KO	0	153.592	infinity	0.0147	0.635594	Usp18	Ubiquitin specific peptidase 18
E14	Up in KO	2697.44	5727.19	1.08624	0.01485	0.638318	Mm.464785	Transcribed locus, embryonic tissue
E14	Up in KO	0	155.37	infinity	0.01485	0.638318	Gm5828	Predicted gene 5828, known processed pseudogene
E14	Up in KO	0	130.283	infinity	0.01615	0.663114	Sfrp5	secreted frizzled-related sequence protein 5
E14	Up in KO	0	130.283	infinity	0.01615	0.663114	Tescl	tescalcin-like
E14	Up in KO	0	130.283	infinity	0.01615	0.663114	7630403G23Tik	RIKEN cDNA 7630403G23 gene, known lincRNA
E14	Up in KO	0	180.537	infinity	0.0162	0.663507	1700007P06Rik	RIKEN cDNA 1700007P06 gene, known antisense
E14	Up in KO	1822.71	4186.12	1.19953	0.01625	0.663506	Gm8206	Predicted gene 8206, known protein coding
E14	Up in KO	608.211	2038.86	1.74512	0.0164	0.667156	Gm28153	predicted gene 28513, ncRNA
E14	Up in KO	0	127.858	infinity	0.0176	0.686774	Gm26576	Predicted gene 26576, known lincRNA
E14	Up in KO	0	127.858	infinity	0.0176	0.686774	Hist1h2bl	Histone cluster 1, H2bl
E14	Up in KO	0	77.1998	infinity	0.01775	0.69018	Aire	autoimmune regulator (autoimmune polyendocrinopathy candidiasis ectodermal dystrophy)
E14	Up in KO	54.8168	254.801	2.21668	0.01875	0.714886	Mas1	MAS1 oncogene
E14	Up in KO	1410.69	3567.83	1.33864	0.01905	0.714886	Nr2c2	nuclear receptor subfamily 2, group C, member 2
E14	Up in KO	0	102.286	infinity	0.0191	0.714886	Gm12028	Predicted gene 12028, known processed pseudogene
E14	Up in KO	0	102.286	infinity	0.0191	0.714886	Mcidas	multicilliate differentiaion and DNA synthesis associated cell cycle protein
E14	Up in KO	0	102.286	infinity	0.0191	0.714886	Pfn3	Profilin 3
E14	Up in KO	0	102.286	infinity	0.0191	0.714886	Tff2	trefoil factor 2 (spasmolytic protein 1)
E14	Up in KO	0	102.286	infinity	0.0191	0.714886	Spink1	Serine peptidase inhibitor, Kazal type 1
E14	Up in KO	0	102.286	infinity	0.0191	0.714886	A530040E14Rik	RIKEN cDNA A530040E14, known protein coding
E14	Up in KO	0	102.286	infinity	0.0191	0.714886	Gm13530	Predicted gene 13530, known lincRNA
E14	Up in KO	0	102.286	infinity	0.0191	0.714886	Gm20638	Predicted gene 20638, known processed transcript
E14	Up in KO	0	102.286	infinity	0.0191	0.714886	Cd207	CD207 antigen
E14	Up in KO	0	102.286	infinity	0.0191	0.714886	Otog	otogelin
E14	Up in KO	0	51.6282	infinity	0.0192	0.717408	Tph1	tryptophan hydroxylase 1
E14	Up in KO	34.0955	409.145	3.58496	0.01935	0.719992	Gm26618	Predicted gene 26618, ncRNA
E14	Up in KO	87021.5	127629	0.552518	0.0194	0.719992	BC005561	known protein coding
E14	Up in KO	85213.3	132115	0.632649	0.0198	0.727476	Gm2036	protein coding
E14	Up in KO	0	49.3654	infinity	0.01985	0.727507	Defb30	defensin beta 30
E14	Up in KO	28195.2	43443.5	0.623694	0.01995	0.727537	2700099C18Rik	unprocessed pseudogene
E14	Up in KO	1526.67	3953.51	1.37275	0.02	0.727537	Camp	cathelicidin antimicrobial peptide
E14	Up in KO	0	74.0481	infinity	0.02015	0.731784	Gm6288	Predicted gene 6288, known antisense
E14	Up in KO	429.642	1413.31	1.71787	0.02065	0.736572	Gm10406	Predicted gene 10406, known protein coding
E14	Up in KO	0	477.215	infinity	0.02085	0.73711	Calcb	Calcitronin-related polypeptide, beta
E14	Up in KO	0	124.787	infinity	0.021	0.73711	4930486L24Rik	RIKEN cDNA 4930486L24 gene, known protein coding
E14	Up in KO	0	129.313	infinity	0.021	0.73711	Ambn	ameloblastin
E14	Up in KO	0	129.313	infinity	0.021	0.73711	Defb10	defnsin beta 10
E14	Up in KO	56.7486	283.709	2.32175	0.0215	0.744541	Tmc8	Transmembrane channel-like gene family 8
E14	Up in KO	0	101.003	infinity	0.0218	0.746092	Gm13267	Predicted gene 13267, known antisense
E14	Up in KO	258226	374804	0.537502	0.02185	0.746092	Tdrd7	tudor domain containing 7
E14	Up in KO	1121.73	3016.89	1.42734	0.0219	0.746092	Mm.234889	Transcribed, mammary
E14	Up in KO	3434.67	6660.67	0.955494	0.02255	0.75976	Gm3636	predicted gene 3636 known protein coding
E14	Up in KO	0	126.08	infinity	0.0226	0.75976	Ccl4	Chemokine (C-C motif) ligand 4
E14	Up in KO	0	126.08	infinity	0.0226	0.75976	Gm17619	Predicted gene 17619, known lincRNA
E14	Up in KO	834.188	2304.92	1.46627	0.02275	0.75976	Gm3488	Predicted gene 3488, known protein coding
E14	Up in KO	3449.47	7268.49	1.07528	0.023	0.763475	Rint1	RAD50 interactor 1
E14	Up in KO	15690.1	25869.8	0.721414	0.0231	0.764488	Pisd	phosphatidylserine decarboxylase
E14	Up in KO	7376.29	12219.6	0.728228	0.02395	0.773996	Tfap2c	transcription factor AP-2, gamma
E14	Up in KO	0	102.771	infinity	0.0241	0.775428	BC030499	cDNA sequence BC030499, known protein coding
E14	Up in KO	1219.6	3099.58	1.34567	0.0242	0.777509	Lrrc7	leucine rich repeat containing 7
E14	Up in KO	2942.3	5691.83	0.95195	0.02495	0.787804	Camp5	CAMP responsive element binding protein 5
E14	Up in KO	188877	470257	1.31601	0.0251	0.788018	Erdr1	erythroid differentiation regulator 1
E14	Up in KO	1448.02	3334.22	1.20327	0.0252	0.788907	Robo2	Roundabout homolog 2

Table A2.1 E14.5 Differentially Expressed Genes (continued)

Time point	Direction	WT	KO	log2(fold change)	p value	q value	Gene symbol	Gene Name
E14	Up in KO	782.252	2111.13	1.43231	0.0253	0.789791	Kcnb2	potassium voltage gated channel, Shab-related subfamily, member 2
E14	Up in KO	0	102.368	infinity	0.02625	0.807267	Sucnr1	succinate receptor 1
E14	Up in KO	0	26.0566	infinity	0.0267	0.809785	Gm3752	Predicted gene 3752, known protein coding
E14	Up in KO	0	98.7308	infinity	0.02675	0.809785	9430024E24Rik	RIKEN cDNA 9430024E24 gene, known lincRNA
E14	Up in KO	0	98.7308	infinity	0.02675	0.809785	Gm6938	Predicted gene 6938, known lincRNA
E14	Up in KO	1345.44	3105.32	1.20666	0.0272	0.814834	Sema3a	sema domain, immunoglobulin domain (Ig), short basic domain, secreted, (semaphorin) 3A
E14	Up in KO	2598.79	5196.21	0.999619	0.0274	0.814891	Pm20d2	Peptidase M20 domain containing 2
E14	Up in KO	320.672	993.172	1.63095	0.0276	0.81723	Rnf112	Ring finger protein 112
E14	Up in KO	12046.2	19053.9	0.661507	0.02835	0.820637	Rad54b	RAD54 homolog B
E14	Up in KO	213.858	1000.04	2.22533	0.0284	0.820637	Zkscan2	Zinc finger with KRAB and SCAN domains 2
E14	Up in KO	1946.24	4117.6	1.08111	0.02845	0.820637	Nit1	Nitriliase
E14	Up in KO	1946.24	4117.6	1.08111	0.02845	0.820637	Dedd	Death effector domain-containing
E14	Up in KO	3170.95	6041.71	0.930043	0.029	0.826725	Gabrp	gamma-aminobutyric acid (GABA) A receptor, pi
E14	Up in KO	27.412	103.742	1.92012	0.02915	0.829927	Tg	Thyroglobulin
E14	Up in KO	2169.61	4424.26	1.028	0.02945	0.833765	Rbms3	RNA binding motif, single stranded interacting protein
E14	Up in KO	0	25.5716	infinity	0.03005	0.841973	4930451E10Rik	RIKEN cDNA 4930451E10 gene, known antisense
E14	Up in KO	516.404	1583.75	1.61677	0.0301	0.841973	Gm4425	Predicted gene 4425, known lincRNA
E14	Up in KO	0	102.853	infinity	0.0303	0.841973	5031425F14Rik	, known lincRNA
E14	Up in KO	0	74.0481	infinity	0.0303	0.841973	C330013J21Rik	RIKEN cDNA C330013J21 gene, known protein coding
E14	Up in KO	0	102.853	infinity	0.0303	0.841973	Zfp445	zinc finger protein 445
E14	Up in KO	3268.46	6118.29	0.904518	0.03095	0.846983	Dzank1	double zinc ribbon and ankyrin repeat domains 1
E14	Up in KO	0	247.731	infinity	0.031	0.846983	Ankrd61	ankyrin repeat domain 61
E14	Up in KO	0	102.286	infinity	0.03125	0.846983	Gm14858	Predicted gene 14858, known processed transcript
E14	Up in KO	1801.25	3805.89	1.07924	0.03255	0.868316	Slc30a10	solute carrier family 30, member 10
E14	Up in KO	13001.5	20185.3	0.634626	0.0328	0.868737	Sgk3	serum/glucocorticoid regulated kinase 3
E14	Up in KO	0	99.6197	infinity	0.03295	0.868737	Cyp4f17	cytochrome P450, family 4, subfamily f, polypeptide 17
E14	Up in KO	998.999	2436.66	1.28635	0.033	0.868737	Ston1	Stonin 1
E14	Up in KO	229920	317243	0.464457	0.033	0.868737	Eif2s3x	eukaryotic translation initiation factor 2, subunit 3, structural gene X-linked
E14	Up in KO	0	100.105	infinity	0.0333	0.870388	Gm15579	Predicted gene 15579, known antisense
E14	Up in KO	289.41	1280.07	2.14504	0.0336	0.876148	Ccl7	Chemokine (C-C motif) ligand 7
E14	Up in KO	126618	175520	0.471151	0.03465	0.888927	Chchd3	coiled-coil-helix-coiled-coil-helix domain containing 3
E14	Up in KO	277.967	1133.07	2.02725	0.0348	0.888927	CD59a	CD59a antigen
E14	Up in KO	963.886	2419.48	1.32776	0.03495	0.888927	Meis2	Meis homeobox 2
E14	Up in KO	589.068	1407.85	1.25699	0.035	0.888927	Ocin	Occludin
E14	Up in KO	314.951	1027.43	1.70584	0.035	0.888927	Gm14419	Predicted gene 14419, known protein coding
E14	Up in KO	28.4002	125.731	2.14636	0.0352	0.888927	Tulp2	Tubby-like protein 2
E14	Up in KO	0	52.1132	infinity	0.0352	0.888927	4931422A03Rik	RIKEN cDNA 4931422A03 gene, known protein coding
E14	Up in KO	10105.2	16000.1	0.662985	0.0358	0.888927	Mir344g	microRNA 344g
E14	Up in KO	0	101.479	infinity	0.03615	0.888926	Matn1	matrillin 1, cartilage matrix protein
E14	Up in KO	0	101.479	infinity	0.03615	0.888927	Gm7857	Predicted gene 7857, known processed pseudogene
E14	Up in KO	1400.21	2829.4	1.01485	0.03645	0.893309	Lgals4	lectin, galactose binding, soluble 4
E14	Up in KO	238.668	1471.92	2.62462	0.03675	0.893622	Mm.411452	Transcribed locus, mammary
E14	Up in KO	1721.9	3470.71	1.01123	0.03685	0.893622	Gm20754	lincRNA
E14	Up in KO	0	76.3109	infinity	0.037	0.893849	Gm12691	Predicted gene 12691, known processed pseudogene
E14	Up in KO	3232.61	5714.12	0.82183	0.0373	0.8952	Mm.452559	Transcribed locus, brain
E14	Up in KO	324.468	1024.89	1.65932	0.03755	0.899239	Fbxo48	F-box protein 48
E14	Up in KO	0	100.509	infinity	0.03785	0.903474	4930519A11Rik	RIKEN cDNA 4930519A11 gene, known lincRNA
E14	Up in KO	0	26.0566	infinity	0.03815	0.905723	Gm25996	Predicted gene 25996, known miRNA
E14	Up in KO	0	49.3654	infinity	0.0384	0.907741	Gm20319	Predicted gene 20319, known processed transcript
E14	Up in KO	8205.93	12967.4	0.660151	0.0387	0.909946	Tbc1d31	TBC1 domain family, member 31
E14	Up in KO	0	77.1998	infinity	0.0389	0.911727	Cpa5	Carboxypeptidase A5
E14	Up in KO	21996.9	32145.9	0.547331	0.03925	0.913123	Arhgap5	Rho GTPase activating protein 5
E14	Up in KO	0	24.6827	infinity	0.03945	0.914874	1700101G07Rik	RIKEN cDNA 1700101G07 miscRNA
E14	Up in KO	2594.67	4889.84	0.914235	0.0397	0.916808	Entpd6	ectonucleoside triphosphate diphosphohydrolase 6
E14	Up in KO	0	129.798	infinity	0.0397	0.916808	Spo1	SPO11 meiotic protein covalently bound to DSB
E14	Up in KO	0	26.0566	infinity	0.0397	0.916808	Pdx1	pancreatic and duodenal homeobox 1
E14	Up in KO	102.286	702.074	2.77901	0.04025	0.921683	Galntl6	UDP-N-acetyl-alpha-D-galactosamine polypeptide N-acetylgalactosaminyltransferase-like 6
E14	Up in KO	62197.1	86473.3	0.475407	0.04035	0.921683	Tmed4	transmembrane emp24 protein transport domain containing 4
E14	Up in KO	0	179.523	infinity	0.04055	0.921683	Sp9	trans-acting transcription factor 9
E14	Up in KO	20162.3	29834.1	0.565304	0.04065	0.921683	Eif3j2	eukaryotic translation initiation factor 3, subunit J2
E14	Up in KO	117.293	563.303	2.26379	0.04185	0.929008	Tnfrsf13c	Tumor necrosis factor receptor superfamily, member 13c
E14	Up in KO	0	25.5716	infinity	0.042	0.929008	Gm19301	Predicted gene 19301, known processed transcript
E14	Up in KO	73606.9	102016	0.470881	0.0421	0.929008	Sema3c	sema domain, immunoglobulin domain (Ig), short

Table A2.1 E14.5 Differentially Expressed Genes (continued)

Time point	Direction	WT	KO	log2(fold change)	p value	q value	Gene symbol	Gene Name
								basic domain, secreted, (semaphorin) 3C
E14	Up in KO	354.767	1131.05	1.67272	0.0424	0.929008	Ddx43	DEAD (Asp-Glu-Ala-Asp) box polypeptide 43
E14	Up in KO	61219.1	85282.4	0.478265	0.0436	0.92924	Haus3	HAUS augmin-like complex, subunit 3
E14	Up in KO	118.256	1104.35	3.22321	0.04375	0.92924	Grik2	glutamate receptor, ionotropic, kainate 2 (beta 2)
E14	Up in KO	349.046	1252.48	1.8433	0.04405	0.92924	Gm14327	Predicted gene 14327, known protein coding
E14	Up in KO	1678.23	3340.56	0.993147	0.0442	0.92924	Gm3739	Predicted gene 3739, known protein coding
E14	Up in KO	954218	######	0.435517	0.0442	0.92924	Cox7b	cytochrome c oxidase subunit VIIb
E14	Up in KO	1529.45	3223.88	1.07579	0.04445	0.92924	Bbs10	Bardet-Biedl syndrome 10 (human)
E14	Up in KO	495.908	1429.83	1.5277	0.04455	0.92924	Gm16008	predicted gene 26008, ncRNA
E14	Up in KO	0	257.171	infinity	0.04475	0.92924	CD300lg	CD300 antigen like family member G
E14	Up in KO	224.107	1636.75	2.86857	0.04505	0.92924	Col19a1	collagen, type XIX, alpha 1
E14	Up in KO	7061.39	11286.7	0.676606	0.0453	0.92924	Hipk2	Homeodomain interacting protein kinase 2
E14	Up in KO	11098.6	22247.4	1.00325	0.04555	0.92924	Orai1	ORAI calcium release-activated calcium modulator 1
E14	Up in KO	1951.67	3896.57	0.997494	0.04555	0.92924	Hdac9	histone deacetylase 9
E14	Up in KO	947.24	2306.91	1.28416	0.0459	0.92924	Mm.385485	Transcribed locus, extraembryonic tissue
E14	Up in KO	12644.4	19225.5	0.604519	0.0459	0.92924	Mpzl2	myelin protein zero-like 2
E14	Up in KO	53747.2	75281.1	0.486097	0.0461	0.92924	Tnfrsf19	tumor necrosis factor receptor superfamily, member 19
E14	Up in KO	0	336.796	infinity	0.04665	0.92924	9630013D21Rik	RIKEN cDNA 9630013D21 gene, known processed transcript
E14	Up in KO	112077	152845	0.447579	0.0467	0.92924	Mir99ahg	Mir99a and Mirlet7c-1 host gene (non-protein coding)
E14	Up in KO	208.137	803.423	1.94863	0.0474	0.92924	Pzp	Pregnancy zone protein
E14	Up in KO	23327.6	33375.6	0.516759	0.04765	0.92924	6720427I07Rik	lincRNA
E14	Up in KO	515.673	1274.33	1.30522	0.0484	0.92924	Elf5	E74-like factor 5
E14	Up in KO	207.175	945.02	2.1895	0.049	0.92924	Gm33855	Predicted gene 33855, ncRNA
E14	Up in KO	10708.1	16408.4	0.615734	0.0491	0.92924	Gm16344	known antisense
E14	Up in KO	1855.29	3545	0.934146	0.04935	0.92924	Zfp341	zinc finger protein 341
E14	Up in KO	242.233	978.107	2.0136	0.0499	0.92924	Smarca1	SWI/SNF related matrix associated, actin dependent regulator of chromatin, subfamily a-like 1
E14	Down in KO	36384.8	23162.1	-0.651566	0.0262	0.807267	Ak4	p21 protein (Cdc42/Rac)-activated kinase 4
E14	Down in KO	110.609	0	-infinity	0.0295	0.833765	1520401A03Rik	RIKEN cDNA 152041A03 gene, known protein coding
E14	Down in KO	28.3743	0	-infinity	0.0146	0.633761	1700013F07Rik	RIKEN cDNA 1700013F07 gene, known protein coding
E14	Down in KO	85.1229	0	-infinity	0.0494	0.92924	1700019A02Rik	RIKEN cDNA 1700019A02 gene, known protein coding
E14	Down in KO	85.1229	0	-infinity	0.0494	0.92924	1700022N22Rik	RIKEN cDNA 1700022N22 gene, known lincRNA
E14	Down in KO	85.1229	0	-infinity	0.0494	0.92924	1700034J04Rik	RIKEN cDNA 1700034J04 gene, TEC
E14	Down in KO	34.0955	0	-infinity	0.0036	0.285959	1700036A12Rik	RIKEN cDNA 1700036A12 gene, known lincRNA
E14	Down in KO	272.536	26.058	-3.38665	0.0026	0.285959	1700109H08Rik	RIKEN cDNA 1200109H08, known protein coding
E14	Down in KO	2074.4	640.099	-1.69633	0.0204	0.734795	170019G17Rik	RIKEN cDNA 1700019G17 gene, known protein coding
E14	Down in KO	84.1603	0	-infinity	0.0481	0.92924	2210011C24Rik	RIKEN cDNA 2210011C24 gene, known protein coding
E14	Down in KO	11685.5	6820.65	-0.776734	0.02795	0.817984	2310022B05Rik	RIKEN cDNA 2310022B05 gene, protein coding
E14	Down in KO	3143.93	1339.7	-1.23066	0.0244	0.781652	2810433D01Rik	RIKEN cDNA 2810433D01 gene, lincRNA
E14	Down in KO	238.668	0	-infinity	0.00415	0.294623	3110004A20Rik	RIKEN cDNA 3110004A20 gene, known lincRNA
E14	Down in KO	375.05	0	-infinity	0.00235	0.285959	3300002P13Rik	RIKEN cDNA 3300002P13 gene, ncRNA
E14	Down in KO	1983.69	587.097	-1.75651	0.01835	0.707262	3830406C13Rik	RIKEN cDNA 3830406C12 gene, protein coding
E14	Down in KO	1744.68	533.691	-1.70888	0.0278	0.81723	4732491K20Rik	RIKEN cDNA 4732491K20 gene, known lincRNA
E14	Down in KO	272.764	0	-infinity	0.0068	0.402297	4930415F15Rik	RIKEN cDNA 4930415F15 gene, known protein coding
E14	Down in KO	283.743	0	-infinity	0.00345	0.285959	4930455J16Rik	RIKEN cDNA 4930455J16 gene, ncRNA
E14	Down in KO	3201.71	1501.37	-1.09256	0.04395	0.92924	4930469G21Rik	RIKEN cDNA 4930469G21 gene , known antisense
E14	Down in KO	170.477	0	-infinity	0.0093	0.49558	4930527J03Rik	RIKEN cDNA 4930527J03, known pseudogene/TEC
E14	Down in KO	186.447	0	-infinity	0.0042	0.295315	4930539E08Rik	RIKEN cDNA 4930539E08 gene, known protein coding
E14	Down in KO	34.0955	0	-infinity	0.0036	0.285959	4930552P12Rik	RIKEN cDNA 4930552P12 gene, known lincRNA
E14	Down in KO	177.835	0	-infinity	0.0147	0.635594	4933431K23Rik	RIKEN cDNA 4933431K23 gene, known processed transcript
E14	Down in KO	167.358	0	-infinity	0.0128	0.594309	5430427O19Rik	RIKEN cDNA 5430427O19 gene, known protein coding
E14	Down in KO	221.505	0	-infinity	0.02475	0.786	5830432E09Rik	RIKEN cDNA 5830432E09 gene, known lincRNA
E14	Down in KO	90.8441	0	-infinity	0.0454	0.92924	A730013G03Rik	RIKEN cDNA A730013G03, TEC
E14	Down in KO	1166.82	333.886	-1.80516	0.04365	0.92924	A83009H15Rk	RIKEN cDNA A830092H15 gene, known antisense
E14	Down in KO	3758.04	1203.81	-1.64238	0.00335	0.285959	A930005H10Rik	RIKEN cDNA A930005H10 gene, known processed transcript
E14	Down in KO	10898.5	6652.06	-0.712263	0.0371	0.894301	Abca2	ATP-binding cassette, sub-family A (ABC1), member 2
E14	Down in KO	7486.99	4356.55	-0.781198	0.04535	0.92924	Abca7	ATP-binding cassette, sub-family A (ABC1), member 7
E14	Down in KO	4039.1	2085.24	-0.953822	0.03575	0.888927	Abcg1	ATP-binding cassette, sub-family G (WHITE), member 1

Table A2.1 E14.5 Differentially Expressed Genes (continued)

Time point	Direction	WT	KO	log2(fold change)	p value	q value	Gene symbol	Gene Name
E14	Down in KO	1926.88	767.634	-1.32778	0.03395	0.883182	Acaca	Acetyl-Coenzyme A carboxylase alpha
E14	Down in KO	53195.1	30678.9	-0.794048	0.0027	0.285959	Acvr2b	Activin receptor IIB
E14	Down in KO	54.8234	0	-infinity	5.00E-05	0.024453	Adad1	Adenosine deaminase domain containing 1 (testis specific)
E14	Down in KO	97860.6	63714.4	-0.619109	0.0084	0.466836	Adarb2	adenosine deaminase, RNA-specific, B2
E14	Down in KO	36634.6	24576.8	-0.575909	0.0274	0.814891	Add1	adducin 1 (alpha)
E14	Down in KO	13601	6190.89	-1.1355	0.00145	0.26593	Adgrb1	Adhesion G protein-coupled receptor B1
E14	Down in KO	45524.2	31048.4	-0.552115	0.03325	0.870114	Afap1	actin filament associated protein 1
E14	Down in KO	234.586	0	-infinity	0.0003	0.0786	Aipl1	Aryl hydrocarbon receptor-interacting protein-like 1
E14	Down in KO	9104.57	5057.05	-0.848295	0.0221	0.750581	Ajuba	Ajuba LIM protein
E14	Down in KO	34.0955	0	-infinity	0.0036	0.285959	AK157302	cDNA sequence AK157302, known protein coding
E14	Down in KO	10828.4	6471.57	-0.742634	0.03285	0.868737	Ak3	adenylate kinase 3
E14	Down in KO	29373.8	19070.1	-0.623218	0.0227	0.75976	Akt1	thymoma viral proto-oncogene 1
E14	Down in KO	212450	158082	-0.42645	0.0471	0.92924	Aldh1a1	aldehyde dehydrogenase family 1, subfamily A1
E14	Down in KO	4924	2805.77	-0.811435	0.04075	0.921683	Alpl	Alkaline phosphatase, liver/bone/kidney
E14	Down in KO	19869.9	11832.3	-0.747856	0.0152	0.645795	Amer2	APC membrane recruitment 2
E14	Down in KO	6073.5	2951.65	-1.041	0.012	0.582849	Angel1	Angel homolog 1
E14	Down in KO	3252.56	1552.19	-1.06727	0.048	0.92924	Angptl6	Angiopoietin-like 6
E14	Down in KO	163.794	0	-infinity	0.01155	0.574873	Ankrd23	Ankyrin repeat domain 23
E14	Down in KO	1182.27	481.578	-1.29572	0.01555	0.651856	Ano4	Anoctamin 4
E14	Down in KO	409.146	0	-infinity	0.0019	0.285959	Ap1m1	Adaptor-related protein complex AP-1, mu subunit
E14	Down in KO	100701	54379.5	-0.88894	0.00045	0.103162	Apba2	Amyloid beta (A4) precursor protein-binding, family A, member 2
E14	Down in KO	26669.3	17992.5	-0.567783	0.04	0.920837	Apc	adenomatosis polyposis coli
E14	Down in KO	46088.3	31490.7	-0.549475	0.0285	0.820637	Aplp2	amyloid beta (A4) precursor-like protein 2
E14	Down in KO	12169.3	7519.68	-0.694497	0.03115	0.846983	Arhgap1	Rho GTPase activating protein 1
E14	Down in KO	35217	20379.6	-0.789149	0.00465	0.313447	Arhgdia	Rho GDP dissociation inhibitor (GDI) alpha
E14	Down in KO	1292.67	508.442	-1.3462	0.04215	0.929008	Arhgdig	Rho GDP dissociation inhibitor (GDI) gamma
E14	Down in KO	7179.99	3953.23	-0.86095	0.02095	0.73711	Arhgef1	Rho guanine nucleotide exchange factor (GEF) 1
E14	Down in KO	91639.4	63153.9	-0.537096	0.02735	0.814891	Arid1a	AT rich interactive domain 1A (SWI-like)
E14	Down in KO	21239.6	14276.1	-0.573152	0.04585	0.92924	Arrb1	arrestin, beta 1
E14	Down in KO	6675.27	3585.36	-0.896707	0.03795	0.9039	Atic	5-aminoimidazole-4-carboxamide ribonucleotide formyltransferase/IMP cyclohydrolase
E14	Down in KO	63476.9	42539	-0.577445	0.02125	0.739984	Atn1	atrophin 1
E14	Down in KO	969968	685098	-0.501627	0.036	0.888927	atoh7	atonal homolog 7
E14	Down in KO	34.0955	0	-infinity	0.0036	0.285959	Atp5k-ps2	ATP synthase, H+ transporting, mitochondrial F1F0 complex, subunit E, pseudogene 2
E14	Down in KO	35471.6	23990.9	-0.564177	0.02985	0.840075	Atp6v0a1	ATPase, H+ transporting, lysosomal V0 subunit A1
E14	Down in KO	14519.7	9385.03	-0.629583	0.04405	0.92924	Atp6v1d	ATPase, H+ transporting, lysosomal V1 subunit D
E14	Down in KO	2559.63	720.776	-1.82832	0.01275	0.594309	B230303O12Rik	RIKEN cDNA B230303O12 gene
E14	Down in KO	111.572	0	-infinity	0.0309	0.846983	B3gnt3	UDP-GlcNAc:betaGal beta-1,3 N-acetylglucosaminyltransferase 3
E14	Down in KO	27199.4	17796.7	-0.611971	0.02705	0.812164	Bag6	BCL2-associated athanogene 6
E14	Down in KO	41873.6	27548.9	-0.604047	0.02405	0.774952	Banf1	barrier to autointegration factor 1
E14	Down in KO	3943.01	2051.63	-0.942524	0.0217	0.746092	BC017158	cDNA sequence BC017158
E14	Down in KO	1694.33	713.34	-1.24805	0.0484	0.92924	BC043934	cDNA sequence BC043934 lincRNA
E14	Down in KO	47707	17313.5	-1.4623	0.0023	0.285959	Bfsp2	Beaded filament structural protein 2, phakinin
E14	Down in KO	4362.84	2043.79	-1.09402	0.0263	0.807267	Blm	Bloom syndrome, RecQ helicase-like
E14	Down in KO	16727.9	10347	-0.693049	0.02635	0.807675	Brpf1	bromodomain and PHD finger containing, 1
E14	Down in KO	153477	107257	-0.516955	0.02065	0.736572	Bsg	basigin
E14	Down in KO	624.13	25.5734	-4.60913	0.0215	0.744541	Bst1	Bone Marrow stromal cell antigen 1
E14	Down in KO	375.05	0	-infinity	0.00235	0.285959	Bzw1	Basic leucine zipper and W2 domains 1 *** 3 of 3 options***
E14	Down in KO	129.698	0	-infinity	0.041	0.921683	C8a	complement component 8, alpha polypeptide
E14	Down in KO	2946.63	1132.83	-1.37913	0.025	0.788018	Cacnb3	Calcium channel, voltage dependent, beta 3 subunit
E14	Down in KO	160202	107955	-0.569459	0.0104	0.537284	Cacng4	calcium channel, voltage-dependent, gamma subunit 4
E14	Down in KO	52694.3	37738	-0.481629	0.0498	0.92924	Capns1	calpain, small subunit 1
E14	Down in KO	2762.37	1284.48	-1.10472	0.04405	0.92924	Car10	Carbonic anhydrase 10
E14	Down in KO	49868.7	34594.4	-0.527597	0.04125	0.925413	Casz1	Castor zinc finger 1
E14	Down in KO	136.382	0	-infinity	0.01735	0.68676	Cbx3-ps6	Chromobox 3, pseudogene 6
E14	Down in KO	2549.21	766.261	-1.73414	0.0102	0.53321	Ccdc184	Coiled-coil domain containing 184
E14	Down in KO	15257.5	9476.06	-0.687156	0.0359	0.888927	Ccdc72	Coiled-coil domain containing 72
E14	Down in KO	2549.58	711.803	-1.84071	0.00585	0.360635	Ccdc88b	Coiled-coil domain containing 88B
E14	Down in KO	7623.99	4167.21	-0.871465	0.01315	0.602928	Ccdc9	Coiled-coil domain containing 9
E14	Down in KO	112.535	0	-infinity	0.02845	0.820637	Cckar	Cholecystokinin A receptor
E14	Down in KO	113.497	0	-infinity	0.02385	0.773035	Ccl3	Chemokine (C-C motif) ligand 3
E14	Down in KO	375.05	0	-infinity	0.00235	0.285959	Ccnd1	Cyclin D1
E14	Down in KO	14975.1	7204.09	-1.05568	0.0027	0.285959	Cd276	CD276 antigen
E14	Down in KO	163.794	0	-infinity	0.0001	0.038611	Cd37	CD37 antigen
E14	Down in KO	272.764	0	-infinity	0.00285	0.285959	Cd79a	CD 79 antigen A (immunoglobulin-associated alpha
E14	Down in KO	50923.9	35222.9	-0.531828	0.03405	0.884737	Cdc37	cell division cycle 37
E14	Down in KO	9861.26	4489.43	-1.13524	0.0034	0.285959	Cdca4	Cell division cycle associated 4
E14	Down in KO	1029.71	283.713	-1.85973	0.04985	0.92924	Cebpa	CCAAT/enhancer binding protein (C/EBP), alpha

Table A2.1 E14.5 Differentially Expressed Genes (continued)

Time point	Direction	WT	KO	log2(fold change)	p value	q value	Gene symbol	Gene Name
E14	Down in KO	18993.8	11805	-0.68613	0.0285	0.820637	Celsr3	cadherin, EGF LAG seven-pass G-type receptor 3
E14	Down in KO	84.1603	0	-infinity	0.0481	0.92924	Ces1a	carboxylesterase 1A
E14	Down in KO	146.63	0	-infinity	0.0208	0.73711	Cfap45	Cilia and flagella associated protein 45
E14	Down in KO	160810	97064.9	-0.728334	0.0024	0.285959	Chd4	chromodomain helicase DNA binding protein 4
E14	Down in KO	39233.6	26889.5	-0.545049	0.0459	0.92924	Chrna4	cholinergic receptor, nicotinic, alpha polypeptide 4
E14	Down in KO	3854.81	1725.54	-1.15962	0.014	0.623709	Cited1	Cbp/p300-interacting transactivator with Glu/Asp-rich carboxy-terminal domain 1
E14	Down in KO	375.05	0	-infinity	0.00235	0.285959	Ck1	CDC-like kinase 1 ***1 of 3 options***
E14	Down in KO	221.505	0	-infinity	0.0103	0.535892	CK137956	cDNA sequence CK137956, known protein coding
E14	Down in KO	421334	262544	-0.682403	0.004	0.287686	Ckb	Creatine kinase, brain
E14	Down in KO	2209.82	817.889	-1.43395	0.024	0.774475	Clec2l	C-type lectin domain family 2, member L
E14	Down in KO	282.049	0	-infinity	0.0003	0.0786	Clec4a3	C-type lectin domain family 4, member a3
E14	Down in KO	164.47	0	-infinity	0.00995	0.52138	Clec4d	C-type lectin domain family 4, member d
E14	Down in KO	340.955	0	-infinity	0.00255	0.285959	Clic1	Chloride intracellular channel 1
E14	Down in KO	55.786	0	-infinity	0.01975	0.727476	Cngb1	Cyclic nucleotide gated channel beta 1
E14	Down in KO	2161.45	810.374	-1.41534	0.02345	0.77028	Cnn1	Calponin 1
E14	Down in KO	6846.94	3479.52	-0.976571	0.01755	0.686774	Cntn1	Contactin 1
E14	Down in KO	49280.2	32898.4	-0.582989	0.04715	0.92924	Col18a1	collagen, type XVIII, alpha 1
E14	Down in KO	503.268	0	-infinity	5.00E-05	0.024453	Col20a1	Collagen, type XX, alpha 1
E14	Down in KO	74473.8	41532	-0.842511	0.0387	0.909946	Col4a2	collagen, type IV, alpha 2
E14	Down in KO	8705.81	5010.67	-0.796976	0.0273	0.814891	Cpsf4	cleavage and polyadenylation specific factor 4
E14	Down in KO	7487.45	4004.73	-0.902769	0.016	0.663114	Creb3l1	cAMP responsive element binding protein 3-like 1
E14	Down in KO	24332.1	13934.1	-0.80424	0.0064	0.383791	Crip2	cysteine rich protein 2
E14	Down in KO	123994	85396.6	-0.538017	0.0421	0.929008	Crmp1	collapsin response mediator protein 1
E14	Down in KO	7029.68	3126.61	-1.16886	0.0051	0.328189	Crx	cone-rod homeobox
E14	Down in KO	101921	70607.7	-0.529551	0.02615	0.807267	Csk	c-src tyrosine kinase
E14	Down in KO	510.238	0	-infinity	0.00015	0.048547	Cst3	Cystain C
E14	Down in KO	6268.43	3167.41	-0.9848	0.01415	0.626586	Ctdp1	CTD (carboxy-terminal domain, RNA polymerase II polypeptide A) phosphatase, subunit 1
E14	Down in KO	51175.3	33089.4	-0.629081	0.01355	0.613598	Ctxn1	cortexin 1
E14	Down in KO	22935.4	12905	-0.829644	0.0038	0.285959	Cux2	Cut-like homeobox 2
E14	Down in KO	88.9189	0	-infinity	0.0455	0.92924	Cxcr3	Chemokine (C-X-C motif) receptor 3
E14	Down in KO	6661.19	3242.83	-1.03853	0.01425	0.628485	Cxx1b	CAAX box 1B
E14	Down in KO	866.876	0	-infinity	5.00E-05	0.024453	Cyb561a3	Cytochrome b561 family, member A3
E14	Down in KO	244.158	25.5716	-3.2552	0.04255	0.929008	Cyp2s1	Cytochrome P450, family 2, subfamily s, polypeptide 1
E14	Down in KO	40230.4	28062.9	-0.519622	0.04905	0.92924	cyth2	cytohesin 2
E14	Down in KO	3937.48	1920.54	-1.03576	0.04355	0.92924	D630003M21Rik	RIKEN cDNA D630003M21 gene, protein coding
E14	Down in KO	34.0955	0	-infinity	0.0036	0.285959	D830013O20Rik	RIKEN D830013O20 gene, protein coding
E14	Down in KO	28744.2	13836	-1.05485	0.0152	0.645795	D930028M14Rik	RIKEN cDNA D930028M14 gene, lincRNA
E14	Down in KO	36698.3	25093.7	-0.548392	0.0331	0.86984	Dapl1	death associated protein-like 1
E14	Down in KO	16806	10900.7	-0.624557	0.03915	0.912726	Dars	aspartyl-tRNA synthetase
E14	Down in KO	85.1369	0	-infinity	0.02025	0.731793	Dcdc2b	Doublecortin domain containing 2b
E14	Down in KO	21914.6	10514.2	-1.05955	0.00145	0.26593	Dctn1	Dynactin 1
E14	Down in KO	9257.62	5561.2	-0.735244	0.04615	0.92924	Ddx23	DEAD (Asp-Glu-Ala-Asp) box polypeptide 23
E14	Down in KO	25421.9	0	-infinity	5.00E-05	0.024453	Ddx3y	DEAD (Asp-Glu-Ala-Asp) box polypeptide 3, Y-linked
E14	Down in KO	24113.1	16352.7	-0.560288	0.04815	0.92924	Dennd2a	DENN/MADD domain containing 2A
E14	Down in KO	4443.49	2072.84	-1.10008	0.01655	0.669545	Deptor	DEP domain containing MTOR-interacting protein
E14	Down in KO	3711.09	1828.28	-1.02136	0.0389	0.911727	Dll3	Delta-like 3
E14	Down in KO	47456.1	32797.2	-0.53302	0.03525	0.888927	Dmwd	dystrophia myotonica-containing WD repeat motif
E14	Down in KO	85.1229	0	-infinity	0.0494	0.92924	Dnajc19-ps	DNAJ (Hsp40), subfamily C, member 19, known processed pseudogene
E14	Down in KO	201.453	0	-infinity	5.00E-05	0.024453	Dnase1l2	Doexyribonuclease 1-like 2
E14	Down in KO	257.421	0	-infinity	5.00E-05	0.024453	Doc2a	Double C2, alpha
E14	Down in KO	37286.6	24109.2	-0.629073	0.0204	0.734795	Dpysl5	dihydropyrimidinase-like 5
E14	Down in KO	11846.9	7202.56	-0.717934	0.03665	0.893622	Dr1	down-regulator of transcription 1
E14	Down in KO	82800.8	58113.6	-0.51077	0.03275	0.868737	Drap1	Dr1 associated protein 1 (negative cofactor 2 alpha)
E14	Down in KO	12501.7	7596.32	-0.718751	0.02875	0.821727	Drg2	developmentally regulated GTP binding protein 2
E14	Down in KO	23750.4	13333.1	-0.832944	0.00375	0.285959	Dtd	D-tyrosyl-tRNA deacylase
E14	Down in KO	7317.18	4019.84	-0.86415	0.03205	0.862294	Dtd2	D-tyrosyl-tRNA deacylase 2
E14	Down in KO	3327.9	1182.44	-1.49285	0.00725	0.419889	Dusp8	Dual specificity phosphatase 8
E14	Down in KO	34973.4	23977.9	-0.544553	0.0357	0.888927	Ecd	ecdysoneless homolog
E14	Down in KO	4258.83	2212.74	-0.944623	0.0475	0.92924	Ece1	Endothelin converting enzyme-like 1
E14	Down in KO	57764.7	41042	-0.493088	0.0409	0.921683	Efnb2	ephrin B2
E14	Down in KO	2838.37	1277.61	-1.15161	0.03285	0.868737	Ehd3	EH-domain containing 3
E14	Down in KO	8020.04	0	-infinity	0.0173	0.68676	Eif2s3y	Eukaryotic translation initiation factor 2, subunit 3, structural gene Y-linked
E14	Down in KO	19382.5	12819.7	-0.596395	0.0424	0.929008	Eif4ebp1	eukaryotic translation initiation factor 4E binding protein 1
E14	Down in KO	109504	72410.6	-0.596706	0.0131	0.601889	Eif5a	eukaryotic translation initiation factor 5A
E14	Down in KO	217296	133920	-0.698289	0.0021	0.285959	Elavl1	ELAV (embryonic lethal, abnormal vision)-like 1(Hu antigen R)
E14	Down in KO	321651	208524	-0.625281	0.01165	0.574873	Elavl3	ELAV (embryonic lethal, abnormal vision,

Table A2.1 E14.5 Differentially Expressed Genes (continued)

Time point	Direction	WT	KO	log2(fold change)	p value	q value	Gene symbol	Gene Name
								Drosophila)-like 3 (Hu antigen C)
E14	Down in KO	7925.07	4773.3	-0.731438	0.0475	0.92924	Ep300	E1A binding protein p300
E14	Down in KO	7726.54	3985.46	-0.955075	0.0165	0.668751	Epas1	Endothelial PAS domain protein 1
E14	Down in KO	360.49	76.3118	-2.23998	0.0151	0.645795	Eps8l1	Epidermal growth factor receptor kinase substrate 8-like 1
E14	Down in KO	340.723	0	-infinity	0.00035	0.086548	Ereg	Epiregulin
E14	Down in KO	14681.6	8675.33	-0.759022	0.0176	0.686774	Eri3	exoribonuclease 3
E14	Down in KO	1107.86	310.739	-1.834	0.04455	0.92924	Erich5	Glutamate rich 5
E14	Down in KO	6058.67	2635.9	-1.20071	0.0046	0.312459	Esyt1	Extended synaptogamin-like protein 1
E14	Down in KO	4644.2	2268.36	-1.03378	0.02	0.727537	Eya1	eyes absent 1 homolog
E14	Down in KO	38626.9	27080.7	-0.512339	0.04485	0.92924	F2r	coagulation factor II (thrombin) receptor
E14	Down in KO	32409.9	15597.8	-1.05509	0.0006	0.132048	Fam110a	Family with sequence similarity 110, member A
E14	Down in KO	21190.9	13154.4	-0.687897	0.0199	0.727507	Fam114a2	family with sequence similarity 114, member A2
E14	Down in KO	5775	2970.44	-0.959146	0.02665	0.809785	Fam166a	Family with sequence similarity 166, member a
E14	Down in KO	3062.48	1323.66	-1.21016	0.02765	0.81723	Fam167a	Family with sequence similarity 167, member A
E14	Down in KO	176128	123023	-0.517696	0.01935	0.719992	Fam195b	family with sequence similarity 195, member B
E14	Down in KO	2524.77	1230.19	-1.03727	0.0386	0.909946	Fam20a	Family with sequence similarity 20, member A
E14	Down in KO	137.059	0	-infinity	0.0171	0.684249	Fam25c	family with sequence similarity 25, member c
E14	Down in KO	139.946	0	-infinity	0.0187	0.714886	Fasl	FAS ligand (TNF superfamily, member 6)
E14	Down in KO	229199	163770	-0.484928	0.0286	0.820637	Fasn	fatty acid synthase
E14	Down in KO	44897.1	31324.6	-0.519324	0.04005	0.921024	Fat1	FAT tumor suppressor homolog 1
E14	Down in KO	20729.1	9972.98	-1.05556	0.001	0.207623	Fbln1	Fibulin 1
E14	Down in KO	20021	12059.2	-0.731377	0.02155	0.744541	Fexf2	Fez family finger 2
E14	Down in KO	222.118	0	-infinity	5.00E-05	0.024453	Fgf1	Fibroblast growth factor 1
E14	Down in KO	3763.4	1786.62	-1.0748	0.03035	0.842299	Fgf18	Fibroblast growth factor 18
E14	Down in KO	83.1977	0	-infinity	0.04915	0.92924	Fgg	fibrinogen gamma chain
E14	Down in KO	12441.2	6433.52	-0.951448	0.00945	0.502357	Fggy	FGGY carbohydrate kinase domain containing
E14	Down in KO	25568.9	17337.3	-0.560508	0.0454	0.92924	Fhl3	four and a half LIM domains 3
E14	Down in KO	59036	28998.8	-1.0256	5.00E-05	0.024453	Fis1	Fisson 1 (mitochondria outer membrane)
E14	Down in KO	9054.43	5307.83	-0.770501	0.0325	0.868316	FIZ1	Fit3 interacting zinc finger protein 1
E14	Down in KO	89845.9	61080.2	-0.556749	0.0161	0.663114	Flna	filamin, alpha
E14	Down in KO	6696.14	3833.89	-0.804521	0.041	0.921683	Foxd1	forkhead box D1
E14	Down in KO	998.268	330.815	-1.5934	0.0487	0.92924	Foxk2	Forkhead box 2
E14	Down in KO	67960.8	45328.7	-0.584279	0.01765	0.687507	Fscn1	fascin homolog 1, actin bundling protein
E14	Down in KO	224406	164197	-0.450683	0.0394	0.914678	Ftl1	ferritin light chain 1
E14	Down in KO	11977.9	7285.06	-0.717364	0.0332	0.86984	G6pc3	glucose 6 phosphatase, catalytic, 3
E14	Down in KO	158646	100675	-0.656106	0.00425	0.297879	Gabarap	Gamm-aminobutyric acid receptor associated protein
E14	Down in KO	153.314	0	-infinity	5.00E-05	0.024453	Gadl	Glutamate decarboxylase 1
E14	Down in KO	9576.2	5575.11	-0.780455	0.03665	0.893622	Gck	glucokinase
E14	Down in KO	32312.9	20418.4	-0.66224	0.0154	0.650524	Gcn1l1	GCN1 general control of amino-acid synthesis 1-like 1
E14	Down in KO	6370.41	3450.69	-0.884502	0.0342	0.885498	Gdap11	ganglioside-induced differentiation-associated protein 1-like 1
E14	Down in KO	140.909	0	-infinity	0.0154	0.650524	Gdf3	Growth differentiation factor 3
E14	Down in KO	175.004	0	-infinity	0.00515	0.328525	Gjd4	Gap junction protein, delta 4
E14	Down in KO	18097.4	11450	-0.660434	0.0304	0.842624	Gkap1	G kinase anchoring protein 1
E14	Down in KO	192.168	0	-infinity	0.0013	0.253189	Gltpd2	Glycolipid transfer protein domain containing 2
E14	Down in KO	2972.7	1354.57	-1.13394	0.0403	0.921683	Gm.387482	http://www.ncbi.nlm.nih.gov/projects/mapview/maps.cgi?TAXID=10090&CHR=14&MAPS=assembly%2Ccntg-r%2CugMm%2Cgenes&BEG=49675900&END=49676500&oview=default
E14	Down in KO	368.366	0	-infinity	0.00245	0.285959	Gm10046	Predicted gene 10046, ncRNA
E14	Down in KO	34.0955	0	-infinity	0.0036	0.285959	Gm10053	Predicted gene 10053, known protein coding
E14	Down in KO	15843.9	8957.43	-0.822771	0.01205	0.582849	Gm10093	Pseudogene
E14	Down in KO	9474.46	4520.32	-1.06762	0.0058	0.359567	Gm10116	Predicted pseudogene, known protein coding
E14	Down in KO	2995.89	1294.54	-1.21055	0.0266	0.809785	Gm10120	Pseudogene
E14	Down in KO	179.763	0	-infinity	0.00605	0.3668	Gm10154	Predicted gene 10154, known processed pseudogene
E14	Down in KO	7047.17	3593.56	-0.971629	0.02515	0.788463	Gm10177	processed transcript
E14	Down in KO	3408.29	1674.8	-1.02506	0.042	0.929008	Gm10182	pseudogene
E14	Down in KO	1431.49	228.933	-2.64452	0.02665	0.809785	Gm10269	Predicted gene 10269, known protein coding
E14	Down in KO	237.474	0	-infinity	0.00215	0.285959	Gm10275	Processed transcript
E14	Down in KO	34.0955	0	-infinity	0.0036	0.285959	Gm10355	Predicted gene 10355, known processed pseudogene ***option 1 of 3***
E14	Down in KO	248.631	0	-infinity	0.00735	0.421247	Gm10451	Predicted gene 10451, known protein coding
E14	Down in KO	65274.4	45258.5	-0.528329	0.03335	0.87066	Gm10499	unprocessed transcript
E14	Down in KO	123.977	0	-infinity	0.01455	0.632839	Gm10912	Predicted gene 10912, known protein coding
E14	Down in KO	2103.76	813.041	-1.37157	0.03075	0.846983	Gm11411	Predicted gene 11411, processed pseudogene
E14	Down in KO	34.0955	0	-infinity	0.0036	0.285959	Gm11469	Predicted gene 11469, known processed pseudogene
E14	Down in KO	130.661	0	-infinity	0.02115	0.73884	Gm11520	Predicted gene 11520, known antisense
E14	Down in KO	137.059	0	-infinity	0.0171	0.684249	Gm11764	Predicted gene 11764, known processed pseudogene
E14	Down in KO	5470.8	2922.61	-0.904495	0.0486	0.92924	Gm11808	known protein coding
E14	Down in KO	96.5652	0	-infinity	0.03605	0.888927	Gm11824	Predicted gene 11824, known processed pseudogene

Table A2.1 E14.5 Differentially Expressed Genes (continued)

Time point	Direction	WT	KO	log2(fold change)	p value	q value	Gene symbol	Gene Name
E14	Down in KO	84.1603	0	-infinity	0.0481	0.92924	Gm11878	Predicted gene 11878, known processed pseudogene
E14	Down in KO	34.0955	0	-infinity	0.0036	0.285959	Gm11914	Predicted gene 11914, known processed pseudogene
E14	Down in KO	34.0955	0	-infinity	0.0036	0.285959	Gm11997	Predicted gene 11997, known processed pseudogene
E14	Down in KO	34.0955	0	-infinity	0.0036	0.285959	Gm12011	Predicted gene 12011, known processed pseudogene
E14	Down in KO	111.572	0	-infinity	0.0309	0.846983	Gm12114	Predicted gene 12114, known lincRNA
E14	Down in KO	34.0955	0	-infinity	0.0036	0.285959	Gm12279	Predicted gene 12279 known antisense
E14	Down in KO	136.382	0	-infinity	0.01735	0.68676	Gm12506	Predicted gene 12506, known lincRNA
E14	Down in KO	85.1229	0	-infinity	0.0494	0.92924	Gm12524	Predicted gene 12524, known lincRNA
E14	Down in KO	34.0955	0	-infinity	0.0036	0.285959	Gm12661	Predicted gene 12661, known processed pseudogene
E14	Down in KO	170.477	0	-infinity	0.0093	0.49558	Gm12697	Predicted gene 12697, known processed pseudogene
E14	Down in KO	113.497	0	-infinity	0.02385	0.773035	Gm12901	Predicted gene 12901, known processed pseudogene
E14	Down in KO	1357.06	486.992	-1.47852	0.04795	0.92924	Gm13344	Predicted gene 13344, known antisense
E14	Down in KO	55.7861	0	-infinity	0.0051	0.328189	Gm13563	Predicted gene 13563, known antisense
E14	Down in KO	279.893	0	-infinity	0.00055	0.122267	Gm13652	Predicted gene 13652, known lincRNA
E14	Down in KO	85.1229	0	-infinity	0.0494	0.92924	Gm13686	Predicted gene 13686, known antisense
E14	Down in KO	165953	116609	-0.509095	0.02085	0.73711	Gm13841	pseudogene
E14	Down in KO	85.1229	0	-infinity	0.0494	0.92924	Gm14018	Predicted gene 14018, known unprocessed pseudogene
E14	Down in KO	34.0955	0	-infinity	0.0036	0.285959	Gm14034	Predicted gene 14034, known processed pseudogene
E14	Down in KO	206.212	0	-infinity	0.00305	0.285959	Gm14222	Predicted gene 14222, known sense intronic
E14	Down in KO	95.6026	0	-infinity	0.03695	0.893622	Gm14317	Predicted gene 14317, known lincRNA
E14	Down in KO	34.0955	0	-infinity	0.0036	0.285959	Gm14591	Predicted gene 14591, known processed pseudogene
E14	Down in KO	144.705	0	-infinity	0.0081	0.4536	Gm14812	Predicted gene 14812, known lincRNA
E14	Down in KO	194.77	0	-infinity	0.01135	0.572915	Gm15221	Predicted gene 15221, known lincRNA
E14	Down in KO	83.1977	0	-infinity	0.04915	0.92924	Gm15298	Predicted gene 15298, known lincRNA
E14	Down in KO	157.11	0	-infinity	0.00585	0.360635	Gm15410	Predicted gene 15410, known antisense
E14	Down in KO	28.3743	0	-infinity	0.0459	0.92924	Gm15877	Predicted gene 15877, known processed pseudogene
E14	Down in KO	34.0955	0	-infinity	0.0036	0.285959	Gm16013	Predicted gene 16013, known lincRNA
E14	Down in KO	28.3743	0	-infinity	0.0402	0.921683	Gm16219	Predicted gene 16219, known processed pseudogene
E14	Down in KO	316.145	0	-infinity	0.0004	0.093651	Gm16386	Predicted gene 16386, known lincRNA
E14	Down in KO	113.497	0	-infinity	0.02385	0.773035	Gm16675	Predicted gene 16675, known lincRNA
E14	Down in KO	32114	20783.4	-0.627774	0.02785	0.81723	Gm1673	Predicted gene 1673, known protein coding
E14	Down in KO	102.286	0	-infinity	0.01755	0.686774	Gm17644	Predicted gene 17644, known lincRNA
E14	Down in KO	34.0955	0	-infinity	0.0036	0.285959	Gm18025	Predicted gene 18025, known protein coding
E14	Down in KO	50004.2	30549.3	-0.710909	0.00615	0.37082	Gm1821	pseudogene
E14	Down in KO	48622	32451.8	-0.583314	0.0219	0.746092	Gm19558	miscRNA
E14	Down in KO	4222.36	1209.45	-1.8037	0.0071	0.413378	Gm19680	Predicted gene 19680, known processed pseudogene
E14	Down in KO	34.0955	0	-infinity	0.0036	0.285959	Gm20513	Predicted gene 20513, known lincRNA
E14	Down in KO	191.882	0	-infinity	0.00575	0.359506	Gm20554	Predicted gene 20554, known lincRNA
E14	Down in KO	110.609	0	-infinity	0.0001	0.038611	Gm20878	Predicted gene 20878, known protein coding
E14	Down in KO	85.1229	0	-infinity	0.0494	0.92924	Gm2115	Predicted gene 2115, known lincRNA
E14	Down in KO	3515.59	1186.76	-1.56674	0.0058	0.359567	Gm22711	Predicted gene 22711, known snoRNA
E14	Down in KO	102.286	0	-infinity	0.01755	0.686774	Gm23481	Predicted gene 23481, known snoRNA
E14	Down in KO	34.0955	0	-infinity	0.0036	0.285959	Gm24365	Predicted gene 24365, known miRNA
E14	Down in KO	141.871	0	-infinity	0.0133	0.604765	Gm25360	Predicted gene 25360, known snRNA
E14	Down in KO	34.0955	0	-infinity	0.0036	0.285959	Gm25509	Predicted gene 25509, known miRNA
E14	Down in KO	34.0955	0	-infinity	0.0036	0.285959	Gm26460	Predicted gene 26460, known miRNA
E14	Down in KO	397.703	0	-infinity	0.0001	0.038611	Gm26559	Predicted gene 26559, known lincRNA
E14	Down in KO	352.166	0	-infinity	0.0145	0.632839	Gm26563	Predicted gene 26563, known lincRNA
E14	Down in KO	111.572	0	-infinity	0.0309	0.846983	Gm26686	Predicted gene 26686, known lincRNA
E14	Down in KO	853.508	127.939	-2.73795	0.04835	0.92924	Gm26799	Predicted gene 26799, known lincRNA
E14	Down in KO	153.314	0	-infinity	0.02085	0.73711	Gm27186	Predicted gene 27186, known processed pseudogene
E14	Down in KO	34.0955	0	-infinity	0.0036	0.285959	Gm27249	Predicted gene 27249, Known processed pseudogene
E14	Down in KO	27.4117	0	-infinity	0.0386	0.909946	Gm2962	Predicted pseudogene 2962, known processed pseudogene
E14	Down in KO	1572.85	588.794	-1.41754	0.0409	0.921683	Gm30234	Predicted gene 30234, lincRNA
E14	Down in KO	283.743	0	-infinity	0.00345	0.285959	Gm31218	Predicted gene 31218, ncRNA
E14	Down in KO	396.741	0	-infinity	0.0001	0.038611	Gm32178	Predicted gene 32178, ncRNA
E14	Down in KO	1601.33	594.452	-1.42963	0.03675	0.893622	Gm32391	Predicted gene 32391, known lincRNA
E14	Down in KO	12855.7	7827.07	-0.715868	0.0332	0.86984	GM3379	pseudogene
E14	Down in KO	1389.73	334.048	-2.05668	0.0392	0.912924	Gm34934	Predicted gene 34934, ncRNA
E14	Down in KO	2258.08	941.383	-1.26224	0.04525	0.92924	Gm35082	Predicted gene 35082, lincRNA
E14	Down in KO	44166.6	22437	-0.977077	0.0381	0.905723	Gm3788	pseudogene
E14	Down in KO	32695.1	20599.7	-0.66645	0.0166	0.669896	Gm3839	Predicted pseudogene 3839, known protein

Table A2.1 E14.5 Differentially Expressed Genes (continued)

Time point	Direction	WT	KO	log2(fold change)	p value	q value	Gene symbol	Gene Name
								coding gene
E14	Down in KO	340.955	0	-infinity	0.00255	0.285959	Gm39487	Predicted gene 3948, ncRNA
E14	Down in KO	2151.54	345.558	-2.63837	0.035	0.888927	Gm39644	Predicted gene 39644, ncRNA
E14	Down in KO	477.337	104.226	-2.19529	0.0355	0.888927	Gm40055	Predicted gene 40055, protein coding
E14	Down in KO	409.146	0	-infinity	0.0019	0.285959	Gm40416	Predicted gene 40416, ncRNA
E14	Down in KO	409.146	0	-infinity	0.0019	0.285959	Gm40755	Predicted gene 40755, ncRNA
E14	Down in KO	369.329	0	-infinity	0.00315	0.285959	Gm41760	Predicted gene 41760, ncRNA
E14	Down in KO	340.955	0	-infinity	0.00255	0.285959	Gm4221	Predicted gene 4221, unknown
E14	Down in KO	82064.6	45572.6	-0.848593	0.0022	0.285959	Gm4366	Pseudogene
E14	Down in KO	2413.35	769.575	-1.6489	0.01665	0.669896	Gm4986	Predicted pseudogene 4986, known processed pseudogene
E14	Down in KO	1630.17	621.075	-1.39218	0.04875	0.92924	Gm5173	Predicted pseudogene, ncRNA
E14	Down in KO	109.647	0	-infinity	0.02465	0.783956	Gm5445	Predicted gene 5445, known processed pseudogene
E14	Down in KO	117.293	0	-infinity	0.0205	0.734795	Gm5451	Predicted gene 5451, known processed pseudogene
E14	Down in KO	4091.04	911.497	-2.16616	0.01615	0.663114	Gm5499	Predicted pseudogene 5499, known processed pseudogene
E14	Down in KO	204.573	0	-infinity	0.006	0.365784	Gm5621	Predicted gene 5621, known processed pseudogene
E14	Down in KO	10469.9	5036.73	-1.05569	0.00435	0.300109	Gm5781	pseudogene
E14	Down in KO	2080.77	296.192	-2.81251	0.0278	0.81723	Gm5796	Predicted gene 5796, protein coding
E14	Down in KO	6896.64	2702.64	-1.35152	0.00305	0.285959	Gm5855	Predicted gene 5855, pseudogene
E14	Down in KO	10865.6	6341	-0.776991	0.0258	0.800855	Gm5884	pseudogene
E14	Down in KO	34.0955	0	-infinity	0.0036	0.285959	Gm6023	Predicted gene 6023, known processed pseudogene
E14	Down in KO	1520.39	275.954	-2.46194	0.01555	0.651856	Gm626	Predicted protein 626, protein coding
E14	Down in KO	116.331	0	-infinity	0.0249	0.787804	Gm6286	Predicted gene 6286, known processed pseudogene
E14	Down in KO	30611.6	19038.3	-0.685174	0.01405	0.624672	Gm6394	pseudogene
E14	Down in KO	34.0955	0	-infinity	0.0036	0.285959	Gm6578	Predicted gene 6578, known transcribed and processed pseudogene
E14	Down in KO	9680.34	5634.16	-0.780858	0.02895	0.82637	Gm6581	pseudogene
E14	Down in KO	1432.17	332.189	-2.10813	0.0372	0.894751	Gm7108	Predicted gene 7108, known processed pseudogene
E14	Down in KO	34.0955	0	-infinity	0.0036	0.285959	Gm7293	Predicted gene 7293, known protein coding
E14	Down in KO	2282.84	923.085	-1.3063	0.0417	0.929008	Gm7337	Predicted gene 7337, processed transcript
E14	Down in KO	60616.7	40591.6	-0.578532	0.02215	0.75112	Gm7338	pseudogene
E14	Down in KO	84.1603	0	-infinity	0.0324	0.867469	Gm8378	Predicted gene 8378, known processed transcript
E14	Down in KO	34.0955	0	-infinity	0.0036	0.285959	Gm8444	Predicted gene 8444, known protein coding
E14	Down in KO	34.0955	0	-infinity	0.0036	0.285959	Gm8837	Predicted gene 8837, known unprocessed pseudogene
E14	Down in KO	1413.76	461.502	-1.61512	0.03505	0.888927	Gm8880	Predicted gene 8880, known processed pseudogene
E14	Down in KO	96.5652	0	-infinity	0.03605	0.888927	Gm9169	Predicted gene 9169, known processed pseudogene
E14	Down in KO	32302.8	18960.4	-0.768674	0.0047	0.313447	Gm9416	Pseudogene
E14	Down in KO	96.5652	0	-infinity	0.03605	0.888927	Gm9800	Predicted gene 9800, known pseudogene
E14	Down in KO	260924	188499	-0.469072	0.0491	0.92924	Gm9844	predicted gene 9844, known protein coding
E14	Down in KO	47185.6	28362.7	-0.73435	0.02025	0.731793	Gng3	guanine nucleotide binding protein (G protein), gamma 3
E14	Down in KO	32618.2	21012.9	-0.6344	0.0238	0.773035	Gpaa1	GPI anchor attachment protein 1
E14	Down in KO	5226.28	2763.11	-0.919492	0.03835	0.907534	Gprin1	G protein-regulated inducer of neurite outgrowth 1
E14	Down in KO	28891.2	19727.2	-0.550443	0.0406	0.921683	Gpx1	glutathione peroxidase 1
E14	Down in KO	2503.21	1180.17	-1.08478	0.04215	0.929008	Gpx3	Glutathione peroxidase 3
E14	Down in KO	38936.8	19483.9	-0.998855	0.00075	0.163426	Grifin	Galectin-related inter-fiber protein
E14	Down in KO	51252.6	35077.1	-0.547096	0.0345	0.888927	Grina	glutamate receptor, ionotropic, N-methyl D-aspartate-associated protein 1 (glutamate binding)
E14	Down in KO	17045.6	10108.7	-0.753797	0.0122	0.587522	Gstm1	glutathione S-transferase, mu 1
E14	Down in KO	2110.89	732.768	-1.52642	0.0332	0.86984	Gulo	Gulonolactone (L-) oxidase
E14	Down in KO	113.497	0	-infinity	0.02385	0.773035	Hao2	Hydroxyacid oxidase 2
E14	Down in KO	######	######	-0.436239	0.04915	0.92924	Hba-a1	hemoglobin alpha, adult chain 1
E14	Down in KO	428559	265917	-0.688517	0.00195	0.285959	Hba-a2	Hemoglobin alpha, adult chain 2
E14	Down in KO	272.764	0	-infinity	0.00285	0.285959	Hbq1a	hemoglobin, theta 1A
E14	Down in KO	337.835	0	-infinity	0.0002	0.060296	Hcn2	Hyperpolarization-activated, cyclic nucleotide-gated K+2
E14	Down in KO	1160.65	331.219	-1.80908	0.03295	0.868737	Hcn3	Hyperpolarization-activated, cyclic nucleotide-gated K+ 3
E14	Down in KO	170.477	0	-infinity	0.0093	0.49558	Hist1h2bh	Histone cluster 1, H2bh
E14	Down in KO	11756	7406.6	-0.666513	0.0482	0.92924	Hist1h3c	histone cluster 1, H3c
E14	Down in KO	1337.69	513.13	-1.38234	0.0372	0.894751	Hmcn2	Hemicentin 2
E14	Down in KO	34.0955	0	-infinity	0.0036	0.285959	Hmga1-rs	High mobility group AT-hook I, related sequence
E14	Down in KO	34.0955	0	-infinity	0.0036	0.285959	Hmgb1-ps1	High mobility group bx 1, pseudogene 1
E14	Down in KO	8002.03	4482.13	-0.836182	0.04095	0.921683	Hopx	HOP homeobox
E14	Down in KO	175.005	0	-infinity	0.01205	0.582849	Hox3dos1	homeobox D3, opposite strand 1
E14	Down in KO	27.4117	0	-infinity	0.0003	0.0786	Hoxa2	Homeobox A2

Table A2.1 E14.5 Differentially Expressed Genes (continued)

Time point	Direction	WT	KO	log2(fold change)	p value	q value	Gene symbol	Gene Name
E14	Down in KO	96.5652	0	-infinity	0.03605	0.888927	Hoxd1	Homeobox D1
E14	Down in KO	4234	2171.49	-0.963337	0.0299	0.840408	Hsf1	Heat shock factor 1
E14	Down in KO	2528.85	746.784	-1.75972	0.01345	0.610325	Hspe1-rs	Heat shock protein 1 (chaperonin 10), related sequence
E14	Down in KO	67110.6	42336.1	-0.664653	0.005	0.324602	Hspg2	Perlecan (heparin sulfate proteoglycan 2)
E14	Down in KO	230.79	0	-infinity	0.00245	0.285959	Htr1f	5-hydroxytryptamine (serotonin) receptor 1F
E14	Down in KO	13525.4	8096.47	-0.740308	0.0199	0.727507	Hyou1	hypoxia up-regulated 1
E14	Down in KO	84.1603	0	-infinity	0.0481	0.92924	Ifi204	Interferon activated gene 204
E14	Down in KO	29002.4	19271.8	-0.589677	0.03205	0.862294	Igf1r	insulin-like growth factor I receptor
E14	Down in KO	1294.59	306.536	-2.07837	0.03575	0.888927	Igfals	Insulin-like growth factor binding protein, acid labile subunit
E14	Down in KO	204.573	0	-infinity	0.006	0.365784	Igsf23	Immunoglobin superfamily, member 23
E14	Down in KO	7510.39	3610.05	-1.05687	0.0133	0.604765	Igsf2l	Immunoglobulin superfamily, member 21
E14	Down in KO	2212.94	1132.18	-0.966857	0.04195	0.929008	Inpp5d	Inositol polyphosphate-5-phosphatase D
E14	Down in KO	10532.9	6260.21	-0.750626	0.031	0.846983	Inpp5k	inositol polyphosphate 5-phosphatase K
E14	Down in KO	27397.6	1801.84	-3.92651	5.00E-05	0.024453	Insm1	Insulinoma-associated 1
E14	Down in KO	27545.8	18014.9	-0.612644	0.0183	0.707262	Ipo4	importin 4
E14	Down in KO	416.506	0	-infinity	5.00E-05	0.024453	Iqca	IQ miotic containing with AAA domain
E14	Down in KO	29185.1	19556.2	-0.577606	0.0366	0.893622	Irf2bp1	interferon regulatory factor 2 binding protein 1
E14	Down in KO	510.894	129.775	-1.97702	0.02365	0.773035	Irf7	Interferon regulatory factor 7
E14	Down in KO	12259	7389.27	-0.73034	0.02495	0.787804	Islr	immunoglobulin superfamily containing leucine-rich repeat
E14	Down in KO	1417.38	564.84	-1.32731	0.04215	0.929008	Jakmip1	Janus kinase and microtubule interacting protein 1
E14	Down in KO	48618.6	30436.2	-0.675717	0.0075	0.427617	Jund	jun D proto-oncogene
E14	Down in KO	7252.14	4399.18	-0.721171	0.04235	0.929008	Kat7	K(lysine) acetyltransferase 7
E14	Down in KO	111.572	0	-infinity	0.00435	0.300109	Katnal1	Katanin p60 subunit A-like 1, depreciated identifier
E14	Down in KO	382.179	0	-infinity	0.00015	0.048547	Kcns1	K+ voltage-gated channel, subfamily s, 1
E14	Down in KO	11719.5	6845.09	-0.775776	0.03575	0.888927	Kctd13	potassium channel tetramerisation domain containing 13
E14	Down in KO	6383.46	3796.57	-0.749643	0.04245	0.929008	Kdm4b	lysine (K)-specific demethylase 4B
E14	Down in KO	5422.02	0	-infinity	5.00E-05	0.024453	Kdm5d	Lysine (K)-specific demethylase 5D
E14	Down in KO	113.497	0	-infinity	0.02385	0.773035	Kif16bos	Kinesin family member 16B, opposite strand
E14	Down in KO	20084.4	12693.9	-0.661933	0.02235	0.756737	Kiz	kizuna centrosomal protein
E14	Down in KO	12524.6	7897.51	-0.665291	0.04575	0.92924	Klf13	Kruppel-like factor 13
E14	Down in KO	231.984	0	-infinity	0.0058	0.359567	Klk1b26	Kallikrein 1-related peptidase b26
E14	Down in KO	130.661	0	-infinity	0.02115	0.73884	Krt78	Keratin 78
E14	Down in KO	807.008	254.504	-1.66489	0.01135	0.572915	Lair1	Leukocyte-associated Ig-like receptor 1
E14	Down in KO	53019.7	35972.4	-0.559639	0.02165	0.746092	Larp4b	La ribonucleoprotein domain family, member 4B
E14	Down in KO	150.426	0	-infinity	0.0004	0.093651	Lctl	Lactase-like
E14	Down in KO	243.196	0	-infinity	0.00885	0.483302	Lhx3	LIM homeobox protein 3
E14	Down in KO	6210.19	3442.72	-0.85109	0.0303	0.841973	Lhx4	Lim homeobox protein 4
E14	Down in KO	340.492	0	-infinity	0.00285	0.285959	LOC102634048	uncharacterized C9orf40 homolog
E14	Down in KO	53134.9	36054.1	-0.559499	0.0263	0.807267	LOC105244208	40S ribosomal protein S6
E14	Down in KO	450.084	0	-infinity	0.00025	0.069646	Lox	Lysyl oxidase
E14	Down in KO	20462.4	13828	-0.565387	0.0408	0.921683	Loxl1	lysyl oxidase-like 1
E14	Down in KO	35785.7	24213.8	-0.563553	0.03705	0.894075	Lpcat1	lysophosphatidylcholine acyltransferase 1
E14	Down in KO	88.9486	24.7029	-1.8483	0.02695	0.812164	Lrp2bp	Lrp2 binding protein
E14	Down in KO	328.94	0	-infinity	0.0023	0.285959	Lsamp	Limbic system-associated membrane protein
E14	Down in KO	16485.7	9603.71	-0.779548	0.01145	0.574873	Lsm12	LSM12 homolog
E14	Down in KO	7569.01	4363.26	-0.794697	0.03785	0.903474	Ly6e	lymphocyte antigen 6 complex, locus E
E14	Down in KO	123.014	0	-infinity	0.02605	0.806341	Ly9	Lymphocyte antigen 9
E14	Down in KO	34.0955	0	-infinity	0.0036	0.285959	M6pr	Mannose-6-phosphate receptor, cation dependent (potentially a pseudogene)
E14	Down in KO	8315.56	4824.55	-0.785418	0.03075	0.846983	Mad1l1	MAD1 mitotic arrest deficient 1-like 1
E14	Down in KO	4413.08	2373.36	-0.894854	0.04815	0.92924	Mamstr	MEF2 activating motif and SAP domain containing transcriptional regulator
E14	Down in KO	6421.21	3690.92	-0.798864	0.04505	0.92924	Man1a	mannosidase 1, alpha
E14	Down in KO	10363.2	6540.85	-0.663914	0.0484	0.92924	Manbal	mannosidase, beta A, lysosomal-like
E14	Down in KO	8045.04	4929.51	-0.706655	0.04885	0.92924	Map3k1	mitogen-activated protein kinase kinase kinase 1
E14	Down in KO	45750.9	29828.7	-0.617097	0.0165	0.668751	Map4k4	mitogen-activated protein kinase 4
E14	Down in KO	31183.9	20658.9	-0.59404	0.0379	0.903687	Map6	microtubule-associated protein 6
E14	Down in KO	3869.87	2054.58	-0.913446	0.04155	0.927416	Mapk4	Mitogen-activated protein kinase 4
E14	Down in KO	129240	93736.2	-0.463375	0.0467	0.92924	Mapt	microtubule-associated protein tau
E14	Down in KO	1361.98	436.253	-1.64247	0.0391	0.912527	Marveld2	MARVEL (membrane-associating) domain containing 2
E14	Down in KO	33578.6	19783.4	-0.763251	0.0071	0.413378	Maz	MYC-associated zinc finger protein (purine-binding transcription factor)
E14	Down in KO	58264.8	38118.6	-0.612128	0.014	0.623708	Mbd3	methyl-CpG binding domain protein 3
E14	Down in KO	5884.68	3199.28	-0.879215	0.03015	0.841973	Mecr	mitochondrial trans-2-enoyl-CoA reductase
E14	Down in KO	29472.1	20198	-0.545138	0.04975	0.92924	Med16	mediator complex subunit 16
E14	Down in KO	26064.3	17647.3	-0.562626	0.0383	0.907327	Med24	mediator complex subunit 24
E14	Down in KO	83.1977	0	-infinity	0.02765	0.81723	Mgl2	Macrophage galactose N-acetyl-galactosamine specific lectin 2
E14	Down in KO	22053	13762.3	-0.680253	0.0198	0.727476	Mgll	monoglyceride lipase
E14	Down in KO	2368.64	1155.98	-1.03495	0.0287	0.821727	Mib2	mindbomb homolog 2
E14	Down in KO	14945.3	9580	-0.641593	0.0483	0.92924	Micu1	mitochondrial calcium uptake 1
E14	Down in KO	34.0955	0	-infinity	0.0036	0.285959	Mir1946b	MicroRNA 1946b

Table A2.1 E14.5 Differentially Expressed Genes (continued)

Time point	Direction	WT	KO	log2(fold change)	p value	q value	Gene symbol	Gene Name
E14	Down in KO	1153.28	308.799	-1.901	0.0462	0.92924	Mm.13196	Transcribed locus
E14	Down in KO	3778.96	1681.59	-1.16817	0.0236	0.773035	Mm.167035	Transcribed locus, brain
E14	Down in KO	340.955	0	-infinity	0.00255	0.285959	Mm.17788	Predicted gene 1788, embryonic expressed
E14	Down in KO	302.491	0	-infinity	0.0039	0.285959	Mm.207427	Transcribed locus, neonate cerebellum or brain
E14	Down in KO	338.566	0	-infinity	0.00015	0.048547	Mm.249787	Transcribed locus
E14	Down in KO	14476.2	9090.87	-0.671191	0.03685	0.893622	Mm.344009	Transcribed locus, eye pancreas and brain
E14	Down in KO	1163.02	204.573	-2.5072	0.04435	0.92924	Mm.3635	Transcribed locus
E14	Down in KO	368.366	0	-infinity	0.00245	0.285959	Mm.366942	Transcribe locus
E14	Down in KO	274.117	0	-infinity	0.0036	0.285959	Mm.372587	Transcribed locus, embryonic, lymph, liver and tumor
E14	Down in KO	1046.69	227.074	-2.20461	0.03905	0.912327	Mm.375873	Transcribe locus
E14	Down in KO	2291.43	301.122	-2.92783	0.00915	0.493562	Mm.385139	Transcribed locus
E14	Down in KO	5876.05	2625.39	-1.16231	0.0055	0.346831	Mm.441538	Transcribed locus
E14	Down in KO	1468.24	330.411	-2.15176	0.036	0.888927	Mm.445017	Transcribed locus
E14	Down in KO	6261.62	3455.33	-0.857713	0.03815	0.905723	Mm439929	Transcribed locus, embryonic, bone marrow, stomach
E14	Down in KO	12546.6	7537.3	-0.735182	0.0326	0.868597	Mmp15	matrix metallopeptidase 15
E14	Down in KO	84.1603	0	-infinity	0.0481	0.92924	Morc1	microrchidia 1
E14	Down in KO	6050.04	3029.33	-0.997944	0.01525	0.646671	Mospd3	Motile sperm domain containing 3
E14	Down in KO	1182.84	400.338	-1.56297	0.05035	0.92924	Mrap2	Melanocortin 2 receptor accessory protein 2
E14	Down in KO	3664.25	1641.84	-1.15821	0.03115	0.846983	Mrps27	mitochondrial ribosomal protein S27
E14	Down in KO	203848	134121	-0.603964	0.00745	0.425869	Msl1	musashi RNA-binding protein 1
E14	Down in KO	304.71	26.0545	-3.54783	0.00465	0.313447	Mst1	Macrophage stimulating 1
E14	Down in KO	29008.2	18920.4	-0.616515	0.02655	0.809785	Msx1	msh homeobox 1
E14	Down in KO	2844.94	1338.49	-1.0878	0.03105	0.846983	Mtmr1	Myotubularin related protein 1
E14	Down in KO	34796.9	22112.6	-0.654086	0.01305	0.600846	Mtmr2	myotubularin related protein 2
E14	Down in KO	10920.9	6258.67	-0.803165	0.02325	0.765997	Mtss1l	metastasis suppressor 1-like
E14	Down in KO	25438.5	16867	-0.592807	0.0316	0.853316	Mul1	mitochondrial ubiquitin ligase activator of NFKB 1
E14	Down in KO	7116.4	4130.37	-0.784876	0.04375	0.92924	Mus81	MUS81 endonuclease homolog
E14	Down in KO	34965.7	24094.9	-0.537209	0.04255	0.929008	Mvb12b	multivesicular body subunit 12B
E14	Down in KO	7242.3	1684.66	-2.10399	5.00E-05	0.024453	Mybl2	Myeloblastosis oncogene-like 2
E14	Down in KO	173.079	0	-infinity	0.006	0.365784	Mybpc3	Myosin binding protein C, cardiac
E14	Down in KO	14460.1	8741.35	-0.726147	0.0382	0.905933	Myo18a	myosin XVIIIA
E14	Down in KO	32032.7	21723.6	-0.560279	0.04085	0.921683	Myrf	myelin regulatory factor
E14	Down in KO	15168.7	9910.54	-0.614058	0.0479	0.92924	Ncaph	non-SMC condensin I complex, subunit H
E14	Down in KO	16514.6	8864.6	-0.897612	0.00525	0.332017	Necab2	N-terminal EF-hand calcium binding protein 2
E14	Down in KO	10416.9	6168.27	-0.755986	0.0344	0.888927	Nes	nestin
E14	Down in KO	12426.5	7632.62	-0.703164	0.02925	0.831698	Nfil3	nuclear factor, interleukin 3, regulated
E14	Down in KO	13762.2	8429.84	-0.707131	0.03085	0.846983	Nhsl1	NHS-like 1
E14	Down in KO	1959.32	845.238	-1.21292	0.0352	0.888927	Ninj1	Ninjurin 1
E14	Down in KO	14692.3	9064.2	-0.696813	0.02755	0.81723	Nipsnap3b	nipsnap homolog 3B
E14	Down in KO	9165.79	5616.6	-0.706563	0.04965	0.92924	Nle1	notchless homolog 1
E14	Down in KO	375.05	0	-infinity	0.00235	0.285959	Nlf3l1	Nigg interacting factor 30-like 1 ***2 of 3 options***
E14	Down in KO	752408	514472	-0.548424	0.01945	0.720632	Nnat	Neuronatin
E14	Down in KO	340.955	0	-infinity	0.00255	0.285959	Nos2	Nitric oxide synthae 2, inducible
E14	Down in KO	8173.19	4315.47	-0.921383	0.01635	0.666353	Notch3	notch 3
E14	Down in KO	159.035	0	-infinity	0.01515	0.645795	Npas4	neuronal PAS domain protein 4
E14	Down in KO	7704.65	3699.89	-1.05825	0.0045	0.306613	Nr1h2	Nuclear receptor subfamily 1, group H, member 2
E14	Down in KO	47435.2	30432.8	-0.640334	0.0492	0.92924	Nr2f6	nuclear receptor subfamily 2, group F, member 6
E14	Down in KO	9821	5754.19	-0.771257	0.02535	0.790231	nrxn3	neurexing III
E14	Down in KO	40410	27375.1	-0.561848	0.02955	0.833765	Nsfl1c	NSFL1 (p97) cofactor (p47)
E14	Down in KO	15249.2	9301.33	-0.713221	0.0245	0.783715	Nudt14	nudix (nucleoside diphosphate linked moiety X)-type motif 14
E14	Down in KO	7545.32	4203.93	-0.843843	0.03625	0.890391	Olfm2	Olfactomedin 2
E14	Down in KO	130.661	0	-infinity	0.02115	0.73884	Olig1	Oligodendrocyte transcription factor 1
E14	Down in KO	8258.8	3875.3	-1.09162	0.0051	0.328189	Opn3	Opsin3
E14	Down in KO	11339.1	7128.16	-0.669702	0.0451	0.92924	Os9	amplified in osteosarcoma
E14	Down in KO	4025.11	1969.9	-1.0309	0.03085	0.846983	Otud1	OUT domain containing 1
E14	Down in KO	60414.6	38760.3	-0.64032	0.00755	0.428248	Otx2	orthodenticle homolog 2
E14	Down in KO	2235.08	829.399	-1.43019	0.02325	0.765997	Ovol2	Ovo-like 2
E14	Down in KO	32485.8	20579.8	-0.658581	0.0133	0.604765	Pabpc4	poly(A) binding protein, cytoplasmic 4
E14	Down in KO	4476.69	2287.11	-0.968906	0.02845	0.820637	Padi2	Peptidyl arginine deaminase, type II
E14	Down in KO	13421	6938.81	-0.951727	0.00415	0.294623	Palm	Paralemmin
E14	Down in KO	40241.6	23451.1	-0.779035	0.00485	0.319577	Parah1b3	Platelet-activating factor acetylhydrolase, isoform 1b, subunit 3
E14	Down in KO	7638.68	4534.62	-0.75234	0.0422	0.929008	Pcbd1	pterin 4 alpha carbinolamine dehydrate/dimerization cofactor of hepatocyte nuclear factor 1 alpha (TCF1)
E14	Down in KO	39880.7	27098	-0.557504	0.027	0.812164	Pcbp3	poly(rC) binding protein 3
E14	Down in KO	53856.3	35045.9	-0.619868	0.0202	0.731793	Pcbp4	poly(rC) binding protein 4
E14	Down in KO	48282.2	26755.8	-0.851644	0.0015	0.272826	Pcdhgb6	Protocadherin gamma subfamily B, 6
E14	Down in KO	8850.5	5157.36	-0.779127	0.03615	0.888927	Pcks1n	proprotein convertase subtilisin/kexin type 1 inhibitor
E14	Down in KO	31065.8	20471.3	-0.601723	0.03365	0.876413	Pcnxl3	pecanex-like 3
E14	Down in KO	4492.21	2104.55	-1.09391	0.01665	0.669896	Pcsk4	Proprotein convertase subtilisin/kexin type 4
E14	Down in KO	1622.86	658.075	-1.30221	0.0393	0.91332	Pde6a	Phosphodiesterase 6A, cGMP-specific, rod, alpha
E14	Down in KO	109.647	24.6833	-2.15126	0.0238	0.773035	Pdzk1	PDZ domain containing 1

Table A2.1 E14.5 Differentially Expressed Genes (continued)

Time point	Direction	WT	KO	log2(fold change)	p value	q value	Gene symbol	Gene Name
E14	Down in KO	43241.6	30357	-0.510391	0.04635	0.92924	Pex19	peroxisomal biogenesis factor 19
E14	Down in KO	240812	159000	-0.598879	0.0069	0.407118	Pfn1	profilin 1
E14	Down in KO	116.331	0	-infinity	0.0249	0.787804	Pglyrp1	Peptidoglycan recognition protein 1
E14	Down in KO	3147.4	1533.98	-1.03689	0.0414	0.926888	Pgrmc1	Progesterone receptor membrane component 1
E14	Down in KO	17871.1	11581.8	-0.625766	0.0357	0.888927	Phactr1	phosphatase and actin regulator 1
E14	Down in KO	55976.5	39346.2	-0.508596	0.0406	0.921683	Phc1	polyhomeotic-like 1
E14	Down in KO	57995	37686.4	-0.621884	0.01185	0.579544	Phc2	polyhomeotic-like 2
E14	Down in KO	34869.9	22836.7	-0.610625	0.02795	0.817984	Phf21b	PHD finger protein 21B
E14	Down in KO	4299.36	1544.64	-1.47685	0.00235	0.285959	Pitnm2	Phosphatidylinositol transfer protein, membrane-associated 2
E14	Down in KO	31226.4	12629.9	-1.30593	5.00E-05	0.024453	Pkd2	Polycystic kidney disease 2
E14	Down in KO	15981.9	10350.5	-0.626731	0.04425	0.92924	Pkdcc	protein kinase domain containing, cytoplasmic
E14	Down in KO	8456.05	5142.93	-0.717395	0.0459	0.92924	Pla2g12a	phospholipase A2, group XIIA
E14	Down in KO	136.382	0	-infinity	0.01735	0.68676	Plac8l1	PLAC8-like 1
E14	Down in KO	104936	61595.3	-0.768611	0.00125	0.247838	Plagl1	Pleiomorphic adenoma gene-like 1
E14	Down in KO	12568.9	8182.24	-0.619289	0.02705	0.812164	Plec	plectin
E14	Down in KO	808.702	254.019	-1.67067	0.00135	0.256128	Plekhb1	Pleckstrin homology domain containing, family B (evectins)
E14	Down in KO	1497.35	383.817	-1.96392	0.00735	0.421247	Plk3	Polo-like kinase 3
E14	Down in KO	13503.8	7999	-0.755475	0.0205	0.734795	Plxnd1	Plexin D1
E14	Down in KO	147797	108170	-0.450317	0.04745	0.92924	Pmel	premelanosome protein
E14	Down in KO	1003.99	232.569	-2.11001	0.03985	0.919307	Pmfbp1	Polyamine modulated factor 1 binding protein 1
E14	Down in KO	4016.13	2193.67	-0.872463	0.0374	0.896622	Pml	promyelocytiv leukemia
E14	Down in KO	7663.56	4689.34	-0.708628	0.0413	0.925591	Pnkp	polynucleotide kinase 3'- phosphatase
E14	Down in KO	136.382	0	-infinity	0.01735	0.68676	Pnliprp1	Pancreatic lipase related protein 1
E14	Down in KO	7366.93	4343.73	-0.762129	0.04285	0.92924	Pnpla3	patatin-like phospholipase domain containing 3
E14	Down in KO	40502.9	26143.2	-0.63159	0.04385	0.92924	Pom121	nuclear pore membrane protein 121
E14	Down in KO	46964.5	24628.5	-0.931239	0.00125	0.247838	Pop4	Processing of precursor 4, ribonuclease P/MRP family
E14	Down in KO	21842	14394.8	-0.601554	0.04205	0.929008	Pou4f1	POU domain, class 4, transcription factor 1
E14	Down in KO	14684.5	9252.41	-0.666392	0.0357	0.888927	Ppme1	protein phosphatase methylesterase 1
E14	Down in KO	53113.2	32430.9	-0.711704	0.0033	0.285959	Ppp2r1a	Protein phosphatase 2, regulatory subunit A, alpha
E14	Down in KO	49779.1	35364.7	-0.493229	0.0467	0.92924	Ppp2r4	protein phosphatase 2A activator, regulatory subunit B
E14	Down in KO	10662.8	6346.04	-0.748655	0.04325	0.92924	Ppp2r5b	protein phosphatase 2, regulatory subunit B', beta
E14	Down in KO	52542.1	30624.6	-0.778783	0.0017	0.285959	Ppp4c	Protein phosphatase 4, catalytic subunit
E14	Down in KO	10018.5	6088.4	-0.718538	0.03535	0.888927	Prc1	protein regulator of cytokinesis 1
E14	Down in KO	14120.1	5894.83	-1.26023	0.00035	0.086548	Prdm1	PR domain containing 1, with ZNF domain
E14	Down in KO	16675.4	10062.6	-0.728726	0.023	0.763475	Prdm13	PR domain containing 1
E14	Down in KO	111.572	0	-infinity	0.0354	0.888927	Prima1	proline rich member anchor 1
E14	Down in KO	15548.2	10053.7	-0.629021	0.0422	0.929008	Prn	prion protein gene complex
E14	Down in KO	2163.04	786.903	-1.4588	0.02265	0.75976	Prokr1	Prokineticin receptor 1
E14	Down in KO	238.668	0	-infinity	0.00415	0.294623	Prr22	Proline rich 22
E14	Down in KO	23545.6	14990.3	-0.651433	0.02595	0.804377	Prrc2a	proline-rich coiled-coil 2A
E14	Down in KO	49855.1	34883.7	-0.515186	0.03865	0.909946	Prrc2b	proline-rich coiled-coil 2B
E14	Down in KO	34.0955	0	-infinity	0.0036	0.285959	Pspn	Persephin
E14	Down in KO	1421.9	489.014	-1.53988	0.0368	0.893622	Ptbp2	Polypyrimidine tract binding protein 2
E14	Down in KO	14661.1	9118.59	-0.685108	0.04055	0.921683	Ptgds	prostaglandin D2 synthase (brain)
E14	Down in KO	9830.44	6126.77	-0.68213	0.04745	0.92924	Ptges2	prostaglandin E synthase 2
E14	Down in KO	17949	7814.35	-1.1997	0.00235	0.285959	Ptgis	Prostaglandin I2 (prostacyclin) synthase
E14	Down in KO	32594.9	21340.3	-0.611066	0.02565	0.797324	Ptms	parathymosin
E14	Down in KO	68810.3	45768.8	-0.588261	0.01835	0.707262	Ptov1	prostate tumor over expressed gene 1
E14	Down in KO	2729	1376.26	-0.987619	0.02685	0.811696	Ptpn6	Protein tyrosine phosphatase, non-receptor type 6
E14	Down in KO	39997.3	24437	-0.710837	0.0073	0.420572	Pttg1	pituitary tumor-transforming gene 1
E14	Down in KO	84.1203	0	-infinity	0.00325	0.285959	Pus3	pseudouridine synthase 3
E14	Down in KO	25029.8	15394.8	-0.701208	0.01265	0.591085	Pvrl1	poliovirus receptor-related 1
E14	Down in KO	2603.75	1021.65	-1.34968	0.02785	0.81723	Pygm	Muscle glycogen phosphorylase
E14	Down in KO	22583.7	15184.2	-0.572707	0.0475	0.92924	R3hdm4	R3H domain containing 4
E14	Down in KO	15243.6	9917.27	-0.620189	0.045	0.92924	Rab11fip4	RAB11 family interacting protein 4 (class II)
E14	Down in KO	139.946	0	-infinity	0.0187	0.714886	Rab42	RAB42, member RAS oncogene family)
E14	Down in KO	33650.2	23259.2	-0.532814	0.0342	0.885498	Ramp2	receptor (calcitonin) activity modifying protein 2
E14	Down in KO	34.0955	0	-infinity	0.0036	0.285959	Rangrf	RAN guanine nucleotide release factor ***option 3 of 3***
E14	Down in KO	28944.7	19210	-0.591446	0.0345	0.888927	Rasl10b	RAS-like, family 10, member B
E14	Down in KO	1897.89	770.786	-1.29999	0.0457	0.92924	Rbfox1	RNA binding protein, fox-1 homolog 1
E14	Down in KO	330.866	0	-infinity	0.00015	0.048547	Rbm20	RNA binding motif protein 20
E14	Down in KO	283.743	0	-infinity	0.00345	0.285959	Rbpj	Recombinant signal binding protein for immuno globulin kappa J region
E14	Down in KO	2902.94	1221.06	-1.24939	0.00495	0.323263	Relb	Avian reticuloendotheliosis viral (v-rel) oncogene related B
E14	Down in KO	102.287	0	-infinity	5.00E-05	0.024453	Rell2	RELT-like 2
E14	Down in KO	7893.37	4271.68	-0.885838	0.02085	0.73711	Rem2	rad and gem related GTP binding protein 2
E14	Down in KO	15636.9	9641.48	-0.69763	0.0277	0.81723	Ret	ret proto-oncogene
E14	Down in KO	251.505	52.1045	-2.27111	0.0001	0.038611	Rfx5	Regulatory Factor X, 5 (influences HLA class II expression)
E14	Down in KO	89.8815	0	-infinity	0.0011	0.22625	Rgs14	Regulator of Gprotein signaling 14
E14	Down in KO	365.246	78.1698	-2.22419	0.0119	0.580699	Rims1	Regulating synaptic membrane exocytosis1
E14	Down in KO	192.168	0	-infinity	0.00265	0.285959	Ripply2	ripply 2 homolog zebrafish

Table A2.1 E14.5 Differentially Expressed Genes (continued)

Time point	Direction	WT	KO	log2(fold change)	p value	q value	Gene symbol	Gene Name
E14	Down in KO	73319.1	50492.3	-0.538125	0.02875	0.821727	Rnasek	Ribonuclease, K
E14	Down in KO	2765.15	1232.85	-1.16536	0.0369	0.893622	Rnf208	Ring finger protein 208
E14	Down in KO	38979.2	16970.5	-1.19967	5.00E-05	0.024453	Rnpep	Arginyl aminopeptidase (aminopeptidase B)
E14	Down in KO	85.1229	0	-infinity	0.0494	0.92924	Rnu12	RNA U12, small nuclear
E14	Down in KO	9697.64	4841	-1.00233	0.0052	0.329803	Robo4	roundabout homolog 4
E14	Down in KO	18479.3	11073.4	-0.738811	0.04785	0.92924	Rp13-ps1	pseudogene
E14	Down in KO	3184.16	1529.45	-1.0579	0.0408	0.921683	RP24-537K9	Pseudogene
E14	Down in KO	81398	55802.6	-0.544662	0.02395	0.773996	Rp9	Retinitis Pigmentosa 9
E14	Down in KO	89781.4	60698.8	-0.564749	0.0205	0.734795	Rpl17-ps3	Pseudogene
E14	Down in KO	88551.3	58277.7	-0.603569	0.01425	0.628485	Rpl19-ps7	Pseudogene
E14	Down in KO	3829.1	1048.92	-1.8681	0.0048	0.319149	Rpl31-ps10	Ribosomal protein L31, pseudogene 10
E14	Down in KO	34.0955	0	-infinity	0.0036	0.285959	Rpl36-ps10	Ribosomal protein L36, pseudogene 10
E14	Down in KO	84.1603	0	-infinity	0.0481	0.92924	Rps15a-ps7	ribosomal protein S15A, pseudogene 7
E14	Down in KO	112.535	0	-infinity	0.02845	0.820637	Rps24-ps2	Ribosomal protein S24, pseudogene 2
E14	Down in KO	374259	207575	-0.8504	0.0098	0.514746	Rps24-ps3	ribosomal protein S24, pseudogene 3
E14	Down in KO	6129.67	3344.68	-0.873941	0.0286	0.820637	Rpusd3	RNA pseudouridylate synthase domain containing 3
E14	Down in KO	19038.8	12455.3	-0.612177	0.04045	0.921683	Rrm2b	ribonucleotide reductase M2 B (TP53 inducible)
E14	Down in KO	50195.3	34802	-0.52838	0.03595	0.888927	Rrp1	ribosomal RNA processing 1 homolog (S. cerevisiae)
E14	Down in KO	9096.28	5419.25	-0.747184	0.04155	0.927416	Rxrb	retinoid x receptor beta
E14	Down in KO	102.286	0	-infinity	0.01755	0.686774	S100a3	S100 calcium binding protein 3
E14	Down in KO	32843.3	20600.3	-0.672935	0.01455	0.632839	Safb	scaffold attachment factor B
E14	Down in KO	36384.8	23162.1	-0.651566	0.0262	0.807267	Samd4b	sterile alpha domain containing 4B
E14	Down in KO	4493.66	2311.05	-0.95934	0.03965	0.916808	Samsn1	SAM domain, SH3 domain and nuclear localization signals, 1
E14	Down in KO	24742.8	15065.7	-0.715746	0.0149	0.639219	Sbk1	SH3-binding kinase 1
E14	Down in KO	10432.3	6354.17	-0.715276	0.03535	0.888927	Scamp3	secretory carrier membrane protein 3
E14	Down in KO	15450.4	8753.96	-0.819641	0.0138	0.621085	Scg3	Secretogranin
E14	Down in KO	34.0955	0	-infinity	0.0036	0.285959	Scgb1a1	secretoglobin, family 1A, member 1 (uteroglobin)
E14	Down in KO	26035.1	15211.3	-0.775313	0.00815	0.455242	Scrib	scribbled homolog
E14	Down in KO	5051.55	1620.23	-1.64053	0.0044	0.30261	Scrt1	Scratch 1
E14	Down in KO	732.188	180.052	-2.0238	0.0266	0.809785	Scube2	Signal peptide, CUB domain, EGF-like 2
E14	Down in KO	17355.9	10831.4	-0.680206	0.02175	0.746092	Sec16a	SEC16 homolog A
E14	Down in KO	2350.32	909.59	-1.36957	0.02625	0.807267	Sema3a	sema domain, immunoglobin domain, short basic domain, secreted, (semaphorin) 3A
E14	Down in KO	1265.54	408.419	-1.63163	0.04065	0.921683	Sema6b	Sema domain, transmembrane domain (TM), and cytoplasmic domain, (semaphorin) 6B
E14	Down in KO	39171.4	26390.4	-0.569785	0.02675	0.809785	Sepw1	selenoprotein W, muscle 1
E14	Down in KO	11719.5	6845.09	-0.775776	0.03575	0.888927	Sez6l2	seizure related 6 homolog like 2
E14	Down in KO	130247	86643.7	-0.588079	0.01305	0.600846	Sgip1	SH3-domain GRB2-like (endophilin) interacting protein 1
E14	Down in KO	56030.4	39966.1	-0.487432	0.0488	0.92924	Sh3pxd2b	SH3 and PX domains 2B
E14	Down in KO	203.379	0	-infinity	5.00E-05	0.024453	Sh3rf2	SH3 domain containing ring finger 2
E14	Down in KO	7818.78	4507.48	-0.794622	0.0303	0.841973	Shisa5	shisa family member 5
E14	Down in KO	3139.72	1601.07	-0.971597	0.04245	0.929008	Shroom2	Shroom family member 2
E14	Down in KO	7859.45	4306.14	-0.868033	0.0232	0.765997	Sipa1	signal-induced proliferation associated gene 1
E14	Down in KO	5677.56	3147.74	-0.850956	0.04325	0.92924	Sirt6	sirtuin6
E14	Down in KO	61.5072	0	-infinity	0.03125	0.846983	Skint8	Selection and upkeep on intraepithelial T cells 8
E14	Down in KO	1081.41	228.044	-2.24553	0.04015	0.921683	Slc10a1	Solute carrier family 20, member 1
E14	Down in KO	28.3743	0	-infinity	0.0454	0.92924	Slc10a6	Solute carrier family 10 (sodium/bile acid cotransporter), member 6
E14	Down in KO	95.6026	0	-infinity	0.0174	0.686774	Slc16a11	Solute carrier family 16 (monocarboxylic acid transporters), member 11
E14	Down in KO	6989.4	3766.42	-0.891974	0.0228	0.760276	Slc24a3	solute carrier family 24 (sodium/potassium/calcium exchanger), member 3
E14	Down in KO	34.0955	0	-infinity	0.0036	0.285959	Slc25a35	Solute carrier family 25, member 35 ***option 2 of 3***
E14	Down in KO	22952.1	14998.1	-0.613842	0.0312	0.846983	Slc25a39	solute carrier family 25, member 39
E14	Down in KO	95.6026	0	-infinity	0.03695	0.893622	Slc26a4	Solute carrier family 26, member 4
E14	Down in KO	4631.95	2132.22	-1.11926	0.0234	0.769787	Slc29a2	solute carrier family 29 (nuceloside transporters), member 2
E14	Down in KO	28160.7	19500.5	-0.530175	0.0477	0.92924	Slc35c2	solute carrier family 35, member C2
E14	Down in KO	11582.9	7349.98	-0.65618	0.04645	0.92924	Slc36a1	solute carrier family 36 (proton/amino acid symporter), member 1
E14	Down in KO	34.0955	0	-infinity	0.0036	0.285959	Slc46a2	Solute carrier family 46, member 2
E14	Down in KO	47582.5	30547.6	-0.63937	0.0114	0.574122	Slc4a5	solute carrier family 4, sodium bicarbonate cotransporter, member 5
E14	Down in KO	1863.61	539.106	-1.78946	0.00725	0.419889	Slc52a3	Solute carrier protein family 52, member 3
E14	Down in KO	96.5652	0	-infinity	0.0198	0.727476	Slc6a20b	Solute carrier family 6 (neurotransmitter transporter), member 20B
E14	Down in KO	80632.7	57299.6	-0.49284	0.03905	0.912327	Slc7a8	solute carrier family 7 (cationic amino acid transporter, y+ system), member 8
E14	Down in KO	192.845	0	-infinity	0.0073	0.420572	Slfn3	Schlafen 3
E14	Down in KO	1889.67	818.211	-1.20759	0.03725	0.894976	Slit1	Slit homolog 1
E14	Down in KO	49336.9	34018.8	-0.536336	0.03885	0.911727	Smarcd1	SWI/SNF related, matrix associated, actin dependent regulator of chromatin, subfamily d,

Table A2.1 E14.5 Differentially Expressed Genes (continued)

Time point	Direction	WT	KO	log2(fold change)	p value	q value	Gene symbol	Gene Name
								member 1
E14	Down in KO	26004.4	17164.1	-0.599363	0.02975	0.838333	Smc1a	structural maintenance of chromosomes 1A
E14	Down in KO	40016.7	23981.9	-0.738656	0.004	0.287686	Sncg	Synuclein, gamma
E14	Down in KO	1514.46	711.481	-1.08991	0.04075	0.921683	Snph	Syntaphilin
E14	Down in KO	58122.9	41593.6	-0.482745	0.0478	0.92924	Snrpb	small nuclear ribonucleoprotein B
E14	Down in KO	47297.4	30692.8	-0.623858	0.0161	0.663114	Snx22	sorting nexin 22
E14	Down in KO	129.698	0	-infinity	0.01955	0.72312	Sohlh2	spermatogenesis and oogenesis specific basic helix-loop-helix 2
E14	Down in KO	8996.69	5693.43	-0.660096	0.04365	0.92924	Sorb2	sorbin and SH3 domain containing 2
E14	Down in KO	12005.9	7584.26	-0.662666	0.04495	0.92924	Sorcs2	sortilin-related VPS10 domain containing receptor 2
E14	Down in KO	210749	143715	-0.552313	0.0144	0.631305	Sox12	SRY (sex determining region Y)-box 12
E14	Down in KO	406.757	0	-infinity	0.00025	0.069646	Sox3	SRY-box containing 3
E14	Down in KO	11687.3	7185.87	-0.70171	0.0341	0.884992	Sparcl1	SPARC-like 1
E14	Down in KO	2087.4	662.682	-1.65532	0.0286	0.820637	Spin1	Spindlin 1
E14	Down in KO	1791	535.55	-1.74167	0.02275	0.75976	Spin4	Spindlin family, member 4
E14	Down in KO	204.573	0	-infinity	0.006	0.365784	Spock1	Sparc/osteonectiv, cwcv and kazal-like domains proteoglycan 1
E14	Down in KO	59512.9	38656.8	-0.622482	0.0095	0.503798	Spon1	spondin 1, (f-spondin) extracellular matrix protein
E14	Down in KO	9907.49	4970.84	-0.99503	0.00785	0.442982	Spp1	Secreted phosphoprotein 1
E14	Down in KO	44303.7	26090.8	-0.763883	0.0138	0.621085	Sppl3	Signal peptide peptidase 3
E14	Down in KO	5728.02	2920.99	-0.97158	0.01595	0.663114	Srd53	Steroid 5 alpha-reductase 3
E14	Down in KO	1439.87	362.852	-1.98848	0.03235	0.867185	Srp54c	Signal recognition particle 54B
E14	Down in KO	170.481	0	-infinity	0.0025	0.285959	Srsf4	Serine/arginine-rich splicing factor 4
E14	Down in KO	4510.99	2001.38	-1.17245	0.0194	0.719992	Sst	Somatostatin
E14	Down in KO	17093.7	10260.5	-0.73637	0.01705	0.684249	St3gal1	ST3 beta-galactoside alpha-2,3-sialyltransferase 1
E14	Down in KO	2925.47	1024.32	-1.514	0.01445	0.632238	Stard8	START domain containing 8
E14	Down in KO	50992.6	35422.7	-0.525613	0.03995	0.920649	Stip1	stress-induced phosphoprotein 1
E14	Down in KO	5577.25	2932.58	-0.927385	0.0305	0.844332	Stk10	Serine/threonine kinase 10
E14	Down in KO	8216	4334.28	-0.922643	0.01285	0.595374	Stmn1	stathmin 1
E14	Down in KO	97892.9	68145.2	-0.522592	0.02555	0.795339	Stmn3	stathmin-like 3
E14	Down in KO	49589.6	35336.8	-0.488866	0.0468	0.92924	Stra6	stimulated by retinoic acid gene 6
E14	Down in KO	119.218	0	-infinity	0.03145	0.850309	Stra6l	STRA6-like
E14	Down in KO	346.213	0	-infinity	0.00385	0.285959	Sulf1	Sulfatase 1
E14	Down in KO	13783.6	8876.71	-0.634861	0.0492	0.92924	Suv39h1	suppressor of variegation 3-9 homolog 1 (Drosophila)
E14	Down in KO	2260.42	896.462	-1.33428	0.0322	0.865272	Syndig1l	Synapse differentiation inducing 1 like
E14	Down in KO	10494.8	5752.28	-0.867471	0.0141	0.625631	Synpo	synaptopodin
E14	Down in KO	14665.6	7789.86	-0.91277	0.0093	0.49558	Syp	synaptophysin
E14	Down in KO	184170	128793	-0.515985	0.03145	0.850309	Syt11	synaptotagmin XI
E14	Down in KO	206.209	24.6818	-3.06259	0.0294	0.833765	Sytl3	Snaptogamin-like 3
E14	Down in KO	22768.2	15148	-0.587895	0.0487	0.92924	Tacc3	transforming, acidic coiled-coil containing protein 3
E14	Down in KO	10602	5884.17	-0.84942	0.01555	0.651856	Tacr1	Tachykinin receptor 1
E14	Down in KO	8057.47	4325.65	-0.897409	0.01545	0.651386	Tada3	Transcriptional adaptor 3
E14	Down in KO	12488.6	7140.51	-0.806516	0.01265	0.591085	Taf6l	TAF6-like RNA polymerase II, p300/CBP-associated factor (PCAF)-associated factor
E14	Down in KO	21355	13057	-0.709747	0.02205	0.750041	Tagln3	transgelin 3
E14	Down in KO	10760.8	6411.64	-0.747013	0.02505	0.788018	Tarbp	TAR (HIV) RNA binding protein 2
E14	Down in KO	42912.4	26388	-0.70151	0.00915	0.493562	Tbc1d13	TBC1 domain family, member 13
E14	Down in KO	2045.07	720.047	-1.50598	0.0357	0.888927	Tbx1	T-box 1
E14	Down in KO	3851.55	1201.46	-1.68064	0.00325	0.285959	Tcap	Titin-cap
E14	Down in KO	2464.01	923.489	-1.41584	0.01575	0.658985	Tceal3	Transcription elongation factor A (SII)-like 3
E14	Down in KO	23388.9	14848.5	-0.65551	0.0278	0.81723	Tcp11	t-complex protein 11
E14	Down in KO	779.309	202.472	-1.94447	0.02185	0.746092	Tdg	Thymine DNA glycosylase
E14	Down in KO	26671.3	17372.4	-0.618496	0.0295	0.833765	Tecr	trans-2,3-enoyl-CoA reductase
E14	Down in KO	35677	25057.9	-0.509725	0.04805	0.92924	Tex261	testis expressed gene 261
E14	Down in KO	349.278	0	-infinity	0.0004	0.093651	Them6	Thioesterase superfamily member 6
E14	Down in KO	218.617	0	-infinity	0.00015	0.048547	Thtpa	Thiamine triphosphatase
E14	Down in KO	174782	125478	-0.478121	0.03255	0.868316	Timm13	translocase of inner mitochondrial membrane 13
E14	Down in KO	1781.53	401.712	-2.14889	0.00605	0.3668	Tinagl1	Tubulointerstital nephritis antigen-like 1
E14	Down in KO	15776.7	10282.6	-0.617593	0.0476	0.92924	Tkfc	triokinase, FMN cyclase
E14	Down in KO	118.256	0	-infinity	0.0071	0.413378	Tlr13	Toll-like receptor 13
E14	Down in KO	88.9189	0	-infinity	0.0455	0.92924	Tlx3	T cell leukemia, homeobox 3
E14	Down in KO	27545.8	18014.9	-0.612644	0.0183	0.707262	Tm9sf1	transmembrane 9 superfamily member 1
E14	Down in KO	32787	20112.1	-0.705058	0.0091	0.493283	Tmem160	Transmembrane protein 160
E14	Down in KO	2777.18	308.88	-3.1685	0.007	0.410816	Tmem178	Transmembrane protein 178
E14	Down in KO	22982.8	15384.2	-0.579103	0.04715	0.92924	Tmem201	Transmembrane protein 201
E14	Down in KO	18518.8	11952.8	-0.631642	0.03535	0.888927	Tmem214	transmembrane protein 214
E14	Down in KO	198.852	0	-infinity	0.0085	0.471204	Tnfaip8l3	Tumor necrosis factor, alpha-induced protein 8-like 3
E14	Down in KO	16882.5	9453.6	-0.836591	0.0122	0.587522	Tnrc18	Trinucleotide repeat containing 18
E14	Down in KO	4005.02	2067.39	-0.954002	0.0468	0.92924	Top3b	Topoisomerase (DNA) III beta
E14	Down in KO	146445	102409	-0.516013	0.02455	0.783956	Tpi1	triosephosphate isomerase 1
E14	Down in KO	18081.6	10830.5	-0.739426	0.01385	0.622063	Trappc9	trafficking protein particle complex 9
E14	Down in KO	163.794	0	-infinity	0.01155	0.574873	Trdv5	T cell receptor delta variable 5
E14	Down in KO	39219.7	24653.1	-0.669808	0.0118	0.579544	Trim28	Tripartite motif-containing 28
E14	Down in KO	83.1977	0	-infinity	0.04915	0.92924	Trim43a	tripartite motif-containing 43A

Table A2.1 E14.5 Differentially Expressed Genes (continued)

Time point	Direction	WT	KO	log2(fold change)	p value	q value	Gene symbol	Gene Name
E14	Down in KO	109851	80124.4	-0.455229	0.04345	0.92924	Trove2	TROVE domain family, member 2
E14	Down in KO	11482.3	7153.31	-0.682724	0.04255	0.929008	Trp53bp2	transformation related protein 53 binding protein 2
E14	Down in KO	59659.4	40226	-0.568622	0.02055	0.735389	Tspan13	tetraspanin 13
E14	Down in KO	19206.6	11392	-0.753578	0.0116	0.574873	Tspan15	tetraspanin 15
E14	Down in KO	124.94	0	-infinity	5.00E-05	0.024453	Ttc16	Tertatricopeptide repeat domain 16
E14	Down in KO	46146.3	32275	-0.515796	0.0411	0.922989	Ttc28	tetratricopeptide repeat domain 28
E14	Down in KO	397.703	0	-infinity	0.0001	0.038611	Ttc32	Tetratricopeptide repeat domain 32
E14	Down in KO	13056.3	5954.12	-1.13278	0.0029	0.285959	Ttc9b	Tetratricopeptide repeat domain 9B
E14	Down in KO	38025.7	23655.7	-0.684786	0.0096	0.507877	Ttll3	tubulin tyrosine ligase-like family, member 3
E14	Down in KO	368.866	0	-infinity	0.0022	0.285959	Tub1b	Tubulin 1B subunit
E14	Down in KO	34447.2	20425.7	-0.754001	0.00645	0.385738	Tubb4a	tubulin, beta 4A, class IVA
E14	Down in KO	19608.7	11243.7	-0.802376	0.00925	0.49558	Tufm	Tu translation elongation factor, mitochondrial
E14	Down in KO	3260.54	1380.79	-1.23962	0.01825	0.707123	Tulp1	Tubby like protein 1
E14	Down in KO	62434.7	43243	-0.529883	0.02995	0.840739	Txn2	thioredoxin
E14	Down in KO	55046.8	34638.7	-0.668277	0.0086	0.473172	Txndc5	thioredoxin domain containing 5
E14	Down in KO	45903.3	26288.8	-0.804148	0.0027	0.285959	U2af2	U2 small nuclear ribonucleoprotein auxiliary factor (U2AF)2
E14	Down in KO	35856.2	24851	-0.528922	0.0461	0.92924	Ube2j2	ubiquitin-conjugating enzyme E2J 2
E14	Down in KO	51493.9	33206.9	-0.632917	0.0128	0.594309	Ube2m	ubiquitin-conjugating enzyme E2M
E14	Down in KO	51329.9	36395.5	-0.496041	0.04335	0.92924	Ube4b	ubiquitination factor E4B
E14	Down in KO	8974.23	5380.51	-0.738046	0.03635	0.891852	Ucp2	uncoupling protein 2 (mitochondrial, proton carrier)
E14	Down in KO	19572.2	6978.47	-1.48782	5.00E-05	0.024453	Unc5c	Unc-5 homolog C
E14	Down in KO	4113.16	2278.3	-0.852288	0.02155	0.744541	unc79	Unc-79 homolog
E14	Down in KO	143.742	0	-infinity	0.01865	0.714886	Upk3a	Uroplakin 3A
E14	Down in KO	10683.5	0	-infinity	0.0173	0.68676	Uty	Ubiquitously transcribed tetratricopeptide repeat gene, Y chromosome
E14	Down in KO	73145.6	51700.2	-0.500601	0.0312	0.846983	Vdac1	voltage-dependent anion channel 1
E14	Down in KO	33650.2	23259.2	-0.532814	0.0342	0.885498	Vps25	vacuolar protein sorting 25
E14	Down in KO	5287.34	2734.2	-0.951426	0.02955	0.833765	Vps37d	vacuolar protein sorting 37D
E14	Down in KO	21079.3	13888.5	-0.601937	0.0436	0.92924	Vps72	vacuolar protein sorting 72
E14	Down in KO	58549.7	36692.8	-0.674164	0.0118	0.579544	Wdr89	WD repeat domain 89
E14	Down in KO	15767.5	8376.99	-0.912454	0.0045	0.306613	Wdtc1	WD and tetratricopeptide repeats 1
E14	Down in KO	7476.41	4003.47	-0.901096	0.02145	0.744541	Wfs1	Wolfram syndrome 1 homolog
E14	Down in KO	85.1229	0	-infinity	0.00035	0.086548	Xir5a	X-linked lymphocyte-regulated 5A
E14	Down in KO	83.1986	0	-infinity	0.01585	0.660657	Xir5b	X-linked lymphocyte-regulated 5B
E14	Down in KO	4258.81	1954.31	-1.12379	0.0231	0.764488	Xk	Kell blood group precursor (McLeod phenotype) homolog
E14	Down in KO	1785.74	385.354	-2.21227	0.0188	0.714886	Ybx1-ps2	Y box protein 1, pseudogene 2
E14	Down in KO	45353.1	30722.7	-0.561895	0.02725	0.814834	Zcchc3	zinc finger, CCHC domain containing 3
E14	Down in KO	1409.96	383.817	-1.87716	0.0126	0.591085	Zfat	Zinc finger and AT hook domain containing
E14	Down in KO	112.535	0	-infinity	0.02845	0.820637	Zfp317	zinc finger protein 317
E14	Down in KO	26983.3	16681.6	-0.693808	0.0148	0.638318	Zfp385a	zinc finger protein 385A
E14	Down in KO	23914.7	15325	-0.642007	0.0244	0.781652	Zfp444	zinc finger protein 444
E14	Down in KO	7130.78	4144.79	-0.78276	0.04535	0.92924	Zfp536	zinc finger protein 536
E14	Down in KO	8878.27	4692.01	-0.920073	0.0158	0.659822	Zfp574	zinc finger protein 584
E14	Down in KO	10561.6	6199.17	-0.768678	0.028	0.818359	Zfp592	Zinc finger protein 592
E14	Down in KO	136.378	0	-infinity	0.0027	0.285959	Zfp600	zinc finger protein 600
E14	Down in KO	159.035	0	-infinity	0.01515	0.645795	Zfp672	Zinc finger protein 672
E14	Down in KO	3654.54	1821.08	-1.00489	0.04245	0.929008	Zfp746	Zinc finger protein 746
E14	Down in KO	6523.31	3092.8	-1.07669	0.00895	0.487553	Zkscan5	Zinc finger with KRAB and SCAN domains 5
E14	Down in KO	17012.4	8580.16	-0.987509	0.00235	0.285959	Zmiz2	Zinc finger, MIZ-type containing 2
E14	Down in KO	164.756	0	-infinity	0.01195	0.581849	Zpf433	Zinc finger protein 433
E14	Down in KO	34990.7	23735.9	-0.559899	0.0352	0.888927	Zswim8	zinc finger SWIM-type containing 8
E14	Down in KO	16188.7	8650.41	-0.904148	0.01885	0.714886	Zyx	zyxin

Table A2.2: E18.5 Differentially Expressed Genes

Time Point	Direction	WT	KO	log2 (fold change)	p value	q value	Gene Symbol	Gene Name
E18	Down in KO	136.413	0	-infinity	5.00E-05	0.012993	4930519F16Rik	RIKEN cDNA 4930519F16 gene; known processed transcript
E18	Down in KO	357.757	0	-infinity	5.00E-05	0.012993	Lox	Lysyl oxidase
E18	Down in KO	357.757	0	-infinity	5.00E-05	0.012993	Lin7b	Lin-7 homolog B
E18	Down in KO	402.476	0	-infinity	5.00E-05	0.012993	Kat5	K(lysine) acetyltransferase 5
E18	Down in KO	406.99	0	-infinity	5.00E-05	0.012993	Mm.316763	Transcribed locus: eye
E18	Down in KO	429.35	0	-infinity	5.00E-05	0.012993	Foxr2	forkhead box R2
E18	Down in KO	434.573	0	-infinity	5.00E-05	0.012993	Itga3	Integrin alpha 3
E18	Down in KO	447.196	0	-infinity	5.00E-05	0.012993	Mm.385768	Transcribed locus: thymus
E18	Down in KO	495.778	0	-infinity	5.00E-05	0.012993	Mm.385743	Transcribed locus: spinal cord
E18	Down in KO	536.847	0	-infinity	5.00E-05	0.012993	Zfp40	zinc finger protein 40
E18	Down in KO	558.995	0	-infinity	5.00E-05	0.012993	Lsamp	Limbic system-associated membrane protein
E18	Down in KO	560.707	0	-infinity	5.00E-05	0.012993	6820431F20Rik	Cadherin 11 pseudogene
E18	Down in KO	662.189	0	-infinity	5.00E-05	0.012993	Cdh12	cadherin 12
E18	Up in KO	0	100.642	infinity	5.00E-05	0.012993	Platr14	pluripotency associated transcript 14
E18	Up in KO	0	126.738	infinity	5.00E-05	0.012993	Als2cl	ALS2 C-terminal like
E18	Up in KO	0	155.442	infinity	5.00E-05	0.012993	Adcy3	adenylate cyclase 3
E18	Up in KO	0	191.846	infinity	5.00E-05	0.012993	Hoxd3	homeobox D3
E18	Up in KO	0	194.436	infinity	5.00E-05	0.012993	Eml6	echinoderm microtubule associated protein like 6
E18	Up in KO	0	221.019	infinity	5.00E-05	0.012993	Ccdc33	coiled-coil domain containing 33
E18	Up in KO	0	222.327	infinity	5.00E-05	0.012993	Dedd	death effector domain-containing
E18	Up in KO	0	232.122	infinity	5.00E-05	0.012993	Stab2	stabilin 2
E18	Up in KO	0	234.737	infinity	5.00E-05	0.012993	Trim66	tripartite motif-containing 66
E18	Up in KO	0	322.059	infinity	5.00E-05	0.012993	Vrk2	vaccinia related kinase 2
E18	Up in KO	0	362.463	infinity	5.00E-05	0.012993	Gm30139	lincRNA
E18	Up in KO	0	366.178	infinity	5.00E-05	0.012993	Grik1	glutamate receptor, ionotropic, kainate 1
E18	Up in KO	0	393.908	infinity	5.00E-05	0.012993	Rnf170	Ring finger protein 170
E18	Up in KO	0	393.908	infinity	5.00E-05	0.012993	Smpd2	sphingomyelin phosphodiesterase 2, neutral
E18	Up in KO	0	436.384	infinity	5.00E-05	0.012993	Cdc34-ps	cell division cycle 34 homolog, pseudogene
E18	Up in KO	0	443.167	infinity	5.00E-05	0.012993	Fer1l6	fer-1-like 6
E18	Up in KO	0	447.906	infinity	5.00E-05	0.012993	Mm.308783	Transcribed locus: brain, epididymis
E18	Up in KO	0	477.435	infinity	5.00E-05	0.012993	Gm39030	unknown
E18	Up in KO	0	483.974	infinity	5.00E-05	0.012993	Gm11425	pseudogene
E18	Up in KO	0	484.635	infinity	5.00E-05	0.012993	Mm.247416	Transcribe locus: testis
E18	Up in KO	0	486.381	infinity	5.00E-05	0.012993	D130079A08Rik	miscRNA
E18	Up in KO	0	500.635	infinity	5.00E-05	0.012993	Mybpc2	myosin binding protein C, fast-type
E18	Up in KO	0	505.673	infinity	5.00E-05	0.012993	Gjb4	gap junction protein, beta 4
E18	Up in KO	0	528.041	infinity	5.00E-05	0.012993	Slc7a11	solute carrier family 7 (cationic amino acid transporter, y+ system), member 11
E18	Up in KO	0	531.149	infinity	5.00E-05	0.012993	Commd10	COMM domain containing 10
E18	Up in KO	0	536.625	infinity	5.00E-05	0.012993	E2f3	E2F transcription factor 3
E18	Up in KO	0	556.186	infinity	5.00E-05	0.012993	Hdac9	Histone deacetylase 9
E18	Up in KO	0	565.209	infinity	5.00E-05	0.012993	Mm.442230	Transcribed locus: bone marrow; intestine; embryonic tissue; skin
E18	Up in KO	0	572.07	infinity	5.00E-05	0.012993	Robo1	Roundabout homolog 1
E18	Up in KO	0	592.654	infinity	5.00E-05	0.012993	Gm33458	lincRNA
E18	Up in KO	0	792.631	infinity	5.00E-05	0.012993	Gm33217	lincRNA
E18	Down in KO	18024.5	3778.1	-2.25423	5.00E-05	0.012993	Aldh1a7	aldehyde dehydrogenase family 1; subfamily A7
E18	Up in KO	1633.86	6915.74	2.0816	5.00E-05	0.012993	Gm7976	lincRNA
E18	Up in KO	9284.08	19872.2	1.09792	5.00E-05	0.012993	Hipk2	homeodomain interacting protein kinase 2
E18	Up in KO	7768.72	20140.2	1.37433	5.00E-05	0.012993	Mid1	midline 1
E18	Down in KO	353967	172226	-1.03931	5.00E-05	0.012993	Klk14	kallikrein related-peptidase 14
E18	Up in KO	121589	335829	1.46572	5.00E-05	0.012993	Erdr1	erythroid differentiation regulator 1
E18	Up in KO	718133	######	1.51283	5.00E-05	0.012993	Malat1	metastasis associated lung adenocarcinoma transcript 1 (non-coding RNA)
E18	Down in KO	123.027	0	-infinity	0.0001	0.020418	Mas1	MAS1 oncogene
E18	Down in KO	345.784	0	-infinity	0.0001	0.020418	Gm39353	unknown
E18	Down in KO	418.488	0	-infinity	0.0001	0.020418	Gm32027	lincRNA
E18	Down in KO	452.276	0	-infinity	0.0001	0.020418	Hgf	hepatocyte growth factor
E18	Down in KO	469.555	0	-infinity	0.0001	0.020418	Kif5a	Kinesin family member 5A
E18	Up in KO	0	182.862	infinity	0.0001	0.020418	1700110I01Rik	lincRNA
E18	Up in KO	0	372.716	infinity	0.0001	0.020418	Mm.373303	Transcribed locus: brain
E18	Up in KO	0	376.793	infinity	0.0001	0.020418	Nlgn1	neuroligin 1
E18	Up in KO	0	379.447	infinity	0.0001	0.020418	1700019L22Rik	lincRNA
E18	Up in KO	0	387.046	infinity	0.0001	0.020418	7530416G11Rik	protein coding
E18	Up in KO	0	387.539	infinity	0.0001	0.020418	Aamdc	Adipogenesis associated Mth938 domain containing
E18	Up in KO	0	419.23	infinity	0.0001	0.020418	Rbfox1	RNA binding protein, fox-1 homolog (C. elegans) 1
E18	Up in KO	0	439.736	infinity	0.0001	0.020418	Ktn1	Kinectin 1
E18	Up in KO	0	451.182	infinity	0.0001	0.020418	Mm.389490	Transcribed locus: spinal cord
E18	Up in KO	0	458.236	infinity	0.0001	0.020418	Parg	Poly (ADP-ribose) glycohydrolase
E18	Down in KO	55475.1	30243.4	-0.875221	0.0001	0.020418	Robo2	Roundabout homolog 2

Table A2.2: E18.5 Differentially Expressed Genes (Continued)

Time Point	Direction	WT	KO	log2 (fold change)	p value	q value	Gene Symbol	Gene Name
E18	Down in KO	136.418	0	-infinity	0.00015	0.025409	Dlec1	deleted in lung and esophageal cancer 1
E18	Down in KO	313.249	0	-infinity	0.00015	0.025409	Mm.134273	Transcribed locus: eye
E18	Down in KO	319.844	0	-infinity	0.00015	0.025409	Gm28153	antisense
E18	Down in KO	338.8	0	-infinity	0.00015	0.025409	Fdx1	Ferredoxin 1
E18	Down in KO	342.38	0	-infinity	0.00015	0.025409	Gm39938	unknown
E18	Down in KO	363.417	0	-infinity	0.00015	0.025409	Mm.222376	Transcribed locus: brain; embryonic tissue; inner ear
E18	Down in KO	380.116	0	-infinity	0.00015	0.025409	Gm41244	unknown
E18	Down in KO	380.116	0	-infinity	0.00015	0.025409	Mm.399169	transcribed locus: mammary gland
E18	Down in KO	474.07	0	-infinity	0.00015	0.025409	Mm.73758	Transcribed locus: unknown
E18	Up in KO	0	197.854	infinity	0.00015	0.025409	Itk	IL2 inducible T cell kinase
E18	Up in KO	0	223.953	infinity	0.00015	0.025409	Pik3r5	phosphoinositide-3-kinase, regulatory subunit 5, p101
E18	Up in KO	0	314.303	infinity	0.00015	0.025409	Phf17	PHD finger protein 17
E18	Up in KO	0	362.255	infinity	0.00015	0.025409	Cdk5rap3	CDK5 regulatory subunit associated protein 3
E18	Up in KO	0	400.123	infinity	0.00015	0.025409	Pcgf1	Polycomb group ring finger 1
E18	Up in KO	0	411.1	infinity	0.00015	0.025409	Mm.459342	Transcribed locus: bone marrow, embryonic tissue
E18	Up in KO	0	411.1	infinity	0.00015	0.025409	Nrg1 1	neuregulin
E18	Up in KO	21631.3	37678.9	0.800638	0.00015	0.025409	Arhgap5	Rho GTPase activating protein 5
E18	Down in KO	424.22	0	-infinity	0.0002	0.029131	Mydgf	myeloid derived growth factor
E18	Up in KO	0	103.301	infinity	0.0002	0.029131	C030005K06Rik	processed transcript
E18	Up in KO	24.6153	320.384	3.70218	0.0002	0.029131	Car9	carbonic anhydrase 9
E18	Up in KO	0	349.917	infinity	0.0002	0.029131	Gm30624	lincRNA
E18	Up in KO	0	377.324	infinity	0.0002	0.029131	Fam19a5	family with sequence similarity 19, member A5
E18	Up in KO	0	381.57	infinity	0.0002	0.029131	Mm.27695	Transcribed locus: embryonic tissue, eye
E18	Up in KO	0	383.615	infinity	0.0002	0.029131	Krt34	keratin 34
E18	Up in KO	0	383.693	infinity	0.0002	0.029131	5730419F03Rik	lincRNA
E18	Up in KO	0	383.693	infinity	0.0002	0.029131	Gm30370	lncRNA
E18	Up in KO	0	383.693	infinity	0.0002	0.029131	Gm32771	lincRNA
E18	Up in KO	0	383.693	infinity	0.0002	0.029131	Vmp1	vacuole membrane protein 1
E18	Up in KO	0	389.662	infinity	0.0002	0.029131	Adgrl2	adhesion G protein-coupled receptor L2
E18	Up in KO	18154.7	32012.4	0.81829	0.0002	0.029131	Gm10040	pseudogene
E18	Up in KO	92000.2	143823	0.644587	0.0002	0.029131	Alad	aminolevulinate, delta-, dehydratase
E18	Down in KO	315.506	0	-infinity	0.00025	0.034234	Nipbl	Nipped-B homolog
E18	Down in KO	369.042	0	-infinity	0.00025	0.034234	atp5l	ATP synthase; H+ transporting; mitochondrial F0 complex; subunit g
E18	Down in KO	398.457	0	-infinity	0.00025	0.034234	Ldhal6b	Lactate dehydrogenase A-like 6B
E18	Down in KO	414.152	0	-infinity	0.00025	0.034234	Gm36377	lincRNA
E18	Down in KO	451.922	0	-infinity	0.00025	0.034234	Nrg1	neuregulin 1
E18	Up in KO	0	257.405	infinity	0.00025	0.034234	Ces5a	carboxylesterase 5A
E18	Up in KO	15019.6	27532.8	0.874311	0.00025	0.034234	Ddx3y	DEAD (Asp-Glu-Ala-Asp) box polypeptide 3, Y-linked
E18	Up in KO	0	421.807	infinity	0.0003	0.040594	Mm.365932	Transcribed locus: unknown
E18	Down in KO	32915	18439.2	-0.83597	0.0003	0.040594	s100a9	S100 calcium binding protein A9 (calgranulin B)
E18	Up in KO	0	184.17	infinity	0.00035	0.046806	Acsm1	acyl-CoA synthetase medium-chain family member 1
E18	Up in KO	2346.33	5048.71	1.10551	0.00035	0.046806	Rapgef3	Rap guanine nucleotide exchange factor (GEF) 3
E18	Down in KO	339.911	0	-infinity	0.0004	0.052874	Sox30	SRY (sex determining region Y)-box 30
E18	Up in KO	227328	461818	1.02255	0.0004	0.052874	Rps24-ps3	ribosomal protein S24, pseudogene 3
E18	Up in KO	0	278.766	infinity	0.00045	0.058469	Gm26615	lincRNA
E18	Down in KO	10190.4	4330.98	-1.23444	0.00045	0.058469	Slc15a2	solute carrier family 15 (H+/peptide transporter); member 2
E18	Up in KO	2458.08	5619.69	1.19296	0.00045	0.058469	Fggy	FGGY carbohydrate kinase domain containing
E18	Down in KO	22013.2	12017.2	-0.873263	0.0005	0.064599	s100a8	S100 calcium binding protein A8 (calgranulin A)
E18	Up in KO	287864	433018	0.58904	0.00055	0.07066	Hba-a1	hemoglobin alpha, adult chain 1
E18	Up in KO	7622.49	14769.1	0.954245	0.0006	0.076653	Tspan10	tetraspanin 10
E18	Up in KO	0	252.667	infinity	0.00065	0.082579	Slc22a6	solute carrier family 22 (organic anion transporter), member 6
E18	Down in KO	149.994	0	-infinity	0.0007	0.08844	Cd164l2	CD164 sialomucin-like 2
E18	Up in KO	0	125.926	infinity	0.00075	0.092708	Odf3	outer dense fiber of sperm tails 3
E18	Up in KO	0	204.715	infinity	0.00075	0.092708	Gm853	Known Protein Coding
E18	Up in KO	0	232.122	infinity	0.00075	0.092708	Lat	linker for activation of T cells
E18	Up in KO	0	253.975	infinity	0.00075	0.092708	Gm4755	lincRNA
E18	Down in KO	2960.74	890.466	-1.73333	0.0009	0.11006	Trp63	transformation related protein 63
E18	Up in KO	3092.45	6700.7	1.11556	0.0009	0.11006	Pdk2	pyruvate dehydrogenase kinase, isoenzyme 2
E18	Up in KO	1900.64	4962.71	1.38464	0.00105	0.12772	Caps2	calcyphosphine 2
E18	Down in KO	77.2899	0	-infinity	0.00115	0.139144	Rbm46os	RNA binding motif protein 46; opposite strand
E18	Up in KO	6019.66	11771.9	0.967588	0.00125	0.150447	Slc11a2	solute carrier family 11 (proton-coupled divalent metal ion transporters), member 2
E18	Down in KO	185.685	0	-infinity	0.0014	0.150906	Lrp8os2	low density lipoprotein receptor-related protein 8; apolipoprotein e receptor;

Table A2.2: E18.5 Differentially Expressed Genes (Continued)

Time Point	Direction	WT	KO	log2 (fold change)	p value	q value	Gene Symbol	Gene Name
								opposite strand 2
E18	Up in KO	0	206.023	infinity	0.0014	0.150906	Gm17116	Antisense
E18	Down in KO	218.22	0	-infinity	0.00175	0.150906	Gm12580	lincRNA
E18	Down in KO	335.397	0	-infinity	0.00195	0.150906	Atg10	autophagy related 10
E18	Down in KO	335.397	0	-infinity	0.00195	0.150906	4930432J09Rik	miscRNA
E18	Down in KO	335.397	0	-infinity	0.00195	0.150906	Gm17250	lincRNA
E18	Down in KO	335.397	0	-infinity	0.00195	0.150906	Gm32647	lincRNA
E18	Up in KO	27914.3	42537.2	0.607719	0.0021	0.150906	Col3a1	collagen, type III, alpha 1
E18	Up in KO	0	143.856	infinity	0.00215	0.150906	Gm9847	Known Protein Coding
E18	Down in KO	181833	122857	-0.565637	0.00215	0.150906	Cacng4	calcium channel; voltage-dependent; gamma subunit 4
E18	Up in KO	0	154.64	infinity	0.0022	0.150906	Zp3	zona pellucida glycoprotein 3
E18	Down in KO	344.637	0	-infinity	0.00225	0.150906	2010111I01Rik	Known Protein coding
E18	Down in KO	344.637	0	-infinity	0.00225	0.150906	Mm.381823	Transcribed locus: liver; brain; skin; thymus; bone marrow; embryonic tissue
E18	Down in KO	290.677	0	-infinity	0.0024	0.150906	Mm.404734	Transcribed locus: brain
E18	Down in KO	290.677	0	-infinity	0.0024	0.150906	Gm34907	lincRNA
E18	Down in KO	290.677	0	-infinity	0.0024	0.150906	Gm32618	lincRNA
E18	Down in KO	290.677	0	-infinity	0.0024	0.150906	Zfp758	zinc finger protein 758
E18	Down in KO	290.677	0	-infinity	0.0024	0.150906	Gm30255	lincRNA
E18	Down in KO	290.677	0	-infinity	0.0024	0.150906	Kcnn2	potassium intermediate/small conductance calcium-activated channel; subfamily N; member 2
E18	Down in KO	290.677	0	-infinity	0.0024	0.150906	Gm31734	lincRNA
E18	Down in KO	290.677	0	-infinity	0.0024	0.150906	Gm40074	unknown
E18	Down in KO	290.677	0	-infinity	0.0024	0.150906	Gm36365	lincRNA
E18	Down in KO	290.677	0	-infinity	0.0024	0.150906	Apex2	apurinic/apyrimidinic endonuclease 2
E18	Down in KO	290.677	0	-infinity	0.0024	0.150906	Slc9a7	solute carrier family 9 (sodium/hydrogen exchanger), member 7
E18	Down in KO	124.233	0	-infinity	0.00245	0.150906	Vil1	villin 1
E18	Down in KO	313.037	0	-infinity	0.00245	0.150906	Gm34421	lincRNA
E18	Down in KO	313.037	0	-infinity	0.00245	0.150906	Gm40441	unknown
E18	Down in KO	313.037	0	-infinity	0.00245	0.150906	3110004A20Rik	RIKEN cDNA 3110004A20 gene; known lincRNA
E18	Up in KO	0	252.836	infinity	0.00245	0.150906	Eef1g	Eukaryotic translation elongation factor 1 gamma
E18	Up in KO	0	252.836	infinity	0.00245	0.150906	Gprin2	G protein regulated inducer of neurite outgrowth 2
E18	Up in KO	0	252.836	infinity	0.00245	0.150906	Rpl23a-ps4	ribosomal protein L23A, pseudogene 4
E18	Up in KO	0	252.836	infinity	0.00245	0.150906	Scg5	Secretogranin V
E18	Down in KO	270.787	0	-infinity	0.0025	0.150906	Mm.387285	Transcribed locus: brain
E18	Down in KO	270.787	0	-infinity	0.0025	0.150906	Gm36894	lincRNA
E18	Down in KO	270.787	0	-infinity	0.0025	0.150906	Fgf12	Fibroblast growth factor 12
E18	Down in KO	270.787	0	-infinity	0.0025	0.150906	Cyp1b1	cytochrome P450; family 1; subfamily b; polypeptide 1
E18	Down in KO	270.787	0	-infinity	0.0025	0.150906	Mm.84630	Transcribed locus: testis
E18	Down in KO	270.787	0	-infinity	0.0025	0.150906	Tbx3os1	T-box 3; opposite strand 1
E18	Down in KO	270.787	0	-infinity	0.0025	0.150906	Mm.472408	Transcribed locus: eye; pancreas
E18	Down in KO	270.787	0	-infinity	0.0025	0.150906	Herc2	hect (homologous to the E6-AP (UBE3A) carboxyl terminus) domain and RCC1 (CHC1)-like domain (RLD) 2
E18	Down in KO	295.403	0	-infinity	0.0025	0.150906	Gemin2	Gem (nuclear organelle) associated protein 2
E18	Down in KO	295.403	0	-infinity	0.0025	0.150906	Vapa	Vesicle-associated membrane protein; associated protein A
E18	Down in KO	283.396	0	-infinity	0.00255	0.150906	Trim62	tripartite motif-containing 62
E18	Down in KO	25999.9	15962.8	-0.703797	0.00255	0.150906	Scand1	SCAN domain-containing 1
E18	Up in KO	0	263.736	infinity	0.0026	0.150906	1110038F14Rik	protein coding
E18	Up in KO	0	263.736	infinity	0.0026	0.150906	Chrm3	cholinergic receptor, muscarinic 3, cardiac
E18	Up in KO	0	263.736	infinity	0.0026	0.150906	Gm.385314	Transcribed locus: eye
E18	Up in KO	0	263.736	infinity	0.0026	0.150906	Gm19462	Predicted gene 19462, unknown
E18	Up in KO	0	263.736	infinity	0.0026	0.150906	Lhfpl3	lipoma HMGIC fusion partner-like 3
E18	Up in KO	0	263.736	infinity	0.0026	0.150906	Mm.10647	Transcribed locus: testis; intestine; thymus
E18	Up in KO	0	263.736	infinity	0.0026	0.150906	Rps2	Ribosomal protein S2
E18	Up in KO	0	263.736	infinity	0.0026	0.150906	Mm.366308	Transcribed locus, brain
E18	Up in KO	0	303.404	infinity	0.0026	0.150906	Gm34269	lincRNA
E18	Up in KO	0	303.404	infinity	0.0026	0.150906	Gm38641	unknown
E18	Up in KO	0	303.404	infinity	0.0026	0.150906	Gm41408	unknown
E18	Up in KO	15839.3	25413.5	0.682089	0.00265	0.150906	Bex4	brain expressed gene 4
E18	Down in KO	320.02	0	-infinity	0.0027	0.150906	Mm.383938	Transcribed locus: brain; eye; mammary; brain; DRG
E18	Up in KO	0	119.88	infinity	0.0027	0.150906	Apex1	apurinic/apyrimidinic endonuclease 1
E18	Down in KO	334.923	0	-infinity	0.00275	0.150906	Mm44303	Transcribed locus: unknown
E18	Down in KO	172.39	0	-infinity	0.0028	0.150906	Cd48	CD48 antigen
E18	Up in KO	4647.96	8812.2	0.922906	0.0028	0.150906	Dtd2	D-tyrosyl-tRNA deacylase 2
E18	Down in KO	123.12	0	-infinity	0.00285	0.150906	Gm8356	predicted gene 8356; Known protein coding
E18	Up in KO	0	278.12	infinity	0.00285	0.150906	Mm.354786	Transcribed locus: skin, thymus,bone marrow, inner ear
E18	Up in KO	0	278.12	infinity	0.00285	0.150906	Mm.428468	Transcribed locus: brain

Table A2.2: E18.5 Differentially Expressed Genes (Continued)

Time Point	Direction	WT	KO	log2 (fold change)	p value	q value	Gene Symbol	Gene Name
E18	Up in KO	0	278.12	infinity	0.00285	0.150906	Mrgprd	MAS-related GPR, member D
E18	Up in KO	1930.27	4533.81	1.23192	0.00285	0.150906	Kdm5d	Lysine (K)-specific demethylase 5D
E18	Up in KO	0	287.712	infinity	0.0029	0.150906	Agbl1	ATP/GTP binding protein-like 1
E18	Up in KO	0	287.712	infinity	0.0029	0.150906	Gm31214	lincRNA
E18	Up in KO	0	287.712	infinity	0.0029	0.150906	Gm40278	unknown
E18	Up in KO	0	287.712	infinity	0.0029	0.150906	Map3k13	mitogen-activated protein kinase kinase kinase 13
E18	Up in KO	0	287.712	infinity	0.0029	0.150906	Shoc2	Soc-2 (suppressor of clear) homolog
E18	Up in KO	0	311.688	infinity	0.0029	0.150906	Mthfsl	5, 10-methenyltetrahydrofolate synthetase-like
E18	Up in KO	0	311.688	infinity	0.0029	0.150906	Tapt1	transmembrane anterior posterior transformation 1
E18	Up in KO	0	311.688	infinity	0.0029	0.150906	Ttc9	Tetratricopeptide repeat domain 9
E18	Down in KO	5071.66	2229.28	-1.18588	0.0029	0.150906	Gm5483	predicted gene 5483; known protein coding
E18	Up in KO	0	301.473	infinity	0.003	0.150906	Mm.98300	Transcribed locus: intestines; testis
E18	Up in KO	0	326.757	infinity	0.003	0.150906	Fat3	FAT tumor suppressor homolog 3
E18	Up in KO	0	328.88	infinity	0.00305	0.150906	4930500H12Rik	lincRNA
E18	Up in KO	0	328.88	infinity	0.00305	0.150906	Mm.427508	Transcribed locus: eye
E18	Down in KO	309.16	0	-infinity	0.0031	0.150906	LOC105242942	lincRNA
E18	Up in KO	0	227.553	infinity	0.0031	0.150906	Mbl2	mannose-binding lectin (protein C) 2
E18	Up in KO	25638.9	38782.7	0.597079	0.0031	0.150906	Prrc2c	proline-rich coiled-coil 2C
E18	Down in KO	246.17	0	-infinity	0.00315	0.150906	Dgka	Diacylglycerol kinase; alpha
E18	Down in KO	246.17	0	-infinity	0.00315	0.150906	Mm.360944	transcribed locus: thymus; embryonic tissue; lung
E18	Down in KO	246.17	0	-infinity	0.00315	0.150906	Gm36205	lincRNA
E18	Down in KO	246.17	0	-infinity	0.00315	0.150906	Tuba1c	Tubulin alpha 1C
E18	Down in KO	246.17	0	-infinity	0.00315	0.150906	Gm41639	unknown
E18	Down in KO	246.17	0	-infinity	0.00315	0.150906	Platr16	pluripotency associated transcript 16
E18	Down in KO	246.17	0	-infinity	0.00315	0.150906	Mm.379861	Transcribed locus: liver; brain; heart; kidney; embryonic tissue
E18	Down in KO	246.17	0	-infinity	0.00315	0.150906	Fah	Fumarylacetoacetate hydrolase
E18	Down in KO	246.17	0	-infinity	0.00315	0.150906	Gm42042	unknown
E18	Down in KO	246.17	0	-infinity	0.00315	0.150906	Tenm3	teneurin transmembrane protein 3
E18	Down in KO	246.17	0	-infinity	0.00315	0.150906	Psd3	pleckstrin and Sec7 domain containing 3
E18	Down in KO	246.17	0	-infinity	0.00315	0.150906	Gm33974	lincRNA
E18	Down in KO	246.17	0	-infinity	0.00315	0.150906	Prg2	proteoglycan 2; bone marrow
E18	Down in KO	316.441	0	-infinity	0.00315	0.150906	Clip4	CAP-GLY domain containing linker protein family; member 4
E18	Down in KO	245.958	0	-infinity	0.0032	0.150906	Slco5a1	solute carrier organic anion transporter family; member 5A1
E18	Down in KO	245.958	0	-infinity	0.0032	0.150906	Gm31616	lincRNA
E18	Down in KO	245.958	0	-infinity	0.0032	0.150906	Gm41421	unknown
E18	Down in KO	245.958	0	-infinity	0.0032	0.150906	Banfos2	barrier to autointegration factor 2; opposite strand
E18	Down in KO	245.958	0	-infinity	0.0032	0.150906	Mm.411452	transcribed locus: mammary gland
E18	Down in KO	245.958	0	-infinity	0.0032	0.150906	Ythdf1	YTH domain family 1
E18	Down in KO	245.958	0	-infinity	0.0032	0.150906	Gm42185	unknown
E18	Down in KO	245.958	0	-infinity	0.0032	0.150906	2610020H08Rik	known protein coding
E18	Down in KO	245.958	0	-infinity	0.0032	0.150906	Gm39259	unknown
E18	Down in KO	245.958	0	-infinity	0.0032	0.150906	Lingo1	leucine rich repeat and Ig domain containing 1
E18	Down in KO	245.958	0	-infinity	0.0032	0.150906	Gm33039	lincRNA
E18	Down in KO	223.598	0	-infinity	0.0033	0.150906	Zbtb18	zinc finger and BTB domain containing 18
E18	Down in KO	223.598	0	-infinity	0.0033	0.150906	Gm38718	unknown
E18	Down in KO	223.598	0	-infinity	0.0033	0.150906	Gm29536	lincRNA
E18	Down in KO	223.598	0	-infinity	0.0033	0.150906	9430060I03Rik	antisense
E18	Down in KO	223.598	0	-infinity	0.0033	0.150906	Nav3	Neuron navigator 3
E18	Down in KO	223.598	0	-infinity	0.0033	0.150906	Syne1	Spectrin repeat containing; nuclear envelope 1
E18	Down in KO	223.598	0	-infinity	0.0033	0.150906	Gm30366	lincRNA
E18	Down in KO	223.598	0	-infinity	0.0033	0.150906	2810408B13Rik	miscRNA
E18	Down in KO	223.598	0	-infinity	0.0033	0.150906	Mtmr9	Myotubularin related protein 9
E18	Down in KO	223.598	0	-infinity	0.0033	0.150906	Gm30455	lincRNA
E18	Down in KO	223.598	0	-infinity	0.0033	0.150906	Gstm6	Glutathione S-transferase; mu 6
E18	Down in KO	223.598	0	-infinity	0.0033	0.150906	Mm.5320	embryonic tissues
E18	Down in KO	223.598	0	-infinity	0.0033	0.150906	Mm.485412	Histone like
E18	Down in KO	223.598	0	-infinity	0.0033	0.150906	Gm31059	lincRNA
E18	Down in KO	223.598	0	-infinity	0.0033	0.150906	Psip1	PC4 and SFRS1 interacting protein 1
E18	Down in KO	223.598	0	-infinity	0.0033	0.150906	Gm32035	lincRNA
E18	Down in KO	223.598	0	-infinity	0.0033	0.150906	Ywhag	tyrosine 3-monooxygenase/tryptophan 5-monooxygenase activation protein; gamma polypeptide
E18	Down in KO	223.598	0	-infinity	0.0033	0.150906	Mm.376466	Transcribed locus: brain
E18	Down in KO	223.598	0	-infinity	0.0033	0.150906	Ppargc1a	peroxisome proliferative activated receptor; gamma; coactivator 1 alpha
E18	Down in KO	223.598	0	-infinity	0.0033	0.150906	Ccdc149	coiled-coil domain containing 149
E18	Down in KO	223.598	0	-infinity	0.0033	0.150906	Tax1bp1	Tax1 (human T cell leukemia virus type I) binding protein 1

Table A2.2: E18.5 Differentially Expressed Genes (Continued)

Time Point	Direction	WT	KO	log2 (fold change)	p value	q value	Gene Symbol	Gene Name
E18	Down in KO	223.598	0	-infinity	0.0033	0.150906	Nagk	N-acetylglucosamine kinase
E18	Down in KO	223.598	0	-infinity	0.0033	0.150906	Bmp10	Bone morphogenetic protein 10
E18	Down in KO	223.598	0	-infinity	0.0033	0.150906	A230057D06Rik	miscRNA
E18	Down in KO	223.598	0	-infinity	0.0033	0.150906	Mm.374610	Transcribed locus: brain
E18	Down in KO	223.598	0	-infinity	0.0033	0.150906	Dlg2	discs, large homolog 2
E18	Down in KO	223.598	0	-infinity	0.0033	0.150906	Gm35712	lincRNA
E18	Down in KO	223.598	0	-infinity	0.0033	0.150906	Mm.444036	Transcribed locus: unknown
E18	Down in KO	223.598	0	-infinity	0.0033	0.150906	Fam220-ps	family with sequence similarity 220; pseudogene
E18	Down in KO	223.598	0	-infinity	0.0033	0.150906	5730403I07Rik	lincRNA
E18	Up in KO	0	299.35	infinity	0.0033	0.150906	Gm36224	lincRNA
E18	Up in KO	0	299.35	infinity	0.0033	0.150906	Nhej1	nonhomologous end-joining factor 1
E18	Up in KO	2390.88	5282.2	1.1436	0.00335	0.150906	Ankrd26	ankyrin repeat domain 26
E18	Up in KO	0	291.142	infinity	0.0034	0.150906	Dusp6	Dual specificity phosphatase 6
E18	Up in KO	0	291.142	infinity	0.0034	0.150906	Gm11546	pseudogene
E18	Up in KO	1036.17	3501.69	1.75679	0.0034	0.150906	Gm29907	lincRNA
E18	Up in KO	0	265.043	infinity	0.00345	0.150906	Gm26843	lincRNA
E18	Up in KO	0	265.043	infinity	0.00345	0.150906	Rapgef2	Rap guanine nucleotide exchange factor (GEF) 2
E18	Up in KO	0	265.043	infinity	0.00345	0.150906	Zfp446	zinc finger protein 446
E18	Up in KO	5920.39	10589.2	0.838829	0.00345	0.150906	Ccdc23	coiled-coil domain containing 23
E18	Up in KO	0	82.22	infinity	0.0035	0.150906	Selp	selectin, platelet
E18	Up in KO	0	206.838	infinity	0.0036	0.150906	Ly6g5b	lymphocyte antigen 6 complex, locus G5B
E18	Up in KO	0	274.067	infinity	0.0036	0.150906	AA623943	pseudogene
E18	Up in KO	0	274.067	infinity	0.0036	0.150906	Mm.121360	Transcribed locus: brain, embryonic tissue, molar
E18	Up in KO	0	274.067	infinity	0.0036	0.150906	Mm.121789	Transcribed locus: unknown
E18	Up in KO	0	274.067	infinity	0.0036	0.150906	Srrt	serrate RNA effector molecule homolog
E18	Up in KO	0	274.067	infinity	0.0036	0.150906	Suz12	Suppressor of zeste 12 homolog
E18	Up in KO	15688.7	24535	0.64511	0.0036	0.150906	Smc2	structural maintenance of chromosomes 2
E18	Up in KO	0	239.76	infinity	0.00365	0.150906	5430437J10Rik	miscRNA
E18	Up in KO	0	239.76	infinity	0.00365	0.150906	Aim1	absent in melanoma 1
E18	Up in KO	0	239.76	infinity	0.00365	0.150906	Cdc6	Cell division cycle 6
E18	Up in KO	0	239.76	infinity	0.00365	0.150906	Ggt5	gamma-glutamyltransferase 5
E18	Up in KO	0	239.76	infinity	0.00365	0.150906	Gm29260	lincRNA
E18	Up in KO	0	239.76	infinity	0.00365	0.150906	Gm34542	lincRNA
E18	Up in KO	0	239.76	infinity	0.00365	0.150906	Mm.357621	Transcribed locus: brain
E18	Up in KO	0	239.76	infinity	0.00365	0.150906	Mm.366239	Transcribed locus: unknown
E18	Up in KO	0	239.76	infinity	0.00365	0.150906	Mm.395110	Transcribed locus: embryonic tissue; brain
E18	Up in KO	293.182	1540.19	2.39324	0.00365	0.150906	Il1rapl2	interleukin 1 receptor accessory protein-like 2
E18	Up in KO	0	267.166	infinity	0.0037	0.150906	Nkain2	Na+/K+ transporting ATPase interacting 2
E18	Down in KO	290.889	0	-infinity	0.00375	0.150906	Apls2	adaptor-related protein complex 1, sigma 2 subunit
E18	Up in KO	0	219.253	infinity	0.0038	0.150906	Gm16433	Pseudogene
E18	Up in KO	0	267.205	infinity	0.0038	0.150906	Gm5564	pseudogene
E18	Up in KO	0	290.327	infinity	0.0038	0.150906	Akap12	A kinase (PRKA) anchor protein (gravin) 12
E18	Up in KO	2354.1	5023.87	1.09363	0.0038	0.150906	Tmem42	transmembrane protein 42
E18	Down in KO	288.632	0	-infinity	0.00385	0.150906	Gm13807	Antisense
E18	Down in KO	268.317	0	-infinity	0.0039	0.150906	Col19a1	Collagen; type XIX; alpha 1
E18	Down in KO	268.317	0	-infinity	0.0039	0.150906	Lin28b	Lin-28 homolog B
E18	Down in KO	268.317	0	-infinity	0.0039	0.150906	Psma2	Proteasome (prosome; macropain) subunit; alpha type 2
E18	Down in KO	268.317	0	-infinity	0.0039	0.150906	Aaed1	AhpC/TSA antioxidant enzyme domain
E18	Down in KO	268.317	0	-infinity	0.0039	0.150906	Mm.364213	Transcribed locus: brain
E18	Down in KO	268.317	0	-infinity	0.0039	0.150906	Chd8	Chromodomain helicase DNA binding protein 8
E18	Down in KO	268.317	0	-infinity	0.0039	0.150906	Gm41296	unknown
E18	Down in KO	268.317	0	-infinity	0.0039	0.150906	Gabrr3	Gamma-aminobutyric acid (GABA) receptor; rho 3
E18	Down in KO	268.317	0	-infinity	0.0039	0.150906	Gm32252	lincRNA
E18	Down in KO	268.317	0	-infinity	0.0039	0.150906	Fbxl17	F-box and leucine-rich repeat protein 17
E18	Down in KO	268.317	0	-infinity	0.0039	0.150906	Gm33732	lincRNA
E18	Down in KO	268.317	0	-infinity	0.0039	0.150906	D030025E07Rik	miscRNA
E18	Down in KO	268.317	0	-infinity	0.0039	0.150906	Gm30340	lincRNA
E18	Down in KO	268.317	0	-infinity	0.0039	0.150906	Gm30402	lincRNA
E18	Down in KO	268.317	0	-infinity	0.0039	0.150906	Gm20674	pseudogene
E18	Down in KO	268.317	0	-infinity	0.0039	0.150906	Mm.416983	Transcribed locus: brain
E18	Up in KO	4112.01	7591.04	0.884456	0.00395	0.152325	Rab36	RAB36, member RAS oncogene family
E18	Down in KO	201.238	0	-infinity	0.004	0.153477	Tmem247	transmembrane protein 247
E18	Down in KO	201.238	0	-infinity	0.004	0.153477	Sixl1	Six-like 1
E18	Down in KO	293.146	0	-infinity	0.00405	0.154359	Gm39234	unknown
E18	Down in KO	293.146	0	-infinity	0.00405	0.154359	Jpx	Jpx transcript, Xist activator (non-protein coding)
E18	Up in KO	0	289.019	infinity	0.00405	0.154359	unknown	
E18	Up in KO	0	267.659	infinity	0.0042	0.15981	Wee1	WEE1 homolog 1
E18	Down in KO	257.633	0	-infinity	0.00425	0.15985	Rprd1a	regulation of nuclear pre-mRNA domain containing 1A

Table A2.2: E18.5 Differentially Expressed Genes (Continued)

Time Point	Direction	WT	KO	log2 (fold change)	p value	q value	Gene Symbol	Gene Name
E18	Down in KO	257.633	0	-infinity	0.00425	0.15985	Mm.398967	Transcribed locus: heart; brain; embryonic tissue; inner ear
E18	Down in KO	257.633	0	-infinity	0.00425	0.15985	Mm.208240	Transcribed locus: thymus
E18	Down in KO	257.633	0	-infinity	0.00425	0.15985	Gm20005	miscRNA
E18	Down in KO	1624.19	143.856	-3.49703	0.0043	0.161201	Gm38697	unknown
E18	Up in KO	0	215.823	infinity	0.0043	0.161201	Gm5084	Known Protein Coding
E18	Down in KO	227.284	0	-infinity	0.00455	0.169186	Usp18	Ubiquitin specific peptidase 18
E18	Down in KO	23178.4	14730.2	-0.653999	0.00455	0.169186	Pisd	phosphatidylserine decarboxylase
E18	Down in KO	2804.71	604.877	-2.21314	0.0046	0.170215	Gm5611	predicted gene 5611; known protein coding
E18	Up in KO	2122.9	4596.51	1.11451	0.0046	0.170215	Fn3krp	fructosamine 3 kinase related protein
E18	Up in KO	0	280.243	infinity	0.00465	0.17151	Mm.339788	Transcribed locus, brain
E18	Up in KO	0	280.243	infinity	0.00465	0.17151	Sec61a1	Sec61 alpha 1 subunit
E18	Up in KO	0	244.537	infinity	0.0047	0.173075	Rnase9	ribonuclease, RNase A family, 9 (non-active)
E18	Down in KO	278.811	0	-infinity	0.0049	0.179861	Armc4	armadillo repeat containing 4
E18	Down in KO	259.572	0	-infinity	0.005	0.182944	Gast	gastrin
E18	Down in KO	2685.63	741.832	-1.85609	0.005	0.182944	Hist1h2ae	histone cluster 1; H2ae
E18	Up in KO	0	129.357	infinity	0.0051	0.186305	Zcchc16	zinc finger, CCHC domain containing 16
E18	Up in KO	6338.19	10907.5	0.783184	0.00515	0.187831	Creld1	cysteine-rich with EGF-like domains 1
E18	Up in KO	11203	18576.8	0.729624	0.0052	0.189353	Tapbpl	TAP binding protein-like
E18	Down in KO	178.878	0	-infinity	0.0053	0.192077	Hepcam	hepatocyte cell adhesion molecule
E18	Down in KO	178.878	0	-infinity	0.0053	0.192077	Gm13003	lincRNA
E18	Up in KO	0	180.739	infinity	0.0053	0.192077	Ccl19	chemokine (C-C motif) ligand 19
E18	Down in KO	123.085	0	-infinity	0.00535	0.193582	Slc22a14	solute carrier family 22 (organic cation transporter); member 14
E18	Up in KO	53016.1	76324.3	0.525713	0.0055	0.198695	Cox5b	cytochrome c oxidase subunit Vb
E18	Down in KO	180.343	0	-infinity	0.00555	0.199556	Cmtm2b	CKLF-like MARVEL transmembrane domain containing 2B
E18	Down in KO	180.343	0	-infinity	0.00555	0.199556	Gm16005	pseudogene
E18	Up in KO	0	153.333	infinity	0.00555	0.199556	Bmx	BMX non-receptor tyrosine kinase
E18	Up in KO	0	189.724	infinity	0.00565	0.202832	Gzmn	granzyme N
E18	Up in KO	7149.99	11968.2	0.743194	0.00575	0.206099	Arhgap42	Rho GTPase activating protein 42
E18	Up in KO	5230.16	9058.22	0.792373	0.0059	0.211144	Zpf105	zinc finger protein 105
E18	Down in KO	173.465	0	-infinity	0.00595	0.212269	Defb47	defensin beta 47
E18	Up in KO	6663.24	11112.7	0.737915	0.00595	0.212269	Prkd2	protein kinase D2
E18	Up in KO	245.094	1272.98	2.3768	0.006	0.213056	Sp110	Sp110 nuclear body protein
E18	Up in KO	4851.41	8603.28	0.826482	0.006	0.213056	Zfp39	zinc finger protein 39
E18	Up in KO	8243.39	14673.2	0.831876	0.006	0.213056	Gm10320	Predicted pseudogene 10320, known protein coding
E18	Up in KO	1651.74	3909.19	1.24288	0.00605	0.214498	Gm11423	Antisense
E18	Up in KO	0	230.814	infinity	0.0061	0.215936	Gm10110	Known Protein Coding
E18	Up in KO	27045.4	39540	0.547929	0.00615	0.21737	Hist1h1c	histone cluster 1, H1c
E18	Up in KO	0	222.322	infinity	0.0062	0.218799	Gm11549	lincRNA
E18	Down in KO	136.417	0	-infinity	0.0063	0.220964	Gm15401	predicted gene 15401; known protein coding
E18	Up in KO	0	167.832	infinity	0.0063	0.220964	Actbl2	actin, beta-like 2
E18	Up in KO	0	167.832	infinity	0.0063	0.220964	Zfp59	zinc finger protein 59
E18	Up in KO	0	236.045	infinity	0.0063	0.220964	Gm26569	lincRNA
E18	Up in KO	449.736	1685.26	1.90582	0.0064	0.224127	Usp35	ubiquitin specific peptidase 35
E18	Up in KO	15998.7	24588.8	0.620047	0.00645	0.225189	Pdhb	pyruvate dehydrogenase (lipoamide) beta
E18	Up in KO	691705	983366	0.507571	0.00645	0.225189	Npm1	nucleophosmin 1
E18	Up in KO	0	181.555	infinity	0.0065	0.226244	9930038B18Rik	lincRNA
E18	Up in KO	1145.39	3000.35	1.38929	0.0065	0.226244	Naaladl2	N-acetylated alpha-linked acidic dipeptidase-like 2
E18	Up in KO	3538.53	6342.82	0.841972	0.00665	0.230762	Rad51d	RAD51 homolog D
E18	Up in KO	13955	21636.8	0.6327	0.00665	0.230762	Pcdhgb6	protocadherin gamma subfamily B, 6
E18	Down in KO	2940.6	455.106	-2.69184	0.00675	0.233877	Camp	cathelicidin antimicrobial peptide
E18	Down in KO	172.319	0	-infinity	0.0068	0.23419	Serpinb1b	serine (or cysteine)peptidase inhibitor; clade B; member 1b
E18	Down in KO	172.319	0	-infinity	0.0068	0.23419	Trim55	tripartite motif-containing 55
E18	Down in KO	172.319	0	-infinity	0.0068	0.23419	Nme7	NME/NM23 family member 7
E18	Up in KO	403.042	2745.36	2.76799	0.0068	0.23419	Cacna1c	Calcium channel, voltage-dependent, L type, alpha 1C subunit
E18	Up in KO	0	176.985	infinity	0.0069	0.236921	Npffr1	neuropeptide FF receptor 1
E18	Up in KO	0	176.985	infinity	0.0069	0.236921	Ogdhl	oxoglutarate dehydrogenase-like
E18	Up in KO	0	109.631	infinity	0.007	0.239635	1700030C12Rik	processed transcript
E18	Up in KO	0	194.423	infinity	0.007	0.239635	Gm13416	pseudogene
E18	Down in KO	156.518	0	-infinity	0.00715	0.244039	Sh2d1b1	SH2 domain containing 1B1
E18	Up in KO	1771.06	3936.23	1.1522	0.00715	0.244039	Gm8206	Predicted gene 8206, known protein coding
E18	Up in KO	0	143.856	infinity	0.00725	0.247083	Gm13563	Predicted gene 13563, known antisense
E18	Down in KO	11535.1	6936.91	-0.733664	0.0073	0.248417	LOC102634333	uncharacterized LOC102634333; protein coding
E18	Down in KO	181.135	0	-infinity	0.00735	0.249747	Gm13530	Predicted gene 13530; known lincRNA
E18	Down in KO	154.58	0	-infinity	0.00745	0.252022	Spaca5	sperm acrosome associated 5
E18	Down in KO	10379.2	6255.91	-0.730407	0.00745	0.252022	Cartpt	CART prepropeptide
E18	Up in KO	29786.2	43169.4	0.535366	0.00745	0.252022	Plagl1	Pleiomorphic adenoma gene-like 1
E18	Up in KO	0	164.44	infinity	0.0076	0.25596	Gm10524	TEC
E18	Up in KO	0	164.44	infinity	0.0076	0.25596	Rergl	RERG/RAS-like
E18	Up in KO	0	164.44	infinity	0.0076	0.25596	Rpl10a-ps2	ribosomal protein L10A, pseudogene 2
E18	Up in KO	0	183.355	infinity	0.00765	0.256887	Chac1	ChaC, cation transport regulator 1

Table A2.2: E18.5 Differentially Expressed Genes (Continued)

Time Point	Direction	WT	KO	log2 (fold change)	p value	q value	Gene Symbol	Gene Name
E18	Down in KO	13179.4	8142.97	-0.694659	0.00765	0.256887	Pde6g	phosphodiesterase 6G; cGMP-specific; rod; gamma
E18	Down in KO	185.685	0	-infinity	0.00775	0.259864	Gm17518	lincRNA
E18	Down in KO	3484.79	1295.61	-1.42744	0.0078	0.261157	Hspe1-rs1	Heat shock protein 1 (chaperonin 10); related sequence 1
E18	Down in KO	125.327	0	-infinity	0.00795	0.265015	Gm16984	lincRNA
E18	Down in KO	163.326	0	-infinity	0.00795	0.265015	Tbc1d21	TBC1 domain family; member 21
E18	Up in KO	0	162.317	infinity	0.00795	0.265015	8030451A03Rik	processed transcript
E18	Up in KO	0	76.7022	infinity	0.008	0.266294	Zan	zonadhesin
E18	Down in KO	170.062	0	-infinity	0.00805	0.266793	Gm11539	pseudogene
E18	Down in KO	175.758	0	-infinity	0.00805	0.266793	Prr22	Proline rich 22
E18	Up in KO	72.7401	381.531	2.39098	0.00805	0.266793	Ptk2b	PTK2 protein tyrosine kinase 2 beta
E18	Down in KO	152.287	0	-infinity	0.0081	0.267675	Mrgprb2	MAS-related GPR; member B2
E18	Up in KO	0	206.023	infinity	0.0081	0.267675	Gm17115	Antisense
E18	Up in KO	0	128.049	infinity	0.00815	0.268938	Htr6	5-hydroxytryptamine (serotonin) receptor 6
E18	Up in KO	38770	55724.8	0.523378	0.0083	0.273493	Lum	lumican
E18	Down in KO	147.702	0	-infinity	0.0084	0.275597	Cldn13	claudin 13
E18	Down in KO	147.702	0	-infinity	0.0084	0.275597	Gzmc	granzyme C
E18	Down in KO	147.702	0	-infinity	0.0084	0.275597	1700012B09Rik	known protein coding
E18	Up in KO	0	171.755	infinity	0.0085	0.277683	Gm11587	lincRNA
E18	Up in KO	215.963	1149.33	2.41194	0.0085	0.277683	Afap1l2	actin filament associated protein 1-like 2
E18	Up in KO	33113.1	47834.6	0.530653	0.0085	0.277683	Sbno1	sno, strawberry notch homolog 1
E18	Down in KO	154.58	0	-infinity	0.00855	0.278521	C230038L03Rik	processed transcript
E18	Up in KO	9701.85	15140	0.642035	0.00855	0.278521	Zfp180	zinc finger protein 180
E18	Up in KO	670.461	2077.47	1.63161	0.0087	0.283004	Gpx3	Glutathione peroxidase 3
E18	Up in KO	0	170.447	infinity	0.00875	0.283823	Fasl	Fas ligand (TNF superfamily, member 6)
E18	Up in KO	13545.4	20501.6	0.59793	0.00875	0.283823	Kalm	kalirin, RhoGEF kinase
E18	Up in KO	22292.2	32995.1	0.56571	0.0088	0.28504	Arid4a	AT rich interactive domain 4A (RBP1-like)
E18	Up in KO	4738.47	8069.97	0.768143	0.00885	0.286254	Cyyr1	cysteine and tyrosine-rich protein 1
E18	Up in KO	321.202	1753.71	2.44886	0.00895	0.288672	Paox	polyamine oxidase (exo-N4-amino)
E18	Up in KO	0	27.4067	infinity	0.009	0.289468	Sds	serine dehydratase
E18	Up in KO	0	151.702	infinity	0.009	0.289468	Aqp6	Aquaporin
E18	Up in KO	1198.21	3002.98	1.32552	0.00905	0.290668	Bbs5	Bardet-Biedl syndrome 5
E18	Up in KO	0	160.194	infinity	0.0091	0.291864	Gm21962	Known Protein Coding
E18	Up in KO	0	155.948	infinity	0.0093	0.297861	Fam209	family with sequence similarity 209
E18	Up in KO	0	161.009	infinity	0.00935	0.299043	Gm15234	lincRNA
E18	Up in KO	14128.4	21330.5	0.594322	0.00945	0.301819	Dancr	differentiation antagonizing non-protein coding RNA
E18	Up in KO	931.971	2613.06	1.48738	0.0095	0.30215	Mm.429720	Transcribed locus: unknown
E18	Up in KO	2906.62	5541.99	0.93106	0.0095	0.30215	Vgll2	vestigial like 2 homolog
E18	Up in KO	0	162.317	infinity	0.00965	0.305958	LOC102635707	uncharacterized locus
E18	Up in KO	19596.6	28526.5	0.541695	0.00965	0.305958	Flna	filamin, alpha
E18	Down in KO	158.776	0	-infinity	0.0097	0.305958	Gja3	gap junction protein; alpha 3
E18	Down in KO	158.776	0	-infinity	0.0097	0.305958	Gm10600	Known protein coding
E18	Down in KO	158.776	0	-infinity	0.0097	0.305958	Gm11454	lincRNA
E18	Up in KO	82617.3	115147	0.478954	0.0097	0.305958	Arid4b	AT rich interactive domain 4B (RBP1-like)
E18	Down in KO	147.773	0	-infinity	0.00975	0.307112	Gm14662	Antisense
E18	Up in KO	0	180.739	infinity	0.00995	0.31255	Aadat	aminoadipate aminotransferase
E18	Up in KO	1962.08	3898.89	0.99068	0.00995	0.31255	Lrp11	low density lipoprotein receptor-related protein 11
E18	Up in KO	0	147.286	infinity	0.01005	0.314396	BC089597	Known Protein Coding
E18	Up in KO	5468.86	12808.9	1.22783	0.01005	0.314396	Luzp1	leucine zipper protein 1
E18	Up in KO	2501.94	4851.44	0.955367	0.0101	0.315528	Fignl2	fidgetin-like 2
E18	Down in KO	140.93	0	-infinity	0.01015	0.316226	Tmc1	transmembrane channel-like gene family 1
E18	Down in KO	8178.73	4836.98	-0.75777	0.01015	0.316226	Ttc8	tetratricopeptide repeat domain 8
E18	Up in KO	1298.32	3002.63	1.20958	0.0103	0.320028	Pcdhl2	protocadherin 12
E18	Up in KO	1138.08	2769.22	1.28288	0.0104	0.322696	Cldn7	claudin 7
E18	Up in KO	0	182.047	infinity	0.0105	0.325358	Prss22	protease, serine 22
E18	Up in KO	0	147.779	infinity	0.01055	0.326024	Casp3	caspase 3
E18	Up in KO	4243.22	7351.96	0.79297	0.01055	0.326024	Trp53bp2	transformation related protein 53 binding protein 2
E18	Up in KO	2037	4036.78	0.986754	0.01065	0.32867	Ecel1	Endothelin converting enzyme-like 1
E18	Down in KO	23965.5	15515.9	-0.627211	0.0107	0.329324	Insm1	Insulinoma-associated 1
E18	Up in KO	11310.3	17236.6	0.607835	0.0107	0.329324	2810474O19Rik	Known Protein Coding
E18	Up in KO	0	149.086	infinity	0.01075	0.330418	AU020206	lincRNA
E18	Down in KO	98.4678	0	-infinity	0.01085	0.331265	BC051019	Protein coding
E18	Up in KO	2509.79	4933.54	0.975059	0.01085	0.331265	Gm22692	miRNA
E18	Up in KO	4642.4	7825.44	0.7533	0.01085	0.331265	Mrps23	mitochondrial ribosomal protein S23
E18	Up in KO	9600.3	16646.1	0.794036	0.01085	0.331265	Arl16	ADP-ribosylation factor-like 16
E18	Up in KO	3072.81	5724.59	0.897616	0.01105	0.336473	Scara3	scavenger receptor class A, member 3
E18	Up in KO	0	177.308	infinity	0.01135	0.345149	Kcns2	K+ voltage-gated channel, subfamily S, 2
E18	Up in KO	0	158.886	infinity	0.01145	0.347727	Zfp672	Zinc finger protein 672
E18	Up in KO	0	145.163	infinity	0.0116	0.351349	Fgf5	fibroblast growth factor 5
E18	Down in KO	33846.7	23345.9	-0.535845	0.0116	0.351349	Frrs1l	ferric-chelate reductase 1 like
E18	Down in KO	4391.38	2241.33	-0.970321	0.01185	0.357501	C130036L24Rik	Processed transcript
E18	Up in KO	1775.07	3822.83	1.10677	0.01195	0.360043	Pde1b	phosphodiesterase 1B, Ca2+-calmodulin dependent

Table A2.2: E18.5 Differentially Expressed Genes (Continued)

Time Point	Direction	WT	KO	log2 (fold change)	p value	q value	Gene Symbol	Gene Name
E18	Up in KO	245.094	1291.69	2.39785	0.01215	0.365587	Lcor	ligand dependent nuclear receptor corepressor
E18	Down in KO	2826.19	1217.35	-1.21511	0.0122	0.366609	D330045A20Rik	Protein coding
E18	Down in KO	138.673	0	-infinity	0.01235	0.370144	Gm26839	lincRNA
E18	Up in KO	0	82.22	infinity	0.01235	0.370144	C130050O18Rik	Known Protein Coding
E18	Up in KO	775.346	2352	1.60098	0.0125	0.374149	Galntl6	UDP-N-acetyl-alpha-D-galactosamine:polypeptide N-acetylgalactosaminyltransferase-like 6
E18	Up in KO	16540.4	24087.3	0.542281	0.01255	0.375155	Golga4	Golgi autoantigen, golgin subfamily a, 4
E18	Down in KO	152.28	25.2846	-2.59039	0.0126	0.376158	Apoh	apolipoprotein H
E18	Up in KO	10572.7	16084.1	0.605287	0.01265	0.377158	Cdca2	cell division cycle associated 2
E18	Down in KO	143.187	0	-infinity	0.0127	0.378156	Krt36	keratin 36
E18	Up in KO	0	274.067	infinity	0.01285	0.382125	Hox3dos1	homeobox D3, opposite strand 1
E18	Up in KO	5886.64	9501.98	0.690784	0.01305	0.387568	Itpripl2	inositol 1,4,5-triphosphate receptor interacting protein-like 2
E18	Up in KO	839.235	2516.26	1.58414	0.0132	0.391514	Eral1	Era (G-protein)-like 1
E18	Down in KO	2980.84	1309.01	-1.18724	0.01325	0.392488	Cntnap5a	Contactin associated protein-like 5A
E18	Down in KO	167.84	0	-infinity	0.0133	0.392951	6430628N08Rik	lincRNA
E18	Down in KO	3934.78	1919.96	-1.03521	0.0133	0.392951	Nf1	neurofibromatosis 1
E18	Up in KO	266.343	989.8	1.89385	0.0134	0.395395	2610035D17Rik	lincRNA
E18	Up in KO	1945.24	3998.51	1.03952	0.01345	0.396359	Ifnar1	interferon (alpha and beta) receptor 1
E18	Down in KO	144.369	0	-infinity	0.0135	0.39732	Alb	albumin
E18	Up in KO	3069.74	4978.19	0.697507	0.01365	0.401219	Ctnnd1	catenin (cadherin associated protein), delta 1
E18	Up in KO	7160.85	11203.1	0.645693	0.0137	0.402172	HMGXB4	HMG box domain containing 4
E18	Up in KO	238.287	1346.37	2.4983	0.01405	0.410864	Atad2b	ATPase family, AAA domain containing 2B
E18	Up in KO	4321.18	7320.35	0.760486	0.01405	0.410864	Prss56	protease, serine 56
E18	Up in KO	2287.23	4617.01	1.01336	0.0141	0.411682	Srm	spermidine synthase
E18	Up in KO	0	134.91	infinity	0.01415	0.411682	Hist1h3b	histone cluster 1, H3b
E18	Down in KO	2963.54	1341.39	-1.1436	0.01415	0.411682	Ltf	lactotransferrin
E18	Up in KO	2812.42	5035.87	0.840427	0.01415	0.411682	Fxyd3	FXYD domain-containing ion transport regulator 3
E18	Up in KO	2266.84	4690.63	1.0491	0.0142	0.412612	Npr2	natriuretic peptide receptor 2
E18	Up in KO	2453.55	4626.21	0.914956	0.01425	0.413539	Gm20667	Sense overlapping
E18	Up in KO	3646.12	6185.61	0.762557	0.0143	0.41394	Amn1	antagonist of mitotic exit network 1
E18	Up in KO	5039.64	8331.87	0.72532	0.0143	0.41394	Osbpl2	oxysterol binding protein-like 2
E18	Down in KO	144.334	0	-infinity	0.01435	0.414338	Zfp960	zinc finger protein 960
E18	Up in KO	219.331	1326.94	2.59692	0.01435	0.414338	Thada	thyroid adenoma associated
E18	Up in KO	5988.79	9711	0.697354	0.01445	0.416175	Zfp521	zinc finger protein 521
E18	Up in KO	22258.7	31618.4	0.506394	0.01445	0.416175	Prrc2b	proline-rich coiled-coil 2B
E18	Down in KO	553523	408680	-0.437672	0.0145	0.417089	Rps27rt	ribosomal protein S27; retrogene
E18	Down in KO	26390.3	18172.6	-0.538245	0.01455	0.418002	Usf1	upstream transcription factor 1
E18	Up in KO	3088.37	5439.23	0.816554	0.0146	0.418387	Prkab1	protein kinase, AMP-activated, beta 1 non-catalytic subunit
E18	Up in KO	3995.57	6939.96	0.796525	0.0146	0.418387	Itga1	Integrin alpha 1
E18	Up in KO	26017.2	37102.6	0.512052	0.01465	0.419294	Sepw1	selenoprotein W, muscle 1
E18	Up in KO	99166.2	134006	0.434376	0.0148	0.423058	Cst3	cystatin C
E18	Up in KO	0	98.5263	infinity	0.01485	0.423957	Cntd1	cyclin N-terminal domain containing 1
E18	Up in KO	622.373	1984.95	1.67325	0.0149	0.424854	Fmo5	flavin containing monooxygenase 5
E18	Down in KO	4896.64	2667.02	-0.876564	0.01495	0.425749	Taf7	TAF7 RNA polymerase II; TATA box binding protein (TBP)-associated factor
E18	Up in KO	17594.2	26121.8	0.570152	0.01505	0.427532	Hs6st1	heparin sulfate 6-O-sulfotransferase 1
E18	Up in KO	1265.64	2853.96	1.1731	0.01515	0.429839	Cped1	cadherin-like and PC-esterase domain containing 1
E18	Up in KO	1484.87	3242.48	1.12677	0.0152	0.430723	Nucks1	nuclear casein kinase and cyclin-dependent kinase substrate 1
E18	Up in KO	784.481	1752.54	1.15964	0.01525	0.431072	Ccbl1	cysteine conjugate-beta lyase 1
E18	Up in KO	47081.6	64331.9	0.450373	0.01525	0.431072	Tma7	translational machinery associated 7 homolog
E18	Up in KO	0	123.311	infinity	0.01535	0.432295	4930519A11Rik	lincRNA
E18	Up in KO	0	123.311	infinity	0.01535	0.432295	Hist1h2bl	Histone cluster 1, H2bl
E18	Up in KO	34243	48227.7	0.494051	0.01535	0.432295	Gapdh	glyceraldehyde-3-phosphate dehydrogenase
E18	Down in KO	126.524	0	-infinity	0.0154	0.43317	Grpr	gastrin releasing peptide receptor
E18	Up in KO	0	132.787	infinity	0.0155	0.435447	Ankrd63	ankyrin repeat domain 63
E18	Up in KO	0	130.172	infinity	0.01555	0.436316	Prss27	protease, serine 27
E18	Up in KO	361549	484135	0.421221	0.01565	0.438584	Nucks1	nuclear casein kinase and cyclin-dependent kinase substrate 1
E18	Up in KO	6522.41	10248.6	0.651952	0.0158	0.442245	Nhsl1	NHS-like 1
E18	Up in KO	689.417	1956.48	1.50481	0.0159	0.443958	Ndufa7	NADH dehydrogenase (ubiquinone) 1 alpha subcomplex, 7
E18	Up in KO	3245.03	5809.14	0.840092	0.0159	0.443958	Mm.452559	Transcribed locus, brain
E18	Up in KO	1592.61	3306.05	1.05371	0.016	0.446205	Daam2	disheveled associated activator of morphogenesis 2
E18	Up in KO	0	128.541	infinity	0.01605	0.447054	Gzme	granzyme E
E18	Up in KO	0	109.627	infinity	0.0162	0.450683	Fer1l5	fer-1-like 5
E18	Up in KO	15170.5	22116	0.543826	0.01625	0.451525	Plekhg1	pleckstrin homology domain containing, family G (with RhoGEF domain) member 1
E18	Up in KO	1826.42	3711.33	1.02292	0.0164	0.45514	Gm9990	Known Protein Coding
E18	Up in KO	3513.99	6061.18	0.786489	0.01645	0.455974	Slc25a10	solute carrier family 25 (mitochondrial

Table A2.2: E18.5 Differentially Expressed Genes (Continued)

Time Point	Direction	WT	KO	log2 (fold change)	p value	q value	Gene Symbol	Gene Name
								carrier, dicarboxylate transporter), member 10
E18	Down in KO	3136.64	1431.41	-1.13178	0.01685	0.466187	Ndnf	neuron-derived neurotrophic factor
E18	Up in KO	0	130.664	infinity	0.0169	0.466187	Ccl1l	chemokine (C-C motif) ligand 11
E18	Up in KO	0	130.664	infinity	0.0169	0.466187	Prl8a9	prolactin family8, subfamily a, member 9
E18	Up in KO	0	217.091	infinity	0.0169	0.466187	Gm9920	Known Protein Coding
E18	Up in KO	2323.38	4306.39	0.890253	0.017	0.468381	Kdmc5	lysine (K)-specific demethylase 5C
E18	Up in KO	0	129.357	infinity	0.0171	0.470569	Zfp626	zinc finger protein 626
E18	Up in KO	0	122.495	infinity	0.0172	0.471618	Ccdc87	coiled-coil domain containing 87
E18	Up in KO	0	122.495	infinity	0.0172	0.471618	Gm15328	lincRNA
E18	Up in KO	0	195.731	infinity	0.0172	0.471618	Cass4	Cas scaffolding protein family member 4
E18	Up in KO	7376.63	11378.8	0.625312	0.01725	0.472423	Xab2	XPA binding protein 2
E18	Up in KO	4625.98	7528.06	0.702519	0.0173	0.473225	Pdgfc	platelet-derived growth factor, C polypeptide
E18	Up in KO	0	137.033	infinity	0.01745	0.476758	4931422A03Rik	RIKEN cDNA 4931422A03 gene, known protein coding
E18	Up in KO	0	125.111	infinity	0.01755	0.478347	Gm13355	pseudogene
E18	Up in KO	0	125.111	infinity	0.01755	0.478347	Gm20939	Known Protein Coding
E18	Up in KO	1358.87	2865.57	1.07641	0.01785	0.485945	Tchp	trichoplein, keratin filament binding
E18	Up in KO	3084	5350.58	0.794894	0.0179	0.486727	Pdlim4	PDZ and LIM domain 4
E18	Down in KO	122.01	0	-infinity	0.01795	0.487507	Lrcc6	leucine rich repeat containing 6
E18	Down in KO	115.202	0	-infinity	0.01805	0.488679	BC048507	known protein coding
E18	Up in KO	46120.2	65515.8	0.506444	0.01805	0.488679	Cep112os2	centrosomal protein 112, opposite strand 2
E18	Down in KO	1768.09	529.349	-1.7399	0.0181	0.488679	Rpl31-ps11	ribosomal protein L31; pseudogene 11
E18	Up in KO	586.399	1538.02	1.39112	0.0181	0.488679	Corin	corin
E18	Up in KO	1607.3	3276.79	1.02764	0.01815	0.489451	Entpd6	ectonucleoside triphosphate diphosphohydrolase 6
E18	Up in KO	12993.1	18870.8	0.538409	0.0182	0.490221	Hip1	huntingtin interacting protein 1
E18	Up in KO	40205.1	54690	0.443899	0.0185	0.496547	Brd2	bromodomain containing 2
E18	Up in KO	84892.5	114236	0.428306	0.0185	0.496547	Cald1	caldesmon 1
E18	Up in KO	717.226	1996.77	1.47717	0.0186	0.498646	Gm40481	unknown
E18	Up in KO	0	240.291	infinity	0.01885	0.503308	Cacna1f	calcium channel, voltage-dependent, alpha 1F subunit
E18	Up in KO	1659.86	3839.15	1.20972	0.01885	0.503308	4930563M21Rik	Known Protein Coding
E18	Up in KO	0	121.188	infinity	0.01895	0.503308	Gm12259	lincRNA
E18	Up in KO	0	121.188	infinity	0.01895	0.503308	Gm22973	snRNA
E18	Up in KO	0	121.188	infinity	0.01895	0.503308	Sirpb1b	signal-regulatory protein beta 1B
E18	Up in KO	393.695	1880.8	2.25619	0.01895	0.503308	Cdk6	cyclin-dependent kinase 6
E18	Down in KO	15460.5	10395.2	-0.57266	0.01895	0.503308	Dtd	D-tyrosyl-tRNA deacylase
E18	Up in KO	0	198.346	infinity	0.0191	0.506117	Ush1c	Usher syndrome 1C
E18	Up in KO	2307.58	4215.49	0.869321	0.01915	0.506268	Sapcd2	suppressor APC domain containing 2
E18	Up in KO	14749.6	21360.7	0.534288	0.01925	0.508324	Fam114a2	family with sequence similarity 114, member A2
E18	Up in KO	511.438	1725.63	1.75449	0.01935	0.509201	Rpusd2	RNA pseudouridylate synthase domain containing 2
E18	Up in KO	2733.21	4879.93	0.836267	0.01935	0.509201	Gm4430	TEC
E18	Up in KO	99524.6	133320	0.421769	0.01935	0.509201	Wdr31	WD repeat domain 31
E18	Up in KO	2353.37	4335.59	0.881499	0.0194	0.50993	Kcnk3	potassium channel, subfamily K, member 3
E18	Down in KO	114.056	0	-infinity	0.01975	0.516163	Il22	interleukin 22
E18	Down in KO	114.056	0	-infinity	0.01975	0.516163	Ankub1	ankrin repeat and ubiquitin domain containing 1
E18	Down in KO	2304.38	769.77	-1.58188	0.01975	0.516163	Acmsd	amino carboxymuconate semialdehyde decarboxylase
E18	Up in KO	8303.7	12400	0.578516	0.0198	0.516879	l7Rn6	lethal, Chr 7, Rinchik 6
E18	Up in KO	0	268.969	infinity	0.0199	0.518307	Gm17231	Antisense
E18	Down in KO	1588.32	485.281	-1.71061	0.0199	0.518307	LOC102640315	lincRNA
E18	Down in KO	172.319	0	-infinity	0.01995	0.518428	Nwd1	NACHT and WD repeat domain containing 1
E18	Up in KO	33975.4	47162	0.473134	0.01995	0.518428	Pfdn2	prefoldin 2
E18	Up in KO	0	27.4067	infinity	0.02	0.519137	BC028777	processed transcript
E18	Up in KO	821.319	2065.57	1.33053	0.02015	0.522438	Rab17	RAB17, member RAS oncogene family
E18	Up in KO	4728.49	7612.44	0.686978	0.0204	0.528321	Gpr153	G protein-coupled receptor 153
E18	Down in KO	1570.07	488.181	-1.68534	0.02045	0.529017	Mm.405422	Transcribed locus: brain
E18	Up in KO	3821.86	6250.53	0.709703	0.0205	0.529711	Bc2l11	BCL2-like 11
E18	Down in KO	101.907	0	-infinity	0.02065	0.531784	Hs6st3	heparin sulfate 6-O-sulfotransferase 3
E18	Down in KO	101.907	0	-infinity	0.02065	0.531784	Gm25076	snoRNA
E18	Up in KO	7713.4	11687	0.599468	0.02065	0.531784	Carnmt1	carnosine N-methyltransferase 1
E18	Up in KO	16694.4	23900.4	0.517673	0.02075	0.533158	Dcaf5	DDB1 and CUL4 associated factor 5
E18	Up in KO	18577.6	26094.9	0.490202	0.02075	0.533158	Kcnk1	potassium channel, subfamily K, member 1
E18	Up in KO	0	368.832	infinity	0.0208	0.533843	Nfe2	nuclear factor, erythroid derived 2
E18	Up in KO	1603.93	2912.37	0.860582	0.021	0.538372	Nr1h2	nuclear receptor subfamily 1, group H, member 2
E18	Up in KO	3617.69	6018.77	0.734398	0.02105	0.53905	Rin3	Ras and Rab interactor 3
E18	Down in KO	38397.3	27821.6	-0.4648	0.02115	0.541005	Zfp365	zinc finger protein 365
E18	Up in KO	25963.2	36125.2	0.476539	0.02125	0.542955	S100a11	S100 calcium binding protein A11
E18	Up in KO	6902.54	10727.1	0.636061	0.0213	0.543625	Maml3	mastermind like 3
E18	Up in KO	0	126.741	infinity	0.02175	0.554492	Sh3tc1	SH3 domain and tetratricopeptide repeats 1
E18	Up in KO	2932	5079.81	0.792893	0.022	0.560241	Cyth1	cytohesin 1
E18	Up in KO	703.93	1841.91	1.38769	0.02205	0.560266	Guca1b	guanylate cyclase activator 1B
E18	Down in KO	7832.9	4891.82	-0.679175	0.02205	0.560266	Ctf1	cardiotrophin 1

Table A2.2: E18.5 Differentially Expressed Genes (Continued)

Time Point	Direction	WT	KO	log2 (fold change)	p value	q value	Gene Symbol	Gene Name
E18	Down in KO	69.3342	0	-infinity	0.02215	0.562182	4933431K23Rik	RIKEN cDNA 4933431K23 gene; known processed transcript
E18	Up in KO	0	107.504	infinity	0.02225	0.564094	Fam83f	family with sequence similarity 83, member F
E18	Up in KO	1361.53	2897.5	1.08957	0.0223	0.564736	BC026513	unknown
E18	Up in KO	11741.8	17224	0.552767	0.02235	0.565376	Anxa6	annexin A6
E18	Up in KO	0	287.75	infinity	0.0224	0.566015	Il1f5	interleukin 1 family, member 5 (delta)
E18	Down in KO	1218.98	451.998	-1.43129	0.02245	0.566027	Podxl2	podocalyxin-like 2
E18	Up in KO	1648.33	3304	1.00321	0.02245	0.566027	Wtip	WT1-interacting protein
E18	Up in KO	6891.63	10576.2	0.617902	0.02255	0.567922	S1pr2	sphingosine-1-phosphate receptor 2
E18	Up in KO	59080.6	78957.1	0.418385	0.0226	0.568555	Ostf1	osteoclast stimulating factor 1
E18	Up in KO	2185.06	4048.77	0.889812	0.02265	0.569187	Gm26751	lincRNA
E18	Up in KO	280.75	1014.76	1.85378	0.0227	0.569817	Atp7a	ATPase, Cu++ transporting, alpha polypeptide
E18	Up in KO	2114.19	3979.95	0.912648	0.0228	0.5717	Parvb	parvin, beta
E18	Up in KO	7712.67	11531.6	0.580296	0.0229	0.573579	Mrpl38	mitochondrial ribosomal protein L38
E18	Down in KO	189.053	0	-infinity	0.02295	0.574202	Gm16010	Antisense
E18	Up in KO	0	149.086	infinity	0.023	0.574824	Il9r	interleukin 9 receptor
E18	Up in KO	0	123.311	infinity	0.0231	0.576693	Gm12977	Antisense
E18	Down in KO	5522.19	3259.9	-0.760415	0.02325	0.579173	Zfp472	zinc finger protein 472
E18	Down in KO	99.6142	0	-infinity	0.0234	0.581643	Zp2	zona pellucida glycoprotein 2
E18	Down in KO	156.518	0	-infinity	0.0234	0.581643	Gm11973	Antisense
E18	Up in KO	828.161	2515.28	1.60274	0.02345	0.582253	Tmem91	transmembrane protein 91
E18	Up in KO	2599.86	4586.48	0.818954	0.02355	0.584101	Tnfrsf11a	tumor necrosis factor receptor superfamily, member 11a, NFKB activator
E18	Up in KO	2102.48	3889.76	0.88759	0.02365	0.584651	Camkmt	calmodulin-lysine N-methyltransferase
E18	Up in KO	7492.01	11466.8	0.614039	0.02365	0.584651	Sh3bgrl3	SH3 domain binding glutamic acid-rich protein-like 3
E18	Up in KO	9647.06	14315.9	0.569459	0.02365	0.584651	Tcerg1	transcription elongation regulator 1 (CA150)
E18	Up in KO	0	102.765	infinity	0.0237	0.584651	Kctd16	potassium channel tetramerisation domain containing 16
E18	Up in KO	3889.2	6376.53	0.713298	0.0237	0.584651	Abhd4	abhydrolase domain containing 4
E18	Up in KO	690.28	1852.24	1.42401	0.02375	0.585253	Mm.401549	Transcribed locus: testis; ovary; inner ear; lymph node
E18	Down in KO	3163.48	1556.98	-1.02276	0.0238	0.585854	Actn3	actinin alpha 3
E18	Down in KO	201.239	0	-infinity	0.02395	0.58828	Frs3os	fibroblast growth factor receptor substrate 3; opposite strand
E18	Up in KO	0	122.495	infinity	0.02405	0.590102	Sall4	sal-like 4
E18	Down in KO	2180.95	1096.36	-0.992238	0.02415	0.591287	Cfap126	cilia and flagella associated protein 126
E18	Up in KO	17250.4	24270.3	0.492562	0.02415	0.591287	Tecr	trans-2,3-enoyl-CoA reductase
E18	Up in KO	0	143.857	infinity	0.02445	0.597299	4930563I02Rik	Protein coding
E18	Down in KO	16559.2	11434.2	-0.534275	0.02445	0.597299	Mm.35291	Transcribed locus: mammary gland; pancreas; thymus; intestine; embryonic tissue; kidney; extraembryonic tissue; lung; heart; eye
E18	Up in KO	2198.76	4021.07	0.870889	0.0245	0.597299	Dennd1b	DENN/MADD domain containing 1B
E18	Up in KO	293528	382454	0.38179	0.0245	0.597299	Sparc	secreted acidic cysteine rich glycoprotein
E18	Up in KO	520.183	1201.66	1.20794	0.02465	0.600194	Cd40	CD40 antigen
E18	Up in KO	0	97.2115	infinity	0.02475	0.600194	Gm5561	pseudogene
E18	Up in KO	0	97.2115	infinity	0.02475	0.600194	Psca	prostate stem cell antigen
E18	Up in KO	0	97.2115	infinity	0.02475	0.600194	S100a3	S100 calcium binding protein A3
E18	Up in KO	0	97.2115	infinity	0.02475	0.600194	Srd5a2	steroid 5 alpha-reductase 2
E18	Up in KO	0	154.148	infinity	0.02485	0.601981	Gm13145	Known Protein Coding
E18	Up in KO	2898.9	4891.39	0.754741	0.02495	0.603125	Snhg17	small nucleolar RNA host gene 17
E18	Up in KO	12493.9	17986	0.525649	0.02495	0.603125	Apoa1bp	apolipoprotein A-I binding protein
E18	Down in KO	31435.9	22716.3	-0.46869	0.025	0.603561	Trmt11	tRNA methyltransferase 11
E18	Up in KO	0	99.8269	infinity	0.0251	0.603561	Gm16485	Known Protein Coding
E18	Up in KO	0	99.8269	infinity	0.0251	0.603561	Gm815	Known Protein Coding
E18	Up in KO	0	99.8269	infinity	0.0251	0.603561	Hgfac	hepatocyte growth factor activator
E18	Up in KO	2048.64	3745.22	0.870379	0.0251	0.603561	Klc2	kinesin light chain 2
E18	Down in KO	225.855	0	-infinity	0.02515	0.604128	Asb14	ankyrin repeat and SOCS box-containing 14
E18	Up in KO	0	78.7906	infinity	0.0252	0.604694	Rapgef3os2	Pas guanine nucleotide exchange factor 3, opposite strand 2
E18	Up in KO	3366.13	5726.84	0.766648	0.02525	0.605259	Khnyn	KH and NYN domain containing
E18	Up in KO	757.749	1760.18	1.21593	0.0253	0.605822	Actg2	actin, gamma 2, smooth muscle, enteric
E18	Down in KO	4583.96	1968	-1.21986	0.02545	0.608141	2310043M15Rik	lincRNA
E18	Up in KO	1146.07	2476.97	1.11189	0.02545	0.608141	Sirt6	sirtuin6
E18	Down in KO	2314.79	1076.59	-1.10441	0.0255	0.608699	Chst9	carbohydrate (N-acetylgalactosamine 4-0) sulfotransferase 9
E18	Down in KO	2614.16	1210	-1.11134	0.0257	0.611476	Pcdhb19	protocadherin beta 19
E18	Up in KO	0	98.5192	infinity	0.02575	0.611476	Gm14273	Antisense
E18	Up in KO	0	98.5192	infinity	0.02575	0.611476	Gm26677	lincRNA
E18	Down in KO	2997.72	1480.03	-1.01824	0.02585	0.613128	Abcb1a	ATP-binding cassette; sub-family B (MDR/TAP); member 1A
E18	Up in KO	3020.22	5229.68	0.79207	0.0259	0.613128	Lrlg3	leucine-rich repeats and immunoglobulin-like domains 3
E18	Down in KO	89389.6	66798.2	-0.420298	0.0259	0.613128	Zbtb20	zinc finger and BTB domain containing 20
E18	Up in KO	3083.82	5128.19	0.733728	0.026	0.614858	Map3k1	mitogen-activated protein kinase kinase kinase 1

Table A2.2: E18.5 Differentially Expressed Genes (Continued)

Time Point	Direction	WT	KO	log2 (fold change)	p value	q value	Gene Symbol	Gene Name
E18	Down in KO	6157.53	3724.75	-0.725209	0.02605	0.615404	Ppp1r14c	protein phosphatase 1; regulatory (inhibitor) subunit 14c
E18	Up in KO	0	104.073	infinity	0.0263	0.620669	Zfp296	zinc finger protein 296
E18	Up in KO	6284.6	9541.59	0.60241	0.02645	0.623353	Pcgf2	polycomb group ring finger 2
E18	Up in KO	1825.16	3361.15	0.88093	0.0265	0.623353	Etv6	ets variant 6
E18	Down in KO	99.6497	0	-infinity	0.02655	0.623353	Ccl17	chemokine (C-C motif) ligand 17
E18	Up in KO	0	105.381	infinity	0.02655	0.623353	Slc9a2	solute carrier family 9 (sodium/hydrogen exchanger), member 2
E18	Up in KO	2517.81	4226.82	0.747403	0.02655	0.623353	Tgfb1i1	transforming growth factor beta 1 induced transcript 1
E18	Up in KO	1604.44	3186.55	0.989922	0.0267	0.624949	Zfp612	zinc finger protein 612
E18	Down in KO	7657.99	4854.35	-0.657687	0.0267	0.624949	Gm21321	pseudogene
E18	Up in KO	41622.1	55815	0.423302	0.0267	0.624949	Ascc2	activating signal cointegrator 1 complex subunit 2
E18	Up in KO	0	287.75	infinity	0.02695	0.629512	Nxpe5	neurexophilin and PC-esterase domain family, member 5
E18	Up in KO	149001	195103	0.388913	0.02695	0.629512	Noct	nocturnin
E18	Up in KO	213956	281631	0.396495	0.027	0.630037	Pnlsr	PNN interacting serine/arginine-rich
E18	Up in KO	2366.99	4099.66	0.792453	0.0272	0.633411	Tead3	TEA domain family member 3
E18	Up in KO	4411.89	7067.68	0.679841	0.0272	0.633411	Jrk	jerky
E18	Up in KO	14976.6	21513.1	0.522501	0.02725	0.63393	Gcm1	glial cells missing homolog 1
E18	Up in KO	2180.88	3625.3	0.733191	0.02745	0.637934	Impdh1	inosine 5'-phosphate dehydrogenase 1
E18	Down in KO	44612.8	33118.4	-0.429822	0.0276	0.640768	1110012L19Rik	Protein coding
E18	Up in KO	2606.07	4557.25	0.80629	0.02765	0.641278	Cdh5	cadherin 5
E18	Up in KO	1209.32	2607.95	1.10872	0.0277	0.641787	LOC100042464	uncharacterized locus
E18	Down in KO	275.378	23.9833	-3.52131	0.0279	0.645113	Abhd15	abhydrolase domain containing 15
E18	Down in KO	1721.43	685.75	-1.32785	0.0279	0.645113	Smim24	Small integral membrane protein 2
E18	Up in KO	0	215.786	infinity	0.02795	0.645617	Masp2	mannan-binding lectin serine peptidase 2
E18	Up in KO	14471.9	20386.2	0.494338	0.02805	0.647273	Senp8	SUMO/sentrin specific peptidase 8
E18	Up in KO	1510.56	3170.59	1.06967	0.0281	0.647773	Mospd2	motile sperm domain containing 2
E18	Up in KO	128.817	582.092	2.17593	0.0282	0.64877	Ccr9	chemokine (C-C motif) receptor 9
E18	Down in KO	5670.89	3414.25	-0.732005	0.0282	0.64877	Mm.414070	Transcribed locus: brain
E18	Up in KO	3508.5	5679.38	0.694879	0.0283	0.648802	Ecscr	endothelial cell surface expressed chemotaxis and apoptosis regulator
E18	Down in KO	91.6963	0	-infinity	0.02835	0.648802	Mrpl48-ps	mitochondrial ribosomal protein L48 pseudogene
E18	Up in KO	26886.2	37272.9	0.471262	0.02835	0.648802	Rsrc1	arginine/serine-rich coiled-coil 1
E18	Up in KO	0	101.95	infinity	0.0284	0.648802	Gcnt3	glucosaminyl (N-acetyl) transferase 3, mucin type
E18	Down in KO	11662.8	7922.74	-0.557844	0.0284	0.648802	Ndufaf6	NADH dehydrogenase (ubiquinone) complex I; assembly factor 6
E18	Down in KO	34514.3	25284.3	-0.448951	0.0284	0.648802	Rgs17	regulator of G-protein signaling 17
E18	Up in KO	27049.7	40200.5	0.571605	0.0284	0.648802	Ccdc88a	coiled coil domain containing 88A
E18	Up in KO	19226.5	27097.5	0.495066	0.0285	0.649789	Khsrp	KH-type splicing regulatory protein
E18	Up in KO	1497.69	3013.12	1.00852	0.02855	0.65028	Fam57b	family with sequence similarity 57, member B
E18	Up in KO	2023.04	3831.14	0.921251	0.0287	0.653046	Zfp804b	zinc finger protein 804B
E18	Up in KO	0	205.531	infinity	0.02885	0.654506	Ccl21a	chemokine (C-C motif) ligand 21A (serine)
E18	Up in KO	6690.04	10142.2	0.600277	0.02885	0.654506	Hmmr	hyaluronan mediated motility receptor (RHAMM)
E18	Up in KO	2995.35	4792.75	0.678129	0.0289	0.65499	Ccdc9	Coiled-coil domain containing 9
E18	Up in KO	1743.11	3311.68	0.925895	0.02905	0.657087	Krt6a	keratin 6A
E18	Up in KO	645.561	1942.13	1.58902	0.02915	0.658698	Park2	Parkinson disease (autosomal recessive, juvenile) 2, parkin
E18	Up in KO	0	137.033	infinity	0.02925	0.659654	5730460C07Rik	lincRNA
E18	Up in KO	0	137.033	infinity	0.02925	0.659654	Rdh8	retinol dehydrogenase 8
E18	Up in KO	0	157.579	infinity	0.0295	0.664636	Smc1b	Structural maintenance of chromosomes 1B
E18	Down in KO	1312.94	326.395	-2.00811	0.0296	0.666233	ifi2712a	Interferon; alpha-inducible protein 27 like 2A
E18	Up in KO	192.457	1190.23	2.62863	0.0297	0.666983	Atg9b	autophagy related 9B
E18	Up in KO	536.055	1590.3	1.56885	0.02975	0.666983	Gm31733	pseudogene
E18	Up in KO	8649.65	12703.7	0.554537	0.02975	0.666983	Osgin2	oxidative stress induced growth inhibitor family member 2
E18	Down in KO	173669	132082	-0.394907	0.0298	0.66745	Gm9385	pseudogene
E18	Down in KO	5397.49	3252.38	-0.730794	0.02985	0.667916	Cmde	colorectal neoplasia differentially expressed (non-protein coding)
E18	Up in KO	0	105.381	infinity	0.02995	0.668844	Crisp2	cysteine-rich secretory protein 2
E18	Up in KO	3903.13	6209.34	0.669808	0.02995	0.668844	Sbf2	SET binding factor 2
E18	Up in KO	5579.56	8465.5	0.601444	0.0302	0.673769	Copz2	coatomer protein complex, subunit zeta 2
E18	Up in KO	997.147	2067.58	1.05207	0.0303	0.675342	Fam45a	family with sequence similarity 45, member A
E18	Down in KO	2088.35	939.725	-1.15206	0.0306	0.680701	Pitx1	paired-like homeodomain transcription factor 1
E18	Up in KO	371.654	1361.53	1.8732	0.0306	0.680701	Fgd3	FYVE, RhoGEF and PH domain containing 3
E18	Up in KO	2552.74	4402.12	0.78615	0.03075	0.68271	Tmem115	Transmembrane protein 115
E18	Up in KO	8733.41	12450.6	0.511603	0.03075	0.68271	Rasgrp2	RAS, guanyl releasing protein 2
E18	Up in KO	0	100.642	infinity	0.03095	0.685818	Fcer2a	Fc receptor, IgE, low affinity II, alpha polypeptide
E18	Up in KO	0	100.642	infinity	0.03095	0.685818	Gm12702	lincRNA

Table A2.2: E18.5 Differentially Expressed Genes (Continued)

Time Point	Direction	WT	KO	log2 (fold change)	p value	q value	Gene Symbol	Gene Name
E18	Up in KO	4010.52	6397.51	0.673719	0.03105	0.686703	Klhl21	kelch-like 21
E18	Up in KO	23993.4	32519.7	0.438675	0.0312	0.689354	Akap2	A kinase (PRKA) anchor protein 2
E18	Up in KO	23993.4	32519.7	0.438675	0.0312	0.689354	Pakap	paralemmin A kinase anchor protein
E18	Up in KO	10551.9	15154.7	0.522262	0.0313	0.690438	Fst	follistatin
E18	Up in KO	1438.89	2899.5	1.01085	0.03135	0.690438	Gm29998	lincRNA
E18	Down in KO	5097.29	3026.98	-0.75185	0.03135	0.690438	Hist1h2ai	histone cluster 1; H2ai
E18	Up in KO	21224.7	29117.5	0.45614	0.0314	0.690438	Cd164	CD164 antigen
E18	Up in KO	0	158.071	infinity	0.03145	0.690873	Col6a4	collagen, type VI, alpha 4
E18	Up in KO	1804.85	3347.14	0.891048	0.03155	0.692404	AI837181	Protein coding
E18	Up in KO	4597.77	7243.49	0.655749	0.0317	0.694364	Dok5	docking protein 5
E18	Up in KO	38365.1	51184.6	0.415917	0.0317	0.694364	Farp1	FERM, RhoGEF (ArhGEF and pleckstrin domain protein 1 (chondrocyte-derived))
E18	Up in KO	3169.7	5268.11	0.732936	0.03175	0.694558	Pex11g	peroxisomal biogenesis factor 11 gamma
E18	Down in KO	805.08	316.957	-1.34484	0.0318	0.694558	Gm14399	protein coding
E18	Up in KO	827.404	2030.36	1.29507	0.0318	0.694558	Rassf10	Ras association (RalGDS/AF-6) domain family (N-terminal) member 10
E18	Up in KO	2453.99	4213.48	0.779882	0.03205	0.698684	Gm6483	Known Protein Coding
E18	Up in KO	3204.25	5394.29	0.751448	0.03205	0.698684	Map1s	microtubule-associated protein 1S
E18	Down in KO	98.5034	0	-infinity	0.03215	0.699287	Atp6v0c-ps2	ATPase, H+ transporting, lysosomal V0 subunit C, pseudogene 2
E18	Up in KO	7315.48	10893.3	0.574424	0.03215	0.699287	Kif13b	kinesin family member 13B
E18	Up in KO	0	121.188	infinity	0.0322	0.699287	5830432E09Rik	lincRNA
E18	Up in KO	7387.83	10996.6	0.57384	0.0322	0.699287	Fam101b	family with sequence similarity 101, member B
E18	Up in KO	14070.4	19652.6	0.482061	0.03225	0.699709	Loxl1	lysyl oxidase-like 1
E18	Up in KO	1905.61	3453.05	0.857617	0.0324	0.701632	Emx2	empty spiracles homeobox 2
E18	Up in KO	31485.7	42177.2	0.421768	0.0325	0.70222	Ptov1	prostate tumor over expressed gene 1
E18	Up in KO	6241.76	9484.78	0.603662	0.03255	0.70222	Rab35	RAB35, member RAS oncogene family
E18	Up in KO	87859.6	115357	0.392827	0.03255	0.70222	Sgip1	SH3-domain GRB2-like (endophilin) interacting protein 1
E18	Up in KO	5201.2	7784.61	0.58178	0.0327	0.704128	Taf6l	TAF6-like RNA polymerase II, p300/CBP-associated factor (PCAF)-associated factor
E18	Up in KO	4350	6729.23	0.629427	0.03275	0.704291	St5	suppression of tumorigenicity 5
E18	Up in KO	972.495	2182.55	1.16625	0.0328	0.704291	Rasl11a	RAS-like, family 11, member A
E18	Up in KO	4883.4	7521.08	0.623052	0.0328	0.704291	Casp2	caspase 2
E18	Up in KO	2711.55	4627.55	0.771129	0.03285	0.704703	Scaf8	SR-related CTD-associated factor 8
E18	Down in KO	1039.72	256.098	-2.02142	0.03295	0.705525	Pank3	Pantothenate kinase 3
E18	Down in KO	4238.27	2583.66	-0.714058	0.03295	0.705525	Mknk1	MAP kinase-interacting serine/threonine kinase 1
E18	Up in KO	27640.3	37285.6	0.431842	0.033	0.705935	Ep400	E1A binding protein p400
E18	Down in KO	329.191	25.2831	-3.70268	0.03325	0.710618	Slc2a2	solute carrier family 2 (facilitated glucose transporter); member 2
E18	Down in KO	17590.6	12524.7	-0.490029	0.0335	0.715292	Atxn3	ataxin 3
E18	Up in KO	475.499	1415.08	1.57336	0.03355	0.715692	Mm.165212	Transcribed locus: brain
E18	Up in KO	0	244.537	infinity	0.03365	0.716488	Mmp28	matrix metallopeptidase 28 (epilysin)
E18	Down in KO	1992.48	881.843	-1.17597	0.03365	0.716488	Gpihbp1	GPI-anchored HDL-binding protein 1
E18	Up in KO	988.153	2166.09	1.13228	0.0338	0.719012	Zfp775	Zinc finger protein 775
E18	Up in KO	0	292.981	infinity	0.0339	0.72047	Vmn1r181	vomeronasal 1 receptor 181
E18	Up in KO	2071.72	3800.69	0.875432	0.03395	0.720862	Col26a1	collagen, type XXVI, alpha 1
E18	Up in KO	0	356.248	infinity	0.03435	0.728004	Aox3	aldehyde oxidase 3
E18	Up in KO	6836.35	10249.6	0.584265	0.03435	0.728004	Arap3	ArfGAP with RhoGAP domain, ankyrin repeat and PH domain 3
E18	Up in KO	855.827	1854.04	1.11528	0.0344	0.728193	Stac3	SH3 and cysteine rich domain 3
E18	Down in KO	1278.22	157.579	-3.01999	0.03445	0.728193	Rpl31-ps16	ribosomal protein L31; pseudogene 16
E18	Up in KO	0	74.5437	infinity	0.0345	0.728193	A830011K09Rik	Antisense
E18	Up in KO	5064.49	7748.82	0.61356	0.03455	0.728193	Tuft1	Tuftelin 1
E18	Up in KO	10148.7	14409.3	0.505716	0.03455	0.728193	Slc50a1	solute carrier family 50 (sugar transporter), member 1
E18	Down in KO	45923.7	34437.5	-0.415257	0.03455	0.728193	Lrp12	low density lipoprotein-related protein 12
E18	Up in KO	0	76.6663	infinity	0.03475	0.730098	Acer1	alkaline ceramidase 1
E18	Up in KO	0	76.6663	infinity	0.03475	0.730098	Defb25	defensin beta 25
E18	Up in KO	0	76.6663	infinity	0.03475	0.730098	Gm13878	pseudogene
E18	Up in KO	1127.83	2342.56	1.05453	0.0348	0.730098	Gm21158	pseudogene
E18	Up in KO	6283.58	9444.5	0.587888	0.0348	0.730098	Espl1	extra spindle pole bodies 1, separase
E18	Up in KO	6551.94	9820.58	0.583885	0.03495	0.732573	Gnb3	guanine nucleotide binding protein (G protein), beta 3
E18	Up in KO	458.729	1354.92	1.56249	0.0351	0.735043	Zfp804a	zinc finger protein 804A
E18	Up in KO	7554.26	11152.7	0.562032	0.03515	0.735416	Cnppd1	cyclin Pas1/PHO80 domain containing 1
E18	Up in KO	0	164.439	infinity	0.03525	0.736603	Gm12146	Antisense
E18	Up in KO	26345.8	35487.1	0.429723	0.03535	0.736603	Prep	prolyl endopeptidase
E18	Up in KO	73731.4	95895.9	0.37919	0.03535	0.736603	Srrm2	serine/arginine repetitive matrix 2
E18	Up in KO	2377.71	4171.8	0.811099	0.0354	0.736603	AI463229	miscRNA
E18	Down in KO	19289.4	13788.9	-0.484303	0.0354	0.736603	Serpini1	serine (or cysteine) peptidase inhibitor; clade I; member 1
E18	Up in KO	0	173.062	infinity	0.03565	0.741131	4933427D06Rik	Known Protein Coding
E18	Up in KO	1954.34	3524.03	0.850548	0.03585	0.743936	Rbm11	RNA binding motif protein 11
E18	Up in KO	67074.8	87576.1	0.384767	0.036	0.746372	Ppil1	peptidylprolyl isomerase (cyclophilin)-like 1
E18	Down in KO	1352.39	462.613	-1.54763	0.0361	0.747767	Gm31501	lincRNA

Table A2.2: E18.5 Differentially Expressed Genes (Continued)

Time Point	Direction	WT	KO	log2 (fold change)	p value	q value	Gene Symbol	Gene Name
E18	Up in KO	279.639	1118.34	1.99972	0.03615	0.748125	Sst	somatostatin
E18	Up in KO	2106.73	3746.18	0.830413	0.0362	0.748482	Kcna2	potassium voltage-gated channel, shaker-related 2subfamily, member 2
E18	Up in KO	18060.6	24893.3	0.462914	0.03625	0.748839	Safb2	scaffold attachment factor B2
E18	Down in KO	1889.46	852.313	-1.14852	0.0364	0.750582	Nmnat3	nicotinamide nucleotide adenylyltransferase 3
E18	Up in KO	6715.13	9930.2	0.564408	0.0364	0.750582	Brca1	breast cancer 1
E18	Up in KO	1602.71	3006.89	0.907755	0.0365	0.751966	Dph2	DPH2 homolog
E18	Down in KO	99.6142	0	-infinity	0.0366	0.753347	Pydc4	pyrin domain containing 4
E18	Up in KO	0	107.504	infinity	0.03665	0.753698	Ifitm7	interferon induced transmembrane protein 7
E18	Up in KO	4531.82	7052.14	0.637972	0.0367	0.754048	Zfp488	zinc finger protein 488
E18	Up in KO	0	82.22	infinity	0.0369	0.756152	4933423P22Rik	Antisense
E18	Down in KO	2358.4	1135	-1.05511	0.03695	0.756152	Gm20300	miscRNA
E18	Up in KO	558.414	1245.86	1.15773	0.037	0.756152	Vgll4	vestigial like 4
E18	Down in KO	4213.26	2598.31	-0.697362	0.037	0.756152	Gnb1l	guanine nucleotide binding protein (G protein); beta polypeptide 1-like
E18	Up in KO	17934.3	24327.1	0.439841	0.03705	0.756152	Racgap1	Rac GTPase-activating protein 1
E18	Up in KO	316.724	1188.51	1.90786	0.0371	0.756152	Fibcd1	fibrinogen C domain containing 1
E18	Up in KO	1003.95	2448.83	1.2864	0.0371	0.756152	3300002I08Rik	Known Protein Coding
E18	Down in KO	20926.7	15097.9	-0.471002	0.0371	0.756152	Actn1	actinin; alpha 1
E18	Up in KO	1279.73	2605.18	1.02554	0.03725	0.757185	Arg1	arginase, liver
E18	Up in KO	10788.8	15442.7	0.517384	0.03725	0.757185	Mm.473923	Transcribed locus: spleen; pineal; heart; stomach; embryonic tissue; brain
E18	Up in KO	4379.2	6834.29	0.642124	0.0374	0.759559	Tmem50b	transmembrane protein 50B
E18	Up in KO	4078.03	6441.9	0.659616	0.0375	0.760914	Sash1	SAM and SH3 domain containing 1
E18	Up in KO	17392.6	23865.1	0.456428	0.0376	0.762267	Txndc5	thioredoxin domain containing 5
E18	Down in KO	114.056	0	-infinity	0.0377	0.763613	Prc1	protein regulator of cytokinesis 1
E18	Down in KO	897.427	307.48	-1.5453	0.03775	0.763613	Tdh	L-threonine dehydrogenase
E18	Up in KO	0	332.933	infinity	0.0378	0.763613	A230056P14Rik	processed transcript
E18	Up in KO	4392.64	6744.7	0.618668	0.0378	0.763613	Plekho2	pleckstrin homology domain containing, family O member 2
E18	Down in KO	7747.03	5060.73	-0.6143	0.0379	0.764617	Mm.300904	Transcribed locus: unknown
E18	Up in KO	1804.27	3304.12	0.872849	0.03795	0.764617	Ifi35	interferon-induced protein 35
E18	Up in KO	1627.47	3046.14	0.90435	0.03805	0.765957	Dusp23	dual specificity phosphatase 23
E18	Up in KO	2575.79	4457.77	0.791309	0.0381	0.766289	Synpo2l	synaptopodin 2-like
E18	Down in KO	123.087	0	-infinity	0.03815	0.766621	Gm16541	Antisense
E18	Down in KO	977.944	309.603	-1.65933	0.0382	0.766951	Rem1	rad and gem related GTP binding protein 1
E18	Up in KO	0	105.381	infinity	0.0383	0.767611	1700067K01Rik	Known Protein Coding
E18	Up in KO	20714.5	28012.6	0.435434	0.0383	0.767611	Ppox	protoporphyrinogen oxidase
E18	Down in KO	1710	719.164	-1.2496	0.03835	0.76794	Mm.381499	Transcribed locus: brain; embryonic tissue
E18	Up in KO	9547.13	13700.1	0.521044	0.0384	0.768269	Coro2b	coronin, actin binding protein, 2B
E18	Up in KO	10438.8	14779.7	0.501663	0.03855	0.770596	Rasa2	RAS p21 protein activator 2
E18	Up in KO	0	80.097	infinity	0.03875	0.771895	Gm13437	pseudogene
E18	Up in KO	0	80.097	infinity	0.03875	0.771895	Krt84	keratin 84
E18	Up in KO	0	80.097	infinity	0.03875	0.771895	Nodal	nodal
E18	Up in KO	35604.2	47075.3	0.402925	0.0389	0.773535	Pold1	polymerase (DNA directed), delta 1, catalytic subunit
E18	Down in KO	5649	3710.82	-0.606258	0.0391	0.776836	Brsk2	BR serine/threonine kinase 2
E18	Up in KO	3793.33	5955.27	0.650701	0.03935	0.777551	Slc7a8	solute carrier family 7 (cationic amino acid transporter, y+ system), member 8
E18	Up in KO	11408.5	16059.2	0.493301	0.0394	0.777551	Nkd2	naked cuticle 2 homolog
E18	Down in KO	228098	177342	-0.363121	0.03945	0.777551	Nupr1	nuclear protein transcription regulator 1
E18	Down in KO	2649.22	1391.76	-0.928654	0.03955	0.777551	Nwd2	NACHT and WD repeat domain containing 2
E18	Up in KO	669.421	1549.7	1.21101	0.03955	0.777551	Cntfr	ciliary neurotrophic factor receptor
E18	Down in KO	26732.4	19617	-0.446485	0.03955	0.777551	Nol11	nucleolar protein 11
E18	Up in KO	3436.5	5553.71	0.692512	0.03965	0.777551	Myosin16	Myosin XVI
E18	Up in KO	13004	18056	0.47352	0.03965	0.777551	Rnf130	ring finger protein 130
E18	Up in KO	0	78.7893	infinity	0.0398	0.777551	Acsbg2	acyl-CoA synthetase bubblegum family member 2
E18	Up in KO	0	78.7893	infinity	0.0398	0.777551	Cd300ld	CD300 molecule-like family member d
E18	Up in KO	0	78.7893	infinity	0.0398	0.777551	Chrna7	cholinergic receptor, nicotinic, alpha polypeptide 7
E18	Down in KO	134.159	0	-infinity	0.03985	0.777551	Sprr1a	small proline-rich protein 1A
E18	Down in KO	134.159	0	-infinity	0.03985	0.777551	1700019A02Rik	RIKEN cDNA 1700019A02 gene; known protein coding
E18	Down in KO	134.159	0	-infinity	0.03985	0.777551	Vmn1r53	vomeronasal 1 receptor 53
E18	Down in KO	134.159	0	-infinity	0.03985	0.777551	Hist1h2bg	histone cluster 1; H2bg
E18	Down in KO	134.159	0	-infinity	0.03985	0.777551	Srp54c	signal recognition particle 54C
E18	Down in KO	134.159	0	-infinity	0.03985	0.777551	Gm13432	Pseudogene
E18	Down in KO	134.159	0	-infinity	0.03985	0.777551	Gm9005	pseudogene
E18	Down in KO	134.159	0	-infinity	0.03985	0.777551	G430049J08Rik	known protein coding
E18	Up in KO	3674.3	6286.16	0.774709	0.03985	0.777551	Cacna1h	calcium channel, voltage-dependent, T type, alpha 1H subunit
E18	Down in KO	1559.86	574.493	-1.44106	0.03995	0.777823	Pex5l	peroxisomal biogenesis factor 5-like
E18	Down in KO	1934.85	883.966	-1.13016	0.04	0.777823	Pcdhb13	protocadherin beta 13
E18	Up in KO	14471.6	20074.3	0.472122	0.04025	0.78202	Akap9	A kinase (PRKA) anchor protein (yotiao) 9
E18	Down in KO	2297.23	1130.3	-1.02318	0.0405	0.784876	Gabrg1	gamma-aminobutyric acid (GABA) A receptor; subunit gamma 1

Table A2.2: E18.5 Differentially Expressed Genes (Continued)

Time Point	Direction	WT	KO	log2 (fold change)	p value	q value	Gene Symbol	Gene Name
E18	Up in KO	851731	######	0.371987	0.0405	0.784876	Hbb-b1	hemoglobin, beta adult
E18	Up in KO	3417.35	5445.38	0.672152	0.04055	0.78518	Fbin7	fibulin 7
E18	Up in KO	7507.96	11030.9	0.555056	0.0406	0.785483	Pcbd2	pterin 4 alpha carbinolamine dehydratase/dimerization cofactor of hepatocyte nuclear factor 1 alpha (TCF1) 2
E18	Up in KO	1476.23	2859.28	0.953738	0.0407	0.786506	2700038G22Rik	lincRNA
E18	Up in KO	8528.47	12272.5	0.525069	0.04075	0.786506	Dpf2	D4, zinc and double PHD fingers family 2
E18	Up in KO	3808.71	5968.18	0.647989	0.04085	0.786506	C630043F03Rik	processed transcript
E18	Up in KO	2738.75	4614.51	0.752663	0.0409	0.786506	Zbtb16	zinc finger and BTB domain containing 16
E18	Up in KO	5480.83	8186.64	0.578877	0.0409	0.786506	Itih5	inter-alpha (globulin) inhibitor H5
E18	Down in KO	4163.77	2416.28	-0.7851	0.04095	0.786506	Mm.407159	Transcribed locus: unknown
E18	Down in KO	570857	446374	-0.354877	0.04095	0.786506	Gm10073	known protein coding
E18	Down in KO	266.272	0	-infinity	0.041	0.786506	4932442L08Rik	known protein coding
E18	Up in KO	3420.11	5526.99	0.692452	0.04105	0.786506	Celf3	CUGBP, Elav-like family member 3
E18	Up in KO	2355.84	4038.35	0.777523	0.0411	0.786506	Crispld1	cysteine-rich secretory protein LCCL domain containing 1
E18	Down in KO	16993.8	12052	-0.49574	0.0411	0.786506	Ttc30a1	tetratricopeptide repeat domain 30A1
E18	Up in KO	19847.9	26921.9	0.439791	0.0411	0.786506	Nsfl1c	NSFL1 (p97) cofactor (p47)
E18	Down in KO	35928.6	26879	-0.41865	0.04135	0.789968	Map3k5	mitogen-activated protein kinase kinase kinase 5
E18	Up in KO	8010.12	11557.6	0.528947	0.04145	0.790558	Arhgef5	Rho guanine nucleotide exchange factor (GEF) 5
E18	Up in KO	473.242	1165.84	1.30072	0.0415	0.790852	Crtc1	CREB regulated transcription coactivator 1
E18	Down in KO	6029.41	3761.42	-0.680739	0.04155	0.791145	Stfa3	stefin A3
E18	Down in KO	804.584	253.159	-1.6682	0.0416	0.791438	Gaint3	UDP-N-acetyl-alpha-D-galactosamine:polypeptide N-acetylgalactosaminyltransferase 3
E18	Up in KO	37155	48814.9	0.393767	0.04175	0.793632	Pes1	pescadillo homolog 1, containing BRCT domain
E18	Up in KO	20137	27564.5	0.452966	0.04185	0.793844	Klhl41	kelch-like 41
E18	Up in KO	1008.19	2121.26	1.07316	0.0419	0.793844	Fancb	Fanconi anemia, complementation group B
E18	Up in KO	3320.47	5232.71	0.656172	0.0419	0.793844	Kdm4b	lysine (K)-specific demethylase 4B
E18	Up in KO	11036.8	15448.7	0.485169	0.04205	0.796026	Galnt7	UDP-N-acetyl-alpha-D-galactosamine: polypeptide N-acetylgalactosaminyltransferase 7
E18	Up in KO	279.639	1035.67	1.88892	0.0421	0.796229	A730046J19Rik	lincRNA
E18	Down in KO	62760.8	47999.7	-0.386838	0.04215	0.796229	Fis1	Fisson 1 (mitochondria outer membrane)
E18	Down in KO	1965.8	854.929	-1.20124	0.0423	0.796801	Gm14420	Protein coding
E18	Up in KO	13626.2	18811.6	0.465238	0.0423	0.796801	Atg5g1	ATP synthase, H+ transporting, mitochondrial F0 complex, subunit C1 (subunit 9)
E18	Down in KO	5465.37	3492.19	-0.646189	0.04235	0.797	Zkscan5	Zinc finger with KRAB and SCAN domains 5
E18	Down in KO	72.7401	0	-infinity	0.0424	0.797	RP23-204O17.2	pseudogene
E18	Up in KO	243.983	970.239	1.99156	0.04245	0.797	Wdr78	WD repeat domain 78
E18	Up in KO	9537.83	13465.9	0.497574	0.04245	0.797	Arfgap1	ADP-ribosylation factor GTPase activating protein 1
E18	Up in KO	25928.6	34563.5	0.414706	0.0425	0.797113	Acta2	actin, alpha 2, smooth muscle, aorta
E18	Up in KO	9854.57	14076	0.51437	0.0426	0.797113	Apopt1	apoptogenic, mitochondrial 1
E18	Down in KO	73.8864	0	-infinity	0.04265	0.797113	Pdcd1	programmed cell death 1
E18	Up in KO	46377.8	60793.1	0.390471	0.04265	0.797113	Ddx24	DEAD (Asp-Glu-Ala-Asp) box polypeptide 24
E18	Up in KO	8373.11	12057.9	0.526141	0.0427	0.797113	Epb41l4a	erythrocyte membrane protein band 4.1 like 4a
E18	Up in KO	0	77.9739	infinity	0.0428	0.798328	Gm9903	Protein coding
E18	Down in KO	3540.01	1997.78	-0.825359	0.0431	0.802615	Bbs10	Bardet-Biedl syndrome 10 (human)
E18	Down in KO	5500.26	3475.77	-0.662166	0.0432	0.803822	Mccc2	methylcrotonoyl-Coenzyme A carboxylase 2 (beta)
E18	Up in KO	290.96	1068.42	1.87659	0.04325	0.804098	Gm39469	unknown
E18	Up in KO	5907.07	8709.76	0.56019	0.04345	0.807161	Hus1	Hus1 homolog
E18	Up in KO	450.019	1367.45	1.60343	0.04365	0.808567	Col24a1	collagen, type XXIV, alpha 1
E18	Up in KO	633.129	1749.56	1.46642	0.04365	0.808567	Gm30364	lincRNA
E18	Down in KO	183.393	0	-infinity	0.0438	0.808567	Gpr50	G-protein-coupled receptor 50
E18	Down in KO	512.7	25.374	-4.33669	0.0438	0.808567	Dbp	D site albumin promoter binding protein
E18	Up in KO	561.061	1475.61	1.39508	0.0438	0.808567	Tusc5	tumor suppressor candidate 5
E18	Up in KO	982.457	2079.09	1.08149	0.0438	0.808567	Mrps27	mitochondrial ribosomal protein S27
E18	Up in KO	0	75.3586	infinity	0.04385	0.808567	A230065H16Rik	Known protein coding
E18	Up in KO	0	75.3586	infinity	0.04385	0.808567	Gm1110	Known Protein Coding
E18	Up in KO	0	75.3586	infinity	0.04385	0.808567	Mc4r	melanocortin 4 receptor
E18	Up in KO	3729.02	5777.87	0.631742	0.0439	0.808567	Tmem106a	transmembrane protein 106A
E18	Up in KO	145.48	1446.41	3.31358	0.04395	0.808567	Cdc37l1	cell division cycle 37-like 1
E18	Up in KO	946.589	1791.58	0.920426	0.04395	0.808567	C4a	complement component 4A (Rodgers blood group)
E18	Up in KO	0	25.2836	infinity	0.0441	0.810362	Gm12482	pseudogene
E18	Up in KO	4948.58	7473.37	0.594745	0.0442	0.810362	Klf12	Kruppel-like factor 12
E18	Up in KO	7244.96	10408.8	0.52276	0.04425	0.810362	Ice2	interactor of little elongation complex ELL subunit 2
E18	Up in KO	28672.7	38019.9	0.407078	0.0443	0.810362	Prom1	prominin 1
E18	Down in KO	76.1436	0	-infinity	0.04435	0.810362	Hist1h2aa	histone cluster 1; H2aa
E18	Down in KO	76.1436	0	-infinity	0.04435	0.810362	Gm13988	pseudogene

Table A2.2: E18.5 Differentially Expressed Genes (Continued)

Time Point	Direction	WT	KO	log2 (fold change)	p value	q value	Gene Symbol	Gene Name
E18	Down in KO	76.1436	0	-infinity	0.04435	0.810362	Gm2716	lincRNA
E18	Down in KO	5168.24	3257.34	-0.665978	0.0444	0.810362	Pcdh15	Protocadherin 15
E18	Up in KO	4254.17	6521.66	0.616359	0.0445	0.810362	Ets2	E26 avian leukemia oncogene 2, 3' domain
E18	Up in KO	0	74.5432	infinity	0.0446	0.810362	Gm4950	Known Protein Coding
E18	Up in KO	6676.67	9714.4	0.540996	0.0446	0.810362	Cat	catalase
E18	Down in KO	96985.2	74861.4	-0.373541	0.0446	0.810362	Rpl17-ps7	pseudogene
E18	Up in KO	364.811	1284.73	1.81625	0.04465	0.810362	B3galt1	UDP-Gal:betaGlcNAc beta 1,3-galactosyltransferase, polypeptide 1
E18	Up in KO	688.271	1577.03	1.19616	0.04465	0.810362	Emilin3	elastin microfibril interfacer 3
E18	Up in KO	6191.75	9112.48	0.557495	0.04465	0.810362	Sept8	septin 8
E18	Up in KO	6926.19	10074	0.540509	0.04465	0.810362	Rapgef5	Rap guanine nucleotide exchange factor (GEF) 5
E18	Up in KO	663686	856124	0.36732	0.0447	0.810626	Hspa8	heat shock protein 8
E18	Down in KO	1081.32	173.062	-2.64342	0.04475	0.81089	Gm9534	unknown
E18	Up in KO	23306	31204.1	0.421035	0.0449	0.812964	Sdf4	stromal cell derived factor 4
E18	Up in KO	1846.42	3232.36	0.807861	0.04515	0.815553	Vwc2	von Willebrand factor C domain containing 2
E18	Down in KO	17988.8	13064.9	-0.461402	0.04515	0.815553	Fbxl6	F-box and leucine-rich repeat protein 6
E18	Up in KO	1104.5	2337.69	1.08169	0.04525	0.816714	Gltscr1	glioma tumor suppressor candidate region gene 1
E18	Up in KO	365.957	1020.96	1.48018	0.0453	0.816972	Fut7	fucosyltransferase 7
E18	Up in KO	3694.56	5797.47	0.650021	0.0454	0.817486	Csmp2	cysteine-serine-rich nuclear protein 2
E18	Up in KO	5922.33	8584.46	0.535563	0.0454	0.817486	Clpb	ClpB caseinolytic peptidase B
E18	Up in KO	599.978	1566.95	1.38498	0.04545	0.817742	Gm30103	lincRNA
E18	Up in KO	97.357	651.521	2.74246	0.0457	0.821202	Grp	gastrin releasing peptide
E18	Up in KO	13207.1	18341.7	0.473806	0.04575	0.821202	Neil3	nei like 3
E18	Down in KO	25378	18851.5	-0.428898	0.04575	0.821202	Frmd3	FERM domain containing 3
E18	Up in KO	3435.09	5422.48	0.658603	0.04585	0.821707	Enpp1	ectonucleotide pyrophosphatase/phosphodiesterase 1
E18	Up in KO	6060.84	8868.86	0.549231	0.04585	0.821707	Mtpap	mitochondrial poly(A) polymerase
E18	Up in KO	1674.1	3033.16	0.857438	0.04615	0.825789	Fzd7	frizzled homolog 7
E18	Down in KO	2814.13	1479.69	-0.927393	0.04625	0.826931	Sohlh1	spermatogenesis and oogenesis specific basic helix-loop-helix 1
E18	Up in KO	1540.33	2841.78	0.883555	0.04635	0.828072	Hhatl	hedgehog acyltransferase-like
E18	Up in KO	9629.74	13502.8	0.487689	0.04645	0.82921	Tnfaip8l1	tumor necrosis factor, alpha-induced protein 8-like 1
E18	Down in KO	1459.72	420.499	-1.79552	0.04655	0.82963	Rasl2-9	RAS-like; family 2; locus 9
E18	Down in KO	6684.66	4430.91	-0.593251	0.0466	0.82963	Mm.366962	Transcribed locus: brain; embryonic tissue
E18	Up in KO	23835.5	31857.5	0.418518	0.0466	0.82963	Ptms	parathymosin
E18	Up in KO	2748.18	4508.43	0.71415	0.0467	0.82963	Zfp623	zinc finger protein 623
E18	Up in KO	12026.7	16835.2	0.485241	0.04675	0.82963	Tfap2c	transcription factor AP-2, gamma
E18	Up in KO	0	73.2356	infinity	0.0468	0.82963	Hmga1-rs	High mobility group AT-hook I, related sequence
E18	Up in KO	8460.09	11991.1	0.503215	0.0468	0.82963	Vps72	vacuolar protein sorting 72
E18	Up in KO	101.907	958.509	3.23354	0.04685	0.829873	Dusp27	dual specificity phosphatase 27 (putative)
E18	Up in KO	1562.02	2785.38	0.834463	0.04695	0.831	Kcnab2	potassium voltage-gated channel, shaker-related subfamily, beta member 2
E18	Up in KO	270.822	924.372	1.77113	0.0472	0.83349	Zfp395	zinc finger protein 395
E18	Up in KO	963.395	2046.05	1.08664	0.0472	0.83349	Pcdh9	protocadherin 9
E18	Up in KO	28238.3	37258.8	0.399929	0.0472	0.83349	Fam160b2	family with sequence similarity 160, member B2
E18	Up in KO	374.986	1196.11	1.67344	0.04735	0.834849	Rnf180	Ring finger protein 180
E18	Down in KO	7751.81	5174.78	-0.583036	0.0475	0.836205	Ass1	argininosuccinate synthetase 1
E18	Up in KO	15327.9	20754.9	0.43729	0.0475	0.836205	Atp2b4	ATPase, Ca++ transporting, plasma membrane 4
E18	Down in KO	13750.9	9837.77	-0.483125	0.0476	0.837321	Uap1l1	UDP-N-acteylglucosamine pyrophosphorylase 1-like 1
E18	Up in KO	32882.9	43277.1	0.396266	0.04765	0.837556	Mcam	melanoma cell adhesion molecule
E18	Up in KO	1113.28	2338.67	1.07087	0.04775	0.838025	Mterf1b	mitochondrial transcription termination factor 1b
E18	Up in KO	196125	248305	0.340341	0.04775	0.838025	Mex3a	mex3 homolog A
E18	Up in KO	4218.08	6504.44	0.624838	0.0478	0.83826	Csdc2	cold shock domain containing C2, RNA binding
E18	Down in KO	5902.54	3810.06	-0.631521	0.0481	0.842874	Fcor	Foxo1 corepressor
E18	Up in KO	703.067	1612.61	1.19766	0.04835	0.845312	Vsig10l	V-set and immunoglobulin domain containing 10 like
E18	Up in KO	2903.83	4678.84	0.688192	0.0484	0.845539	Eps15l1	epidermal growth factor receptor pathway substrate 15-like 1
E18	Up in KO	3772.45	5749.89	0.608034	0.0485	0.845803	Mpp3	membrane protein, palmitoylated 3 (MAGUK p55 subfamily member 3)
E18	Down in KO	1573.6	609.446	-1.3685	0.04855	0.845803	Mm.388137	Transcribed locus: embryonic tissue
E18	Down in KO	101.907	0	-infinity	0.0486	0.845803	Tdo2	tryptophan 2;3-dioxygenase
E18	Up in KO	622.338	1243.98	0.999197	0.0486	0.845803	Fcho1	FCH domain only 1
E18	Up in KO	2868.29	4606.55	0.683499	0.0486	0.845803	Col7a1	collagen, type VII, alpha 1
E18	Up in KO	496.96	1299.23	1.38646	0.04865	0.846029	Tbc1d22a	TBC1 domain family, member 22a
E18	Up in KO	14770.5	20088.6	0.443659	0.0488	0.847993	Prkcsh	protein kinase C substrate 80K-H
E18	Up in KO	16344.9	22266.6	0.446042	0.0489	0.849085	Gns	glucosamine (N-acetyl)-6-sulfatase
E18	Up in KO	34225.7	44717.5	0.385758	0.04905	0.850398	Myo9a	myosin IXa
E18	Down in KO	######	######	-0.355682	0.04905	0.850398	Rps28	ribosomal protein S28

Table A2.2: E18.5 Differentially Expressed Genes (Continued)

Time Point	Direction	WT	KO	log2 (fold change)	p value	q value	Gene Symbol	Gene Name
		#	#					
E18	**Down in KO**	2477.99	1305.13	-0.924984	0.04915	0.851487	Ccdc113	coiled-coil domain containing 113
E18	**Up in KO**	22.3598	82.22	1.87858	0.04935	0.854304	4930417H01Rik	processed transcript
E18	**Up in KO**	13164	18025.9	0.453473	0.04965	0.858198	Shisa2	shisa family member 2
E18	**Down in KO**	149.994	0	-infinity	0.04975	0.858629	3110099E03Rik	lincRNA
E18	**Up in KO**	1277.83	2324.91	0.863483	0.04975	0.858629	Acap3	ArfGAP with coiled-coil, ankyrin repeat and PH domains 3
E18	**Down in KO**	70.4829	0	-infinity	0.0499	0.859272	Gm9923	known protein coding
E18	**Down in KO**	70.4829	0	-infinity	0.0499	0.859272	Gm11989	pseudogene
E18	**Down in KO**	70.4829	0	-infinity	0.0499	0.859272	Rpsa-ps4	ribosomal protein S4; pseudogene 4
E18	**Down in KO**	6533.7	4330.72	-0.593292	0.04995	0.85948	Cdyl	chromodomain protein; Y chromosome-like

BIBLIOGRAPHY

1. Hubel, D., *Eye, Brain and Vision*. 1988, NY: Scientific American Library.
2. Baye, L. and B. Link, *Interkinetic nuclear migration and the selection of neurogenic cell divisions during vertebrate retinogenesis.* The Journal of neuroscience : the official journal of the Society for Neuroscience, 2007. **27**(38): p. 10143-10152.
3. Hatakeyama, J. and R. Kageyama, *Retinal cell fate determination and bHLH factors.* Seminars in Cell & Developmental Biology, 2004. **15**(1): p. 83-89.
4. Livesey, F.J. and C.L. Cepko, *Vertebrate neural cell-fate determination: lessons from the retina.* Nat Rev Neurosci, 2001. **2**(2): p. 109-18.
5. Nathans, J., D. Thomas, and D.S. Hogness, *Molecular genetics of human color vision: the genes encoding blue, green, and red pigments.* Science, 1986. **232**(4747): p. 193-202.
6. Lamb, T.D. and E.N. Pugh, *Phototransduction, Dark Adaptation, and Rhodopsin Regeneration The Proctor Lecture.* Investigative Ophthalmology & Visual Science, 2006. **47**(12): p. 5138-5152.
7. Roesch, K., et al., *The transcriptome of retinal Müller glial cells.* The Journal of comparative neurology, 2008. **509**(2): p. 225-238.
8. Vecino, E., et al., *Glia-neuron interactions in the mammalian retina.* Prog Retin Eye Res, 2015.
9. MacDonald, R.B., et al., *Muller glia provide essential tensile strength to the developing retina.* J Cell Biol, 2015. **210**(7): p. 1075-83.
10. MacNeil, M.A. and R.H. Masland, *Extreme diversity among amacrine cells: implications for function.* Neuron, 1998. **20**(5): p. 971-82.
11. Wässle, H., et al., *Glycinergic transmission in the mammalian retina.* Frontiers in Molecular Neuroscience, 2009. **2**.
12. Dacey, D.M., *Primate retina: cell types, circuits and color opponency.* Progress in Retinal and Eye Research, 1999. **18**(6): p. 737-763.
13. Kolb, H., K.A. Linberg, and S.K. Fisher, *Neurons of the human retina: a Golgi study.* J Comp Neurol, 1992. **318**(2): p. 147-87.
14. Sernagor, E., S.J. Eglen, and R.O.L. Wong, *Development of Retinal Ganglion Cell Structure and Function.* Progress in Retinal and Eye Research, 2001. **20**(2): p. 139-174.
15. Agathocleous, M. and W.A. Harris, *From progenitors to differentiated cells in the vertebrate retina.* Annual review of cell and developmental biology, 2009. **25**: p. 45-69.
16. Cepko, C.L., et al., *Cell fate determination in the vertebrate retina.* Proceedings of the National Academy of Sciences, 1996. **93**(2): p. 589-595.
17. Heavner, W. and L. Pevny, *Eye Development and Retinogenesis.* Cold Spring Harbor Perspectives in Biology, 2012. **4**(12).
18. Stenkamp, D.L., *Neurogenesis in the Fish Retina*, in *International Review of Cytology*, W.J. Kwang, Editor. 2007, Academic Press. p. 173-224.
19. Ohsawa, R. and R. Kageyama, *Regulation of retinal cell fate specification by multiple transcription factors.* Brain Research, 2008. **1192**: p. 90-98.
20. Giacinti, C. and A. Giordano, *RB and cell cycle progression.* Oncogene, 2006. **25**(38): p. 5220-7.
21. Dyer, M.A. and C.L. Cepko, *Regulating proliferation during retinal development.* Nat Rev Neurosci, 2001. **2**(5): p. 333-42.
22. Zaghloul, N.A., B. Yan, and S.A. Moody, *Step-wise specification of retinal stem cells during normal embryogenesis.* Biol. Cell, 2005. **97**(5): p. 321-337.

23. Brown, N., et al., *Math5 is required for retinal ganglion cell and optic nerve formation.* Development (Cambridge, England), 2001. **128**(13): p. 2497-2508.
24. Wang, S.W., et al., *Brn3b/Brn3c double knockout mice reveal an unsuspected role for Brn3c in retinal ganglion cell axon outgrowth.* Development, 2002. **129**(2): p. 467-77.
25. Li, S., et al., *Foxn4 controls the genesis of amacrine and horizontal cells by retinal progenitors.* Neuron, 2004. **43**(6): p. 795-807.
26. Inoue, T., et al., *Math3 and NeuroD regulate amacrine cell fate specification in the retina.* Development, 2002. **129**(4): p. 831-42.
27. Hatakeyama, J., et al., *Roles of homeobox and bHLH genes in specification of a retinal cell type.* Development, 2001. **128**(8): p. 1313-22.
28. Huang, L., et al., *Bhlhb5 is required for the subtype development of retinal amacrine and bipolar cells in mice.* Dev Dyn, 2014. **243**(2): p. 279-89.
29. Dyer, M.A., et al., *Prox1 function controls progenitor cell proliferation and horizontal cell genesis in the mammalian retina.* Nat Genet, 2003. **34**(1): p. 53-8.
30. Ohsawa, R. and R. Kageyama, *Regulation of retinal cell fate specification by multiple transcription factors.* Brain Research, 2008. **1192**(0): p. 90-98.
31. Tomita, K., et al., *Mammalian achaete-scute and atonal homologs regulate neuronal versus glial fate determination in the central nervous system.* EMBO J, 2000. **19**(20): p. 5460-72.
32. Swaroop, A., D. Kim, and D. Forrest, *Transcriptional regulation of photoreceptor development and homeostasis in the mammalian retina.* Nat Rev Neurosci, 2010. **11**(8): p. 563-576.
33. Jia, L., et al., *Retinoid-related orphan nuclear receptor RORbeta is an early-acting factor in rod photoreceptor development.* Proc Natl Acad Sci U S A, 2009. **106**(41): p. 17534-9.
34. Mears, A.J., et al., *Nrl is required for rod photoreceptor development.* Nat Genet, 2001. **29**(4): p. 447-52.
35. Yoshida, S., et al., *Expression profiling of the developing and mature Nrl-/- mouse retina: identification of retinal disease candidates and transcriptional regulatory targets of Nrl.* Hum Mol Genet, 2004. **13**(14): p. 1487-503.
36. Mitton, K.P., et al., *The leucine zipper of NRL interacts with the CRX homeodomain. A possible mechanism of transcriptional synergy in rhodopsin regulation.* J Biol Chem, 2000. **275**(38): p. 29794-9.
37. Roberts, M.R., et al., *Retinoid X receptor (gamma) is necessary to establish the S-opsin gradient in cone photoreceptors of the developing mouse retina.* Invest Ophthalmol Vis Sci, 2005. **46**(8): p. 2897-904.
38. Nathans, J., *The evolution and physiology of human color vision: insights from molecular genetic studies of visual pigments.* Neuron, 1999. **24**(2): p. 299-312.
39. Moosajee, M., *Genes and the eye.* Journal of the Royal Society of Medicine, 2005. **98**(5): p. 206-207.
40. Sohocki, M.M., et al., *Prevalence of Mutations Causing Retinitis Pigmentosa and Other Inherited Retinopathies.* Human mutation, 2001. **17**(1): p. 42-51.
41. Hamel, C., *Retinitis pigmentosa.* Orphanet J Rare Dis, 2006. **1**: p. 40.
42. Shintani, K., D.L. Shechtman, and A.S. Gurwood, *Review and update: Current treatment trends for patients with retinitis pigmentosa.* Optometry - Journal of the American Optometric Association, 2009. **80**(7): p. 384-401.
43. Hartong, D.T., E.L. Berson, and T.P. Dryja, *Retinitis pigmentosa.* Lancet, 2006. **368**(9549): p. 1795-1809.
44. Hamel, C.P., *Cone rod dystrophies.* Orphanet Journal of Rare Diseases, 2007. **2**: p. 7-7.

45. Daiger, S.P. *RenNet: Genes and Mapped Loci Causing Retinal Diseases*. 1996-2015 31 July 2015 [cited 2015 3 August]; Available from: http://www.sph.uth.tmc.edu/RetNet/.
46. Peachey, N.S., et al., *GPR179 is required for depolarizing bipolar cell function and is mutated in autosomal-recessive complete congenital stationary night blindness.* Am J Hum Genet, 2012. **90**(2): p. 331-9.
47. Li, Z., et al., *Recessive mutations of the gene TRPM1 abrogate ON bipolar cell function and cause complete congenital stationary night blindness in humans.* Am J Hum Genet, 2009. **85**(5): p. 711-9.
48. Dryja, T.P., et al., *Night blindness and abnormal cone electroretinogram ON responses in patients with mutations in the GRM6 gene encoding mGluR6.* Proc Natl Acad Sci U S A, 2005. **102**(13): p. 4884-9.
49. Wutz, K., et al., *Thirty distinct CACNA1F mutations in 33 families with incomplete type of XLCSNB and Cacna1f expression profiling in mouse retina.* Eur J Hum Genet, 2002. **10**(8): p. 449-56.
50. Pearring, J.N., et al., *A role for nyctalopin, a small leucine rich repeat protein, in localizing the TRPM1 channel to retinal depolarizing bipolar cell dendrites.* The Journal of neuroscience : the official journal of the Society for Neuroscience, 2011. **31**(27): p. 10060-10066.
51. Gal, A., et al., *Heterozygous missense mutation in the rod cGMP phosphodiesterase beta-subunit gene in autosomal dominant stationary night blindness.* Nat Genet, 1994. **7**(1): p. 64-8.
52. McLaughlin, M.E., et al., *Recessive mutations in the gene encoding the beta-subunit of rod phosphodiesterase in patients with retinitis pigmentosa.* Nat Genet, 1993. **4**(2): p. 130-4.
53. Eblimit, A., et al., *Spata7 is a retinal ciliopathy gene critical for correct RPGRIP1 localization and protein trafficking in the retina.* Hum Mol Genet, 2015. **24**(6): p. 1584-601.
54. Cremers, F.P., J.A. van den Hurk, and A.I. den Hollander, *Molecular genetics of Leber congenital amaurosis.* Hum Mol Genet, 2002. **11**(10): p. 1169-76.
55. Sohocki, M.M., et al., *A Range of Clinical Phenotypes Associated with Mutations in CRX, a Photoreceptor Transcription-Factor Gene.* The American Journal of Human Genetics, 1998. **63**(5): p. 1307-1315.
56. Swaroop, A., et al., *Leber congenital amaurosis caused by a homozygous mutation (R90W) in the homeodomain of the retinal transcription factor CRX: direct evidence for the involvement of CRX in the development of photoreceptor function.* Hum Mol Genet, 1999. **8**(2): p. 299-305.
57. Swain, P.K., et al., *Mutations in the cone-rod homeobox gene are associated with the cone-rod dystrophy photoreceptor degeneration.* Neuron, 1997. **19**(6): p. 1329-36.
58. Spear, P.D., *Neural bases of visual deficits during aging.* Vision Research, 1993. **33**(18): p. 2589-2609.
59. Barber, A.J., et al., *Neural apoptosis in the retina during experimental and human diabetes. Early onset and effect of insulin.* Journal of Clinical Investigation, 1998. **102**(4): p. 783-791.
60. Hitchcock, P.F. and P.A. Raymond, *The Teleost Retina as a Model for Developmental and Regeneration Biology.* Zebrafish, 2004. **1**(3): p. 257-271.
61. Morris, A.C., *The Genetics of Ocular Disorders: Insights from the Zebrafish.* Birth Defects Research C Embryo Today, 2011. **in press**.

62. Kimmel, C.B., et al., *Stages of embryonic development of the zebrafish.* Developmental Dynamics, 1995. **203**(3): p. 253-310.
63. Hill, M.A. ***Embryology*** *Mouse Development*. 2015 August 6, 2015]; Available from: https://embryology.med.unsw.edu.au/embryology/index.php/Mouse_Development
64. O'Rahilly, R., *Early human development and the chief sources of information on staged human embryos.* Eur J Obstet Gynecol Reprod Biol, 1979. **9**(4): p. 273-80.
65. Parichy, D.M., et al., *Normal table of postembryonic zebrafish development: Staging by externally visible anatomy of the living fish.* Developmental Dynamics, 2009. **238**(12): p. 2975-3015.
66. Koster, R.W. and S.E. Fraser, *Tracing transgene expression in living zebrafish embryos.* Dev Biol, 2001. **233**(2): p. 329-46.
67. Brockerhoff, S. and J. Fadool, *Genetics of photoreceptor degeneration and regeneration in zebrafish.* Cellular and Molecular Life Sciences, 2011. **68**(4): p. 651-659.
68. Fadool, J.M. and J.E. Dowling, *Zebrafish: A model system for the study of eye genetics.* Progress in Retinal and Eye Research, 2008. **27**(1): p. 89-110.
69. Morris, A.C., T. Scholz, and J.M. Fadool, *Rod Progenitor Cells in the Mature Zebrafish Retina Recent Advances in Retinal Degeneration*, R.E. Anderson, M.M. LaVail, and J.G. Hollyfield, Editors. 2008, Springer New York. p. 361-368.
70. Ingham, P.W., *The power of the zebrafish for disease analysis.* Hum Mol Genet, 2009. **18**(R1): p. R107-12.
71. Bill, B., et al., *A primer for morpholino use in zebrafish.* Zebrafish, 2009. **6**(1): p. 69-77.
72. Eisen, J.S. and J.C. Smith, *Controlling morpholino experiments: don't stop making antisense.* Development, 2008. **135**(10): p. 1735-43.
73. Irion, U., J. Krauss, and C. Nusslein-Volhard, *Precise and efficient genome editing in zebrafish using the CRISPR/Cas9 system.* Development, 2014. **141**(24): p. 4827-30.
74. Kleinstiver, B.P., et al., *Engineered CRISPR-Cas9 nucleases with altered PAM specificities.* Nature, 2015. **523**(7561): p. 481-5.
75. Li, J., et al., *Intron targeting-mediated and endogenous gene integrity-maintaining knockin in zebrafish using the CRISPR/Cas9 system.* Cell Res, 2015. **25**(5): p. 634-7.
76. Varshney, G.K., et al., *High-throughput gene targeting and phenotyping in zebrafish using CRISPR/Cas9.* Genome Res, 2015. **25**(7): p. 1030-42.
77. Fadool, J.M., *Development of a rod photoreceptor mosaic revealed in transgenic zebrafish.* Developmental Biology, 2003. **258**(2): p. 277-290.
78. Goto, Y., et al., *A novel human insulinoma-associated cDNA, IA-1, encodes a protein with "zinc-finger" DNA-binding motifs.* The Journal of biological chemistry, 1992. **267**(21): p. 15252-15257.
79. Breslin, M.B., et al., *Neuroendocrine differentiation factor, IA-1, is a transcriptional repressor and contains a specific DNA-binding domain: identification of consensus IA-1 binding sequence.* Nucleic Acids Research, 2002. **30**(4): p. 1038-1045.
80. Xie, J., et al., *The Zinc-Finger Transcription Factor INSM1 Is Expressed during Embryo Development and Interacts with the Cbl-Associated Protein.* Genomics, 2002. **80**(1): p. 54-61.
81. Lan, M.S. and M.B. Breslin, *Structure, expression, and biological function of INSM1 transcription factor in neuroendocrine differentiation.* The FASEB Journal, 2009. **23**(7): p. 2024-2033.
82. de Caestecker, M.P., et al., *The Smad4 activation domain (SAD) is a proline-rich, p300-dependent transcriptional activation domain.* J Biol Chem, 2000. **275**(3): p. 2115-22.

83. Zilfou, J.T., et al., *The corepressor mSin3a interacts with the proline-rich domain of p53 and protects p53 from proteasome-mediated degradation.* Mol Cell Biol, 2001. **21**(12): p. 3974-85.
84. Tatemoto, K. and V. Mutt, *Chemical determination of polypeptide hormones.* Proc Natl Acad Sci U S A, 1978. **75**(9): p. 4115-9.
85. Wang, H.-W., et al., *Identification of an INSM1-binding site in the insulin promoter: negative regulation of the insulin gene transcription.* Journal of Endocrinology, 2008. **198**(1): p. 29-39.
86. Candal, E., et al., *Ol-insm1b, a SNAG family transcription factor involved in cell cycle arrest during medaka development.* Developmental biology, 2007. **309**(1): p. 1-17.
87. Lukowski, C.M., R.G. Ritzel, and A.J. Waskiewicz, *Expression of two insm1-like genes in the developing zebrafish nervous system.* Gene Expression Patterns, 2006. **6**(7): p. 711-718.
88. Forbes-Osborne, M.A., S.G. Wilson, and A.C. Morris, *Insulinoma-associated 1a (Insm1a) is required for photoreceptor differentiation in the zebrafish retina.* Developmental Biology, 2013. **380**(2): p. 157-171.
89. Duggan, A., et al., *Transient expression of the conserved zinc finger gene INSM1 in progenitors and nascent neurons throughout embryonic and adult neurogenesis.* The Journal of comparative neurology, 2008. **507**(4): p. 1497-1520.
90. Desai, C. and H.R. Horvitz, *Caenorhabditis elegans mutants defective in the functioning of the motor neurons responsible for egg laying.* Genetics, 1989. **121**(4): p. 703-21.
91. Stivers, C., et al., *Nerfin-1 and -2, novel Drosophila Zn-finger transcription factor genes expressed in the developing nervous system.* Mech Dev, 2000. **97**(1-2): p. 205-10.
92. Kuzin, A., et al., *Nerfin-1 is required for early axon guidance decisions in the developing Drosophila CNS.* Dev Biol, 2005. **277**(2): p. 347-65.
93. Kuzin, A., et al., *The Drosophila nerfin-1 mRNA requires multiple microRNAs to regulate its spatial and temporal translation dynamics in the developing nervous system.* Dev Biol, 2007. **310**(1): p. 35-43.
94. Morris, A.C., et al., *Microarray Analysis of XOPS-mCFP Zebrafish Retina Identifies Genes Associated with Rod Photoreceptor Degeneration and Regeneration.* Investigative Ophthalmology & Visual Science, 2011. **52**(5): p. 2255-2266.
95. Ramachandran, R., X.-F. Zhao, and D. Goldman, *Insm1a-mediated gene repression is essential for the formation and differentiation of Müller glia-derived progenitors in the injured retina.* Nature cell biology, 2012.
96. Mellitzer, G., et al., *IA1 is NGN3-dependent and essential for differentiation of the endocrine pancreas.* The EMBO journal, 2006. **25**(6): p. 1344-1352.
97. Farkas, L.M., et al., *Insulinoma-Associated 1 Has a Panneurogenic Role and Promotes the Generation and Expansion of Basal Progenitors in the Developing Mouse Neocortex.* Neuron, 2008. **60**(1): p. 40-55.
98. Gierl, M., et al., *The zinc-finger factor Insm1 (IA-1) is essential for the development of pancreatic beta cells and intestinal endocrine cells.* Genes & development, 2006. **20**(17): p. 2465-2478.
99. Jacob, J., et al., *Insm1 (IA-1) is an essential component of the regulatory network that specifies monoaminergic neuronal phenotypes in the vertebrate hindbrain.* Development (Cambridge, England), 2009. **136**(14): p. 2477-2485.
100. Rosenbaum, J., A. Duggan, and J. Garcia-Anoveros, *Insm1 promotes the transition of olfactory progenitors from apical and proliferative to basal, terminally dividing and neuronogenic.* Neural Development, 2011. **6**(1): p. 6.

101. Wildner, H., et al., *Insm1 (IA-1) is a crucial component of the transcriptional network that controls differentiation of the sympatho-adrenal lineage.* Development, 2008. **135**(3): p. 473-481.
102. Wilson, M.E., D. Scheel, and M.S. German, *Gene expression cascades in pancreatic development.* Mech Dev, 2003. **120**(1): p. 65-80.
103. Murtaugh, L.C. and D.A. Melton, *Genes, signals, and lineages in pancreas development.* Annu Rev Cell Dev Biol, 2003. **19**: p. 71-89.
104. Edlund, H., *Pancreatic organogenesis--developmental mechanisms and implications for therapy.* Nat Rev Genet, 2002. **3**(7): p. 524-32.
105. Gu, G., J.R. Brown, and D.A. Melton, *Direct lineage tracing reveals the ontogeny of pancreatic cell fates during mouse embryogenesis.* Mech Dev, 2003. **120**(1): p. 35-43.
106. Rindi, G., et al., *The "normal" endocrine cell of the gut: changing concepts and new evidences.* Ann N Y Acad Sci, 2004. **1014**: p. 1-12.
107. Gotz, M. and W.B. Huttner, *The cell biology of neurogenesis.* Nat Rev Mol Cell Biol, 2005. **6**(10): p. 777-88.
108. Kriegstein, A.R. and M. Gotz, *Radial glia diversity: a matter of cell fate.* Glia, 2003. **43**(1): p. 37-43.
109. Gal, J.S., et al., *Molecular and morphological heterogeneity of neural precursors in the mouse neocortical proliferative zones.* J Neurosci, 2006. **26**(3): p. 1045-56.
110. Konno, D., et al., *Neuroepithelial progenitors undergo LGN-dependent planar divisions to maintain self-renewability during mammalian neurogenesis.* Nat Cell Biol, 2008. **10**(1): p. 93-101.
111. Haubensak, W., et al., *Neurons arise in the basal neuroepithelium of the early mammalian telencephalon: A major site of neurogenesis.* Proceedings of the National Academy of Sciences of the United States of America, 2004. **101**(9): p. 3196-3201.
112. Smart, I.H., et al., *Unique morphological features of the proliferative zones and postmitotic compartments of the neural epithelium giving rise to striate and extrastriate cortex in the monkey.* Cereb Cortex, 2002. **12**(1): p. 37-53.
113. Rakic, P., *Developmental and evolutionary adaptations of cortical radial glia.* Cereb Cortex, 2003. **13**(6): p. 541-9.
114. Miyata, T., et al., *Asymmetric production of surface-dividing and non-surface-dividing cortical progenitor cells.* Development, 2004. **131**(13): p. 3133-45.
115. Pontious, A., et al., *Role of intermediate progenitor cells in cerebral cortex development.* Dev Neurosci, 2008. **30**(1-3): p. 24-32.
116. Huber, K., *The sympathoadrenal cell lineage: Specification, diversification, and new perspectives.* Developmental Biology, 2006. **298**(2): p. 335-343.
117. Shah, N.M., A.K. Groves, and D.J. Anderson, *Alternative Neural Crest Cell Fates Are Instructively Promoted by TGFβ Superfamily Members.* Cell, 1996. **85**(3): p. 331-343.
118. Anderson, D.J., et al., *Antibody markers identify a common progenitor to sympathetic neurons and chromaffin cells in vivo and reveal the timing of commitment to neuronal differentiation in the sympathoadrenal lineage.* J Neurosci, 1991. **11**(11): p. 3507-19.
119. Howard, M.J., et al., *The transcription factor dHAND is a downstream effector of BMPs in sympathetic neuron specification.* Development, 2000. **127**(18): p. 4073-81.
120. Schneider, C., et al., *Bone morphogenetic proteins are required in vivo for the generation of sympathetic neurons.* Neuron, 1999. **24**(4): p. 861-70.
121. Reissmann, E., et al., *Involvement of bone morphogenetic protein-4 and bone morphogenetic protein-7 in the differentiation of the adrenergic phenotype in developing sympathetic neurons.* Development, 1996. **122**(7): p. 2079-88.

122. Goridis, C. and H. Rohrer, *Specification of catecholaminergic and serotonergic neurons.* Nat Rev Neurosci, 2002. **3**(7): p. 531-41.
123. Murdoch, B. and A.J. Roskams, *Olfactory epithelium progenitors: insights from transgenic mice and in vitro biology.* J Mol Histol, 2007. **38**(6): p. 581-99.
124. Kawauchi, S., et al., *Molecular signals regulating proliferation of stem and progenitor cells in mouse olfactory epithelium.* Dev Neurosci, 2004. **26**(2-4): p. 166-80.
125. Smart, I.H., *Location and orientation of mitotic figures in the developing mouse olfactory epithelium.* J Anat, 1971. **109**(Pt 2): p. 243-51.
126. Breslin, M.B., M. Zhu, and M.S. Lan, *NeuroD1/E47 Regulates the E-box Element of a Novel Zinc Finger Transcription Factor, IA-1, in Developing Nervous System.* Journal of Biological Chemistry, 2003. **278**(40): p. 38991-38997.
127. Liu, W.-D., et al., *INSM1 functions as a transcriptional repressor of the neuroD/β2 gene through the recruitment of cyclin D1 and histone deacetylases.* Biochem J, 2006. **397**(1): p. 169-177.
128. Zhang, M., A. Kimura, and A.R. Saltiel, *Cloning and Characterization of Cbl-associated Protein Splicing Isoforms.* Molecular Medicine, 2003. **9**(1-2): p. 18-25.
129. Baumann, C.A., et al., *CAP defines a second signalling pathway required for insulin-stimulated glucose transport.* Nature, 2000. **407**(6801): p. 202-7.
130. Zhang, T., et al., *Insulinoma-associated antigen-1 zinc-finger transcription factor promotes pancreatic duct cell trans-differentiation.* Endocrinology, 2010. **151**(5): p. 2030-9.
131. Zhang, T., et al., *Functional role of an islet transcription factor, INSM1/IA-1, on pancreatic acinar cell trans-differentiation.* Journal of Cellular Physiology, 2012. **227**(6): p. 2470-2479.
132. Zhang, T., et al., *Zinc Finger Transcription Factor INSM1 Interrupts Cyclin D1 and CDK4 Binding and Induces Cell Cycle Arrest.* Journal of Biological Chemistry, 2009. **284**(9): p. 5574-5581.
133. Zhang, T., et al., *Extra-nuclear activity of INSM1 transcription factor enhances insulin receptor signaling pathway and Nkx6.1 expression through RACK1 interaction.* Cell Signal, 2014. **26**(4): p. 740-7.
134. Turner, D., E. Snyder, and C. Cepko, *Lineage-independent determination of cell type in the embryonic mouse retina.* Neuron, 1990. **4**(6): p. 833-845.
135. Andreazzoli, M., *Molecular regulation of vertebrate retina cell fate.* Birth Defects Research Part C: Embryo Today: Reviews, 2009. **87**(3): p. 284-295.
136. Bilitou, A. and S.-i. Ohnuma, *The role of cell cycle in retinal development: Cyclin-dependent kinase inhibitors co-ordinate cell-cycle inhibition, cell-fate determination and differentiation in the developing retina†.* Developmental Dynamics, 2010. **239**(3): p. 727-736.
137. Wang, H.-W., et al., *Identification of an INSM1-binding site in the insulin promoter: negative regulation of the insulin gene transcription.* The Journal of endocrinology, 2008. **198**(1): p. 29-39.
138. Westerfield, M., *The Zebrafish Book: A Guide for the Laboratory Use of Zebrafish (brachydanio rerio).* 1995, Eugene, OR: University of Oregon Press.
139. Morris, A.C., et al., *Cone Survival Despite Rod Degeneration in XOPS-mCFP Transgenic Zebrafish.* Investigative Ophthalmology & Visual Science, 2005. **46**(12): p. 4762-4771.
140. Kennedy, B.N., et al., *Identification of a Zebrafish Cone Photoreceptor–Specific Promoter and Genetic Rescue of Achromatopsia in the nof Mutant.* Investigative Ophthalmology & Visual Science, 2007. **48**(2): p. 522-529.

141. Schroeter, E.H., R.O.L. Wong, and R.G. Gregg, *In vivo development of retinal ON-bipolar cell axonal terminals visualized in nyx::MYFP transgenic zebrafish.* Visual Neuroscience, 2006. **23**(05): p. 833-843.
142. Bernardos, R.L. and P.A. Raymond, *GFAP transgenic zebrafish.* Gene Expression Patterns, 2006. **6**(8): p. 1007-1013.
143. Bill, B.R., et al., *A primer for morpholino use in zebrafish.* Zebrafish, 2009. **6**(1): p. 69-77.
144. Wilson, J.M., R.M. Bunte, and A.J. Carty, *Evaluation of Rapid Cooling and Tricaine Methanesulfonate (MS222) as Methods of Euthanasia in Zebrafish (Danio rerio).* Journal of the American Association for Laboratory Animal Science, 2009. **48**(6): p. 785-789.
145. Morris, A.C., et al., *Genetic dissection reveals two separate pathways for rod and cone regeneration in the teleost retina.* Developmental Neurobiology, 2008. **68**(5): p. 605-619.
146. Chen, J., A. Rattner, and J. Nathans, *The Rod Photoreceptor-Specific Nuclear Receptor Nr2e3 Represses Transcription of Multiple Cone-Specific Genes.* The Journal of Neuroscience, 2005. **25**(1): p. 118-129.
147. Ochocinska, M.J. and P.F. Hitchcock, *Dynamic expression of the basic helix-loop-helix transcription factor neuroD in the rod and cone photoreceptor lineages in the retina of the embryonic and larval zebrafish.* The Journal of Comparative Neurology, 2007. **501**(1): p. 1-12.
148. Zhang, Y., et al., *The Expression of <italic>irx7</italic> in the Inner Nuclear Layer of Zebrafish Retina Is Essential for a Proper Retinal Development and Lamination.* PLoS ONE, 2012. **7**(4): p. e36145.
149. Stenkamp, D.L. and R.A. Frey, *Extraretinal and retinal hedgehog signaling sequentially regulate retinal differentiation in zebrafish.* Developmental Biology, 2003. **258**(2): p. 349-363.
150. Masai, I., et al., *Midline Signals Regulate Retinal Neurogenesis in Zebrafish.* Neuron, 2000. **27**(2): p. 251-263.
151. Hu, M. and S. Easter, *Retinal neurogenesis: the formation of the initial central patch of postmitotic cells.* Developmental biology, 1999. **207**(2): p. 309-321.
152. Peterson, R.E., et al., *Müller cell differentiation in the zebrafish neural retina: Evidence of distinct early and late stages in cell maturation.* The Journal of Comparative Neurology, 2001. **429**(4): p. 530-540.
153. Scheer, N., et al., *An instructive function for Notch in promoting gliogenesis in the zebrafish retina.* Development, 2001. **128**(7): p. 1099-1107.
154. Bernardos, R.L., et al., *Late-Stage Neuronal Progenitors in the Retina Are Radial Müller Glia That Function as Retinal Stem Cells.* The Journal of Neuroscience, 2007. **27**(26): p. 7028-7040.
155. Qin, Z., L.K. Barthel, and P.A. Raymond, *Genetic evidence for shared mechanisms of epimorphic regeneration in zebrafish.* Proceedings of the National Academy of Sciences, 2009. **106**(23): p. 9310-9315.
156. Quastler, H. and F.G. Sherman, *Cell population kinetics in the intestinal epithelium of the mouse.* Experimental Cell Research, 1959. **17**(3): p. 420-438.
157. Yang, Z., et al., *Math5 determines the competence state of retinal ganglion cell progenitors.* Developmental Biology, 2003. **264**(1): p. 240-254.
158. Kay, J.N., et al., *Retinal Ganglion Cell Genesis Requires lakritz, a Zebrafish atonal Homolog.* Neuron, 2001. **30**(3): p. 725-736.
159. Poggi, L., et al., *Influences on neural lineage and mode of division in the zebrafish retina in vivo.* The Journal of Cell Biology, 2005. **171**(6): p. 991-999.

160. Brzezinski, J., L. Prasov, and T. Glaser, *Math5 defines the ganglion cell competence state in a subpopulation of retinal progenitor cells exiting the cell cycle.* Developmental biology, 2012. **365**(2): p. 395-413.
161. Ma, W., et al., *A role of ath5 in inducing neuroD and the photoreceptor pathway.* The Journal of neuroscience : the official journal of the Society for Neuroscience, 2004. **24**(32): p. 7150-7158.
162. Morrow, E.M., et al., *NeuroD regulates multiple functions in the developing neural retina in rodent.* Development, 1999. **126**(1): p. 23-36.
163. Ochocinska, M.J. and P.F. Hitchcock, *NeuroD regulates proliferation of photoreceptor progenitors in the retina of the zebrafish.* Mechanisms of development, 2009. **126**(3-4): p. 128-141.
164. Liu, Y., et al., *Isolation and Characterization of a Zebrafish Homologue of the Cone Rod Homeobox Gene.* Investigative Ophthalmology & Visual Science, 2001. **42**(2): p. 481-487.
165. Shen, Y.-c. and P.A. Raymond, *Zebrafish cone-rod (crx) homeobox gene promotes retinogenesis.* Developmental Biology, 2004. **269**(1): p. 237-251.
166. Chen, S., et al., *Crx, a novel Otx-like paired-homeodomain protein, binds to and transactivates photoreceptor cell-specific genes.* Neuron, 1997. **19**(5): p. 1017-1030.
167. Furukawa, T., E. Morrow, and C. Cepko, *Crx, a novel otx-like homeobox gene, shows photoreceptor-specific expression and regulates photoreceptor differentiation.* Cell, 1997. **91**(4): p. 531-541.
168. Furukawa, T., et al., *Retinopathy and attenuated circadian entrainment in Crx-deficient mice.* Nature genetics, 1999. **23**(4): p. 466-470.
169. Blackshaw, S., et al., *Comprehensive analysis of photoreceptor gene expression and the identification of candidate retinal disease genes.* Cell, 2001. **107**(5): p. 579-589.
170. Livesey, F., et al., *Microarray analysis of the transcriptional network controlled by the photoreceptor homeobox gene Crx.* Current biology : CB, 2000. **10**(6): p. 301-310.
171. Alvarez-Delfin, K., et al., *Tbx2b is required for ultraviolet photoreceptor cell specification during zebrafish retinal development.* Proceedings of the National Academy of Sciences, 2009. **106**(6): p. 2023-2028.
172. Cheng, H., et al., *Photoreceptor-specific nuclear receptor NR2E3 functions as a transcriptional activator in rod photoreceptors.* Human Molecular Genetics, 2004. **13**(15): p. 1563-1575.
173. Akhmedov, N., et al., *A deletion in a photoreceptor-specific nuclear receptor mRNA causes retinal degeneration in the rd7 mouse.* Proceedings of the National Academy of Sciences of the United States of America, 2000. **97**(10): p. 5551-5556.
174. Nelson, S.M., et al., *The developmental sequence of gene expression within the rod photoreceptor lineage in embryonic zebrafish.* Developmental Dynamics, 2008. **237**(10): p. 2903-2917.
175. Bernardos, R.L., et al., *Notch–Delta signaling is required for spatial patterning and Müller glia differentiation in the zebrafish retina.* Developmental Biology, 2005. **278**(2): p. 381-395.
176. Richard, I.D., H.R. David, and A.H. William, *Xotch inhibits cell differentiation in the xenopus retina.* Neuron, 1995. **14**.
177. Nelson, B., et al., *Transient inactivation of Notch signaling synchronizes differentiation of neural progenitor cells.* Developmental biology, 2007. **304**(2): p. 479-498.
178. Clark, B., et al., *Loss of Llgl1 in retinal neuroepithelia reveals links between apical domain size, Notch activity and neurogenesis.* Development (Cambridge, England), 2012. **139**(9): p. 1599-1610.

179. Yeo, S.-Y., et al., *Fluorescent protein expression driven by her4 regulatory elements reveals the spatiotemporal pattern of Notch signaling in the nervous system of zebrafish embryos.* Developmental biology, 2007. **301**(2): p. 555-567.
180. Johnson, D., S. Donovan, and M. Dyer, *Mosaic deletion of Rb arrests rod differentiation and stimulates ectopic synaptogenesis in the mouse retina.* The Journal of comparative neurology, 2006. **498**(1): p. 112-128.
181. Kay, J.N., B.A. Link, and H. Baier, *Staggered cell-intrinsic timing of ath5 expression underlies the wave of ganglion cell neurogenesis in the zebrafish retina.* Development, 2005. **132**(11): p. 2573-2585.
182. Zhang, J., et al., *Rb regulates proliferation and rod photoreceptor development in the mouse retina.* Nature genetics, 2004. **36**(4): p. 351-360.
183. Kettleborough, R.N.W., et al., *A systematic genome-wide analysis of zebrafish protein-coding gene function.* Nature, 2013. **496**(7446): p. 494-497.
184. Rossi, A., et al., *Genetic compensation induced by deleterious mutations but not gene knockdowns.* Nature, 2015. **524**(7564): p. 230-233.
185. Kok, F.O., et al., *Reverse Genetic Screening Reveals Poor Correlation between Morpholino-Induced and Mutant Phenotypes in Zebrafish.* Developmental Cell, 2015. **32**(1): p. 97-108.
186. Pillai-Kastoori, L., et al., *Sox11 Is Required to Maintain Proper Levels of Hedgehog Signaling during Vertebrate Ocular Morphogenesis.* PLoS Genet, 2014. **10**(7): p. e1004491.
187. Malicki, J., et al., *Analysis of gene function in the zebrafish retina.* Methods, 2002. **28**(4): p. 427-438.
188. Costa, V., et al., *Uncovering the complexity of transcriptomes with RNA-Seq.* J Biomed Biotechnol, 2010. **2010**: p. 853916.
189. Rosenbaum, J.N., A. Duggan, and J. García-Añoveros, *Insm1 promotes the transition of olfactory progenitors from apical and proliferative to basal, terminally dividing and neuronogenic.* Neural development, 2011. **6**: p. 6.
190. Mu, X., et al., *Gene expression in the developing mouse retina by EST sequencing and microarray analysis.* Nucleic Acids Research, 2001. **29**(24): p. 4983-4993.
191. Marquardt, T. and P. Gruss, *Generating neuronal diversity in the retina: one for nearly all.* Trends in Neurosciences, 2002. **25**(1): p. 32-38.
192. Goecks, J., A. Nekrutenko, and J. Taylor, *Galaxy: a comprehensive approach for supporting accessible, reproducible, and transparent computational research in the life sciences.* Genome Biol, 2010. **11**(8): p. R86.
193. Blankenberg, D., et al., *Galaxy: A Web-Based Genome Analysis Tool for Experimentalists*, in *Current Protocols in Molecular Biology*. 2001, John Wiley & Sons, Inc.
194. Giardine, B., et al., *Galaxy: a platform for interactive large-scale genome analysis.* Genome Res, 2005. **15**(10): p. 1451-5.
195. Andrews, S., *FastQC: a quality control tool for high throughput sequence data.* 2010.
196. Blankenberg, D., et al., *Manipulation of FASTQ data with Galaxy.* (1367-4811 (Electronic)).
197. Trapnell, C., et al., *Transcript assembly and quantification by RNA-Seq reveals unannotated transcripts and isoform switching during cell differentiation.* Nat Biotechnol, 2010. **28**(5): p. 511-5.
198. Huang da, W., B.T. Sherman, and R.A. Lempicki, *Systematic and integrative analysis of large gene lists using DAVID bioinformatics resources.* Nat Protoc, 2009. **4**(1): p. 44-57.

199. Su, A.I., et al., *A gene atlas of the mouse and human protein-encoding transcriptomes.* Proc Natl Acad Sci U S A, 2004. **101**(16): p. 6062-7.
200. Su, A.I., et al., *Large-scale analysis of the human and mouse transcriptomes.* Proc Natl Acad Sci U S A, 2002. **99**(7): p. 4465-70.
201. Wu, C., et al., *BioGPS: an extensible and customizable portal for querying and organizing gene annotation resources.* Genome Biology, 2009. **10**(11): p. R130.
202. Chen, E.Y., et al., *Enrichr: interactive and collaborative HTML5 gene list enrichment analysis tool.* BMC Bioinformatics, 2013. **14**: p. 128.
203. Rubin, S.M., *Deciphering the Rb phosphorylation code.* Trends in biochemical sciences, 2013. **38**(1): p. 12-19.
204. Szklarczyk, D., et al., *STRING v10: protein-protein interaction networks, integrated over the tree of life.* Nucleic Acids Res, 2015. **43**(Database issue): p. 28.
205. Swaroop, A., D. Kim, and D. Forrest, *Transcriptional regulation of photoreceptor development and homeostasis in the mammalian retina.* Nature reviews. Neuroscience, 2010. **11**(8): p. 563-576.
206. Marshall, J. and J. Heckenlively, *Retinitis pigmentosa.* 1988, Philadelphia: J.B.

Lippincott Co.
207. Wong, F., *How shall research in the treatment of retinitis pigmentosa proceed?* Archives of Ophthalmology, 1993. **111**(6): p. 754-756.
208. Sowka, J.W., *Shedding Light on a Pale Optic Nerve.* Review of Optometry, 2011(November 2011).
209. Rivolta, C., et al., *Retinitis pigmentosa and allied diseases: numerous diseases, genes, and inheritance patterns.* Human Molecular Genetics, 2002. **11**(10): p. 1219-1227.
210. Zelinger, L., et al., *A missense mutation in DHDDS, encoding dehydrodolichyl diphosphate synthase, is associated with autosomal-recessive retinitis pigmentosa in Ashkenazi Jews.* Am J Hum Genet, 2011. **88**(2): p. 207-15.
211. Bleeker-Wagemakers, L.M., et al., *Evidence for nonallelic genetic heterogeneity in autosomal recessive retinitis pigmentosa.* Genomics, 1992. **14**(3): p. 811-2.
212. Leutelt, J., et al., *Autosomal recessive retinitis pigmentosa locus maps on chromosome 1q in a large consanguineous family from Pakistan.* Clin Genet, 1995. **47**(3): p. 122-4.
213. Berson, E.L., *Retinitis pigmentosa. The Friedenwald Lecture.* Invest Ophthalmol Vis Sci, 1993. **34**(5): p. 1659-76.
214. John, S.K., et al., *Loss of cone molecular markers in rhodopsin-mutant human retinas with retinitis pigmentosa.* Mol Vis, 2000. **6**: p. 204-15.
215. Sibulesky, L., et al., *Safety of <7500 RE (<25000 IU) vitamin A daily in adults with retinitis pigmentosa.* Am J Clin Nutr, 1999. **69**(4): p. 656-63.
216. Berson, E.L., et al., *A randomized trial of vitamin A and vitamin E supplementation for retinitis pigmentosa.* Arch Ophthalmol, 1993. **111**(6): p. 761-72.
217. Chatzinoff, A., et al., *Eleven-cis vitamin a in the treatment of retinitis pigmentosa: A negative study.* Archives of Ophthalmology, 1968. **80**(4): p. 417-419.
218. Berson, E.L., et al., *Clinical trial of docosahexaenoic acid in patients with retinitis pigmentosa receiving vitamin A treatment.* Arch Ophthalmol, 2004. **122**(9): p. 1297-305.
219. Bahrami, H., M. Melia, and G. Dagnelie, *Lutein supplementation in retinitis pigmentosa: PC-based vision assessment in a randomized double-masked placebo-controlled clinical trial [NCT00029289].* BMC Ophthalmol, 2006. **6**: p. 23.
220. Berson, E.L., et al., *Clinical Trial of Lutein in Patients with Retinitis Pigmentosa Receiving Vitamin A.* Archives of ophthalmology, 2010. **128**(4): p. 403-411.

221. Hoffman, D.R., et al., *Four-year placebo-controlled trial of docosahexaenoic acid in X-linked retinitis pigmentosa (DHAX trial): a randomized clinical trial.* JAMA Ophthalmol, 2014. **132**(7): p. 866-73.
222. Hoffman, D.R., et al., *A randomized, placebo-controlled clinical trial of docosahexaenoic acid supplementation for X-linked retinitis pigmentosa.* Am J Ophthalmol, 2004. **137**(4): p. 704-18.
223. Hughbanks-Wheaton, D.K., et al., *Safety assessment of docosahexaenoic acid in X-linked retinitis pigmentosa: the 4-year DHAX trial.* Invest Ophthalmol Vis Sci, 2014. **55**(8): p. 4958-66.
224. Wheaton, D.H., et al., *Biological safety assessment of docosahexaenoic acid supplementation in a randomized clinical trial for X-linked retinitis pigmentosa.* Arch Ophthalmol, 2003. **121**(9): p. 1269-78.
225. Birch, D.G., et al., *Randomized Trial of Ciliary Neurotrophic Factor Delivered by Encapsulated Cell Intraocular Implants for Retinitis Pigmentosa.* American journal of ophthalmology, 2013. **156**(2): p. 283-292.e1.
226. Nakazawa, M., et al., *Effect of nilvadipine on central visual field in retinitis pigmentosa: a 30-month clinical trial.* Ophthalmologica, 2011. **225**(2): p. 120-6.
227. Nakazawa, M., et al., *Long-Term Effects of Nilvadipine against Progression of the Central Visual Field Defect in Retinitis Pigmentosa: An Extended Study.* BioMed Research International, 2013. **2013**: p. 6.
228. Kumar, A., et al., *Efficacy of oral valproic acid in patients with retinitis pigmentosa.* J Ocul Pharmacol Ther, 2014. **30**(7): p. 580-6.
229. Hacein-Bey-Abina, S., et al., *LMO2-associated clonal T cell proliferation in two patients after gene therapy for SCID-X1.* Science, 2003. **302**(5644): p. 415-9.
230. Dave, U.P., N.A. Jenkins, and N.G. Copeland, *Gene therapy insertional mutagenesis insights.* Science, 2004. **303**(5656): p. 333.
231. Gore, M.E., *Adverse effects of gene therapy: Gene therapy can cause leukaemia: no shock, mild horror but a probe.* Gene Ther, 0000. **10**(1): p. 4-4.
232. Nori, S., et al., *Long-term safety issues of iPSC-based cell therapy in a spinal cord injury model: oncogenic transformation with epithelial-mesenchymal transition.* Stem Cell Reports, 2015. **4**(3): p. 360-73.
233. Kawamata, S., et al., *Design of a Tumorigenicity Test for Induced Pluripotent Stem Cell (iPSC)-Derived Cell Products.* J Clin Med, 2015. **4**(1): p. 159-71.
234. Santos, A., et al., *Preservation of the inner retina in retinitis pigmentosa. A morphometric analysis.* Arch Ophthalmol, 1997. **115**(4): p. 511-5.
235. Campbell, L.J., J.J. Willoughby, and A.M. Jensen, *Two types of Tet-On transgenic lines for doxycycline-inducible gene expression in zebrafish rod photoreceptors and a gateway-based tet-on toolkit.* PloS one, 2012. **7**(12).
236. Illing, M.E., et al., *A Rhodopsin Mutant Linked to Autosomal Dominant Retinitis Pigmentosa Is Prone to Aggregate and Interacts with the Ubiquitin Proteasome System.* Journal of Biological Chemistry, 2002. **277**(37): p. 34150-34160.
237. Dryja, T.P., et al., *A point mutation of the rhodopsin gene in one form of retinitis pigmentosa.* Nature, 1990. **343**(6256): p. 364-366.
238. Berson, E.L., et al., *Ocular findings in patients with autosomal dominant retinitis pigmentosa and a rhodopsin gene defect (Pro-23-His).* Arch Ophthalmol, 1991. **109**(1): p. 92-101.

239. Rajan, R.S. and R.R. Kopito, *Suppression of wild-type rhodopsin maturation by mutants linked to autosomal dominant retinitis pigmentosa.* J Biol Chem, 2005. **280**(2): p. 1284-91.
240. Heckenlively, J.R., J.A. Rodriguez, and S.P. Daiger, *Autosomal dominant sectoral retinitis pigmentosa. Two families with transversion mutation in codon 23 of rhodopsin.* Arch Ophthalmol, 1991. **109**(1): p. 84-91.
241. Farrar, G.J., et al., *Autosomal dominant retinitis pigmentosa: absence of the rhodopsin proline----histidine substitution (codon 23) in pedigrees from Europe.* Am J Hum Genet, 1990. **47**(6): p. 941-5.
242. Fishman, G.A., et al., *Ocular findings associated with a rhodopsin gene codon 58 transversion mutation in autosomal dominant retinitis pigmentosa.* Arch Ophthalmol, 1991. **109**(10): p. 1387-93.
243. Jacobson, S.G., et al., *Retinal function and rhodopsin levels in autosomal dominant retinitis pigmentosa with rhodopsin mutations.* Am J Ophthalmol, 1991. **112**(3): p. 256-71.
244. Inglehearn, C., et al., *Evidence against a second autosomal dominant retinitis pigmentosa locus close to rhodopsin on chromosome 3q.* Am J Hum Genet, 1993. **53**(2): p. 536-7.
245. Andreasson, S., et al., *A six-generation family with autosomal dominant retinitis pigmentosa and a rhodopsin gene mutation (arginine-135-leucine).* Ophthalmic Paediatr Genet, 1992. **13**(3): p. 145-53.
246. Chuang, J.Z., et al., *Structural and functional impairment of endocytic pathways by retinitis pigmentosa mutant rhodopsin-arrestin complexes.* J Clin Invest, 2004. **114**(1): p. 131-40.
247. Ponjavic, V., et al., *Autosomal dominant retinitis pigmentosa with a rhodopsin mutation (Arg-135-Trp). Disease phenotype in a Swedish family.* Acta Ophthalmol Scand, 1997. **75**(2): p. 218-23.
248. Souied, E., et al., *Retinitis punctata albescens associated with the Arg135Trp mutation in the rhodopsin gene.* Am J Ophthalmol, 1996. **121**(1): p. 19-25.
249. Sung, C.H., et al., *Rhodopsin mutations in autosomal dominant retinitis pigmentosa.* Proc Natl Acad Sci U S A, 1991. **88**(15): p. 6481-5.
250. Keen, T.J., et al., *Autosomal dominant retinitis pigmentosa: Four new mutations in rhodopsin, one of them in the retinal attachment site.* Genomics, 1991. **11**(1): p. 199-205.
251. Robinson, P.R., et al., *Constitutively active mutants of rhodopsin.* Neuron, 1992. **9**(4): p. 719-725.
252. Li, T., et al., *Transgenic mice carrying the dominant rhodopsin mutation P347S: Evidence for defective vectorial transport of rhodopsin to the outer segments.* Proceedings of the National Academy of Sciences, 1996. **93**(24): p. 14176-14181.

VITA

Marie A. Forbes-Osborne

Education

2001-2008,	University of Kentucky, Lexington Ky. B.S. Biology, December 2005
2009	University of Kentucky, Lexington Ky. PhD in Biology begun

Scholastic Honors

2013	National Eye Institute, Association for Research in Vision and Ophthalmology Annual Meeting Travel Fellowship.
2012-2013	Gertrude Flora Ribble Graduate Fellowship, University of Kentucky, Department of Biology.
2012	College of Arts and Sciences Outstanding Teaching Assistant Award, University of Kentucky.
2011	Graduate Student Travel Fellowship, University of Kentucky.
2011	Gertrude Flora Ribble Travel Fellowship, University of Kentucky, Department of Biology.
2011-2012	Gertrude Flora Ribble Summer Mini-Grant, University of Kentucky, Department of Biology.
2011-2013	Outstanding Poster Award: Bluegrass Society for Neuroscience Spring Neuroscience Day.

Research Publications

Forbes-Osborne, M.A., Wilson, S.G., Morris, A.C. Insulinoma-associated 1a is required for photoreceptor development in the zebrafish retina. Developmental Biology, 2013. 380(2): p157-171.

Morris, A.C., Forbes-Osborne, M.A., Pillai, L.S., Fadool J.M. Microarray Analysis of XOPS-mCFP Zebrafish Retina Identifies Genes Associated with Rod Photoreceptor Degeneration and Regeneration. Investigative Ophthalmology & Visual Science, 2011. 52(5): p. 2255-2266.

Research Presentations

2011	"Genetic Models of Photoreceptor Degeneration and Regeneration in Zebrafish" Midwest Regional Zebrafish Meeting. Rochester, MN.

Marie A. Forbes Osborne